

UNCLASSIFIED

AD NUMBER

AD912061

LIMITATION CHANGES

TO:

Approved for public release; distribution is unlimited.

FROM:

Distribution authorized to U.S. Gov't. agencies only; Test and Evaluation; DEC 1971. Other requests shall be referred to Air Force Aeronautical Systems Division, SDXT, Wright-Patterson AFB, OH 45433.

AUTHORITY

asd, usaf ltr, 8 apr 1974

THIS PAGE IS UNCLASSIFIED

Eg 2

AEDC-TR-71-271

12 JUN 1972



AERODYNAMIC CHARACTERISTICS OF A 0.12-SCALE MODEL OF THE A-9A AIRCRAFT AT MACH NUMBERS FROM 0.30 TO 0.80

Warren E. White

ARO, Inc.

December 1971

This document has been approved for public release

its distribution is unlimited. per TAB 74-10

dtg. 10 May '74

Distribution limited to U.S. Government agencies only;
this report contains information on test and evaluation of
military hardware; December 1971; other requests for this
document must be referred to Aeronautical Systems
Division (SDXT), Wright-Patterson AFB, OH 45433.

**PROPELLION WIND TUNNEL FACILITY
ARNOLD ENGINEERING DEVELOPMENT CENTER
AIR FORCE SYSTEMS COMMAND
ARNOLD AIR FORCE STATION, TENNESSEE**

PROPERTY OF U S AIR FORCE
AEDC LIBRARY
F40600-72-C-0003

NOTICES

When U. S. Government drawings specifications, or other data are used for any purpose other than a definitely related Government procurement operation, the Government thereby incurs no responsibility nor any obligation whatsoever, and the fact that the Government may have formulated, furnished, or in any way supplied the said drawings, specifications, or other data, is not to be regarded by implication or otherwise, or in any manner licensing the holder or any other person or corporation, or conveying any rights or permission to manufacture, use, or sell any patented invention that may in any way be related thereto.

Qualified users may obtain copies of this report from the Defense Documentation Center.

References to named commercial products in this report are not to be considered in any sense as an endorsement of the product by the United States Air Force or the Government.

**AERODYNAMIC CHARACTERISTICS OF A
0.12-SCALE MODEL OF THE A-9A AIRCRAFT
AT MACH NUMBERS FROM 0.30 TO 0.80**

**Warren E. White
ARO, Inc.**

Distribution limited to U.S. Government agencies only;
this report contains information on test and evaluation of
military hardware; December 1971; other requests for this
document must be referred to Aeronautical Systems
Division (SDXT), Wright-Patterson AFB, OH 45433.

FOREWORD

The work reported herein was done at the request of the Aeronautical Systems Division (ASD), Air Force Systems Command (AFSC), for the Northrop Corporation, Hawthorne, California, under Program Element 64211F, System 329A.

The results of the test presented were obtained by ARO, Inc. (a subsidiary of Sverdrup & Parcel and Associates, Inc.), contract operator of the Arnold Engineering Development Center (AEDC), AFSC, Arnold Air Force Station, Tennessee, under Contract F40600-72-C-0003. The tests were conducted from August 17 through 24, 1971, under ARO Project No. PB0190. The manuscript was submitted for publication on November 1, 1971.

This technical report has been reviewed and is approved.

George F. Garey
Lt Colonel, USAF
AF Representative, PWT
Directorate of Test

Duncan W. Rabey, Jr.
Colonel, USAF
Director of Test

ABSTRACT

Wind tunnel tests were conducted at Mach numbers from 0.30 to 0.80 and Reynolds numbers from 2.3 to 7.0 million on a 0.12-scale model of the A-9A aircraft to determine the effects of control surface deflections on the aerodynamic characteristics of the airplane. The results showed that the horizontal stabilizer was 20 to 50 percent more effective in pitching moment per degree of deflection than the elevator, the rudder remained effective at all Mach numbers, and the aileron deflections produced significant effects on lift, drag, and pitching and rolling moment. Minimum drag was increased by approximately 100 and 600 percent for speed brake deflections of 20 and 60 deg, respectively, at Mach numbers from 0.70 to 0.80.

Distribution limited to U.S. Government agencies only; this report contains information on test and evaluation of military hardware; December 1971; other requests for this document must be referred to Aeronautical Systems Division (SDXT), Wright-Patterson AFB, OH 45433.

CONTENTS

	<u>Page</u>
ABSTRACT	iii
NOMENCLATURE	vi
I. INTRODUCTION	1
II. APPARATUS	
2.1 Test Facility	1
2.2 Test Article	1
2.3 Instrumentation	2
III. TEST CONDITIONS AND PROCEDURE	
3.1 Test Description	2
3.2 Accuracy of Measurements	3
IV. RESULTS AND DISCUSSION	
4.1 General	3
4.2 Longitudinal Stability and Control	4
4.3 Lateral Stability and Control	4
4.4 Directional Stability and Control	4
4.5 Speed Brake Effectiveness	5
V. CONCLUSIONS	5

APPENDIXES

I. ILLUSTRATIONS

Figure

1. Schematic of Model Installation	9
2. Photograph of Model Installation	10
3. Model Sketch	12
4. Dimensional Sketches of Model Components	13
5. Effect of Tail Components	21
6. Stabilizer Effectiveness	31
7. Elevator Effectiveness	46
8. Aileron Effectiveness	61
9. Rudder Effectiveness	85
10. Speed Brake Effectiveness	105

II. TABLES

I. Index to Model Components	120
II. Summary of Test Data	122

NOMENCLATURE

b	Reference wing span, 82.08 in.
BETA	Sideslip angle, deg
BL	Buttock line, in.
C_D	Drag coefficient, drag/ $q_\infty S$
C_L	Lift coefficient, lift/ $q_\infty S$
C_Q	Rolling-moment coefficient, rolling moment/ $q_\infty S_b$
C_m	Pitching-moment coefficient, pitching moment/ $q_\infty S \bar{c}$
C_n	Yawing-moment coefficient, yawing moment/ $q_\infty S_b$
C_Y	Side-force coefficient, side force/ $q_\infty S$
\bar{c}	Reference chord, 14.46 in.
F.S.	Fuselage station, in.
H_L	Control surface hinge line
M_∞	Free-stream Mach number
q_∞	Free-stream dynamic pressure, psf
Re	Reynolds number based on model \bar{c}
S	Reference wing area, 8.064 sq ft
WL	Waterline, in.
α	Angle of attack, deg
δ_{AL}	Left aileron only, positive, trailing edge down, deg
δ_B	Speedbrake deflection, measured from the centerline of the aileron trailing edge, deg
δ_E	Elevator deflection, positive, trailing edge down, deg
δ_H	Horizontal stabilizer incidence angle, positive, leading edge up, deg
δ_R	Rudder deflection, positive, trailing edge left, deg

SECTION I INTRODUCTION

Wind tunnel investigations of a 0.12-scale model of the A-9A aircraft were conducted in the Propulsion Wind Tunnel (16T) for the Northrop Corporation at Mach numbers of 0.30, 0.60, 0.70, 0.75, and 0.80 at angles of attack and sideslip from -10 to 20 deg and 0 to 5 deg, respectively. Configuration variables included elevator, rudder, aileron, and speed brake deflections, horizontal tail dihedral angles, horizontal stabilizer incidence angles, external stores, and exit-nozzle core cowls. In addition, internal-duct drag was determined from the pressure data obtained from the exit nozzle and core cowl rakes. The primary purpose of the test was to obtain data at high subsonic Mach numbers at high Reynolds numbers.

SECTION II APPARATUS

2.1 TEST FACILITY

Tunnel 16T is a continuous flow, closed-circuit, variable density wind tunnel capable of operating at Mach numbers from 0.15 to 1.60. The test section is 16 by 16 ft in cross section and 40 ft long. Perforated walls in the test section allow continuous operation through the Mach number range with a minimum of wall interference. A more extensive description of the test facility is given in the Test Facilities Handbook.¹ The sting support system was composed of a vertical support strut, sting support boom, and the high-angle-of-attack sting support system with an auxiliary roll mechanism.

The high-angle-of-attack sting support system was utilized to obtain angles of attack from -12 to 20 deg and also enable variations in sideslip by rolling the sting. Location of the model in the test section and details of the perforated walls are shown in Fig. 1 (Appendix I). Photographs of the model are presented in Fig. 2.

2.2 TEST ARTICLE

2.2.1 Aircraft Model

The test article was a 0.12-scale model of the A-9A aircraft which represented the prototype configuration. Details of the model are presented in Figs. 3 and 4 where the complete configuration is shown and the individual components are identified. The aileron (left wing only), elevators, and rudder were remotely controlled, whereas the speed brakes, horizontal tail dihedral, and horizontal stabilizer incidence angles were set manually during configuration changes. The model had flow-through inlets with ducts to simulate exit nozzles. The wing incidence angle was 0 deg with respect to the fuselage waterline. A 0.10-in.-wide boundary-layer trip was composed of number 80 grit and was located 0.80 in. from the leading edge of both surfaces of the wings and vertical and horizontal

¹Test Facilities Handbook (Ninth Edition). "Propulsion Wind Tunnel Facility, Vol. 4." Arnold Engineering Development Center, July 1971.

stabilizers. In addition, a 0.10-in.-wide boundary-layer trip was affixed 0.80 in. aft of the nose. The index to model components and the configurations tested are listed in Table I (Appendix II).

2.2.2 Pylons and Store Models

The stores tested during this investigation were the MK-82 500-lb Bomb and the BLU-1/B Napalm Bomb. Sketches of these stores, associated pylons, and dispenser racks are presented in Figs. 4e, f, g, and h. All stores and pylons were nonmetric and were installed symmetrically on the parent model about its plane of symmetry.

2.3 INSTRUMENTATION

The overall aerodynamic forces and moments on the model were measured with a six-component, internal, strain-gage balance. The sensing components of the balance consisted of forward and aft normal-force elements (for determination of normal force and pitching moment), forward and aft side-force elements (for determination of side force and yawing moment), an axial-force element, and a rolling-moment element. Static pressures were measured at the sting entrance to the model and within the model cavity. A rake was attached to the model and positioned to measure pressures at the exit plane of the engine duct. The sting pitch angle was determined from the output of a strain-gaged angular position indicator. Sting roll angle was determined from the output of a potentiometer. The aileron, elevator, and rudder were instrumented with strain-gage hinge moment beams. The rotational angle of these surfaces was determined from the outputs of potentiometers. Electrical signals from the balances, pressure transducers, model attitude systems, and hinge-moment beams were digitized and recorded on magnetic tape, as well as fed directly to a computer for on-line data reduction. The balance and hinge-moment outputs were also recorded on an oscillograph for monitoring model dynamics.

SECTION III TEST CONDITIONS AND PROCEDURE

3.1 TEST DESCRIPTION

The test was conducted at Mach numbers from 0.30 to 0.80 and Reynolds numbers of 2.3, 4.5, and 7.0 million based on the wing mean aerodynamic chord. The total pressure ranged from approximately 3660 psfa at $M_\infty = 0.60$ and $Re = 7.0 \times 10^6$ to 1071 psfa at $M_\infty = 0.8$ and $Re = 2.3 \times 10^6$. Total temperature was maintained at approximately 105°F for all Mach numbers.

Tunnel conditions were held constant at each Mach number, while the angle of attack was varied from -10 to 20 deg. For related configurations, combinations of a constant beta of 5 deg and angles of attack were obtained by pitching and rolling the model. The maximum angle of attack was limited to lower values in certain cases because of reaching dynamic load limits. Model variables included remotely controlled aileron, elevator, and rudder angles of 0, ± 5 , ± 10 , ± 20 , and ± 30 deg; 0, ± 5 , and ± 10 deg; and 0, 10, 20, and 30 deg, respectively. Additional configurations consisted of manually controlled

speedbrake, horizontal tail dihedral, and horizontal stabilizer incidence angles of 0, -20, and -60 deg; 0 and 10 deg; and 0 and ± 2 deg, respectively.

3.2 ACCURACY OF MEASUREMENTS

The precision of setting and maintaining Mach number is estimated to be within ± 0.004 for Mach numbers of 0.3 and ± 0.003 and for Mach numbers from 0.60 to 0.80. Flow angularity corrections in the vertical plane of the tunnel, deduced from the upright and inverted runs, have been applied. Measured force and moment data on the balance were corrected for weight tares. No corrections have been made for cavity pressure base drag; however, internal duct drag-force data were measured and subtracted from the total drag force of the model. In addition to the measured drag values, interpolated values were used where measured data were not available.

The estimated uncertainties in the static-force data are given in the following table and are based on 95-percent probability.

<u>Parameter</u>	<u>M_∞</u>				
	<u>0.30</u>	<u>0.60</u>	<u>0.70</u>	<u>0.75</u>	<u>0.80</u>
a	± 0.1	± 0.1	± 0.1	± 0.1	± 0.1
β	± 0.1	± 0.1	± 0.1	± 0.1	± 0.1
C_L	± 0.0158	± 0.0083	± 0.0060	± 0.0047	± 0.0037
C_m	± 0.0031	± 0.0082	± 0.0010	± 0.0011	± 0.0011
C_Y	± 0.0104	± 0.0028	± 0.0025	± 0.0023	± 0.0022
C_n	± 0.0006	± 0.0002	± 0.0002	± 0.0008	± 0.0002
C_Q	± 0.0004	± 0.0001	± 0.0001	± 0.0005	± 0.0001
C_D	± 0.0031	± 0.0019	± 0.0020	± 0.0012	± 0.0011

SECTION IV RESULTS AND DISCUSSION

4.1 GENERAL

The primary purpose of this investigation was to determine the effects of deflecting the aileron, elevator, rudder, and speed brakes on the aerodynamic forces and moments. These forces and moments were reduced to aerodynamic coefficients in the stability axes system about a moment reference center that was located at the quarter chord of the mean aerodynamic chord. The large volume of data obtained during this test precludes making detailed analysis of all the test data. Consequently, this report includes only the analysis of data from aileron, elevator, rudder, and speed brake deflections of the basic model with and without the empennage for nominal Reynolds numbers of 2.3 and 4.5 million at Mach numbers 0.3 and from 0.60 to 0.80, respectively. The complete test is documented in Table II where the part numbers are presented for each model configuration and test conditions for which data were obtained.

4.2 LONGITUDINAL STABILITY AND CONTROL

Presented in Fig. 5 are the curves of C_N , C_m , and C_D obtained during the tail component buildup tests. The ailerons, elevator, and rudder remained at zero, whereas the horizontal tail was installed at -2-deg incidence angle. As expected, Configurations XD₆ and XD₆S₁₋₅ V₂ d₂ r₃ (see Table I) were statically unstable, since these configurations were without a horizontal tail. The complete model was longitudinally statically stable for the Mach numbers and Reynolds numbers shown. The increase in drag at a lift coefficient of zero for the addition of the vertical tail and the horizontal tail were approximately 11 and 40 percent, 11 and 31 percent, 11 and 33 percent, 4 and 20 percent, and 0 and 10 percent for Mach numbers of 0.30, 0.60, 0.70, 0.75, and 0.80, respectively.

Presented in Fig. 6 are data showing the effectiveness of the horizontal stabilizer for providing longitudinal control as well as the increase in drag because of the change in incidence angle of the horizontal stabilizer. The data showed that linear changes in C_m were produced by deflecting the horizontal stabilizer at Mach numbers of 0.30, 0.60, and 0.70 until buffet onset or stall occurred. The stabilizer effectiveness remained unchanged as free-stream Mach number was increased from 0.30 to 0.70 but decreased with further increases in Mach number. The deflection of the horizontal tail to ± 2 deg showed an incremental shift in the lift curve.

The effects of deflecting the elevator on the aerodynamic characteristics of the A-9A model are presented in Fig. 7. Deflections of the horizontal stabilizer and the elevator showed similar effects in pitching moments but with different orders of magnitude which were attributable to the difference in surface areas. The stabilizer was 20 to 50 percent more effective in pitching moment per degree of deflection than the elevator.

4.3 LATERAL STABILITY AND CONTROL

Figure 8 shows a noticeable effect on the lift, drag, pitching moment, and rolling-moment coefficients attributable to aileron deflections. The data showed that as the aileron on the left wing was deflected ± 10 deg a proportional increase occurred in C_l at $M_\infty = 0.30, 0.60$, and 0.70 . However, at $M_\infty = 0.75$ and 0.80 , the negative 10-deg (trailing edge up) deflection did not produce an equivalent ΔC_l to the values obtained for the positive aileron deflection. At $M_\infty = 0.80$, a reversal in the sign of the rolling moment occurred for model angles of attack between 1 and 9 deg for $\delta_{AL} = -10$ deg. This anomaly in the data was eliminated when the speed brakes were deflected 20 and 60 deg at $M_\infty = 0.75$ and 0.80 for $\delta_{AL} = -10$ deg as shown in Figs. 8f and g. Therefore, the reversal in rolling moment at $M_\infty = 0.80$ for the negative 10-deg aileron deflection is attributed to some type of local flow separation which reduced the aileron's effectiveness.

4.4 DIRECTIONAL STABILITY AND CONTROL

The changes in aerodynamic coefficients resulting from rudder deflections at $\beta = 0$ deg are presented in Fig. 9. These data show that the rudder effectiveness was essentially

constant for C_Y , C_n , and $C\dot{\theta}$ up to 20 deg. At rudder deflection angles greater than 20 deg, there was less rudder effectiveness. The rudder remained effective for all Mach numbers.

4.5 SPEED BRAKE EFFECTIVENESS

For data presented in Fig. 10 with the speed brakes deflected, the elevator and the rudder were at 0 deg, whereas the horizontal stabilizer incidence angle was at -2 deg. Deflecting the speed brake 60 deg reduced the value of the lift curve slope and significantly delayed the onset of buffet at Mach numbers of 0.70, 0.75, and 0.80. The speed brake deflection angle of 20 and 60 deg increased the minimum drag by 100 and 600 percent, respectively. The deflection of the speed brake from 20 to 60 deg produced a large destabilizing moment.

SECTION V CONCLUSIONS

The results of a test conducted at Mach numbers from 0.3 to 0.8 to determine the aerodynamic characteristics of the A-9A aircraft led to the following remarks:

1. The stabilizer effectiveness remained unchanged as free-stream Mach number was increased from 0.30 to 0.70 but decreased with a further increase in free-stream Mach number.
2. The effectiveness of the aileron to produce a corresponding rolling moment for a negative aileron deflection was reduced to zero for angles of attack from approximately 1 to 9 deg at Mach number 0.80.
3. The rudder remained effective for all Mach numbers from 0.30 to 0.80.
4. Increasing the deflection angle of the speed brakes produced a destabilizing pitching moment and delayed the onset of wing buffet.
5. Minimum drag was increased by factors of approximately 100 and 600 percent for speed brake deflection angles of 20 and 60 deg, respectively, at Mach numbers from 0.70 to 0.80.
6. The horizontal stabilizer was 20 to 50 percent more effective in pitching moment per deg of deflection than the elevator.

APPENDIXES
I. ILLUSTRATIONS
II. TABLES

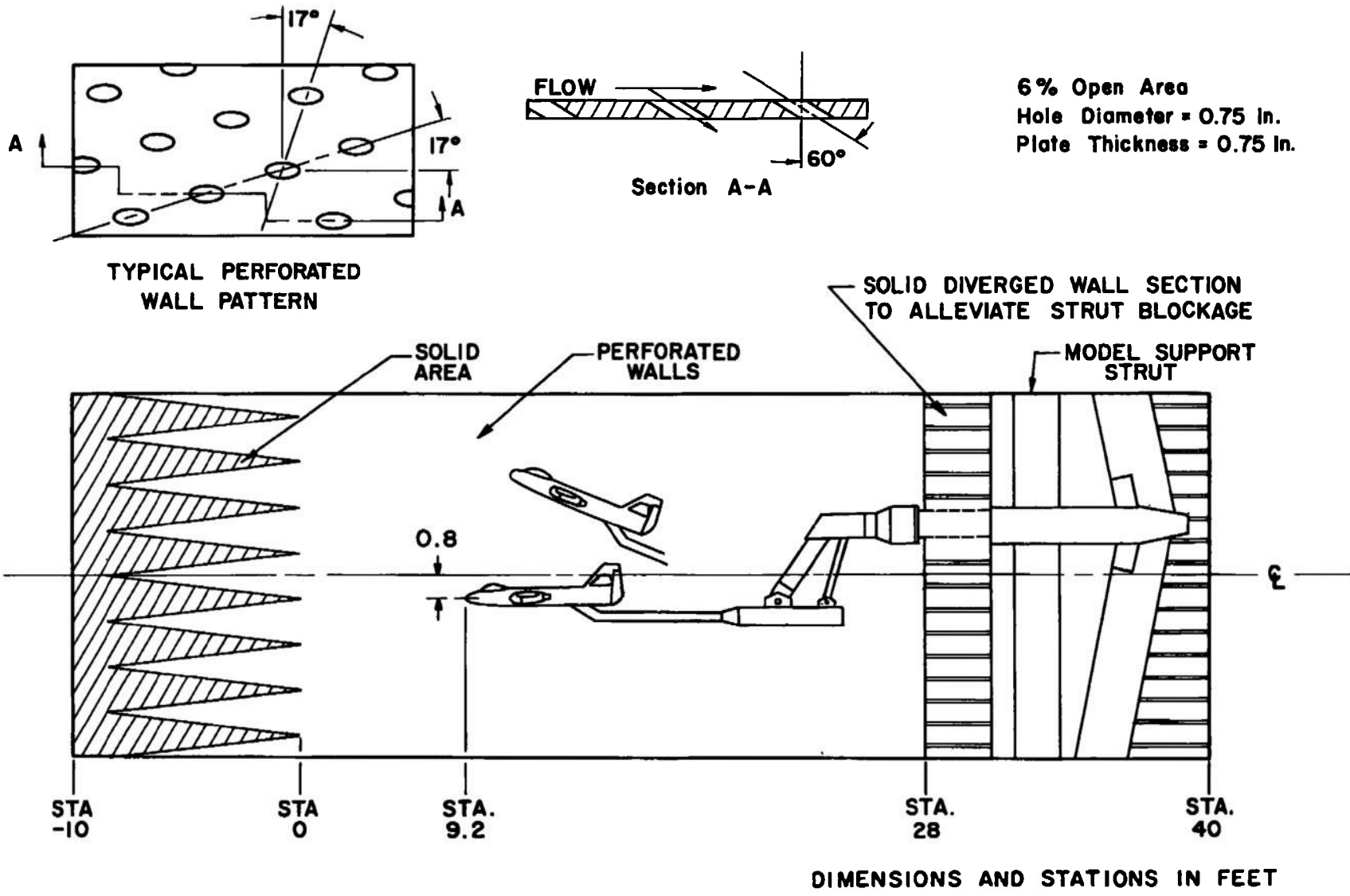
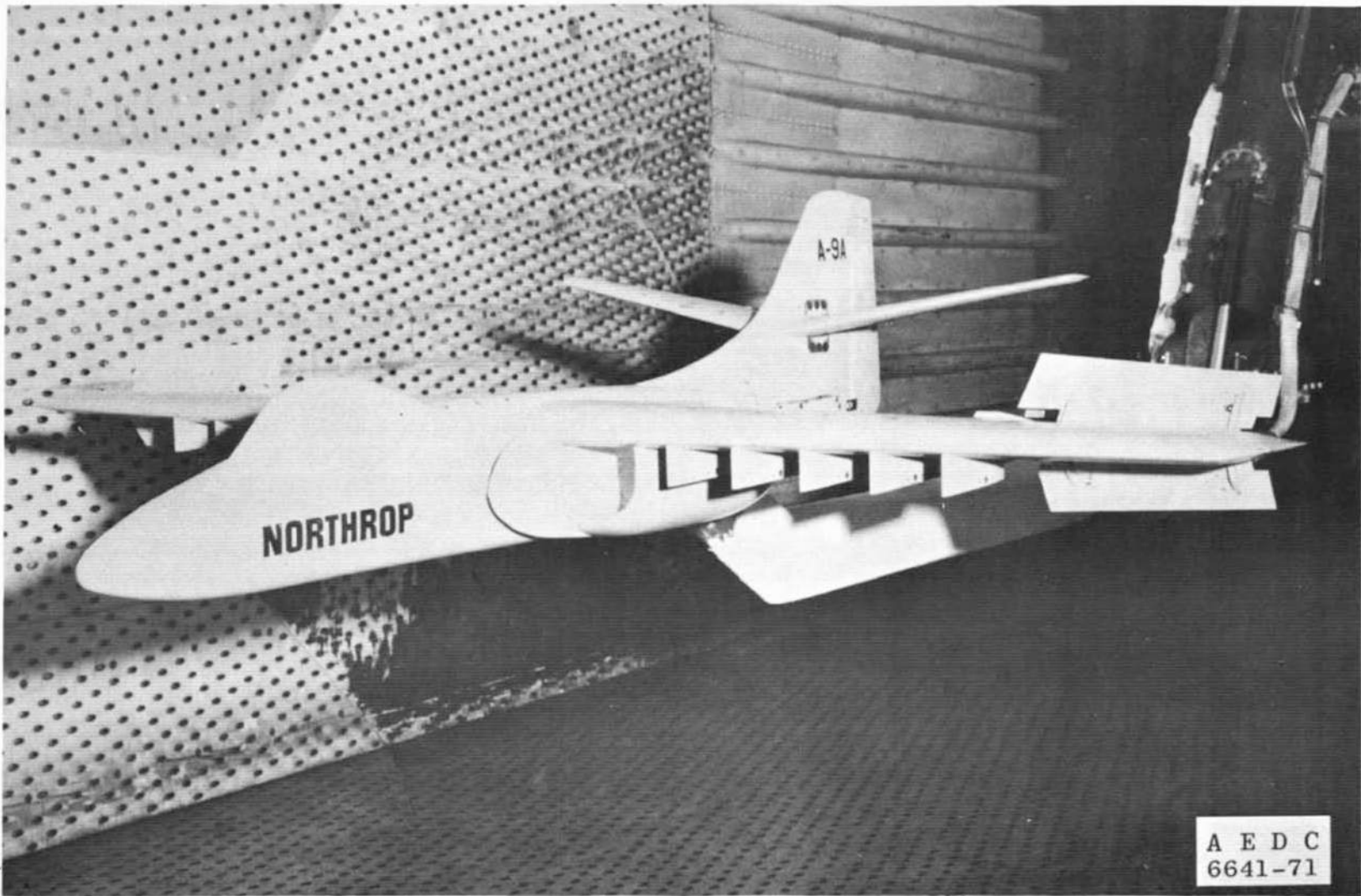
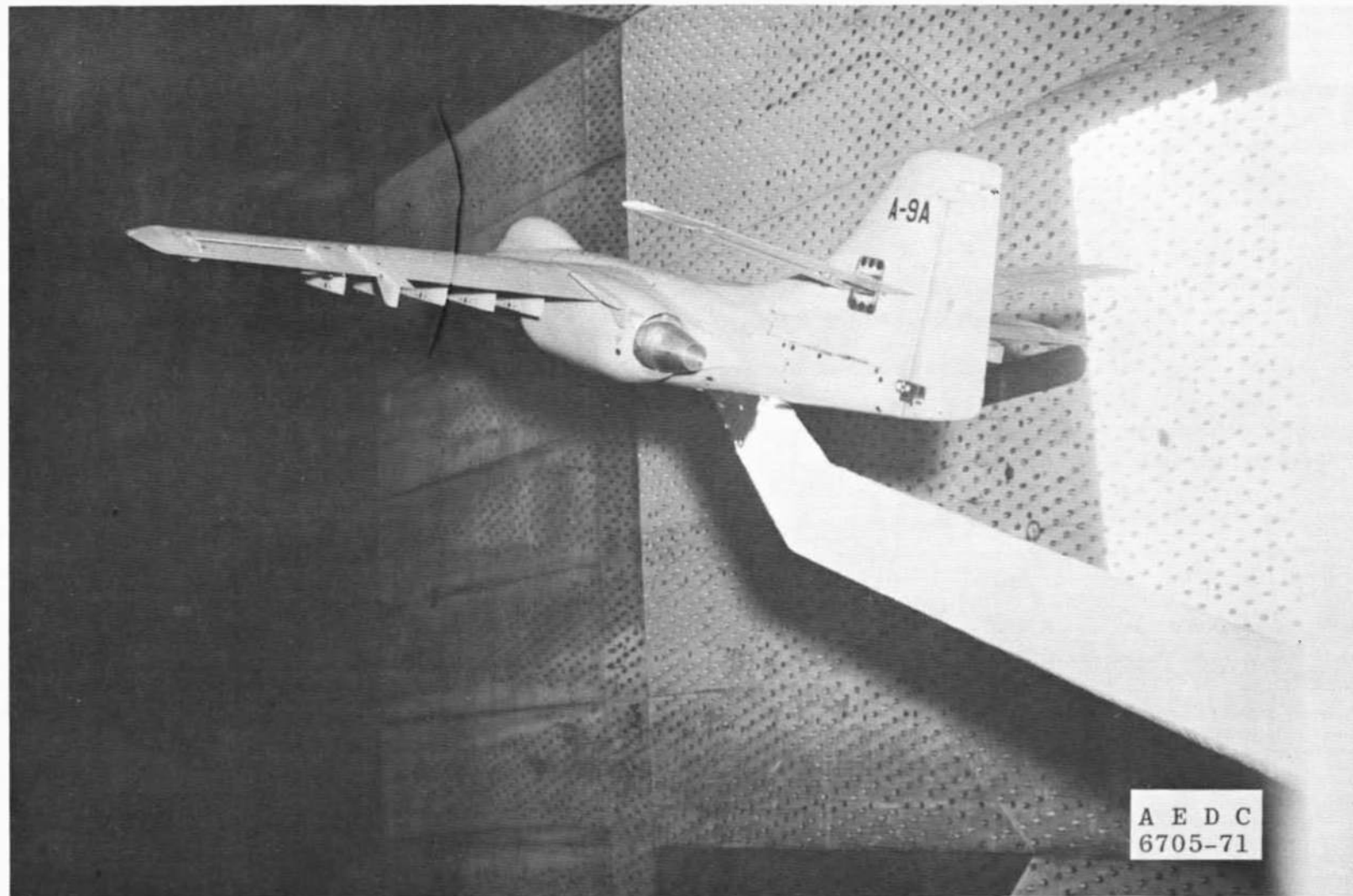


Fig. 1 Schematic of Model Installation



a. Speed Brake Extended
Fig. 2 Photograph of Model Installation



b. Speed Brake Retracted
Fig. 2 Concluded

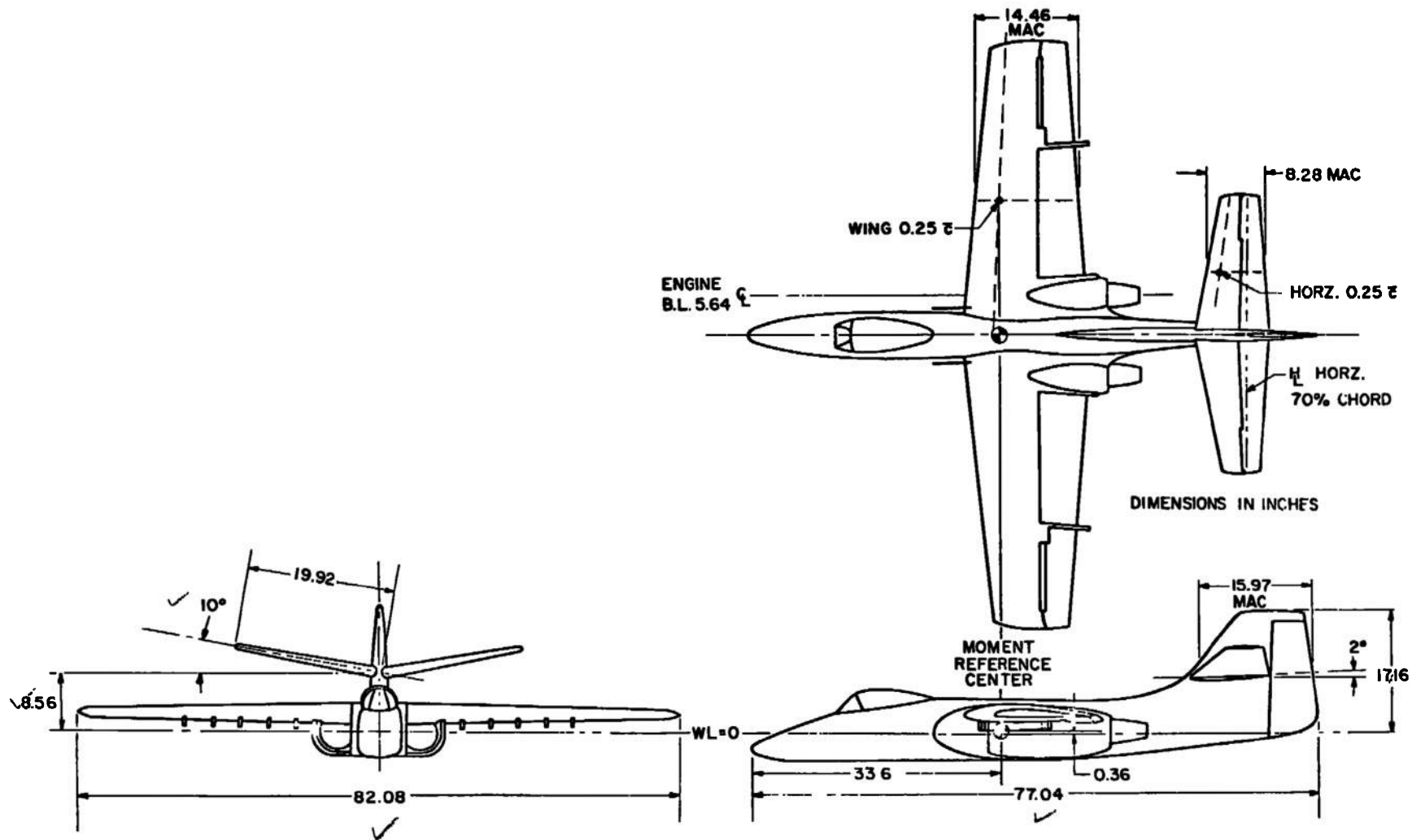
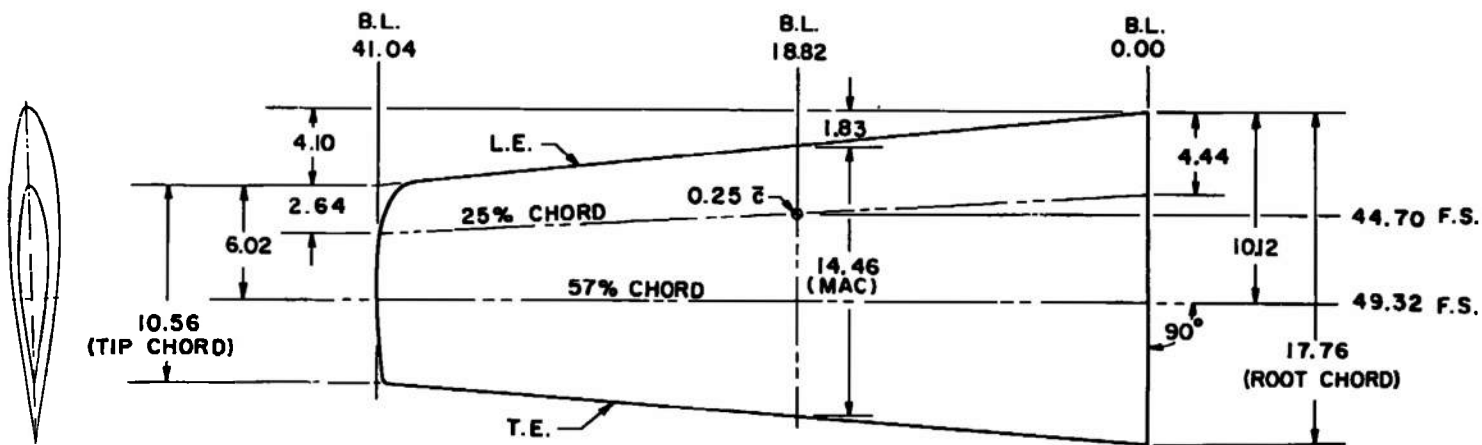


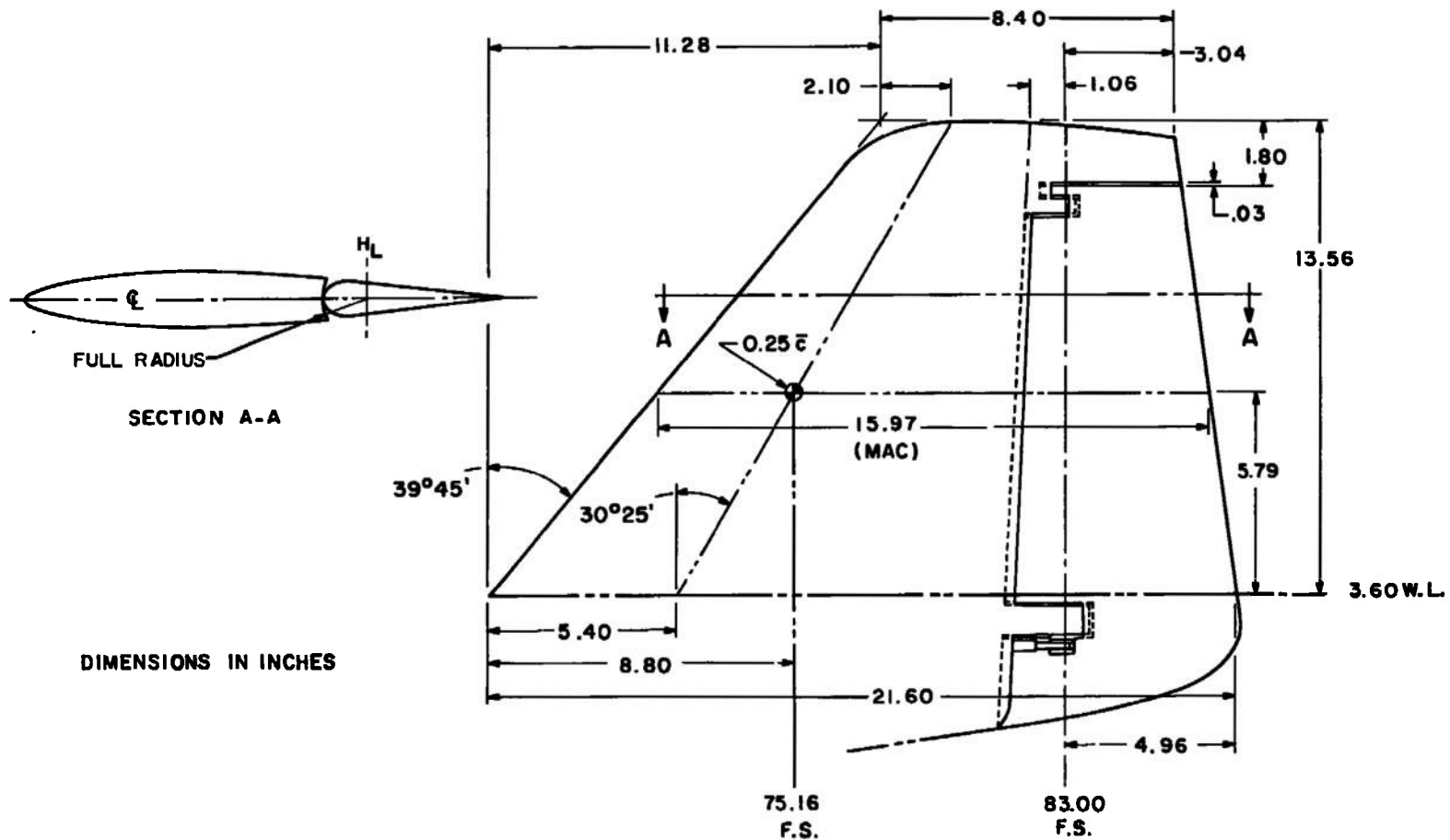
Fig. 3 Model Sketch



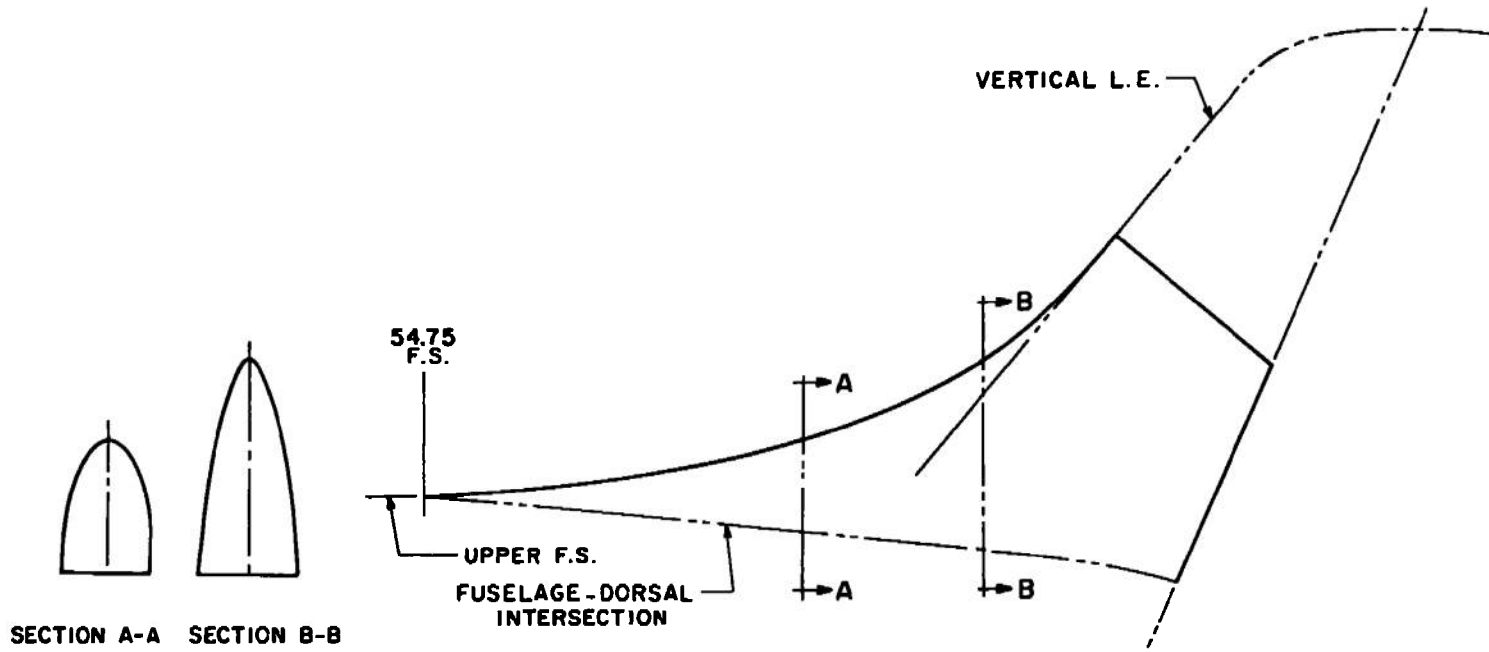
DIMENSIONS IN INCHES

a. Wing

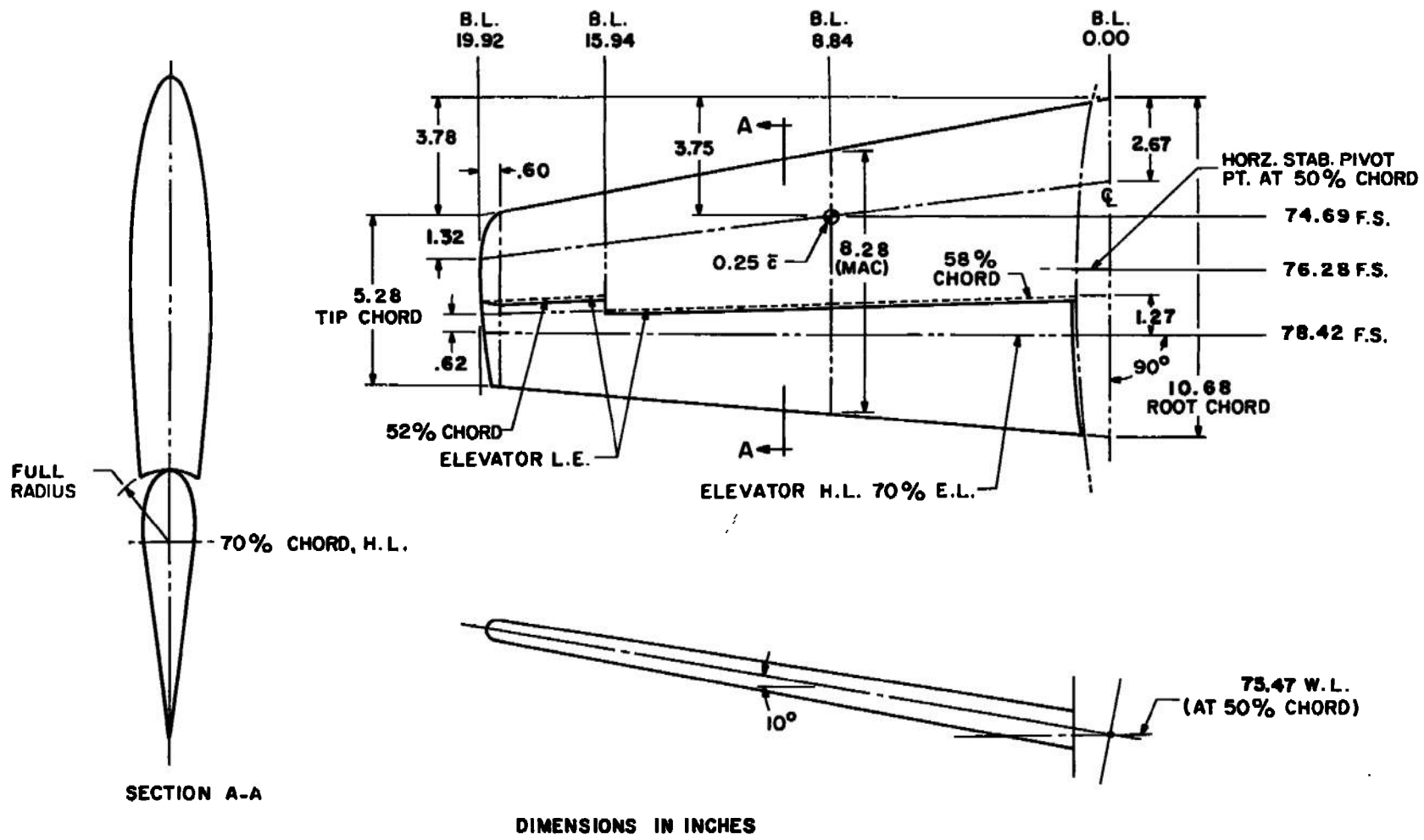
Fig. 4 Dimensional Sketches of Model Components



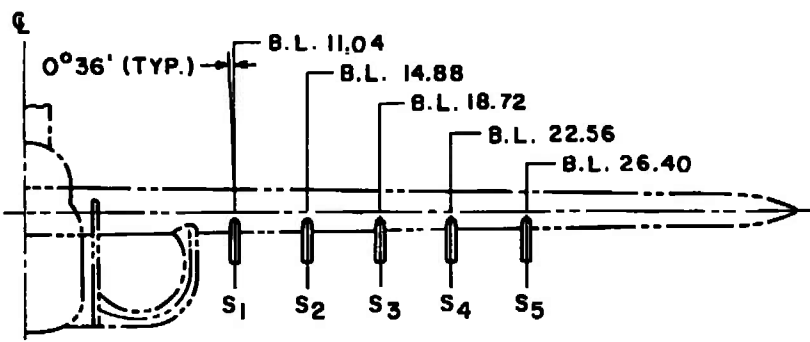
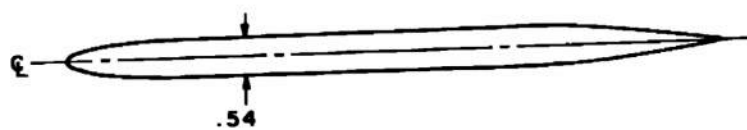
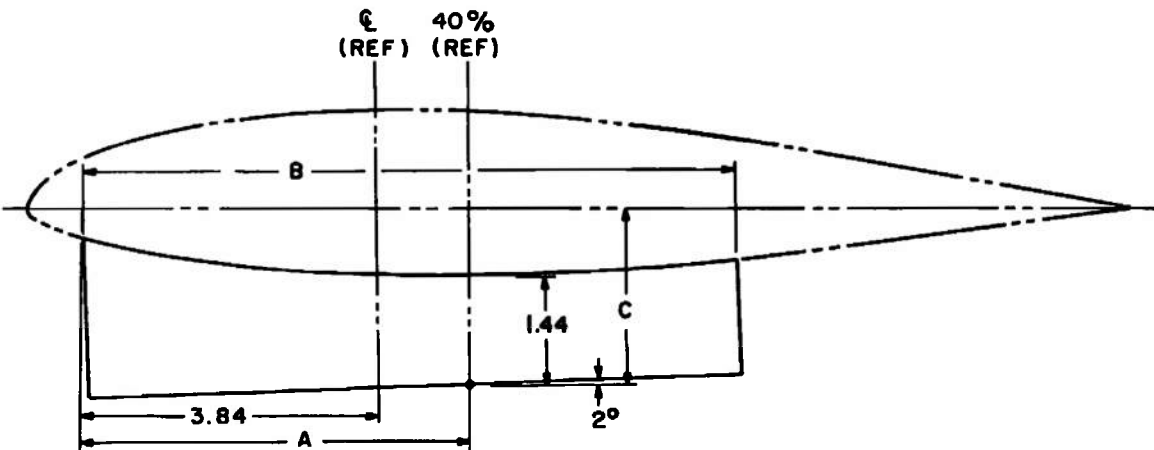
b. Vertical Tail
Fig. 4 Continued



c. Dorsal Fin
Fig. 4 Continued



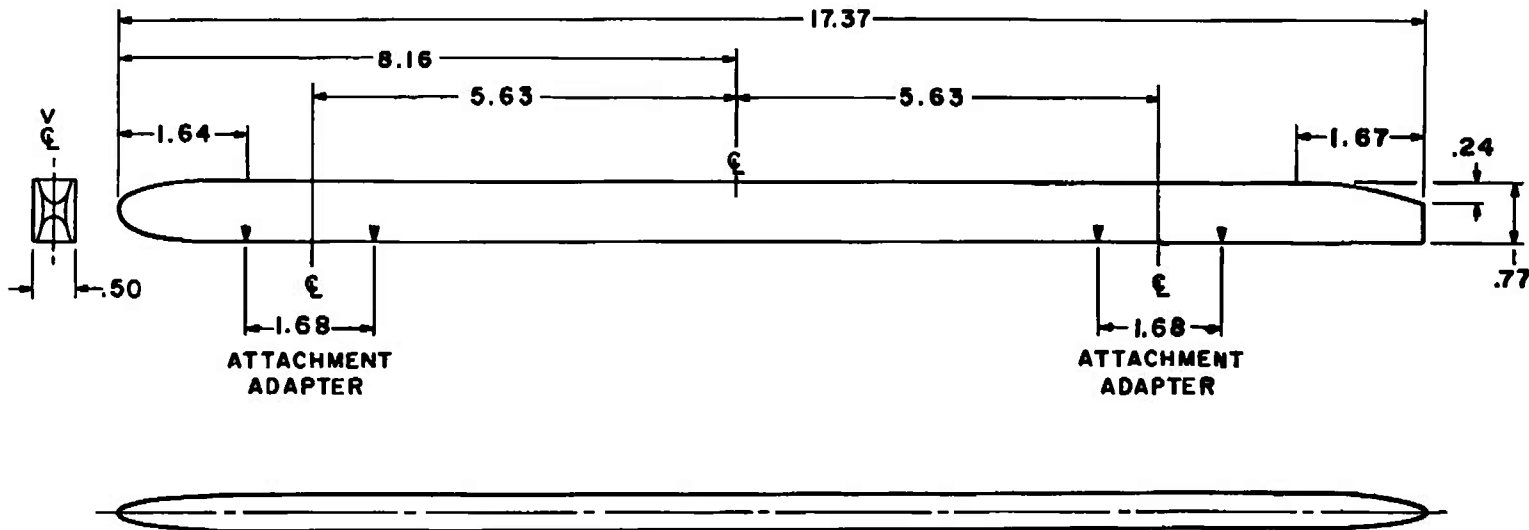
d. Horizontal Tail
Fig. 4 Continued



B.L.	A	B	C
11.04	5.32	9.67	2.38
14.88	5.31	9.13	2.34
18.72	5.06	8.60	2.30
22.56	4.92	8.09	2.26
26.40	4.79	7.52	2.22

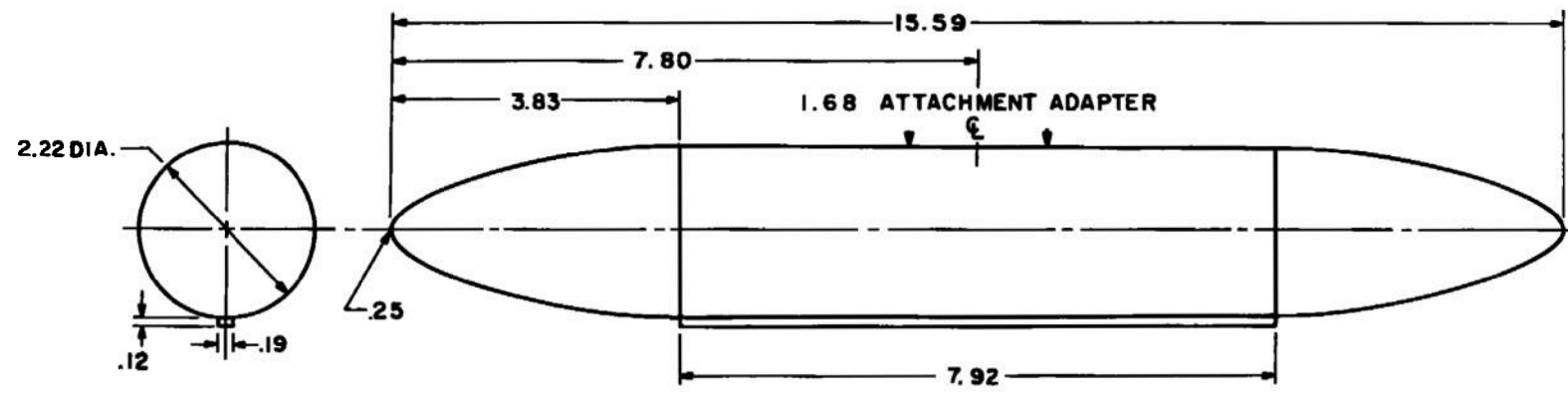
DIMENSIONS IN INCHES

e. Wing Pylon Locations
Fig. 4 Continued



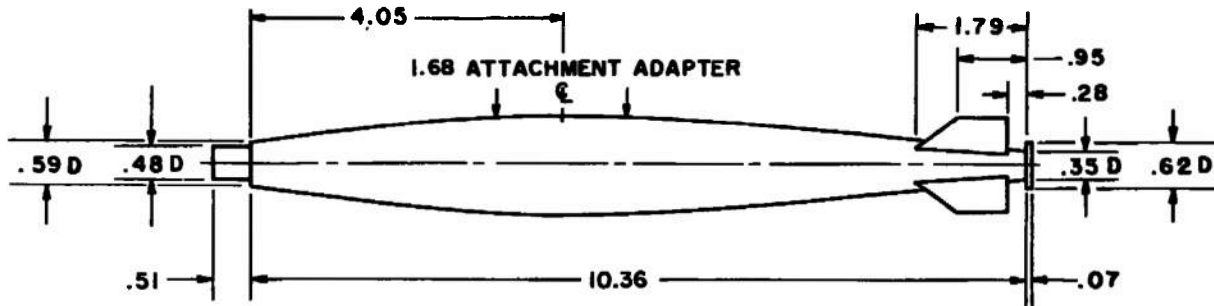
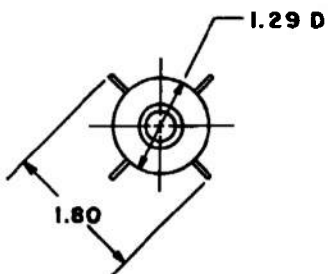
DIMENSIONS IN INCHES

f. Pylon Extension Rack
Fig. 4 Continued



DIMENSIONS IN INCHES

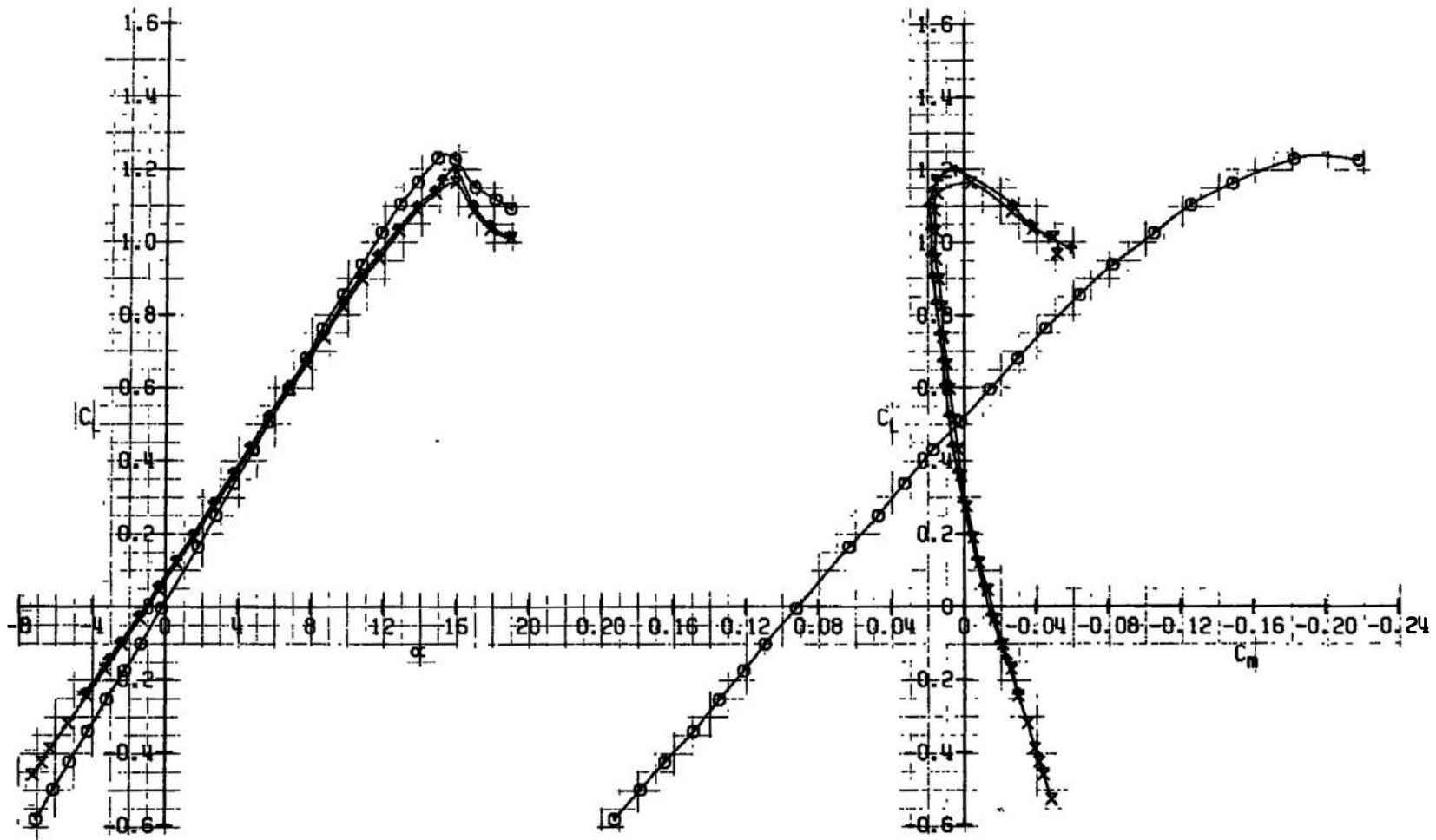
g. BLU-1/B
Fig. 4 Continued



DIMENSIONS IN INCHES

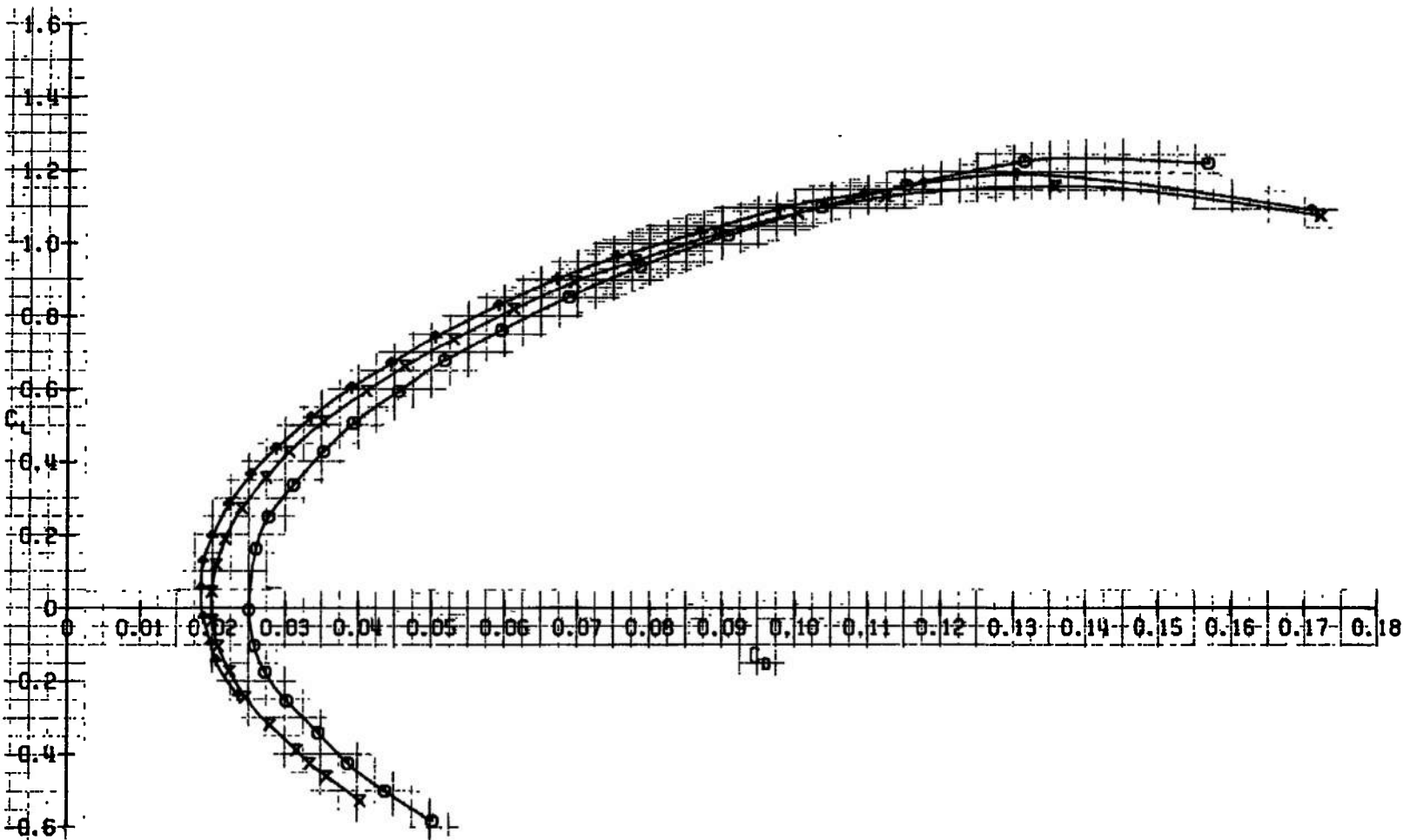
h. MK-82
Fig. 4 Concluded

CONFIGURATION: H_2S_1S H_2P_1P $B_3C_2N_2$		N_{α}	R_{α}	RET	SH	WF	AB	AOL	AB	PN
SYM	CONFIGURATION: σ	-	-	-	-	-	-	-	-	-
\uparrow	D_2S_1S	-	-	0.30	2/3	-	0	0	0	427
X	D_2S_1S $V_2D_2P_3$	-	-	0.30	2/3	-	0	0	0	937
O	D_2S_1S $V_2D_2P_3$ $H_2C_2N_2$	-	-	0.30	2/3	-	0	0	0	46



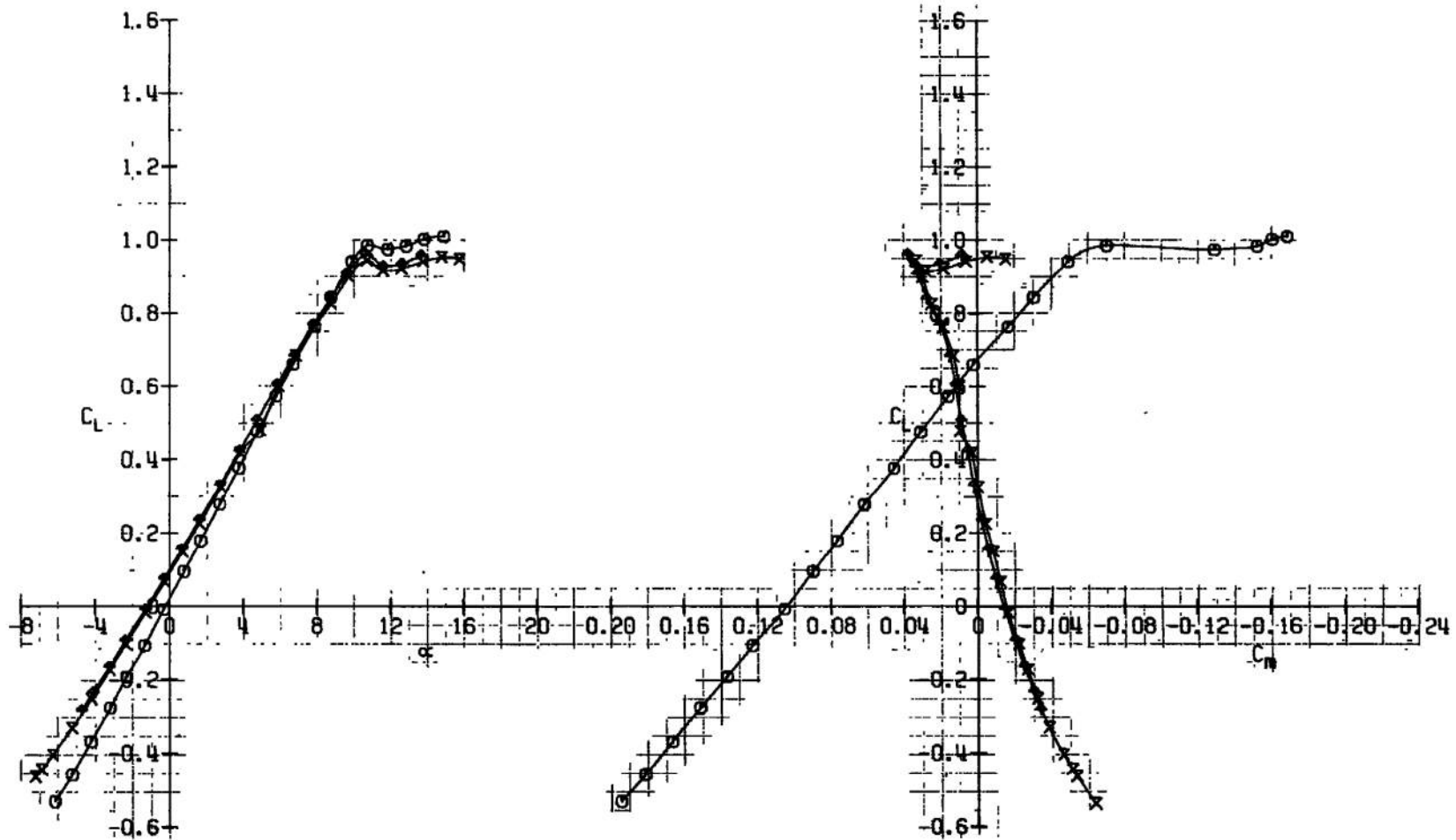
a. $M_a = 0.30$

Fig. 5 Effect of Tail Components

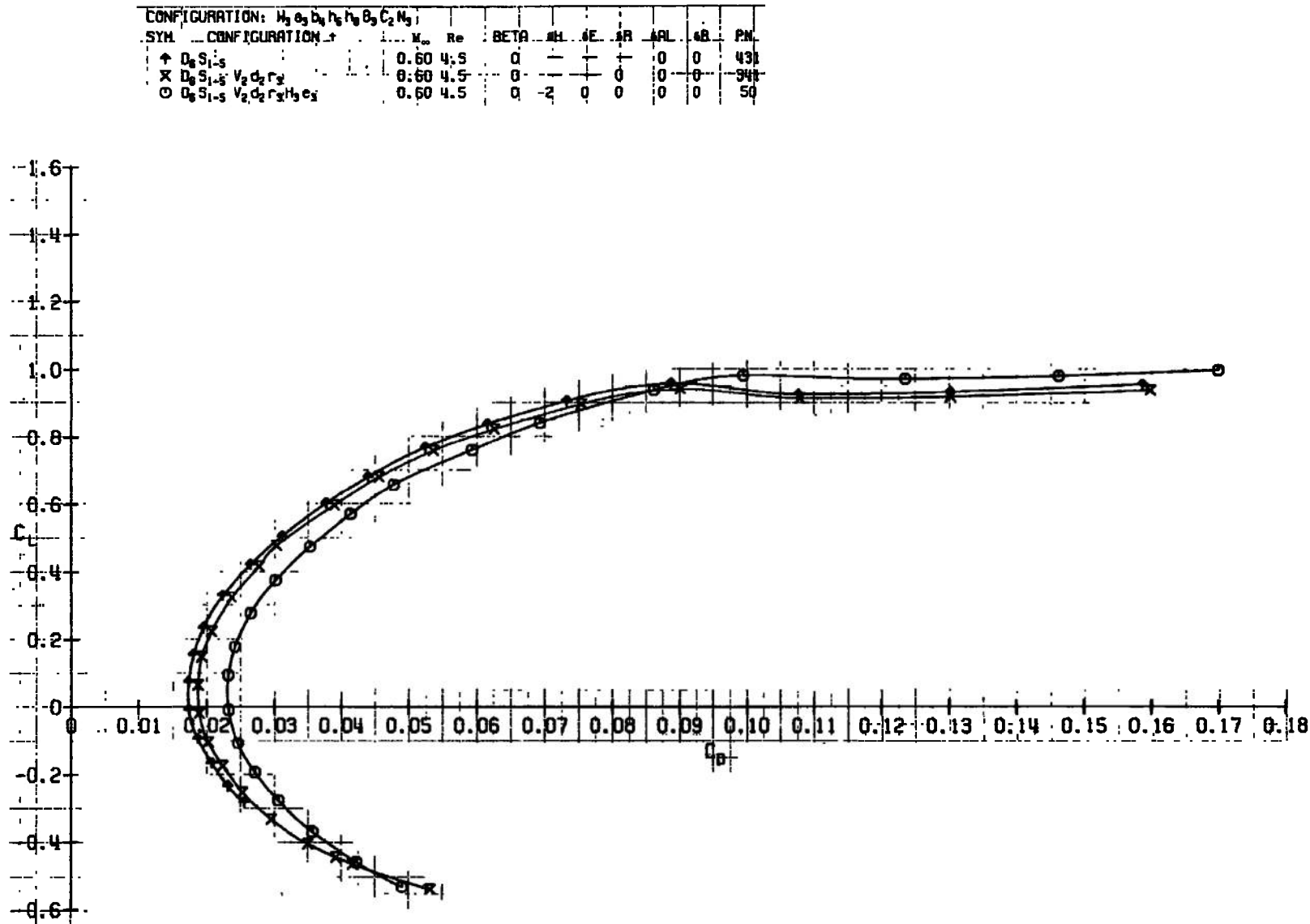


a. Concluded
Fig. 5 Continued

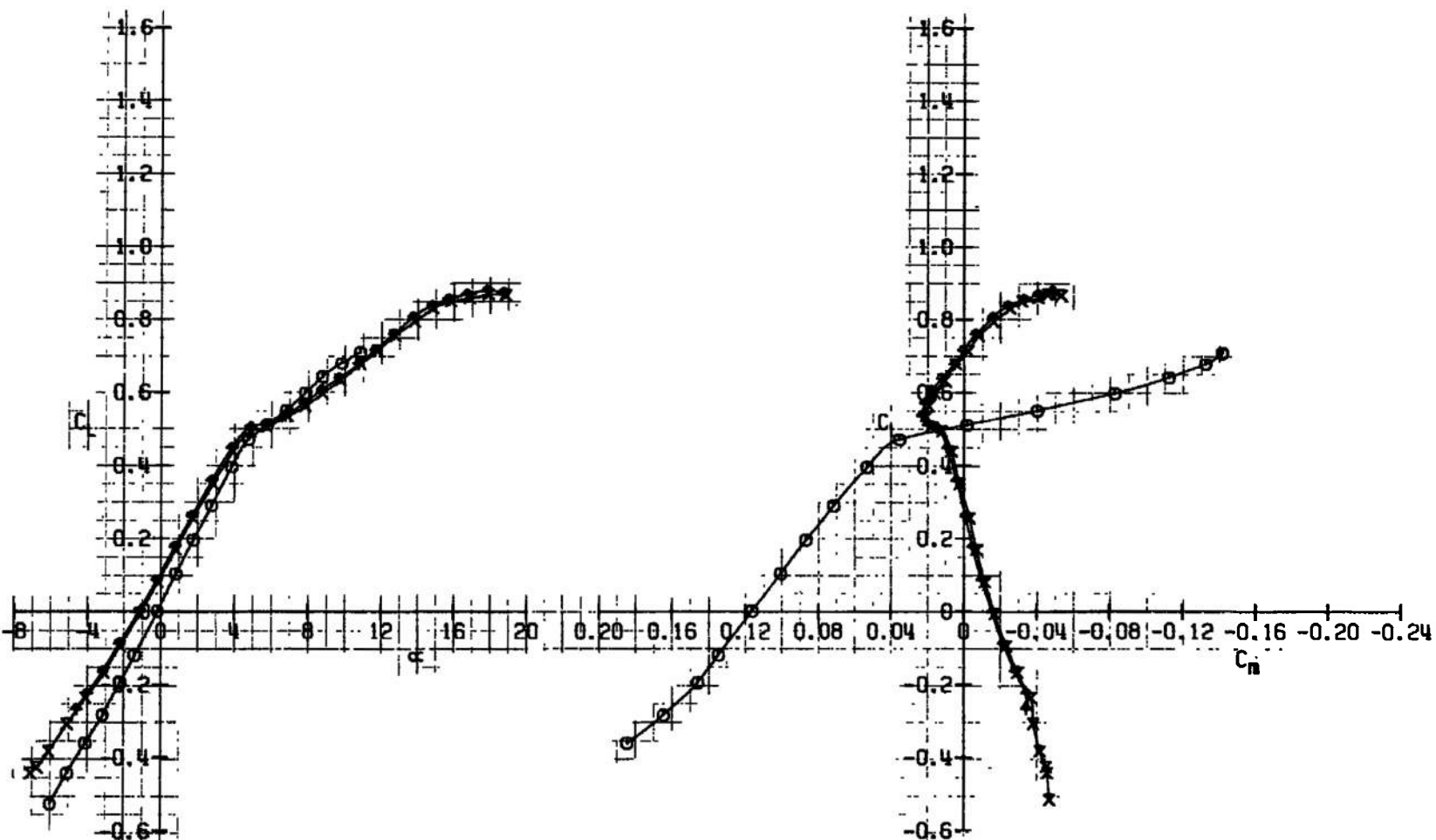
CONFIGURATION: W ₉ B ₄ H ₈ F ₈ B ₃ C ₂ N ₃		SYM.	M _∞	Re	BETAPLANE						
CONFIGURATION	*				BETAPLANE	SH	SE	SP	SOL	SR	PN
↑ D ₆ S ₁₋₅			0.60	4.5	0	1	1	0	0	0	431
X D ₆ S ₁₋₅ V ₂ d ₂ r ₃			0.60	4.5	-	0	1	0	0	0	341
○ D ₆ S ₁₋₅ V ₂ d ₂ r ₃ H ₃ e ₃			0.60	4.5	0	-2	0	0	0	0	50



b. M_∞ = 0.60
Fig. 5 Continued

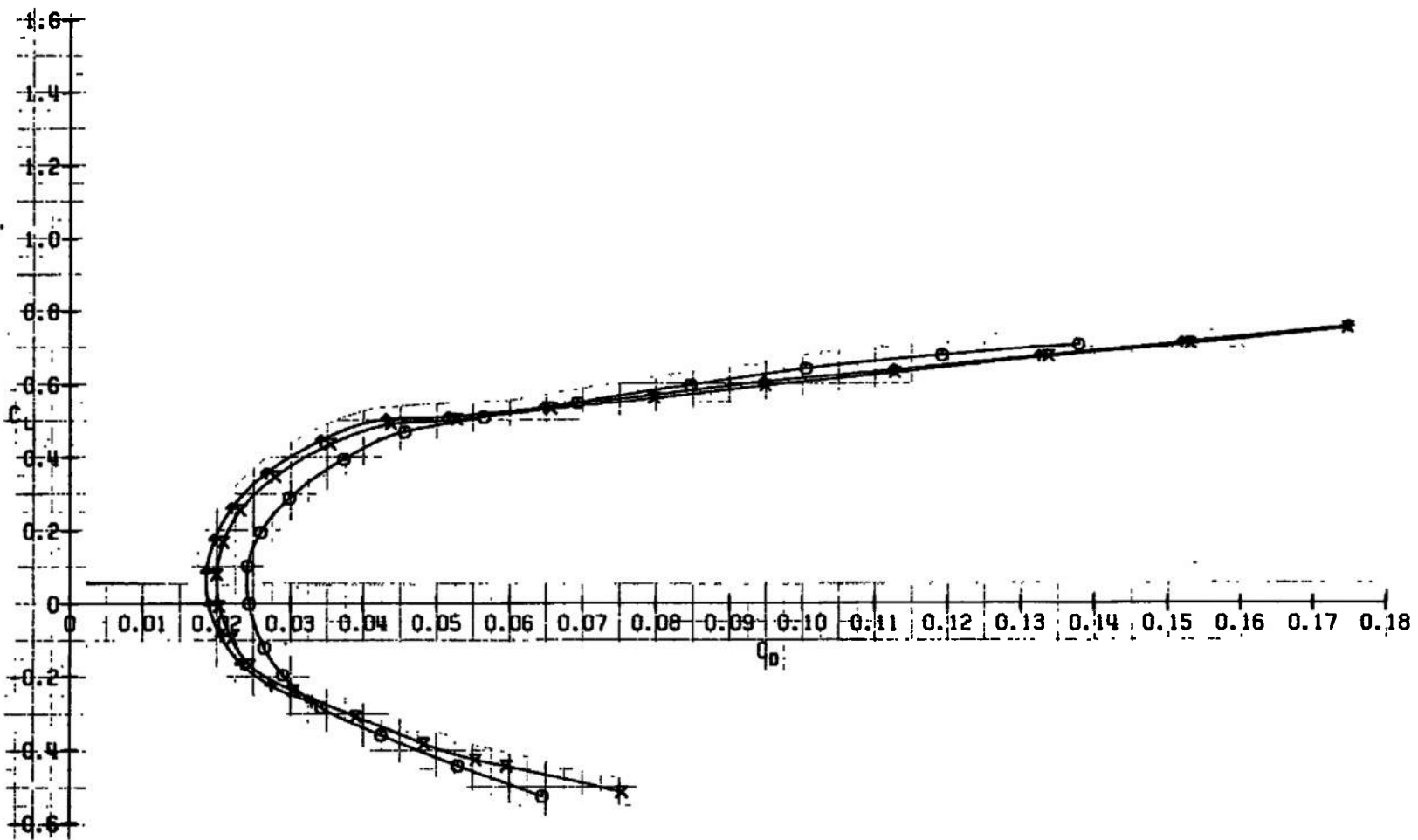


b. Concluded
Fig. 5 Continued

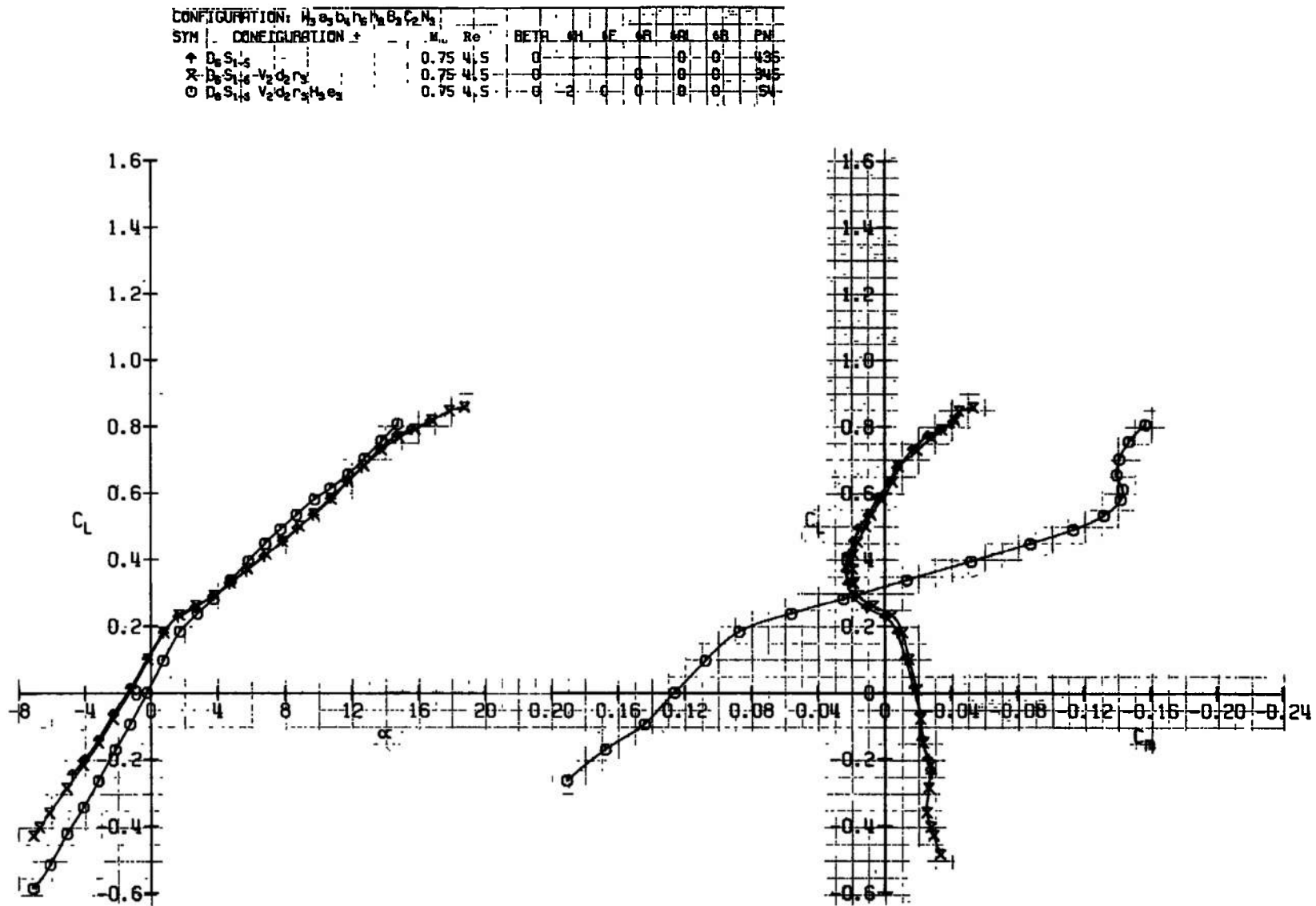


c. $M_\infty = 0.70$
Fig. 5 Continued

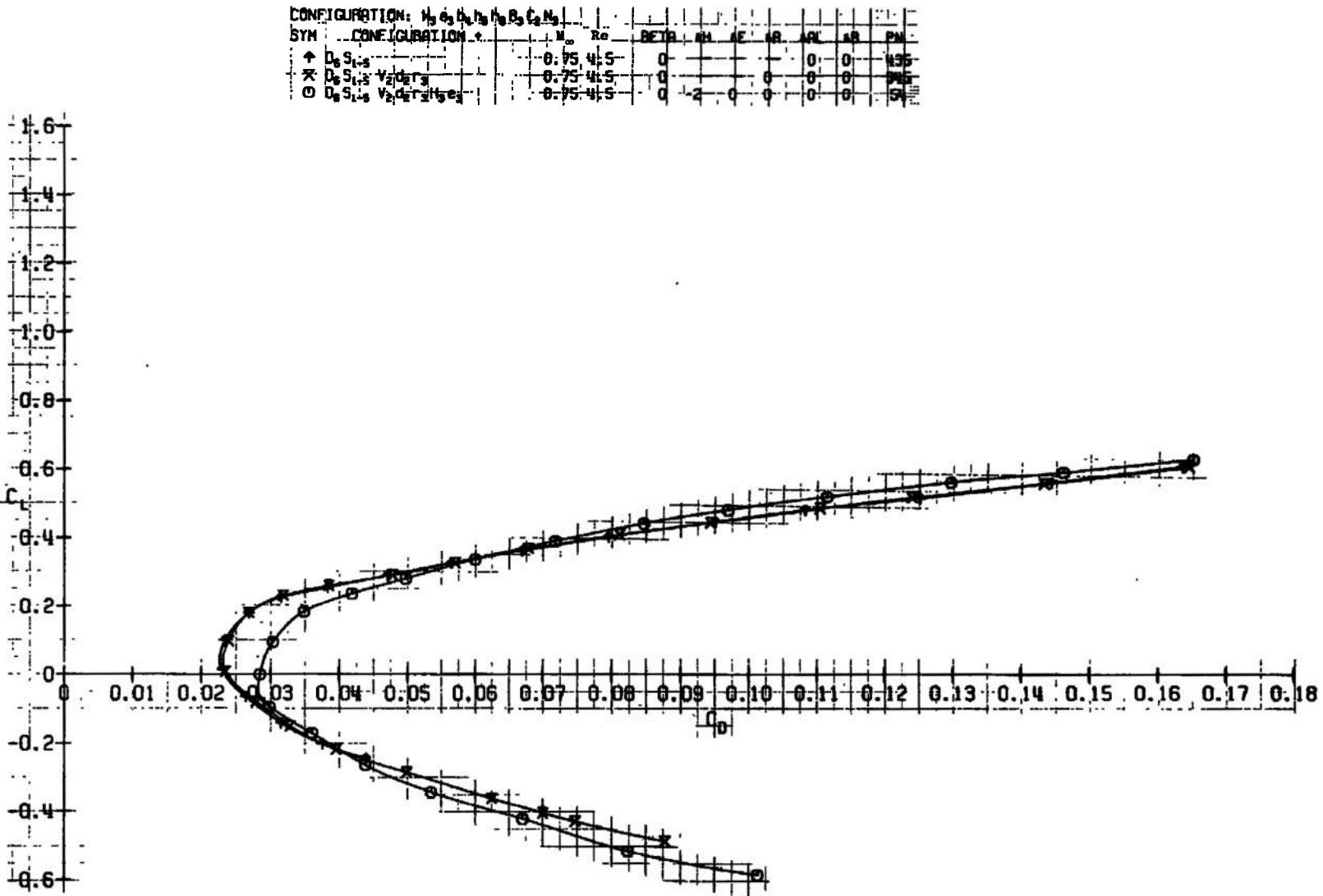
CONFIGURATION: $W_3 S_3 B_3 h_3 h_3 B_3 C_2 N_3$		M _a	Re	BETA	SH	SE	SR	SI	AB	PM
SYM		0.70	4.5	0	+	-	0	0	0	439
↑ D ₆ S ₁₋₅		0.70	4.5	0	-	0	0	0	0	949
X D ₆ S ₁₋₅ V ₂ d ₆ r ₃		0.70	4.5	0	-2	0	0	0	0	52



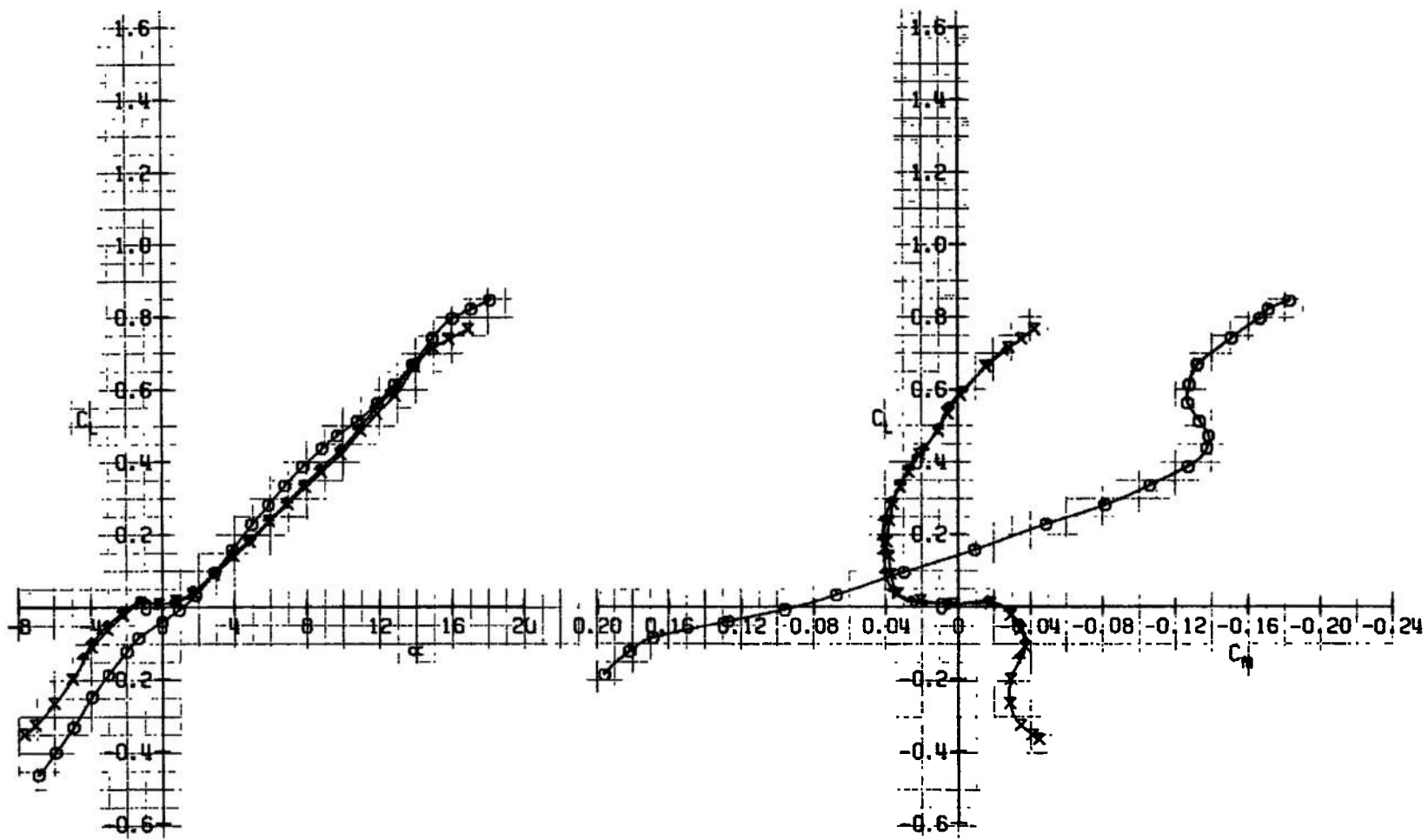
c. Concluded
Fig. 5 Continued



d. $M_\infty = 0.75$
Fig. 5 Continued

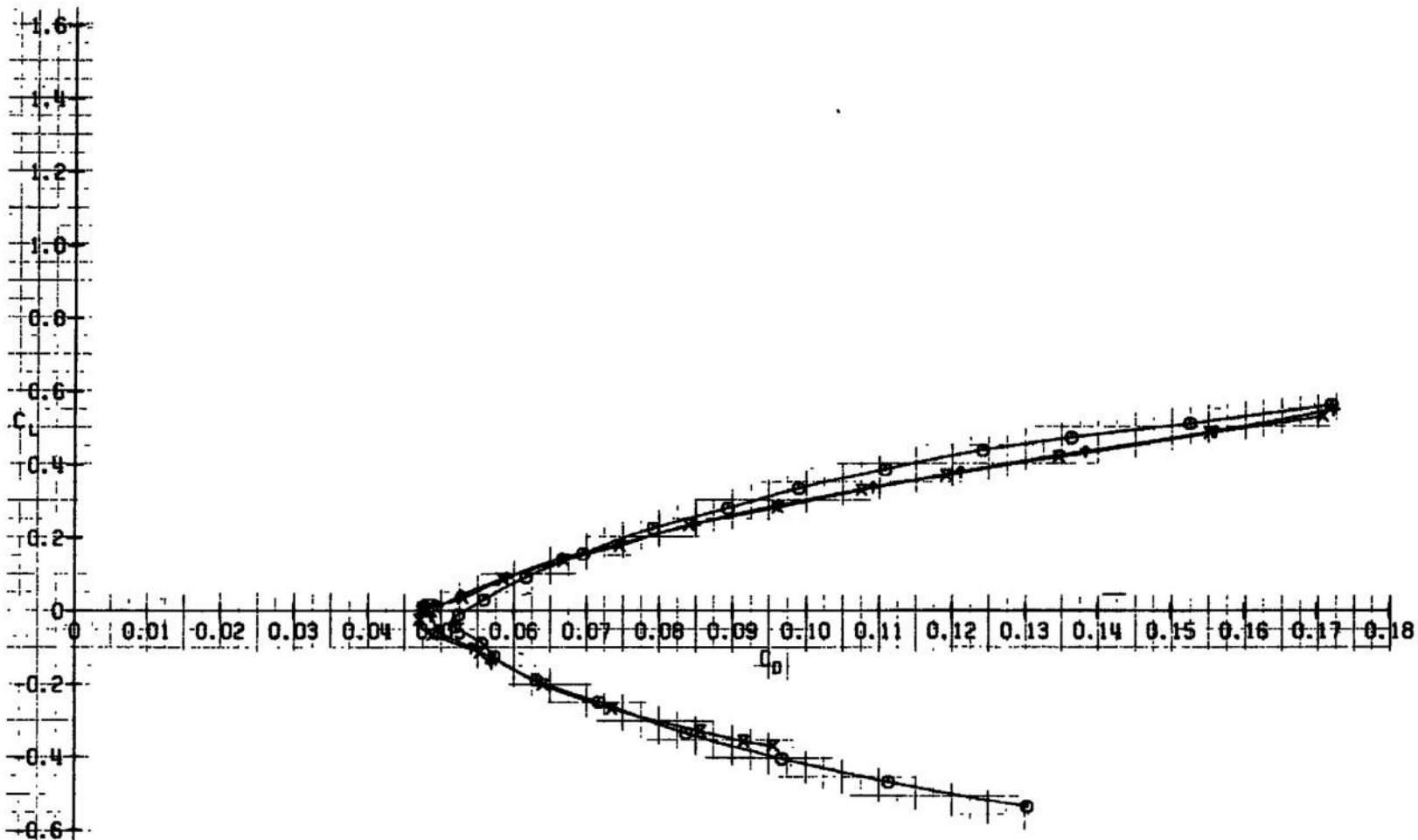


d. Concluded
Fig. 5 Continued



e. $M_\infty = 0.80$
Fig. 5 Continued

CONFIGURATION: $M_\infty = 4.5, \alpha = 0^\circ, \beta = 0^\circ$		M_∞	Re	SERIAL	AM	AF	AB	AC	AB	PW
SYM.		0.00	4.5	0	0	0	0	0	0	437
+ D ₂ S ₁ S ₂		0.00	4.5	0	0	0	0	0	0	377
X D ₂ S ₁ S ₂ V ₂ D ₂ V ₃		0.00	4.5	0	-2	0	0	0	0	358



e. Concluded
Fig. 5 Concluded

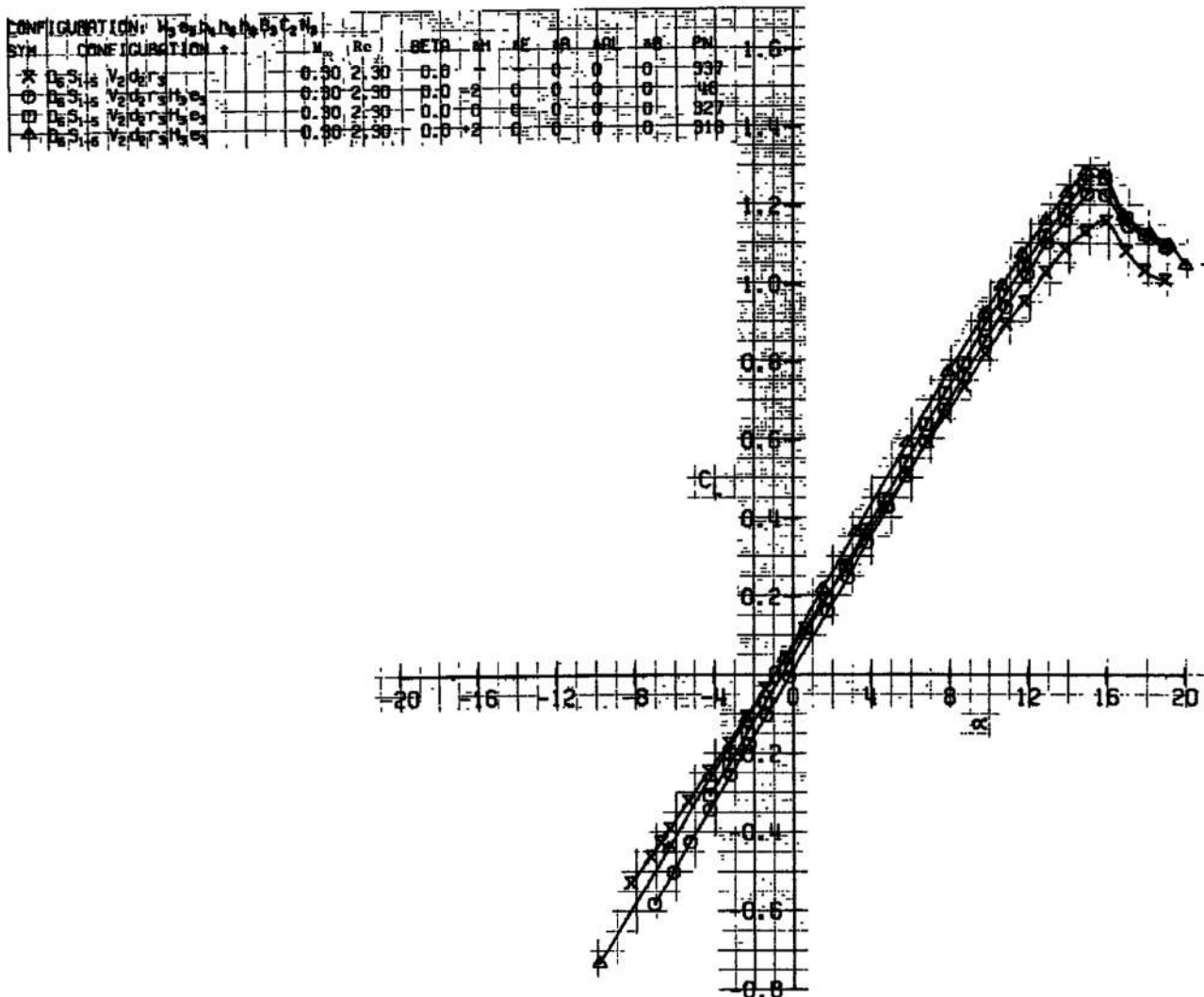
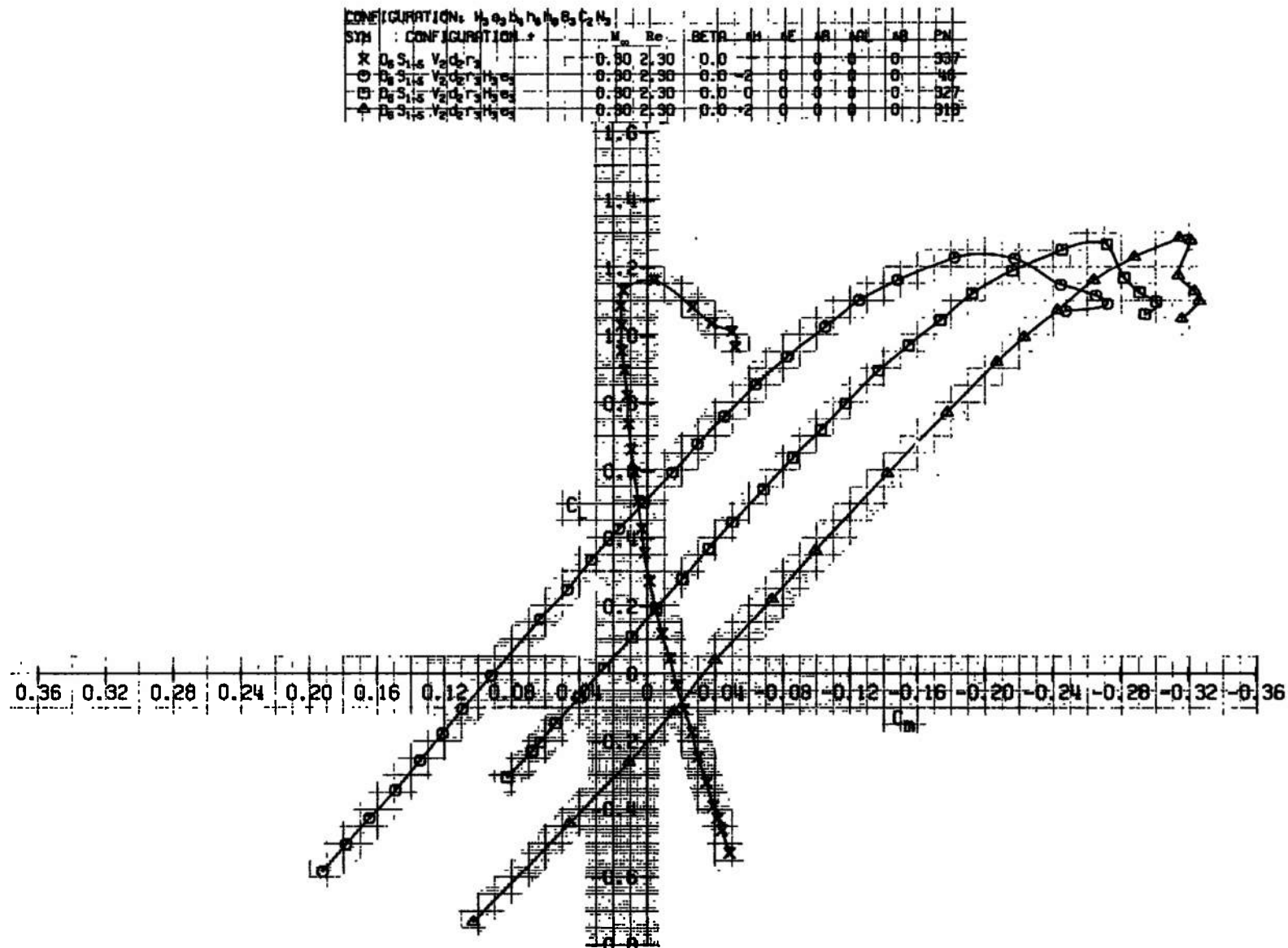
a. $M_\infty = 0.30$

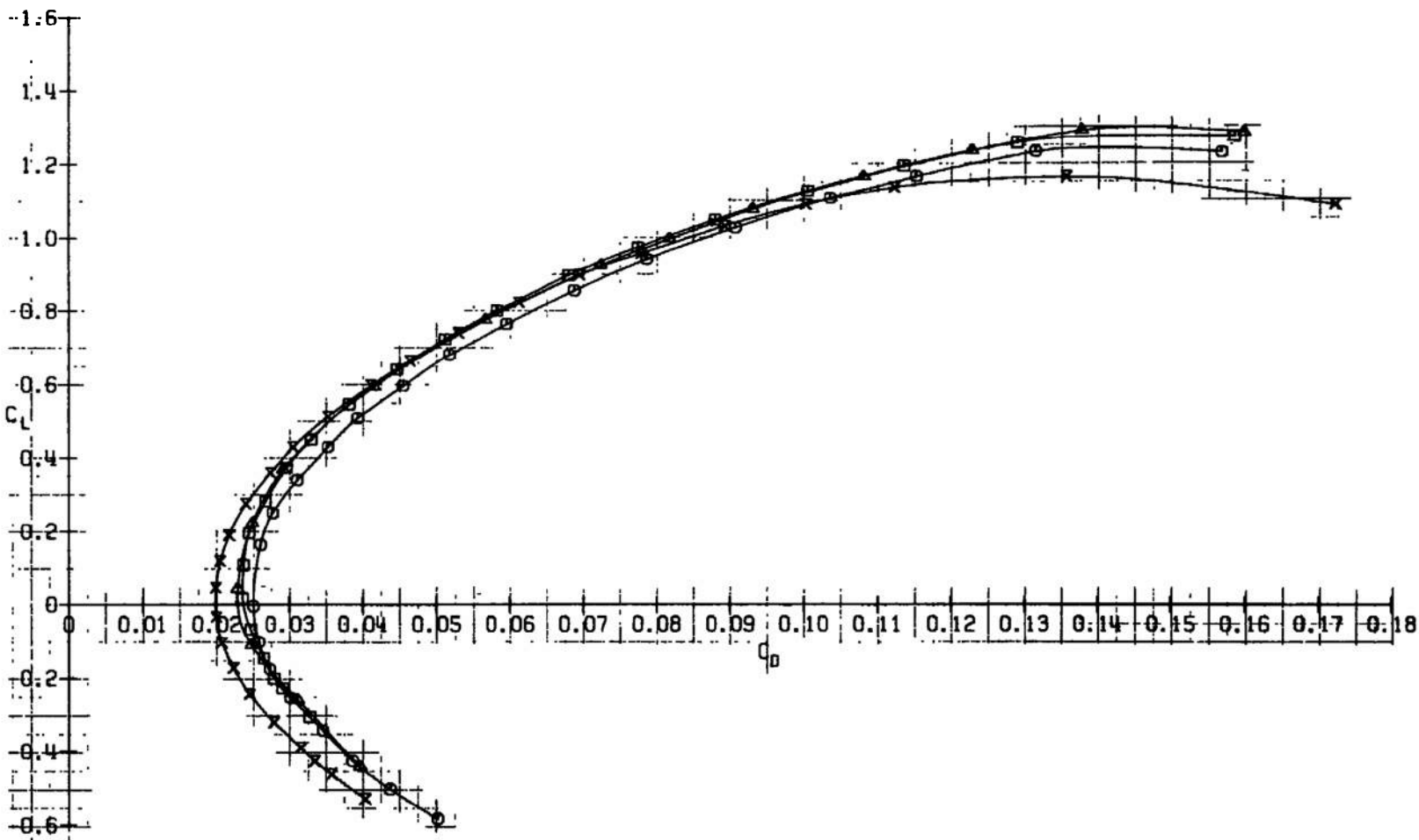
Fig. 6 Stabilizer Effectiveness



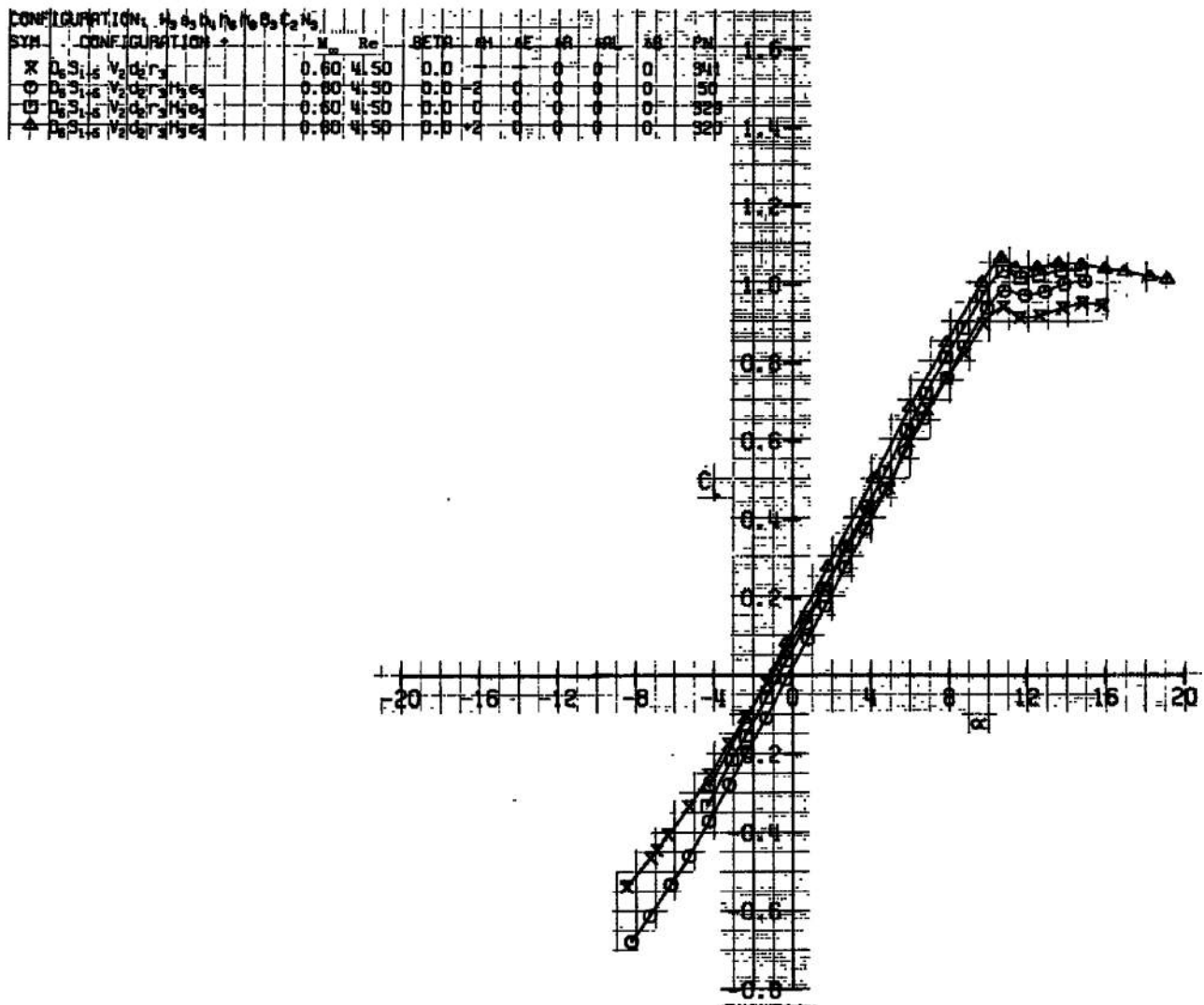
a. Continued
Fig. 6 Continued

CONFIGURATION: $W_3 B_3 B_4 H_5 H_6 B_3 C_2 N_3$

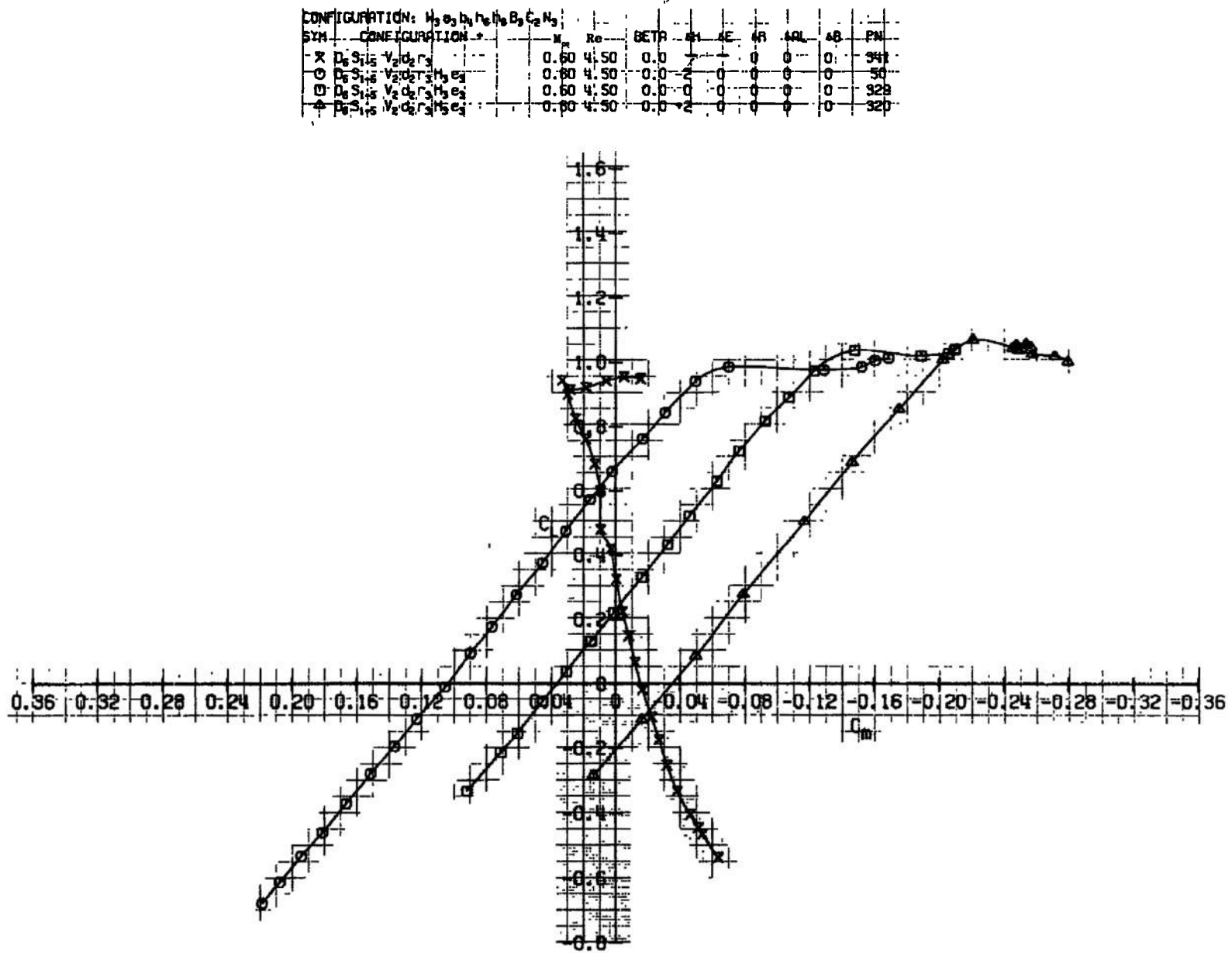
SYM	CONFIGURATION	M_∞	Re	BETB	OH	SE	SR	WL	AB	PN
X	$D_6 S_{1-s} V_2 d_2 r_3$	0.30	2.30	0.0	+	0	0	0	-	337
O	$D_6 S_{1-s} V_2 d_2 r_3 H_3 e_3$	0.30	2.30	0.0	-2	0	0	0	-	46
□	$D_6 S_{1-s} V_2 d_2 r_3 H_3 e_3$	0.30	2.30	0.0	0	0	0	0	-	327
△	$D_6 S_{1-s} V_2 d_2 r_3 H_3 e_3$	0.30	2.30	0.0	*2	0	0	0	-	318



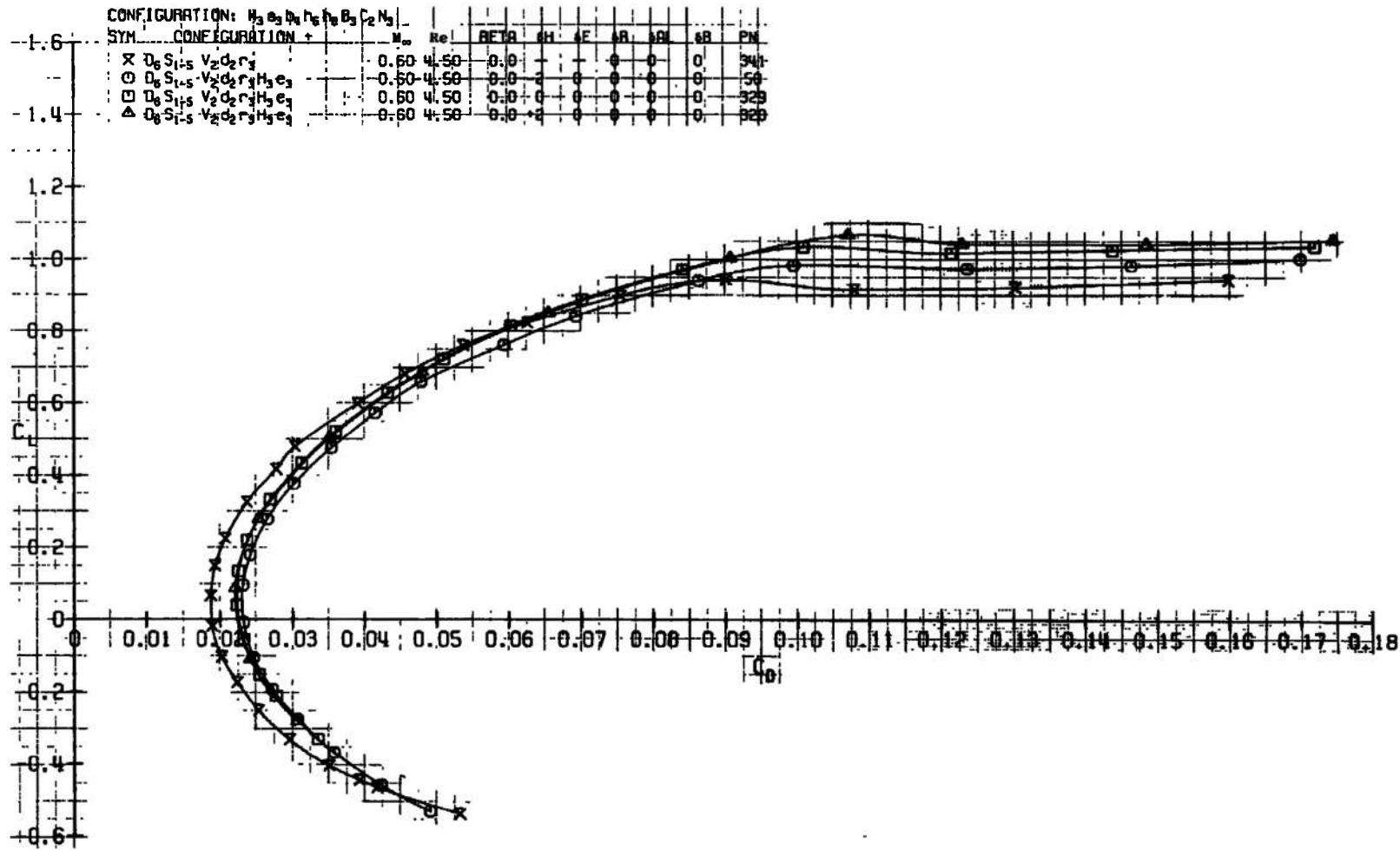
a. Concluded
Fig. 6 Continued



b. $M_\infty = 0.60$
Fig. 6 Continued

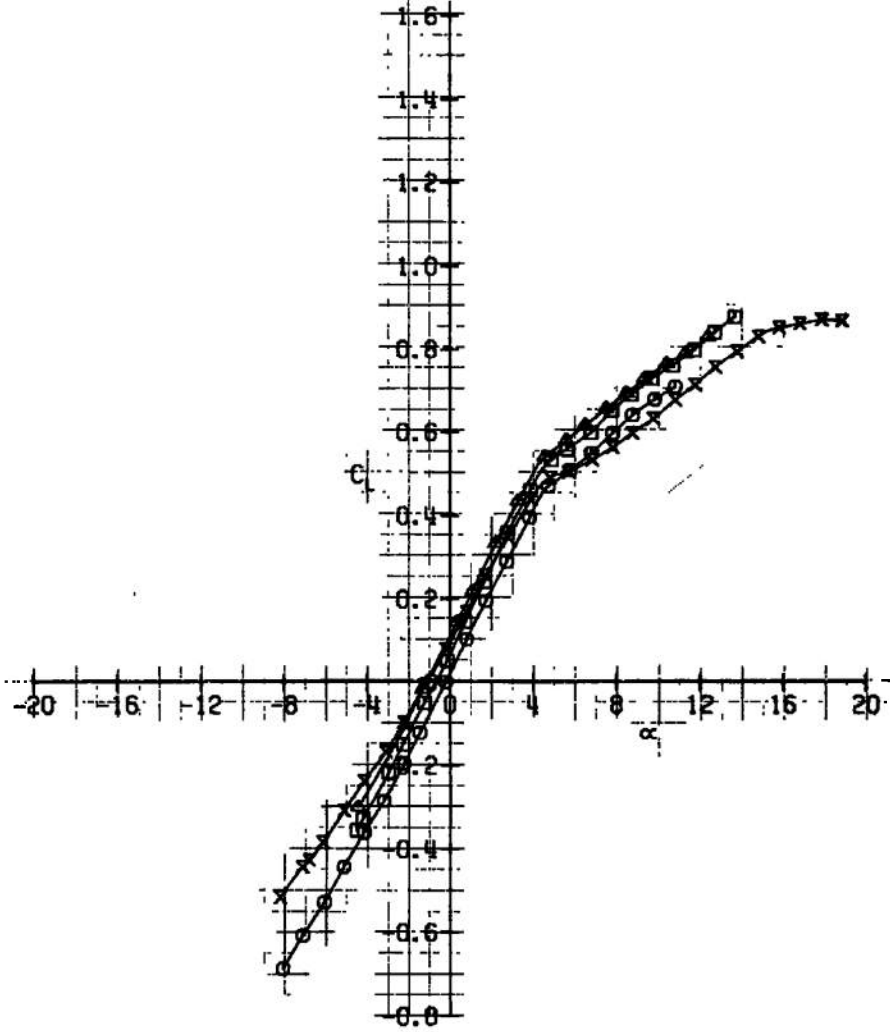


b. Continued
Fig. 6 Continued



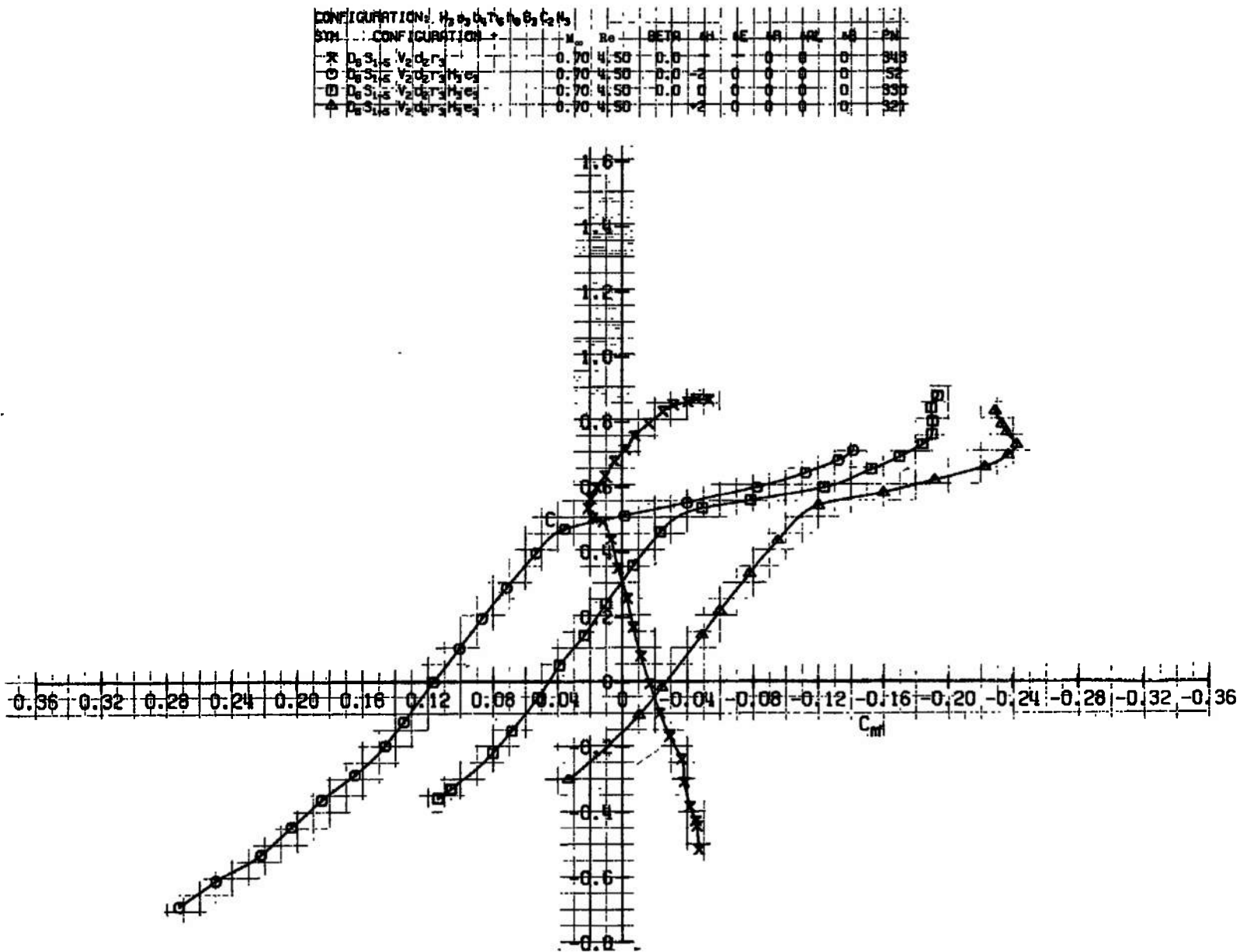
b. Concluded
Fig. 6 Continued

CONFIGURATION: $H_3e_3b_4h_6B_3C_2N_3$		M_∞	Re	BETA	SH	AE	AB	ABL	AB	PN
SYM										
CONFIGURATION										
$\times D_6S_{1/2} V_2d_2r_3$		0.70	4.50	0.0	-1	0	0	0	0	945
$\ominus D_6S_{1/2} V_2d_2r_3H_3e_3$		0.70	4.50	0.0	-2	0	0	0	0	52
$\square D_6S_{1/2} V_2d_2r_3H_3e_3$		0.70	4.50	0.0	0	0	0	0	0	930
$\Delta D_6S_{1/2} V_2d_2r_3H_3e_3$		0.70	4.50	-2	0	0	0	0	0	321



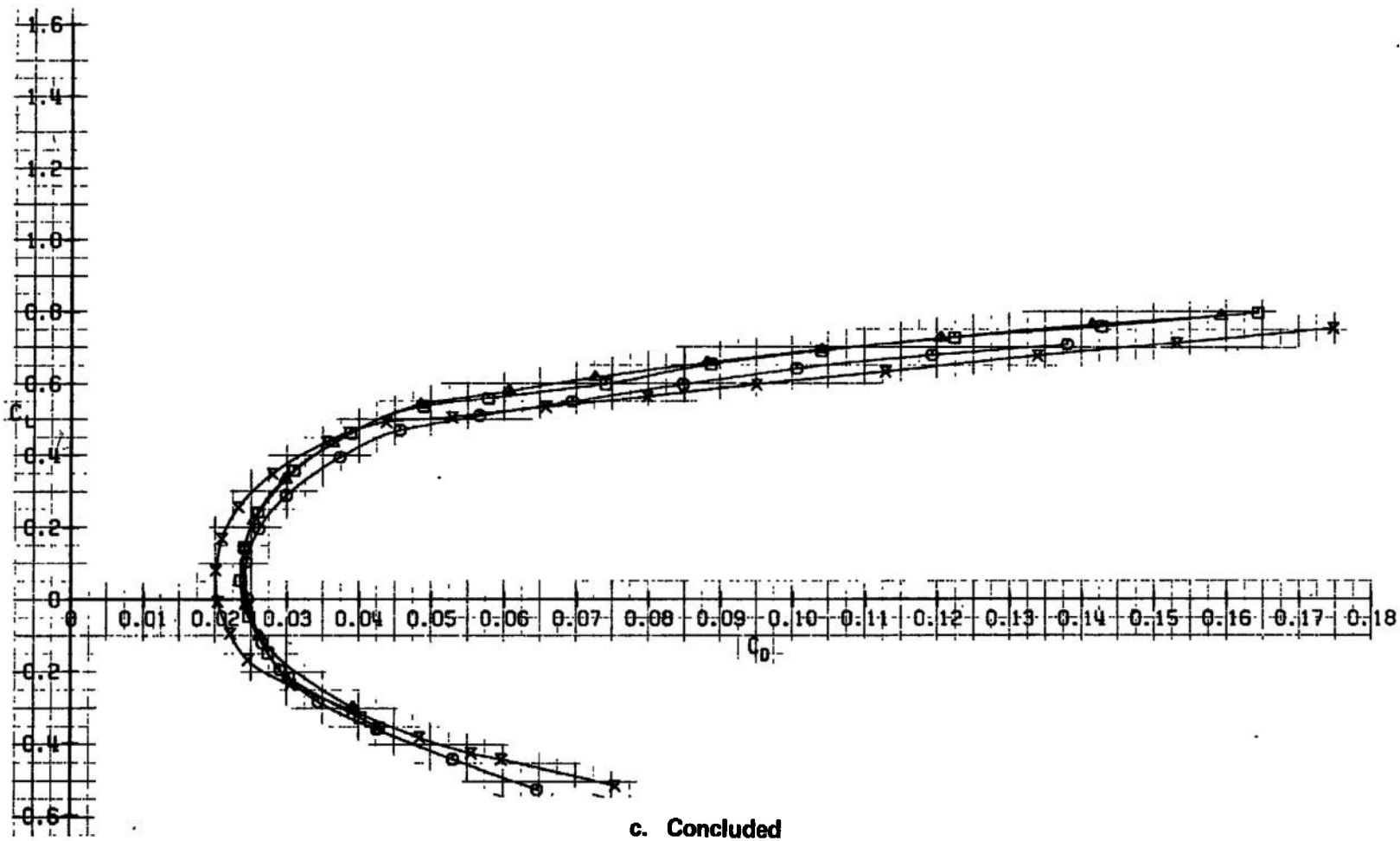
c. $M_\infty = 0.70$

Fig. 6 Continued



c. Continued
Fig. 6 Continued

CONFIGURATION: H ₂ B ₂ N ₂ H ₂ B ₃ C ₂ N ₃		M _∞	Re	BETR	CH	CF	IR	IBL	EB	PN
X	D ₁ S _{1.5} V ₂ d ₂ r ₃	0.70	4.50	0.0	+	0	0	0	0	343
O	D ₁ S _{1.5} V ₂ d ₂ r ₃ H ₂ C ₃	0.70	4.50	-0.0	2	0	0	0	0	52
□	D ₁ S _{1.5} V ₂ d ₂ r ₃ H ₂ C ₃	0.70	4.50	0.0	0	0	0	0	0	330
▲	D ₁ S _{1.5} V ₂ d ₂ r ₃ H ₂ C ₃	0.70	4.50	0.0	2	0	0	0	0	321



c. Concluded
Fig. 6 Continued

CONFIGURATION: $W_3 B_3 b_4 h_6 H_3 C_2 N_3$		M _∞	Re	BETA	AH	AE	SR	AL	AB	PN
SYM. CONFIGURATION +										
X	D ₆ S ₁₋₅ V ₂ d ₂ r ₃	0.75	4.50	0.0	-	-	0	0	0	345
O	B ₆ S ₁₋₅ V ₂ d ₂ r ₃ H ₃ e ₃	0.75	4.50	0.0	-2	0	0	0	0	54
□	D ₆ S ₁₋₅ V ₂ d ₂ r ₃ H ₃ e ₃	0.75	4.50	0.0	0	0	0	0	0	931
▲	D ₆ S ₁₋₅ V ₂ d ₂ r ₃ H ₃ e ₃	0.75	4.50	0.0	+2	0	0	0	0	922

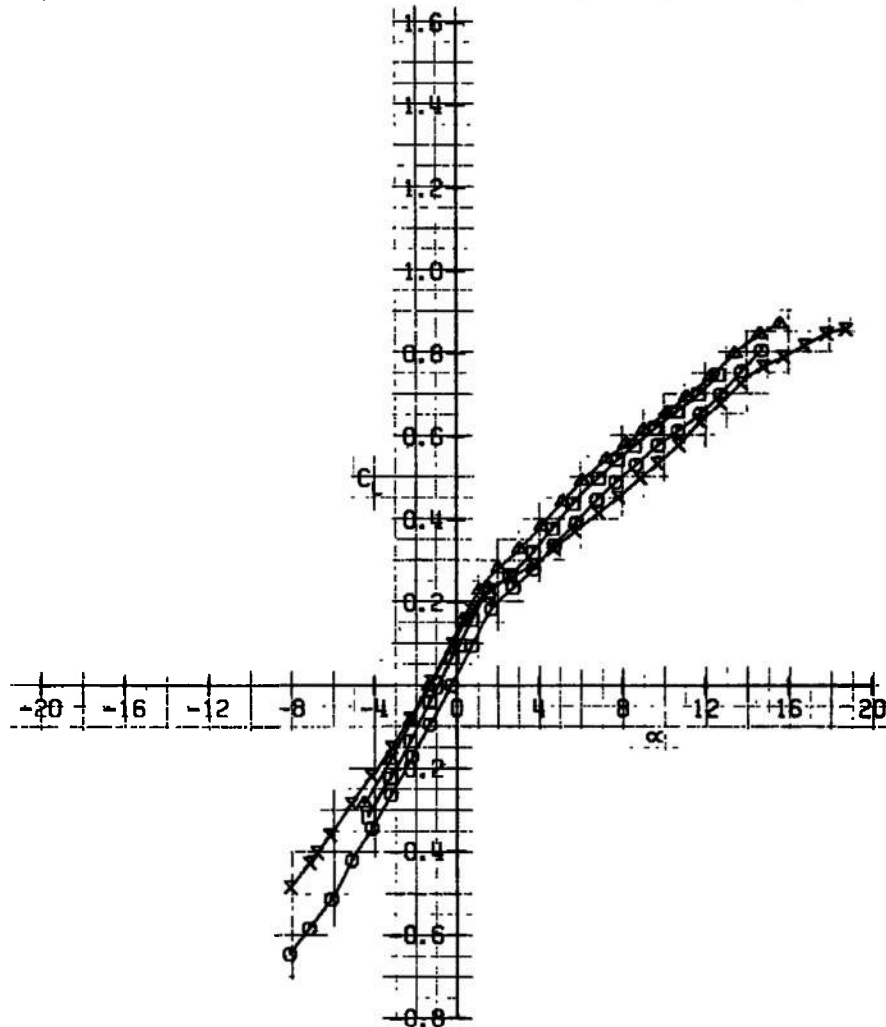
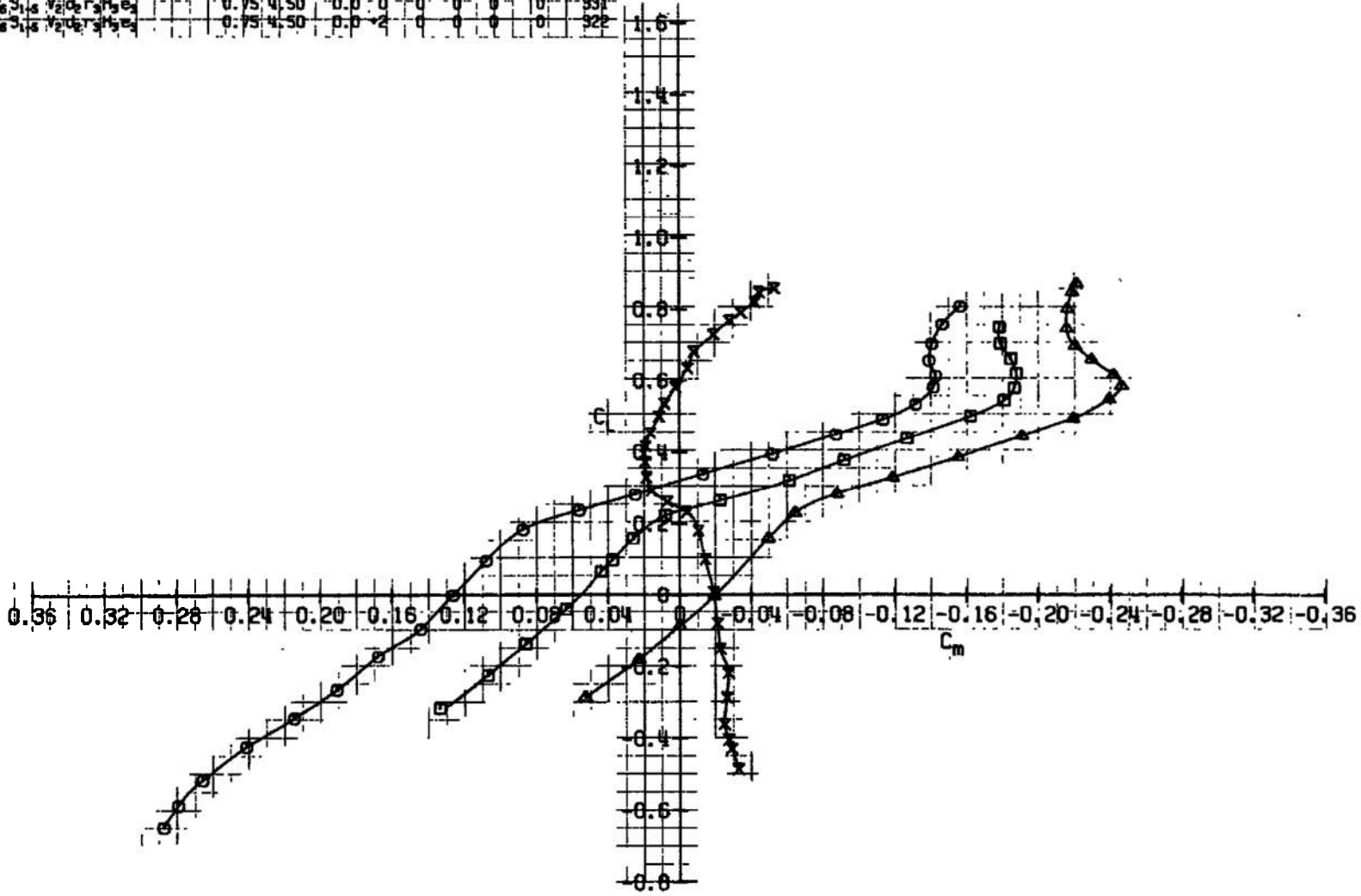
d. $M_\infty = 0.75$

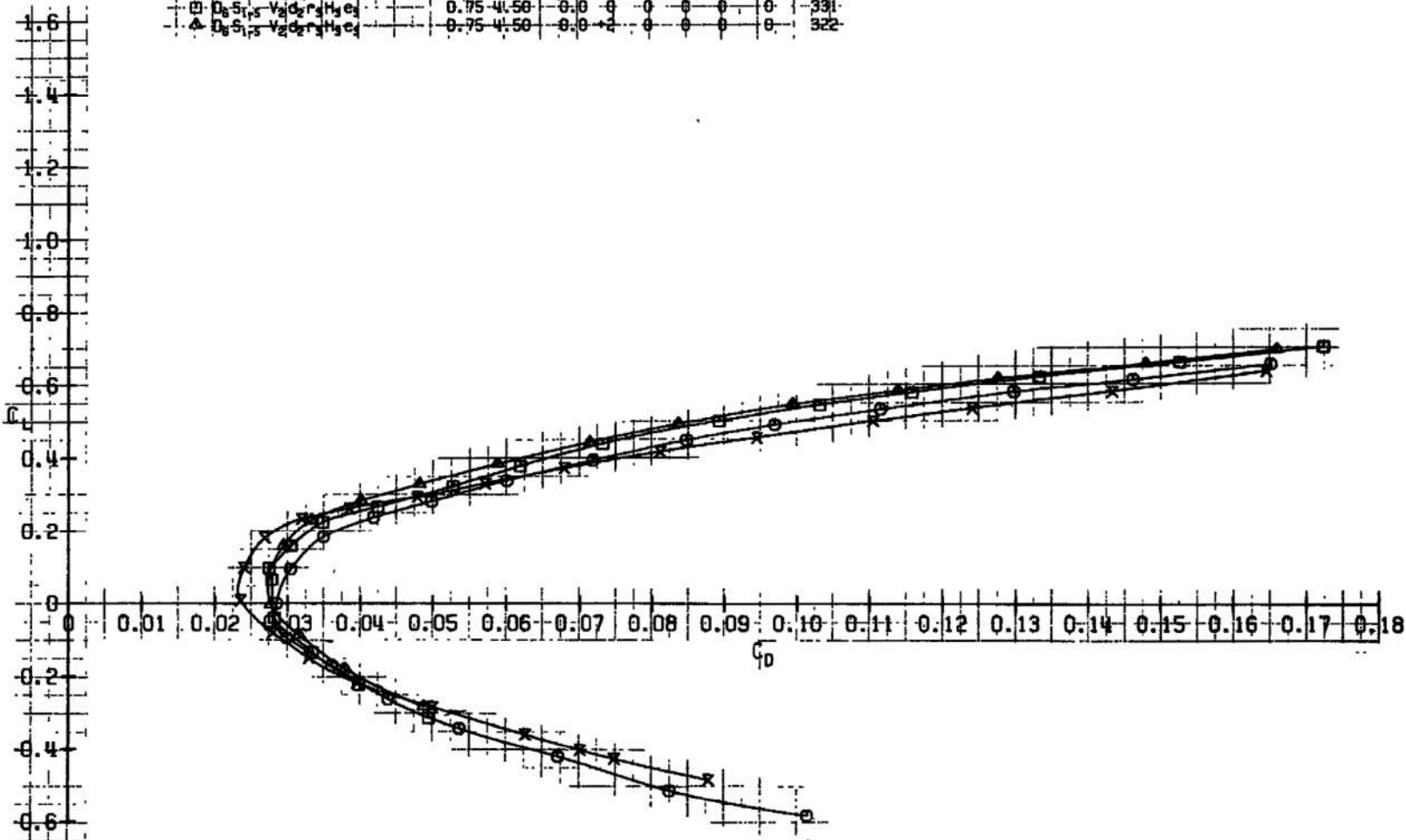
Fig. 6 Continued

CONFIGURATION: $H_3S_3O_4H_6B_3C_2N_3$		M_∞	Re	BETA	δA	δC	δH	δM	ΔB	PM
X	$D_6S_1S_5V_2d_2r_3$	0.75	4.50	0.0	0	0	0	0	0	945
O	$D_6S_1S_5V_2d_2r_3h_2e_3$	0.75	4.50	0.0	-2	0	0	0	0	59
□	$D_6S_1S_5V_2d_2r_3h_2e_4$	0.75	4.50	0.0	0	0	0	0	0	531
▲	$D_6S_1S_5V_2d_2r_3h_2e_5$	0.75	4.50	0.0	-2	0	0	0	0	922

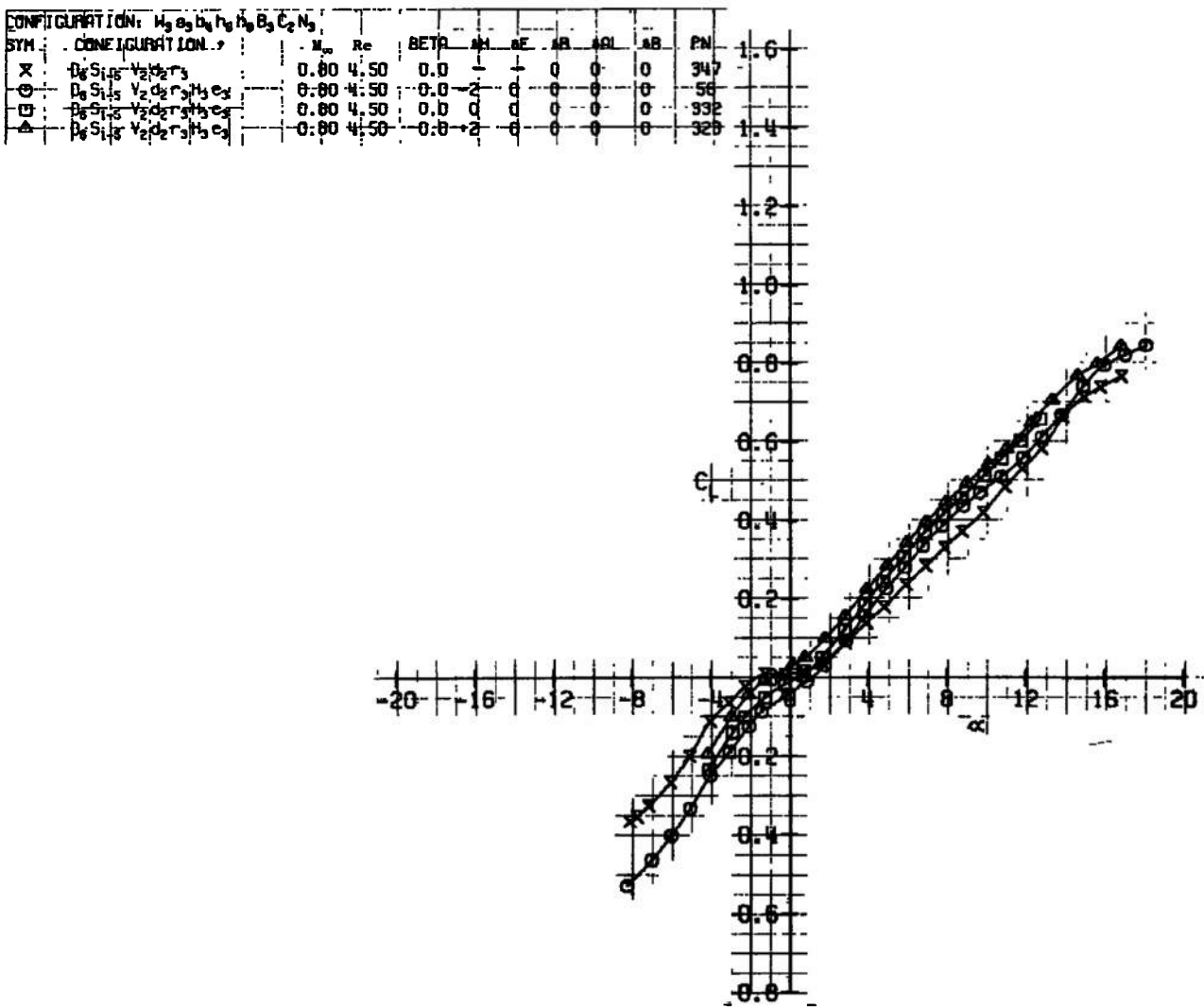


d. Continued
Fig. 6 Continued

CONFIGURATION $H_3S_1S_0^+N_2^+B_3C_2N_3^-$		M ₀	Re	BETB	SH	AF	AR	AB	PN
X	D ₆ S _{1,5} V ₂ O ₂ P ₃	-0.75	4.50	-0.0	-0	0	0	0	345
○	D ₆ S _{1,5} V ₂ O ₂ P ₃ H ₃ C ₃	0.75	4.50	0.0	-2	0	0	0	54
□	D ₆ S _{1,5} V ₂ O ₂ P ₃ H ₃ C ₃	0.75	41.50	-0.0	0	0	0	0	331
△	D ₆ S _{1,5} V ₂ O ₂ P ₃ H ₃ C ₄	0.75	41.50	0.0	-4	0	0	0	322

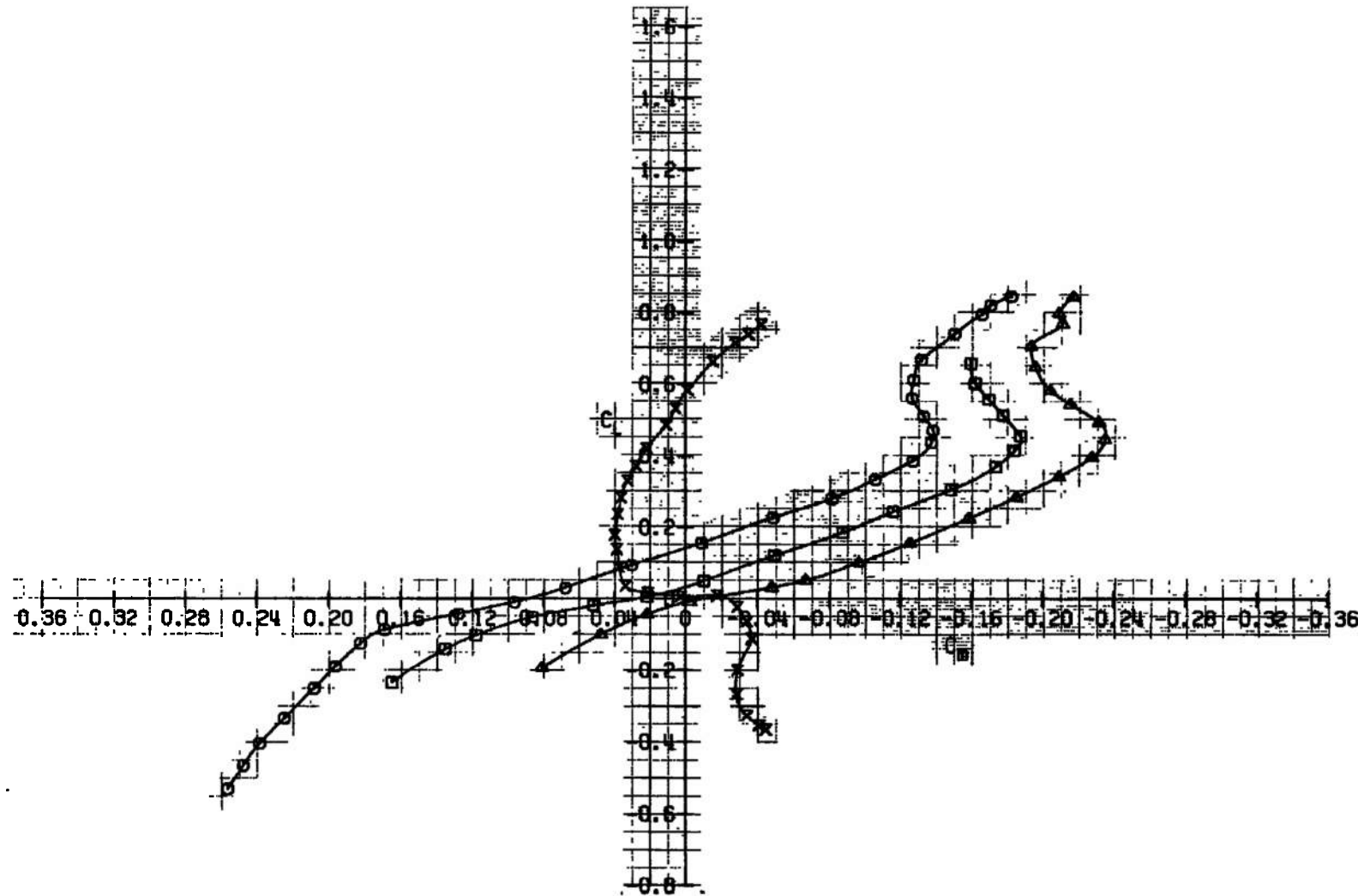


d. Concluded
Fig. 6 Continued



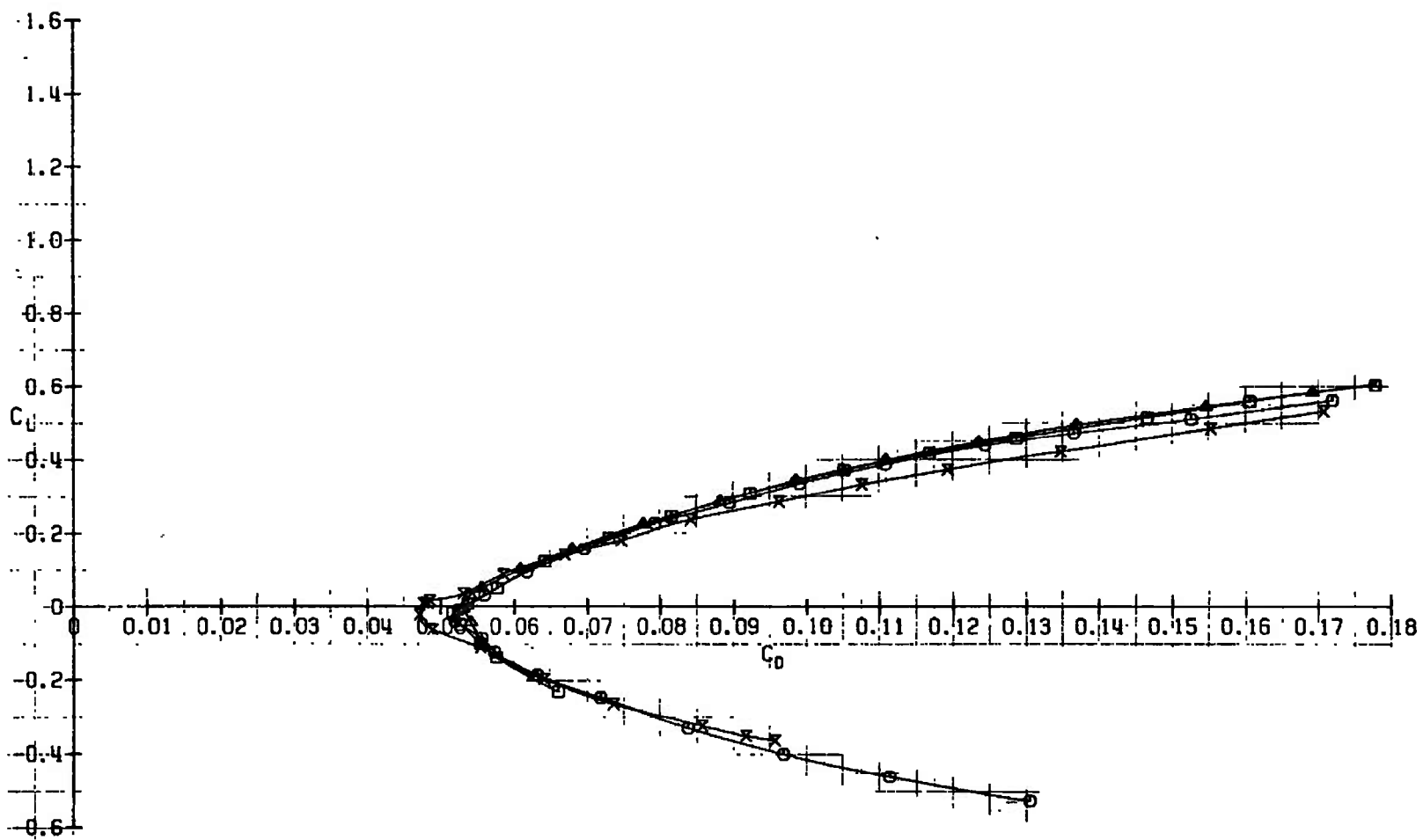
e. $M_\infty = 0.80$
Fig. 6 Continued

CONFIGURATION: $M_3 e_3 b_4 h_5 B_3 C_2 N_3$		SYM.	CONFIGURATION	M_∞	Re	BETA	PH	PF	PA	AL	AB	PN
						0.0	0	0	0	0	0	
X	$D_3 S_{1-5} V_2 d_2 r_3$			0.80	4.50	0.0	0	0	0	0	0	347
O	$D_3 S_{1-5} V_2 d_2 r_3 H_3 e_3$			0.80	4.50	0.0	-2	0	0	0	0	56
S	$D_3 S_{1-5} V_2 d_2 r_3 H_3 e_3$			0.80	4.50	0.0	0	0	0	0	0	932
A	$D_3 S_{1-5} V_2 d_2 r_3 H_3 e_3$			0.80	4.50	0.0	2	0	0	0	0	329



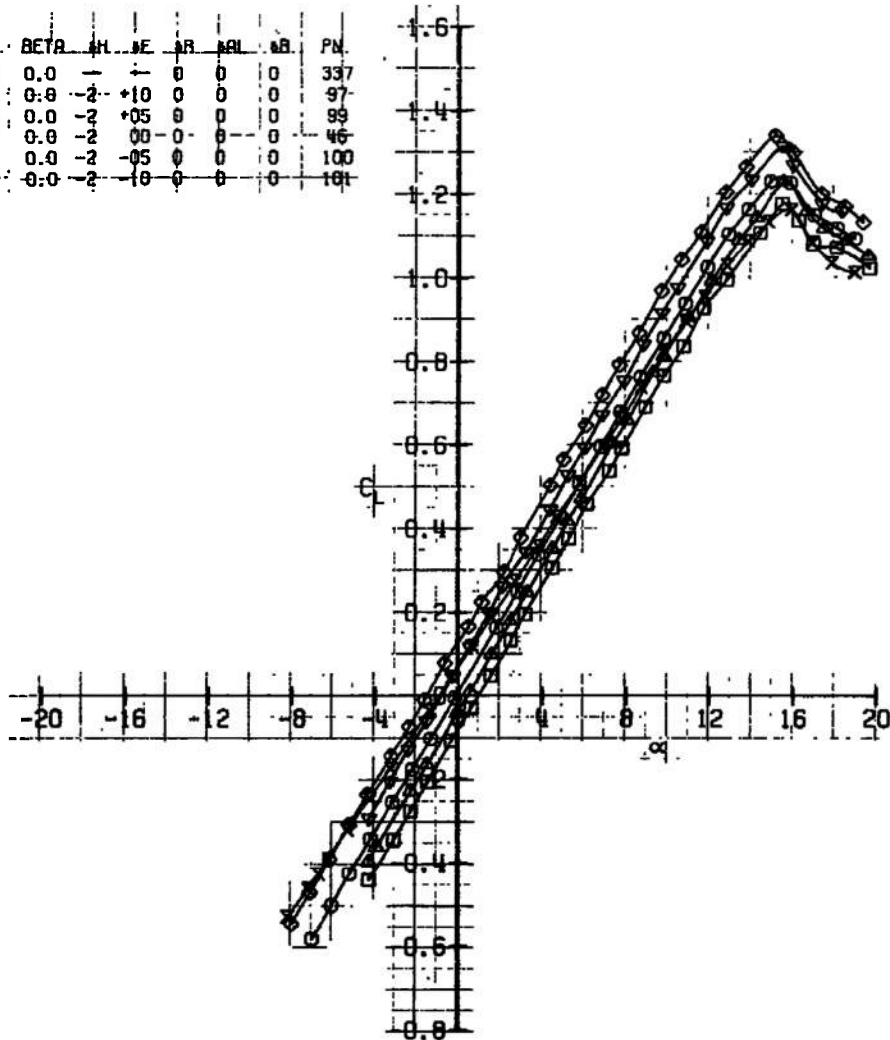
e. Continued
Fig. 6 Continued

CONFIGURATION: $W_3 S_3 B_4 h_6 h_8 B_3 C_2 N_3$		M_∞	Re	BETR	CH	AF	SR	SP	SB	PN
X	$D_6 S_{1-6} V_2 d_2 r_3$	0.80	4.50	0.0	+	0	0	0	0	347
O	$I_{3-1-3} V_2 d_2 r_3 H_3 e_3$	0.80	4.50	0.0	-2	0	0	0	0	56
\square	$I_3 S_{1-5} V_2 d_2 r_3 H_3 e_3$	0.80	4.50	0.0	0	0	0	0	0	332
Δ	$I_3 S_{1-5} V_2 d_2 r_3 H_3 e_3$	0.80	4.50	0.0	-2	0	0	0	0	323



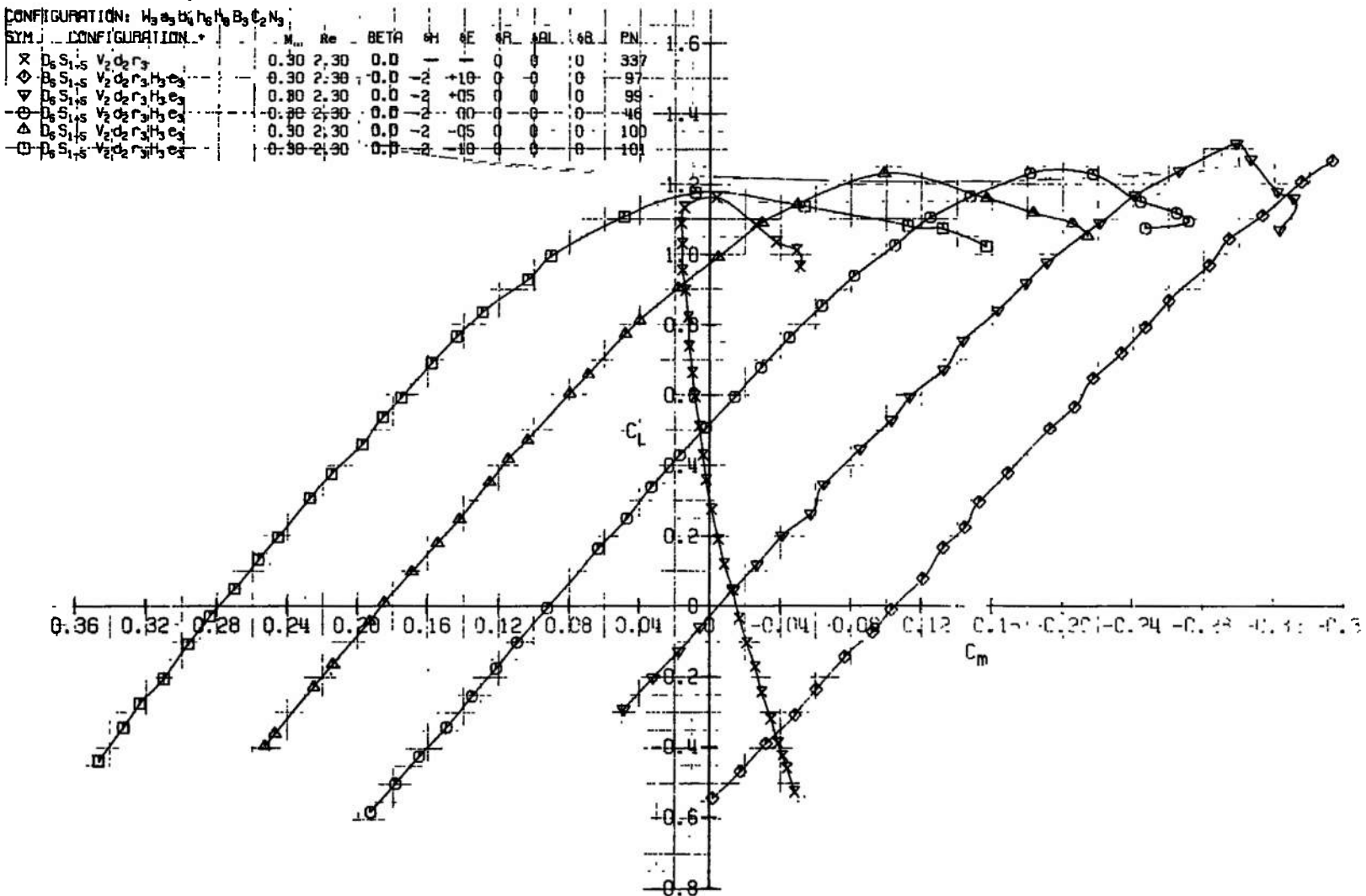
e. Concluded
Fig. 6 Concluded

CONFIGURATION: $M_2 e_3 b_3 h_6 l_6 B_3 C_2 N_3$									
SYM	CONFIGURATION	M_∞	Re	BETA	H	LE	LR	RL	PW
X	$D_6 S_{1-5} V_2 d_2 r_3$	0.30	2.30	0.0	-1	-1	0	0	337
◊	$D_6 S_{1-5} V_2 d_2 r_3 H_3 e_3$	0.30	2.30	0.0	-2	+10	0	0	97
▽	$D_6 S_{1-5} V_2 d_2 r_3 H_3 e_3$	0.30	2.30	0.0	-2	+03	0	0	99
○	$D_6 S_{1-5} V_2 d_2 r_3 H_3 e_3$	0.30	2.30	0.0	-2	00	0	0	96
△	$D_6 S_{1-5} V_2 d_2 r_3 H_3 e_3$	0.30	2.30	0.0	-2	-05	0	0	100
□	$D_6 S_{1-5} V_2 d_2 r_3 H_3 e_3$	0.30	2.30	0.0	-2	-10	0	0	101

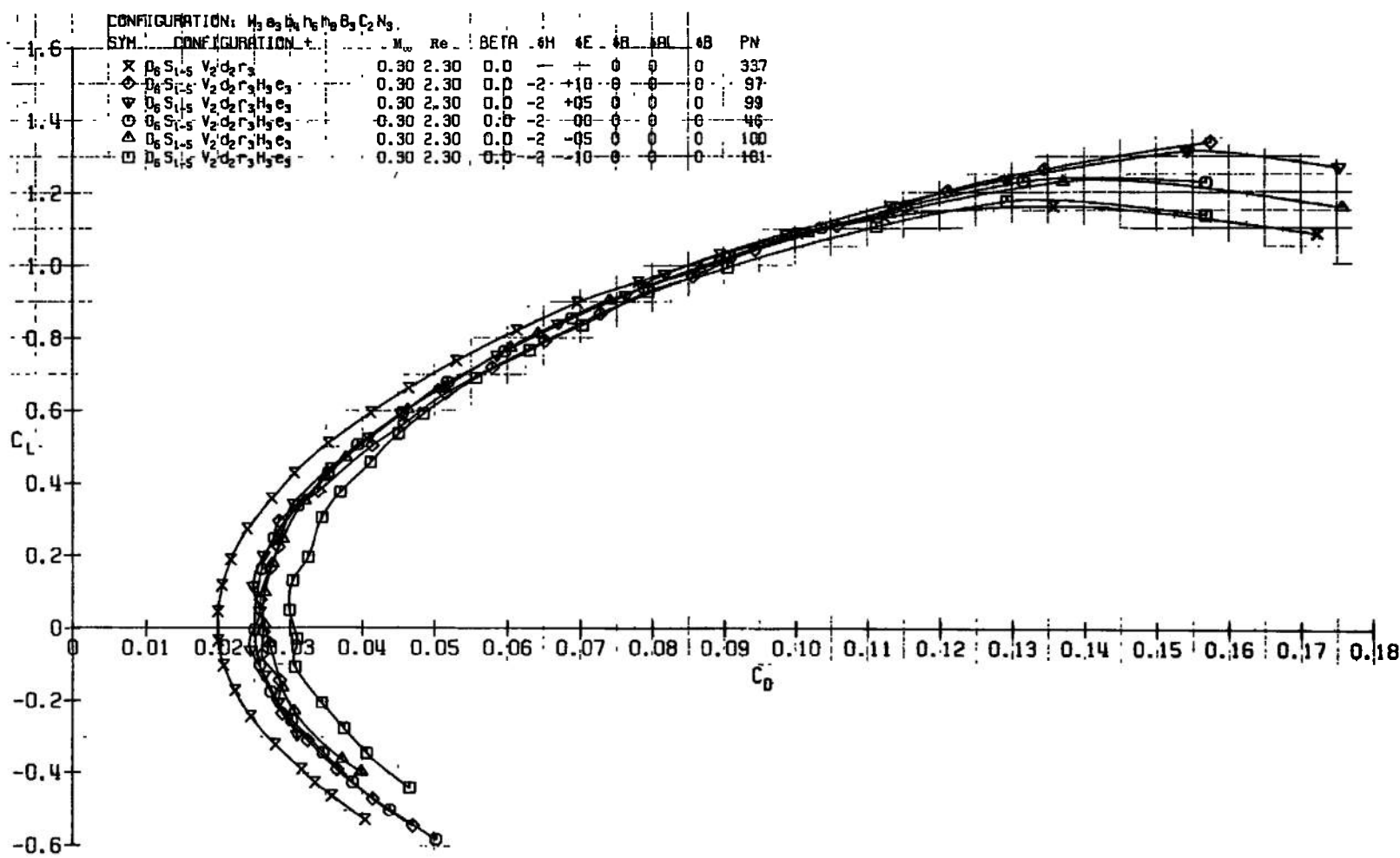


a. $M_\infty = 0.30$

Fig. 7 Elevator Effectiveness

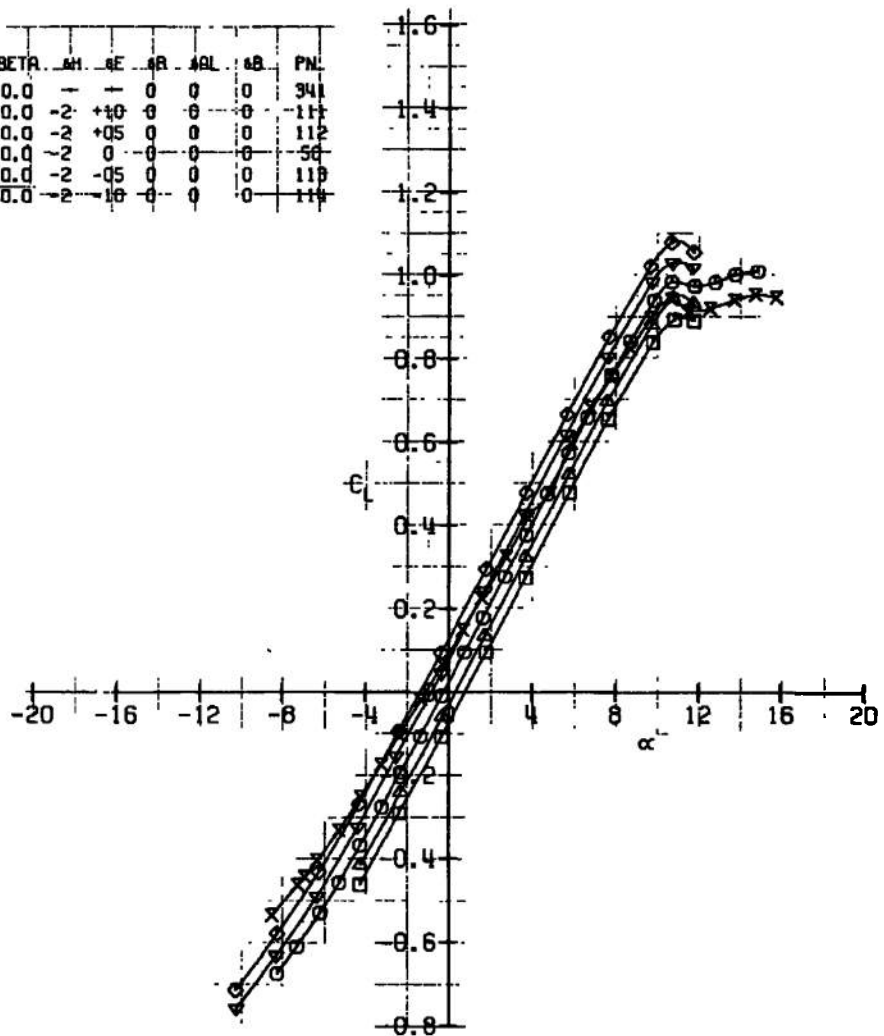


a. Continued
Fig. 7 Continued



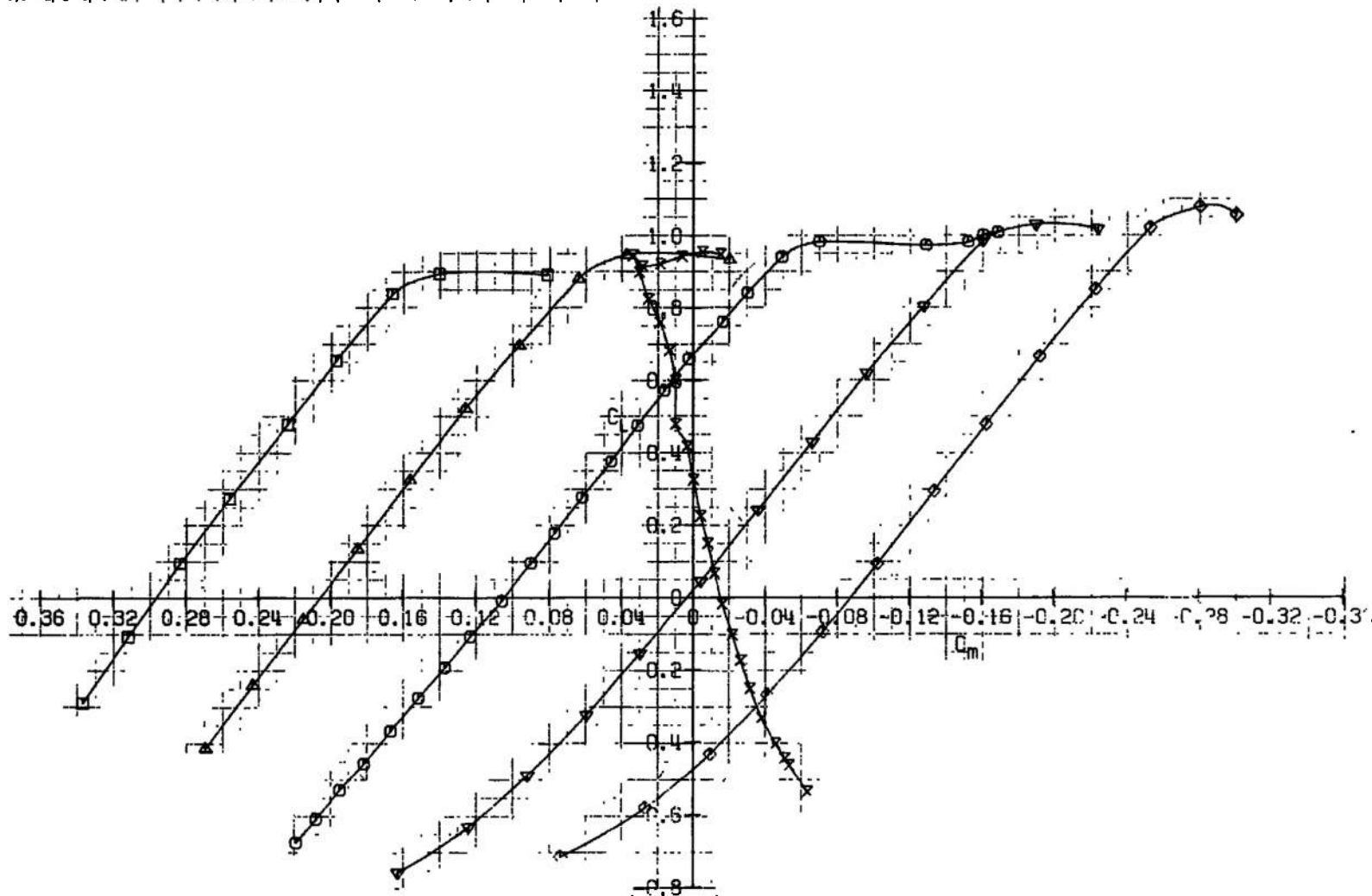
a. Concluded
Fig. 7 Continued

CONFIGURATION: $H_3O_3D_3H_6B_3C_2N_3$		M _a	Re.	BETA	AH	AE	AR	AL	AB	PM
X	D ₆ S ₁₋₅ V ₂ d ₂ r ₃	0.60	4.50	0.0	-	-	0	0	0	341
◊	D ₆ S ₁₋₅ V ₂ d ₂ r ₃ H ₃ e ₃	0.60	4.50	0.0	-2	+10	0	0	0	111
▽	D ₆ S ₁₋₅ V ₂ d ₂ r ₃ H ₃ e ₃	0.60	4.50	0.0	-2	+05	0	0	0	112
○	D ₆ S ₁₋₅ V ₂ d ₂ r ₃ H ₃ e ₃	0.60	4.50	0.0	-2	0	-0	0	0	56
△	D ₆ S ₁₋₅ V ₂ d ₂ r ₃ H ₃ e ₃	0.60	4.50	0.0	-2	-05	0	0	0	113
□	D ₆ S ₁₋₅ V ₂ d ₂ r ₃ H ₃ e ₃	0.60	4.50	0.0	-2	-10	0	0	0	114



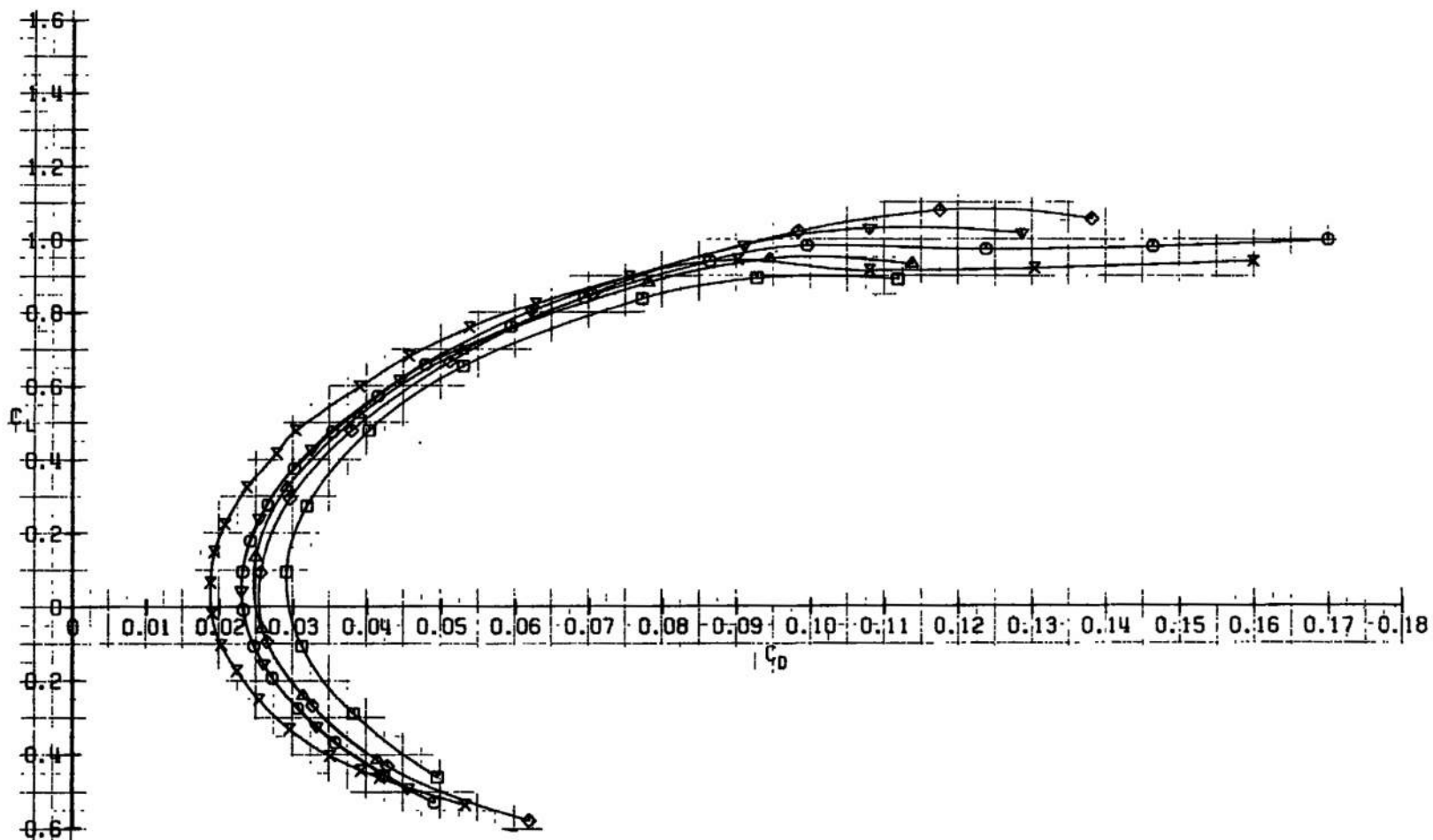
b. $M_a = 0.60$
Fig. 7 Continued

CONFIGURATION: $H_2S_4B_4H_6B_3C_2N_3$		M_∞	Re	βT_0	α	δE	δR	δL	δR	PN
X	$D_6S_{1,6}V_2d_2r_3$	0.60	4.50	0.0	-1	0	0	0	0	341
◊	$D_6S_{1,6}V_2d_2r_3h_2$	0.60	4.50	0.0	-2	+0	0	0	0	111
▼	$D_6S_{1,6}V_2d_2r_3h_2^2$	0.60	4.50	0.0	-3	+0.5	0	0	0	112
○	$D_6S_{1,6}V_2d_2r_3h_2^3$	0.60	4.50	0.0	-4	0	0	0	0	50
▲	$D_6S_{1,6}V_2d_2r_3h_2^4$	0.60	4.50	0.0	-5	0	0	0	0	113
□	$D_6S_{1,6}V_2d_2r_3h_2^5$	0.60	4.50	0.0	-6	0	0	0	0	114

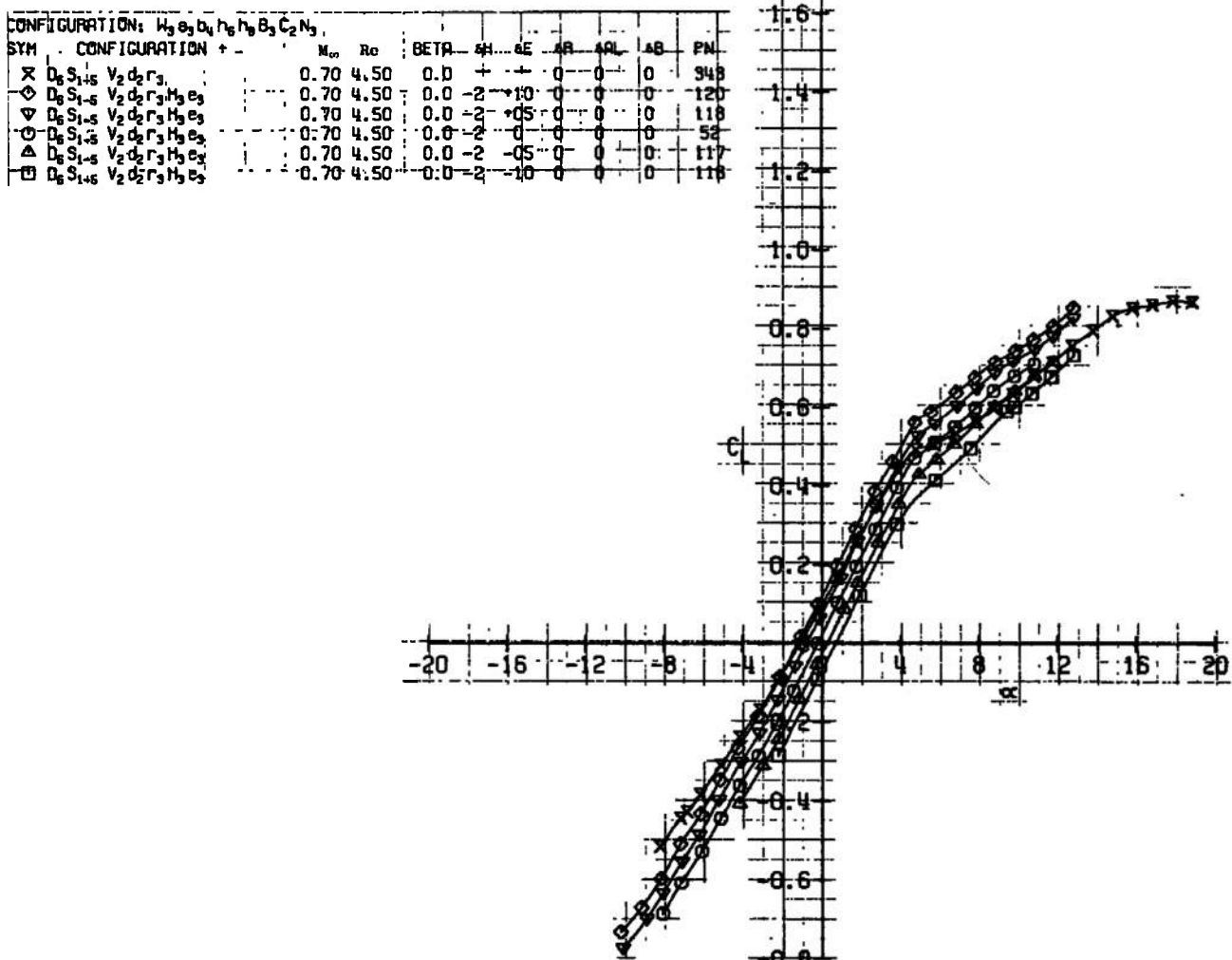


b. Continued
Fig. 7 Continued

CONFIGURATION: $H_3^+e^-h_6^+h_6^-B_3^-[C_2N_3]$		M_∞	Re	BETR	AH	AF	AR	API	6B.	PN.
SYN. 1-DONE [CURVATURE]										
X	D ₆ S ₁ s V ₂ d ₂ rg	0.60	4.50	0.0	-1	0	0	0	0	341
◊	D ₆ S ₁ s V ₂ d ₂ r ₃ H ₃ e ₃	0.60	4.50	0.0	-2	+10	0	0	0	111
▽	D ₆ S ₁ s V ₂ d ₂ r ₃ H ₃ e ₃	0.60	4.50	0.0	-3	+05	0	0	0	112
○	D ₆ S ₁ s V ₂ d ₂ r ₃ H ₃ e ₃	0.60	4.50	0.0	-2	-0	0	0	0	50
△	D ₆ S ₁ s V ₂ d ₂ r ₃ H ₃ e ₃	0.60	4.50	0.0	-2	-05	0	0	0	113
■	D ₆ S ₁ s V ₂ d ₂ r ₃ H ₃ e ₃	0.60	4.50	0.0	-2	+10	0	0	0	114

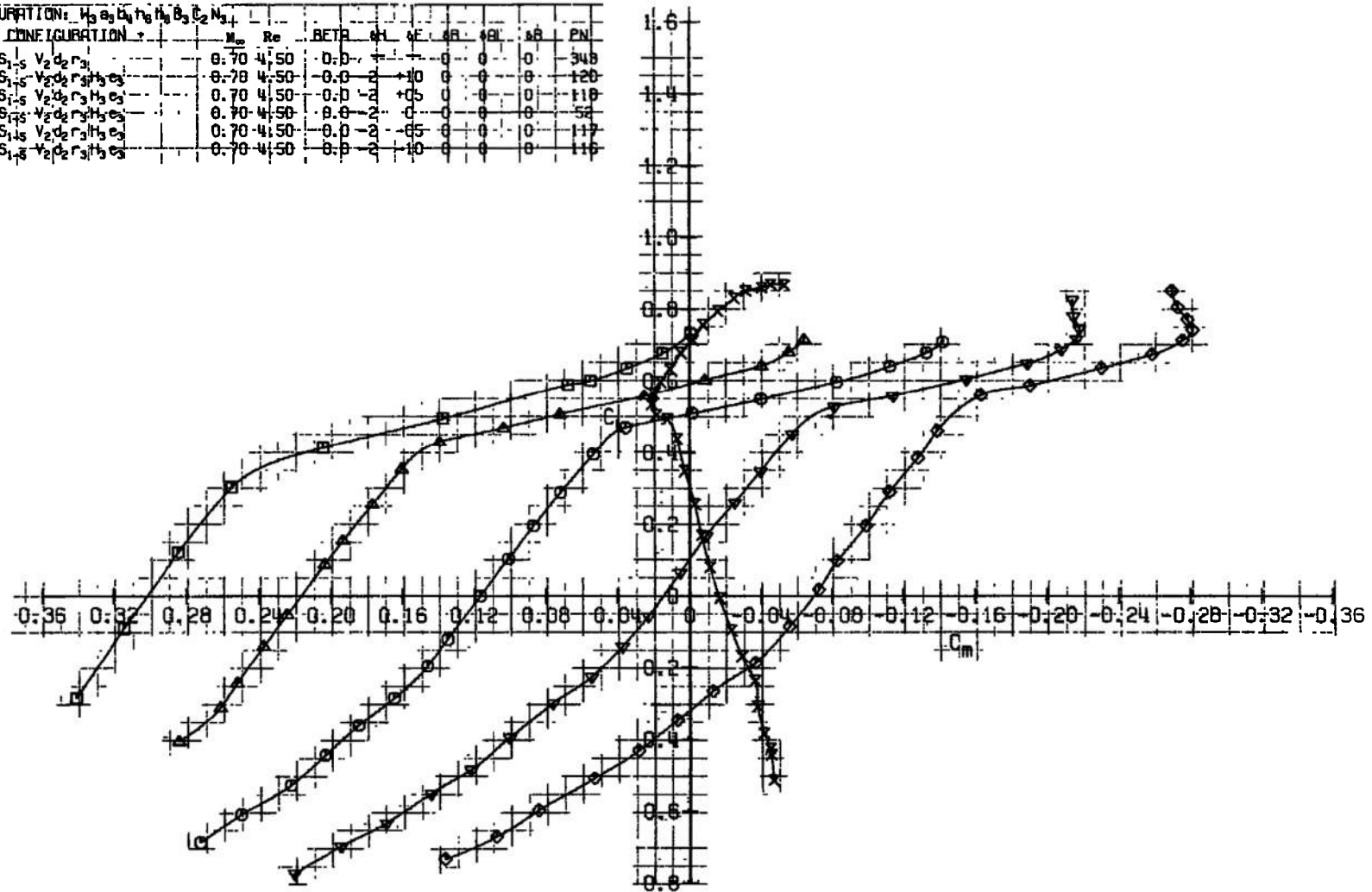


b. Concluded
Fig. 7 Continued

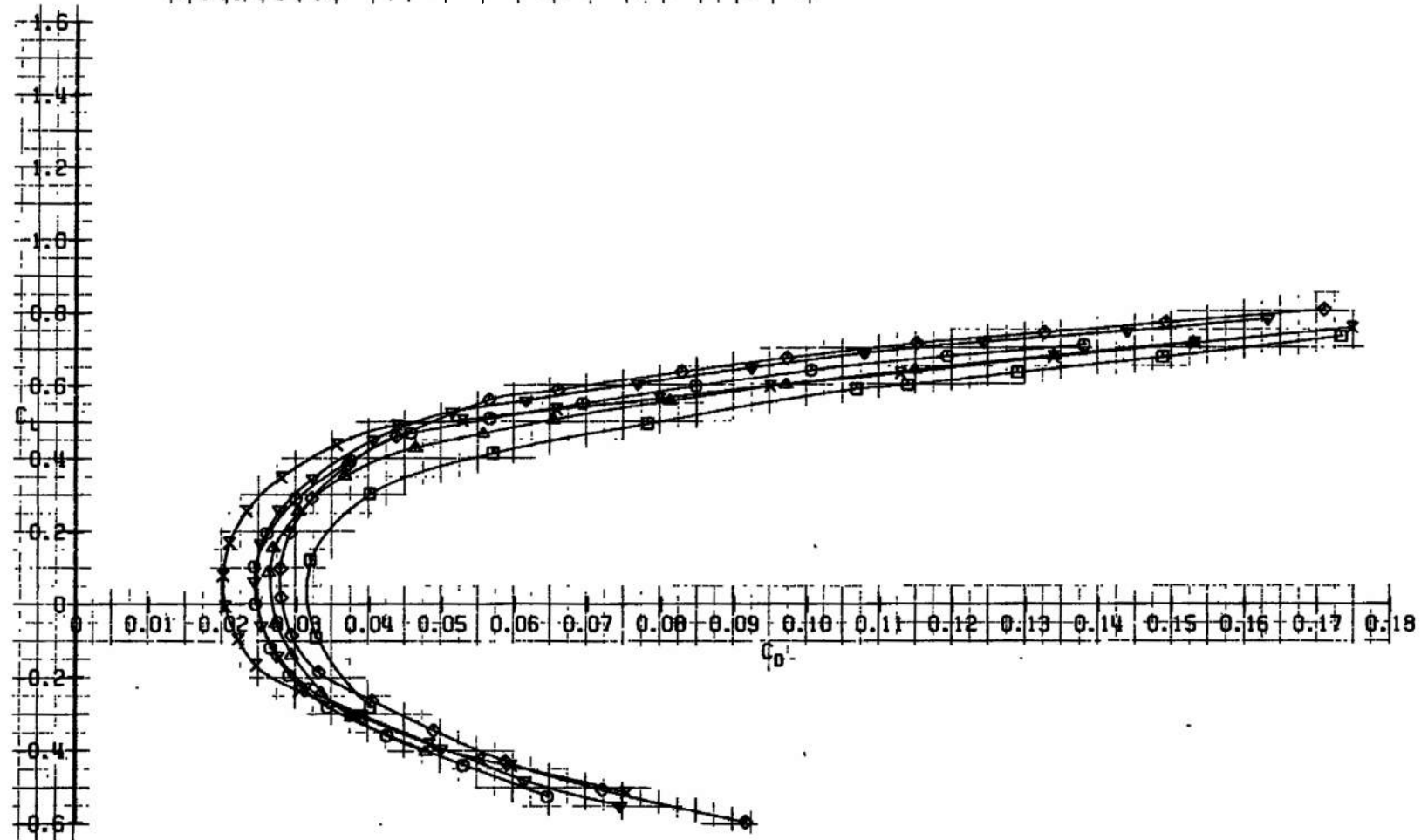


c. $M_\infty = 0.70$
Fig. 7 Continued

CONFIGURATION: H ₂ e ₃ D ₃ H ₂ H ₂ B ₃ C ₂ N ₃		M _∞	Re	BETA	AL	WF	AR	BL	AB	PN
SYM	CONFIGURATION									
X	D ₆ S ₁₋₅ V ₂ D ₂ r ₃	0.70	4.50	-0.0	+10	0	0	0	0	348
◊	D ₆ S ₁₋₅ V ₂ D ₂ r ₃ H ₃ e ₃	0.70	4.50	-0.0	+10	0	0	0	0	120
▽	D ₆ S ₁₋₅ V ₂ D ₂ r ₃ H ₃ e ₃	0.70	4.50	-0.0	+10	0	0	0	0	110
○	D ₆ S ₁₋₅ V ₂ D ₂ r ₃ H ₃ e ₃	0.70	4.50	-0.0	+10	0	0	0	0	50
△	D ₆ S ₁₋₅ V ₂ D ₂ r ₃ H ₃ e ₃	0.70	4.50	-0.0	+10	0	0	0	0	117
□	D ₆ S ₁₋₅ V ₂ D ₂ r ₃ H ₃ e ₃	0.70	4.50	-0.0	+10	0	0	0	0	110



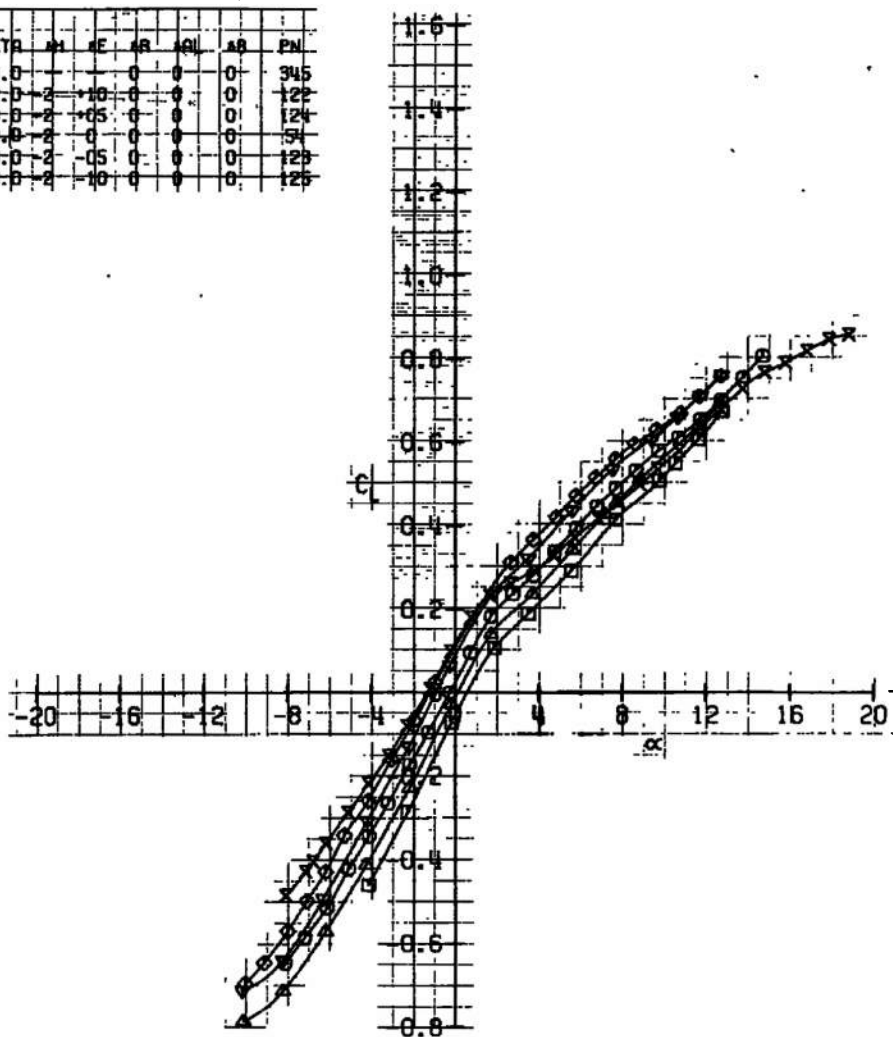
c. Continued
Fig. 7 Continued



c. Concluded
Fig. 7 Continued

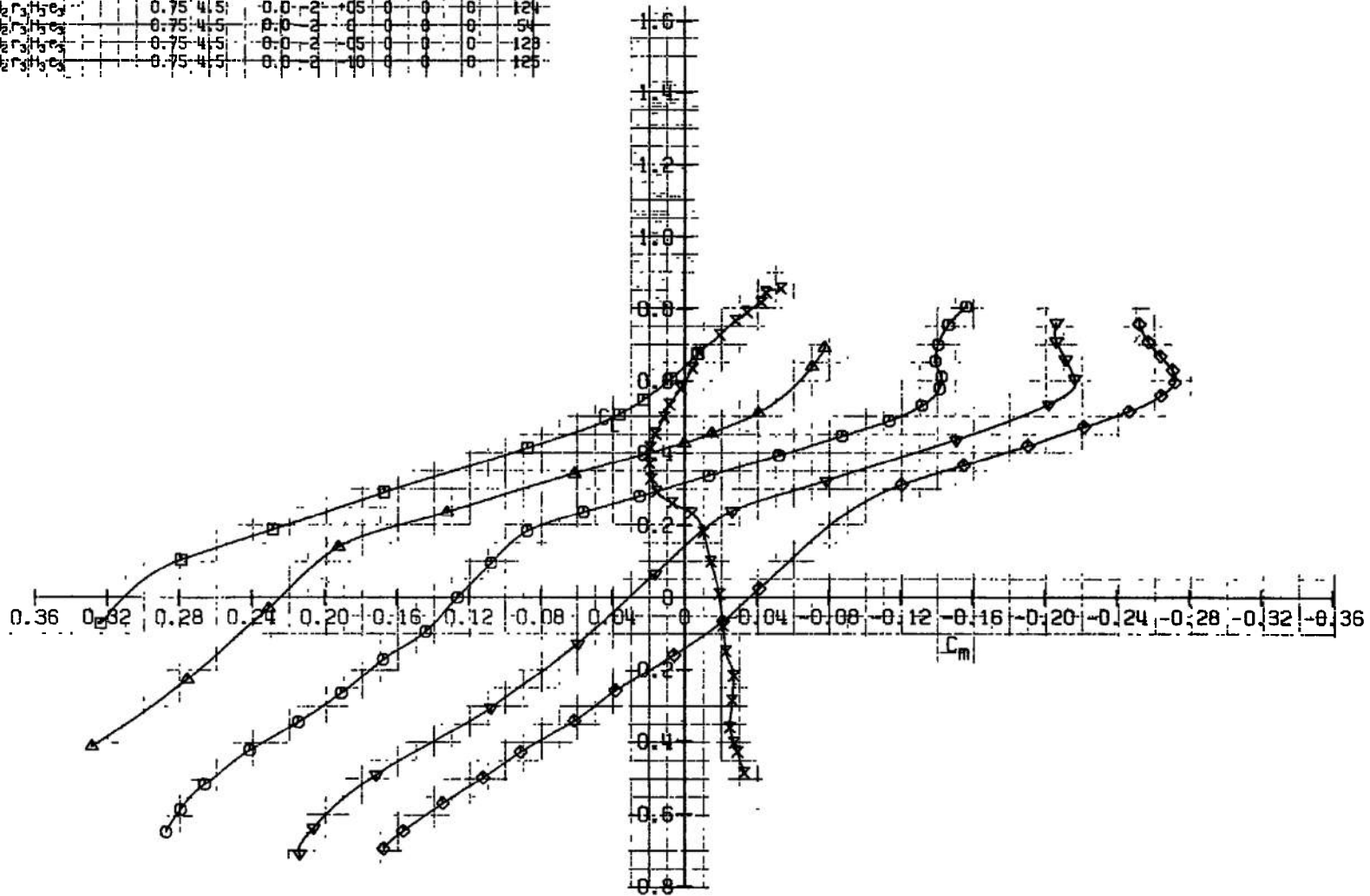
CONFIGURATION: $N_2S_3D_4H_2B_3C_2N_3$		M_∞	Re	BETA	AH	AF	DR	ML	SB	PN
X	$D_6S_1S_3V_2D_2R_3$	-	-	0.70	4.50	0.0	-	0	0	343
O	$D_6S_1S_3V_2D_2R_3H_2C_3$	-	-	0.70	4.50	0.0	-2	-0	0	120
V	$D_6S_1S_3V_2D_2R_3H_2C_3$	-	-	0.70	4.50	0.0	-2	-0.05	0	116
D	$D_6S_1S_3V_2D_2R_3H_2C_3$	-	-	0.70	4.50	0.0	-2	0	0	52
A	$D_6S_1S_3V_2D_2R_3H_2C_3$	-	-	0.70	4.50	0.0	-2	-0.05	0	117
B	$D_6S_1S_3V_2D_2R_3H_2C_3$	-	-	0.70	4.50	0.0	-2	-0	0	116

CONFIGURATION, $H_3S_1sH_4He^+H_2S_1sC_2N_2$	SYM.	CONFIGURATION, $H_3S_1sH_4He^+H_2S_1sC_2N_2$	M_∞	Re	BETR	AH	FE	GR	AGL	AB	PN
X $D_6S_{1s}V_2d_{3s}T_5$	-	-	0.75	4.50	0.0	-	0	0	0	0	345
◊ $D_6S_{1s}V_2d_{3s}T_5$	-	-	0.75	4.50	0.0	-2	-10	0	0	0	128
▽ $D_6S_{1s}V_2d_{3s}T_5H_2S_1s$	-	-	0.75	4.50	0.0	-2	-05	0	0	0	124
○ $D_6S_{1s}V_2d_{3s}T_5H_2S_1s$	-	-	0.75	4.50	0.0	-2	0	0	0	0	125
△ $D_6S_{1s}V_2d_{3s}T_5H_2S_1s$	-	-	0.75	4.50	0.0	-2	-05	0	0	0	123
□ $D_6S_{1s}V_2d_{3s}T_5H_2S_1s$	-	-	0.75	4.50	0.0	-2	10	0	0	0	120

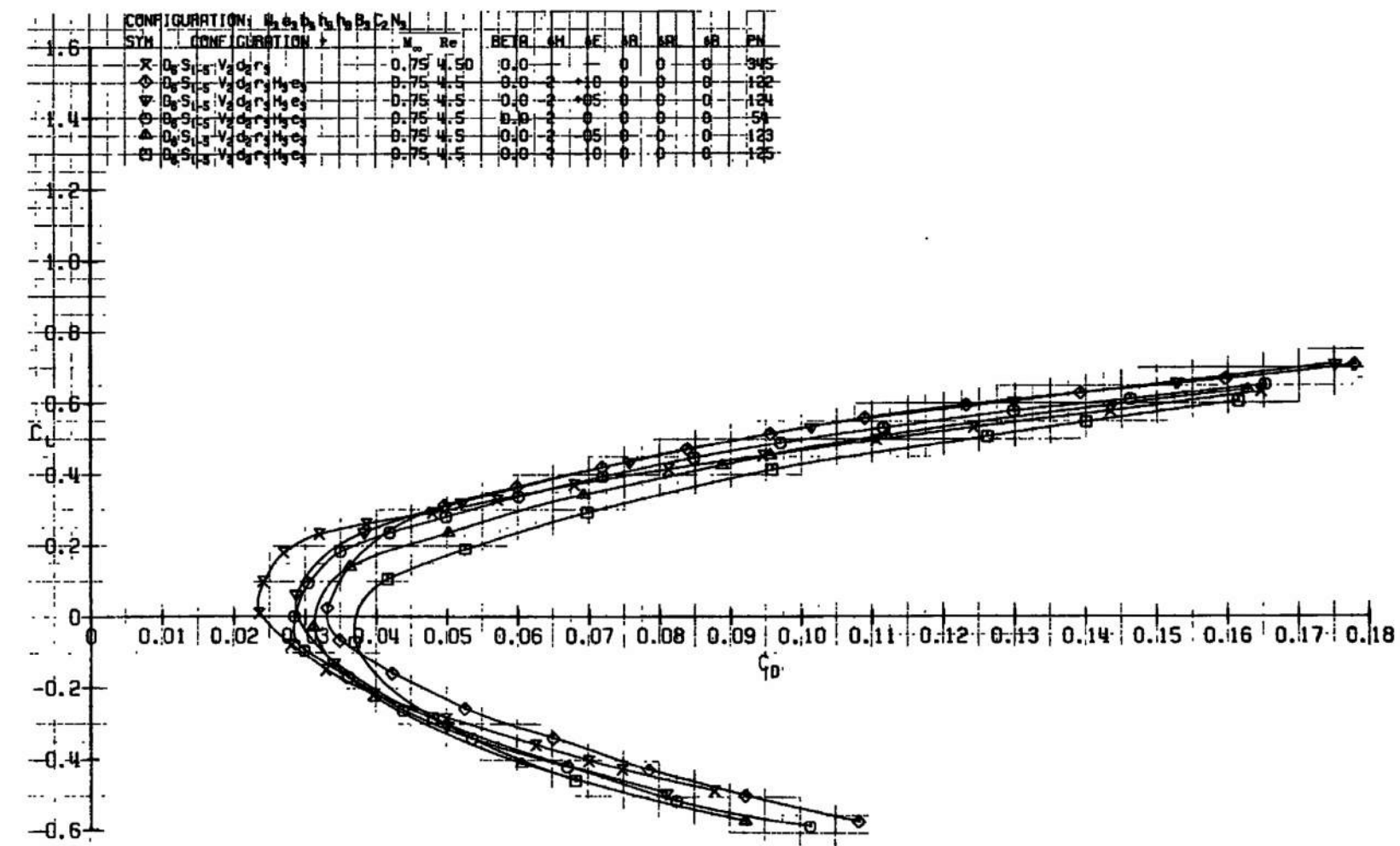


d. $M_\infty = 0.75$
Fig. 7 Continued

CONFIGURATION: H ₃ H ₄ H ₅ H ₆ B ₃ C ₂ N ₃		M _∞	Re	BETA	SH	SE	SR	SL	SP	PN
SYM	CONFIGURATION:	-	-	-	-	-	-	-	-	-
X	H ₃ S ₁ H ₅ V ₂ H ₂ r ₃	0.75	4.5	0.0	0	0	0	0	0	345
◊	H ₃ S ₁ H ₅ V ₂ H ₂ r ₃ H ₃ e ₃	0.75	4.5	-0.8	-2	-10	0	0	0	122
▼	H ₃ S ₁ H ₅ V ₂ H ₂ r ₃ H ₅ e ₃	0.75	4.5	0.0	-2	-0.5	0	0	0	124
○	H ₃ S ₁ H ₅ V ₂ H ₂ r ₃ H ₅ e ₃	0.75	4.5	0.0	-2	0	0	0	0	54
△	H ₃ S ₁ H ₅ V ₂ H ₂ r ₃ H ₅ e ₃	0.75	4.5	0.0	-2	-0.5	0	0	0	123
□	H ₃ S ₁ H ₅ V ₂ H ₂ r ₃ H ₅ e ₃	0.75	4.5	0.0	-2	-10	0	0	0	125



d. Continued
Fig. 7 Continued

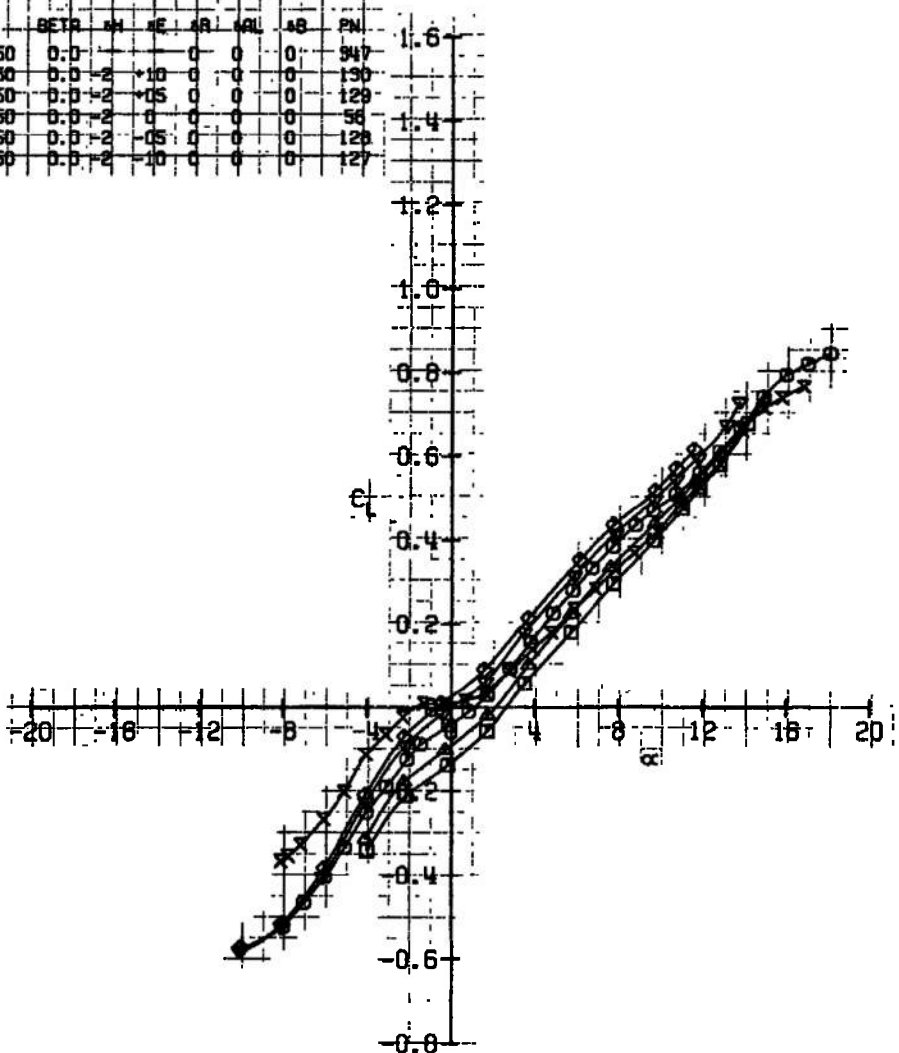


d. Concluded
Fig. 7 Continued

CONFIGURATION: $W_{0.80} S_{1.0} V_{2.0} \delta_{1.0} B_{0.5} C_{0.5}$

STAB. CONFIGURATION:

	M_∞	Re	BETA	ME	MR	ML	AS	PM
X $S_{1.0} V_{2.0} \delta_{1.0} B_{0.5} C_{0.5}$	0.80	4.50	0.0	0	0	0	0	947
◊ $S_{1.0} V_{2.0} \delta_{1.0} B_{0.5} C_{0.5}$	0.80	4.50	0.0 -2	+10	0	0	0	130
▽ $S_{1.0} V_{2.0} \delta_{1.0} B_{0.5} C_{0.5}$	0.80	4.50	0.0 -2	+05	0	0	0	129
○ $S_{1.0} V_{2.0} \delta_{1.0} B_{0.5} C_{0.5}$	0.80	4.50	0.0 -2	0	0	0	0	56
△ $S_{1.0} V_{2.0} \delta_{1.0} B_{0.5} C_{0.5}$	0.80	4.50	0.0 -2	-05	0	0	0	120
□ $S_{1.0} V_{2.0} \delta_{1.0} B_{0.5} C_{0.5}$	0.80	4.50	0.0 -2	-10	0	0	0	127

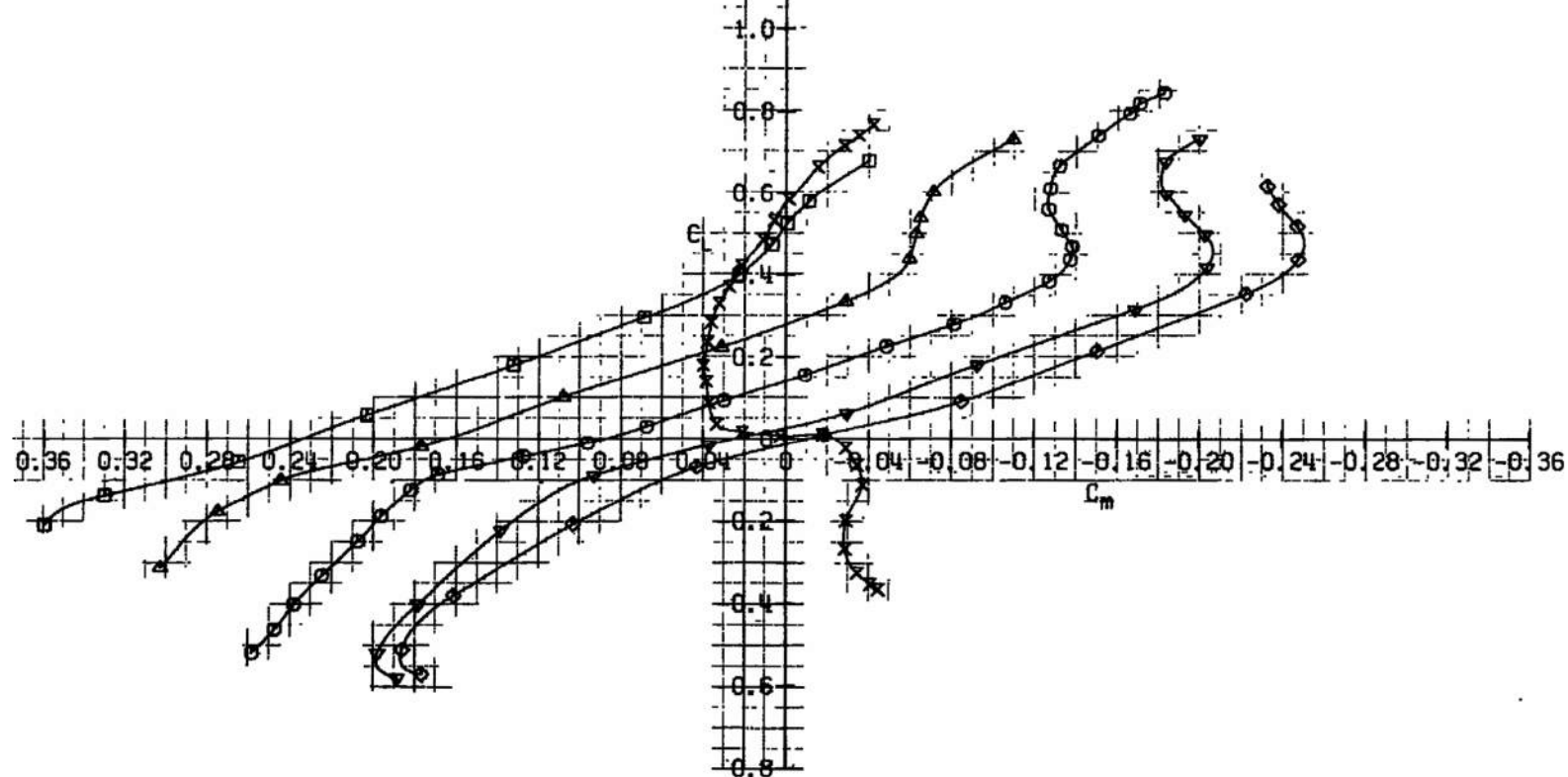


e. $M_\infty = 0.80$

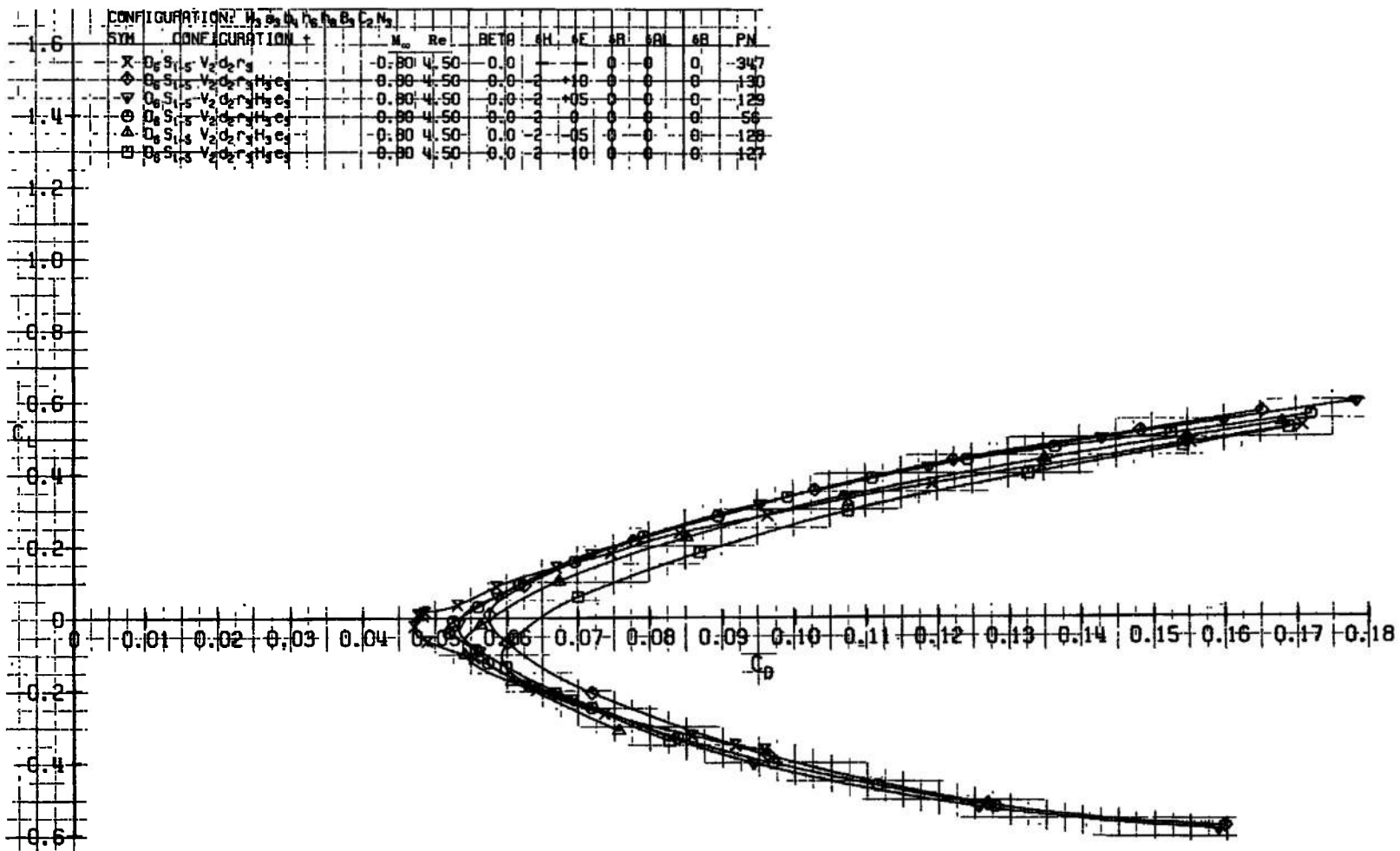
Fig. 7 Continued

CONFIGURATION: $H_3^+e_3^+b_1^+b_2^+b_3^+c_2^-N_3^-$

SYM. CONFIGURATION

M₀ Re BETD SHL AF LR AL PR PNX D₆S₁e₃V₂d₂r₃D₆S₁e₃V₂d₂r₃H₃e₃D₆S₁e₃V₂d₂r₃H₃e₃D₆S₁e₃V₂d₂r₃H₃e₃D₆S₁e₃V₂d₂r₃H₃e₃D₆S₁e₃V₂d₂r₃H₃e₃D₆S₁e₃V₂d₂r₃H₃e₃

e. Continued
Fig. 7 Continued



e. Concluded
Fig. 7 Concluded

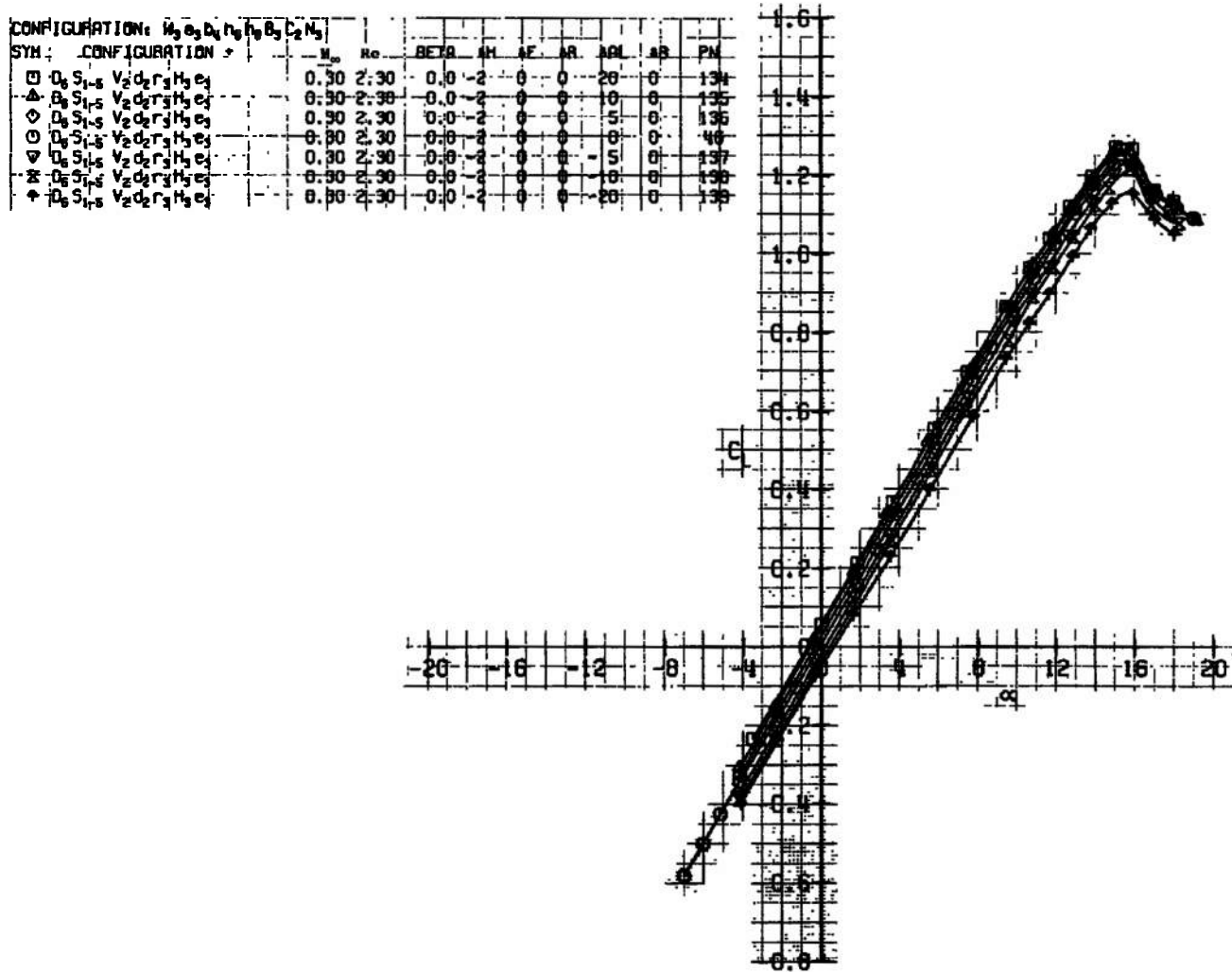
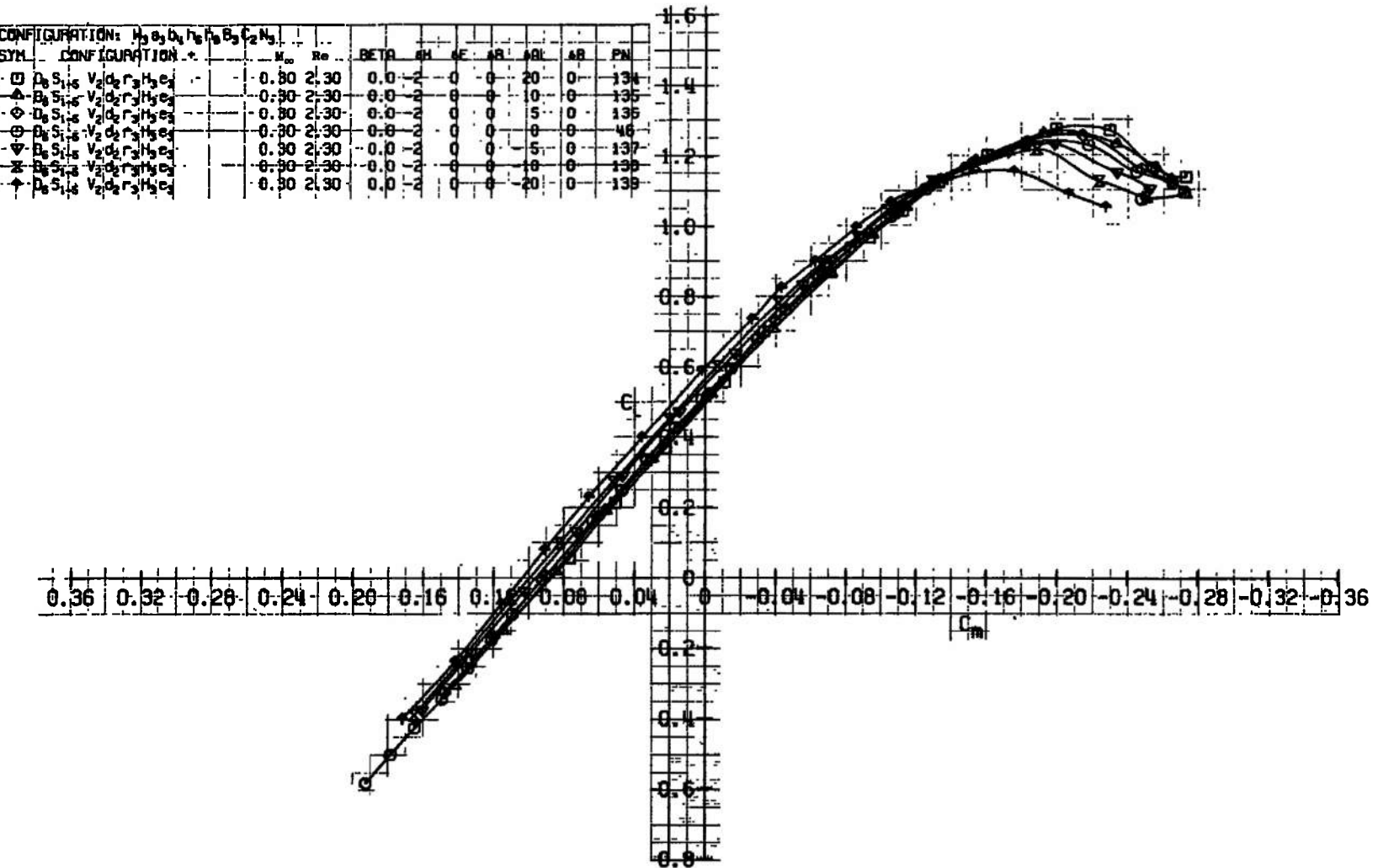
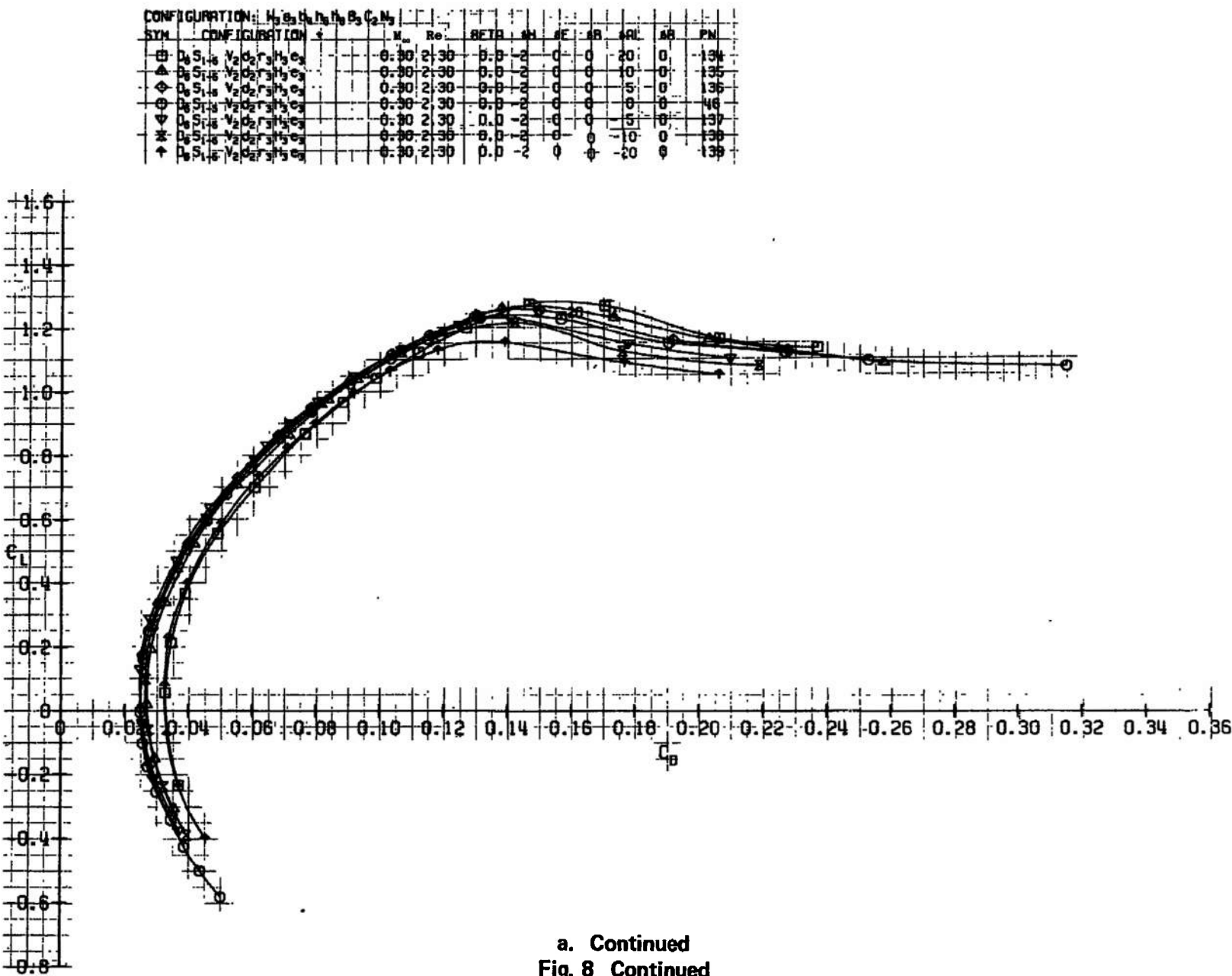
a. $M_0 = 0.30$

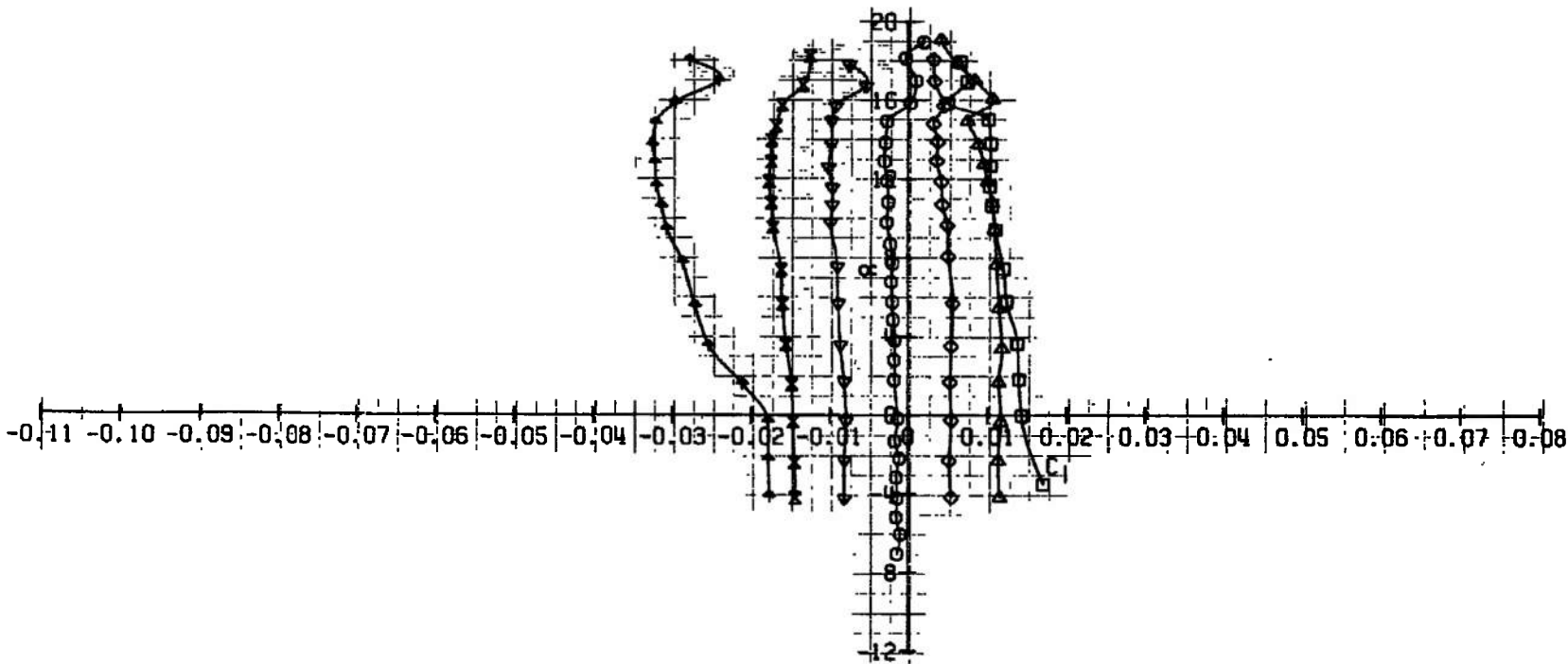
Fig. 8 Aileron Effectiveness



a. Continued
Fig. 8 Continued

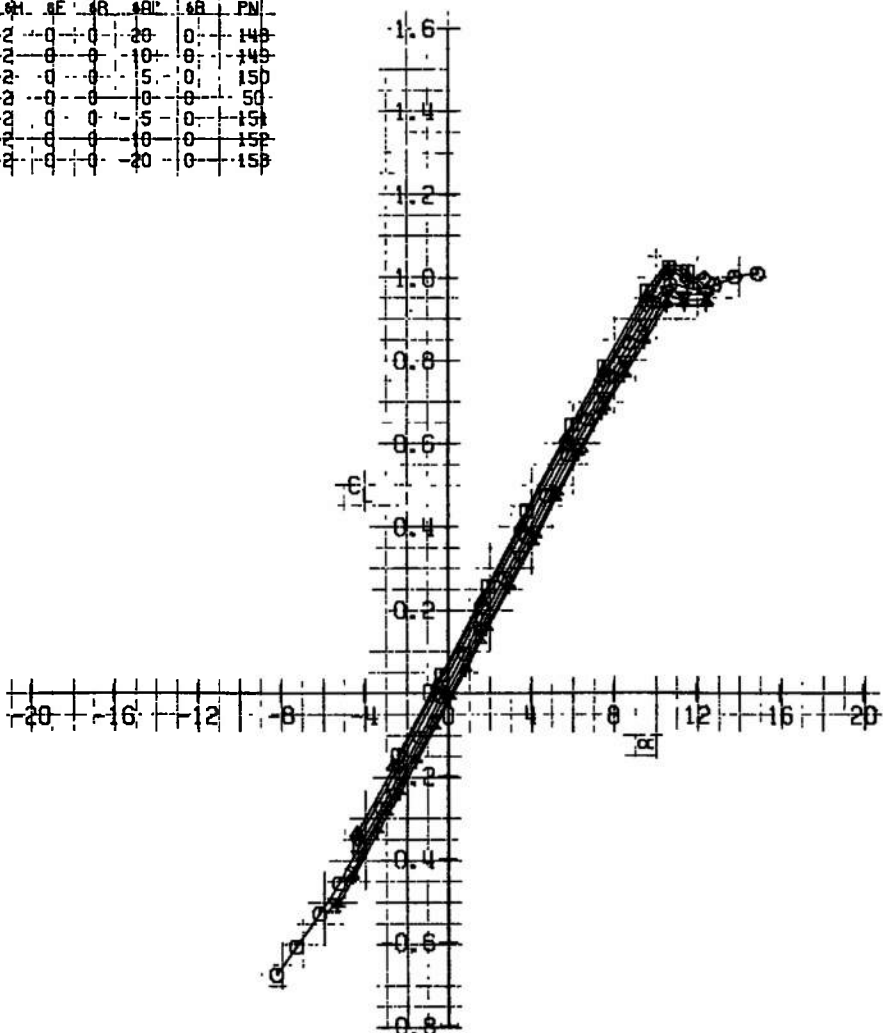


CONFIGURATION: $M_0 S_0 C_0 T_0 M_0 B_0 C_2 M_0$		M_∞	Re	BETR	SH	SF	SL	SB	-PN
□ - $D_0 S_{1/2} V_2 D_2 r_3 M_0 e_3$		0.30	2.30	0.0	2	0	20	0	134
△ - $D_0 S_{1/2} V_2 D_2 r_3 M_0 e_3$		0.30	2.30	0.0	2	0	10	0	135
◇ - $D_0 S_{1/2} V_2 D_2 r_3 M_0 e_3$		0.30	2.30	0.0	2	0	5	0	136
○ - $D_0 S_{1/2} V_2 D_2 r_3 M_0 e_3$		0.30	2.30	0.0	2	0	0	0	146
▽ - $D_0 S_{1/2} V_2 D_2 r_3 M_0 e_3$		0.30	2.30	0.0	2	0	5	0	137
× - $D_0 S_{1/2} V_2 D_2 r_3 M_0 e_3$		0.30	2.30	0.0	2	0	10	0	138
◆ - $D_0 S_{1/2} V_2 D_2 r_3 M_0 e_3$		0.30	2.30	0.0	2	0	20	0	139



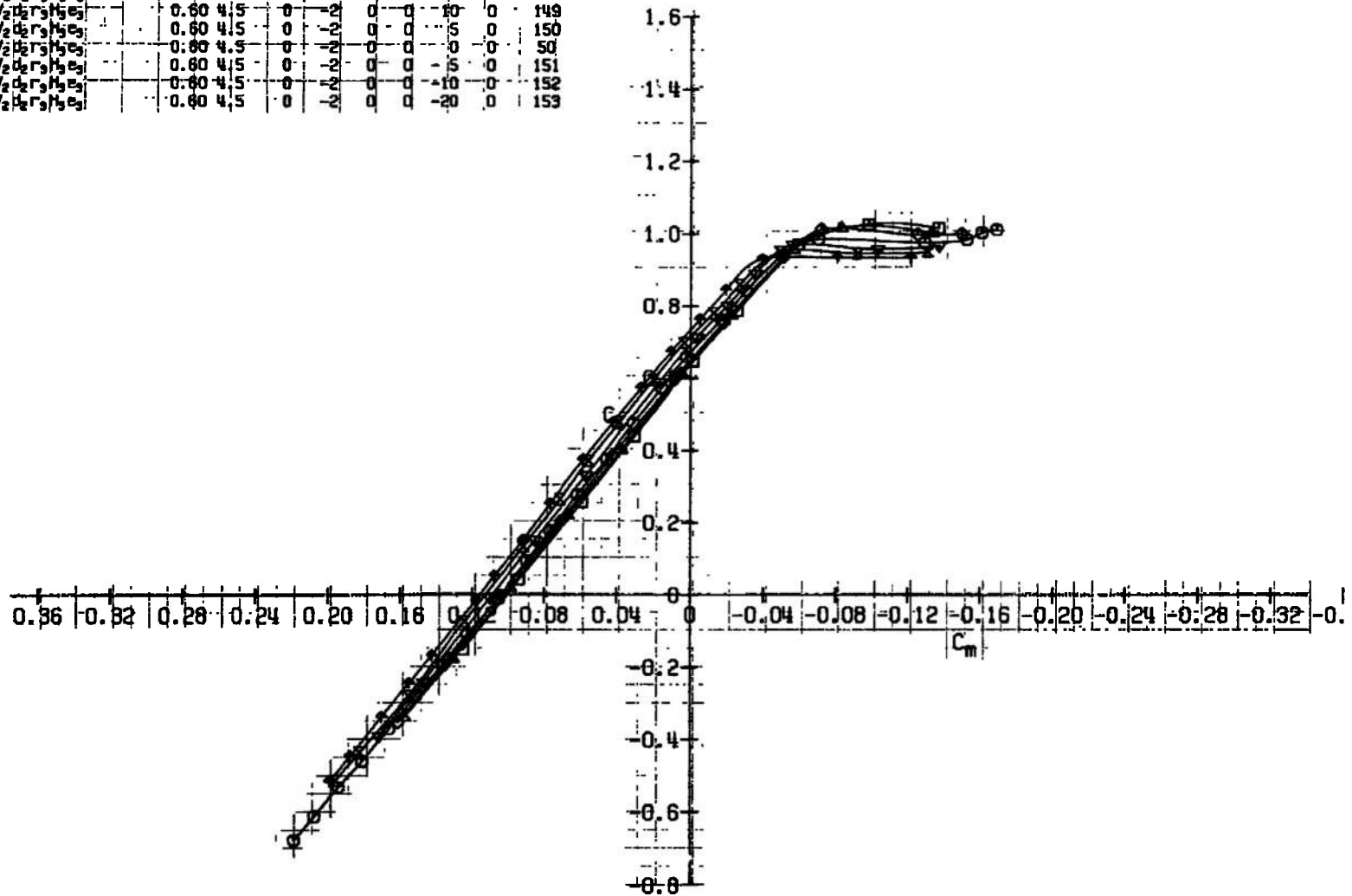
a. Concluded
Fig. 8 Continued

SYM	CONFIGURATION	M_∞	Re	BETA	SH	SE	SL	SP	LR	PN
□	$D_6 S_{1+5} V_2' d_2 r_3 H_3 e_3$	0.60	4.5	0	-2	0	0	20	0	148
△	$D_6 S_{1+5} V_2 d_2 r_3 H_3 e_3$	0.60	4.5	0	-2	0	0	10	0	149
◊	$D_6 S_{1+5} V_2 d_2 r_3 H_3 e_3$	0.60	4.5	0	-2	0	0	15	0	150
○	$D_6 S_{1+5} V_2 d_2 r_3 H_3 e_3$	0.60	4.5	0	-2	0	0	0	0	50
▽	$D_6 S_{1+5} V_2 d_2 r_3 H_3 e_3$	0.60	4.5	0	-2	0	0	-5	0	151
×	$D_6 S_{1+5} V_2 d_2 r_3 H_3 e_3$	0.60	4.5	0	-2	0	0	10	0	152
†	$H_6 S_{1+5} V_2' d_2 r_3 H_3 e_3$	0.60	4.5	0	-2	0	0	20	0	153

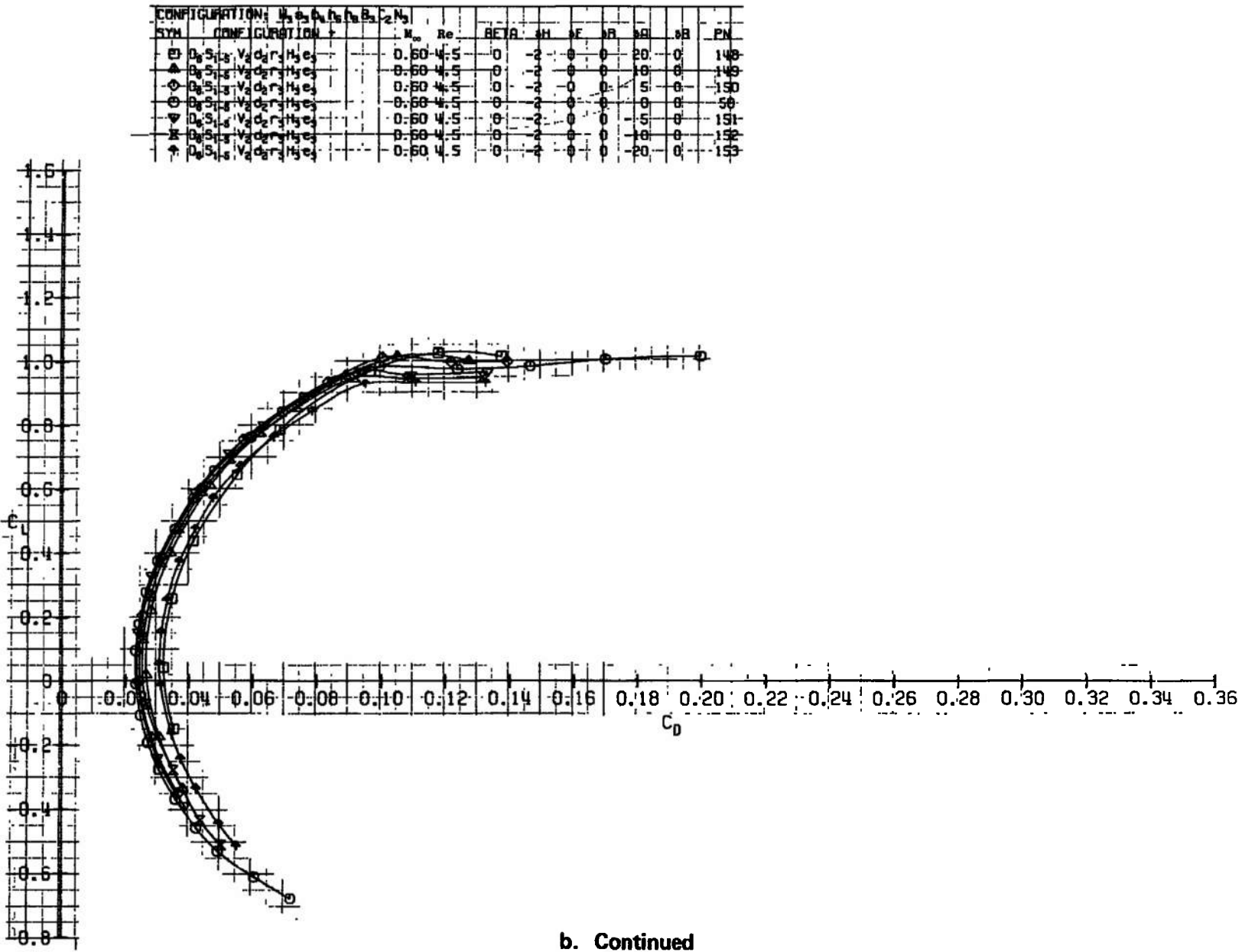


b. $M_\infty = 0.60$
Fig. 8 Continued

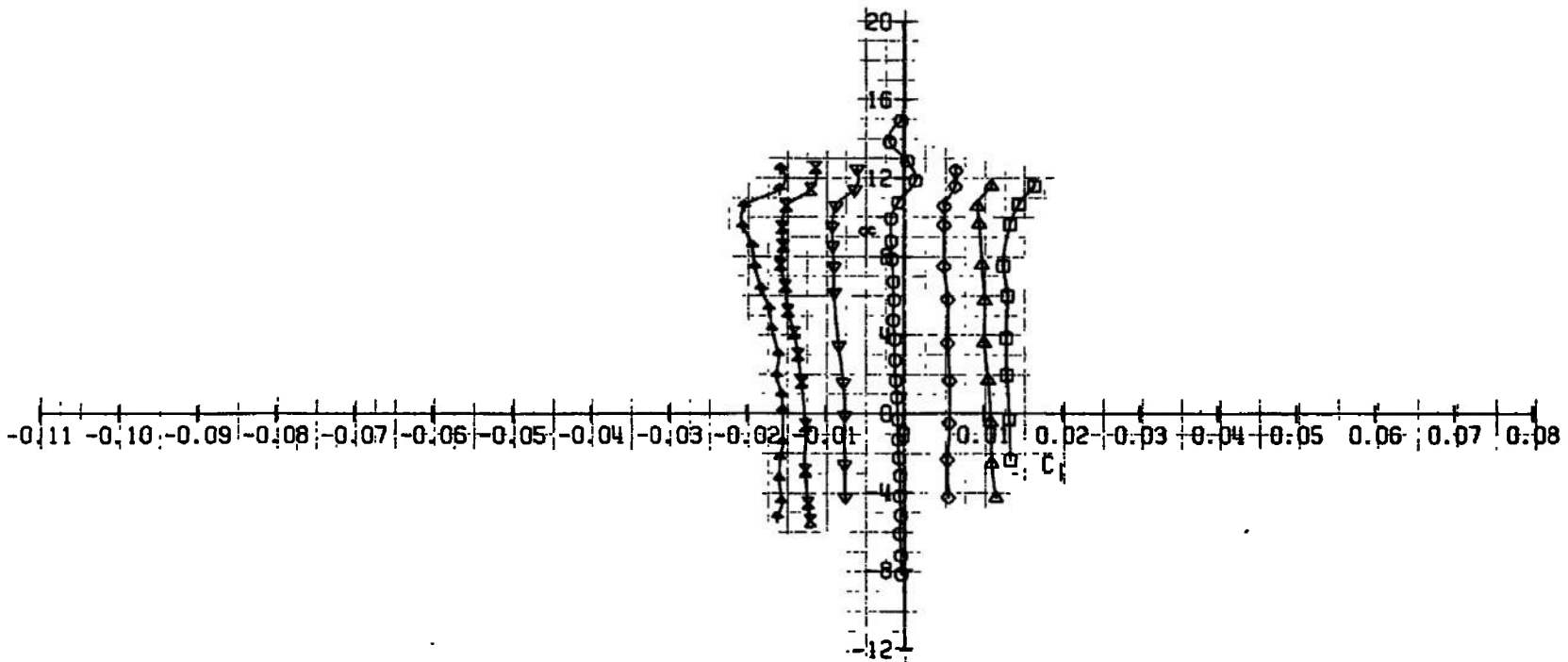
CONFIGURATION: $W_3 S_3 B_3 H_3 H_3 B_3 C_2 N_3$	SYM.	CONFIGURATION	M_∞	Re	BETA	OH	OE	OR	OL	OB	PN
\square $D_6 S_{1-6} V_2 d_2 r_3 H_3 e_3$			0.60	4.5	0	-2	0	0	20	0	146
\triangle $D_6 S_{1-6} V_2 d_2 r_3 H_3 e_3$			0.60	4.5	0	-2	0	0	10	0	149
\diamond $D_6 S_{1-6} V_2 d_2 r_3 H_3 e_3$			0.60	4.5	0	-2	0	0	5	0	150
\circ $D_6 S_{1-6} V_2 d_2 r_3 H_3 e_3$			0.60	4.5	0	-2	0	0	0	0	50
∇ $D_6 S_{1-6} V_2 d_2 r_3 H_3 e_3$			0.60	4.5	0	-2	0	0	-5	0	151
\times $D_6 S_{1-6} V_2 d_2 r_3 H_3 e_3$			0.60	4.5	0	-2	0	0	-10	0	152
\dagger $D_6 S_{1-6} V_2 d_2 r_3 H_3 e_3$			0.60	4.5	0	-2	0	0	-20	0	153



b. Continued
Fig. 8 Continued

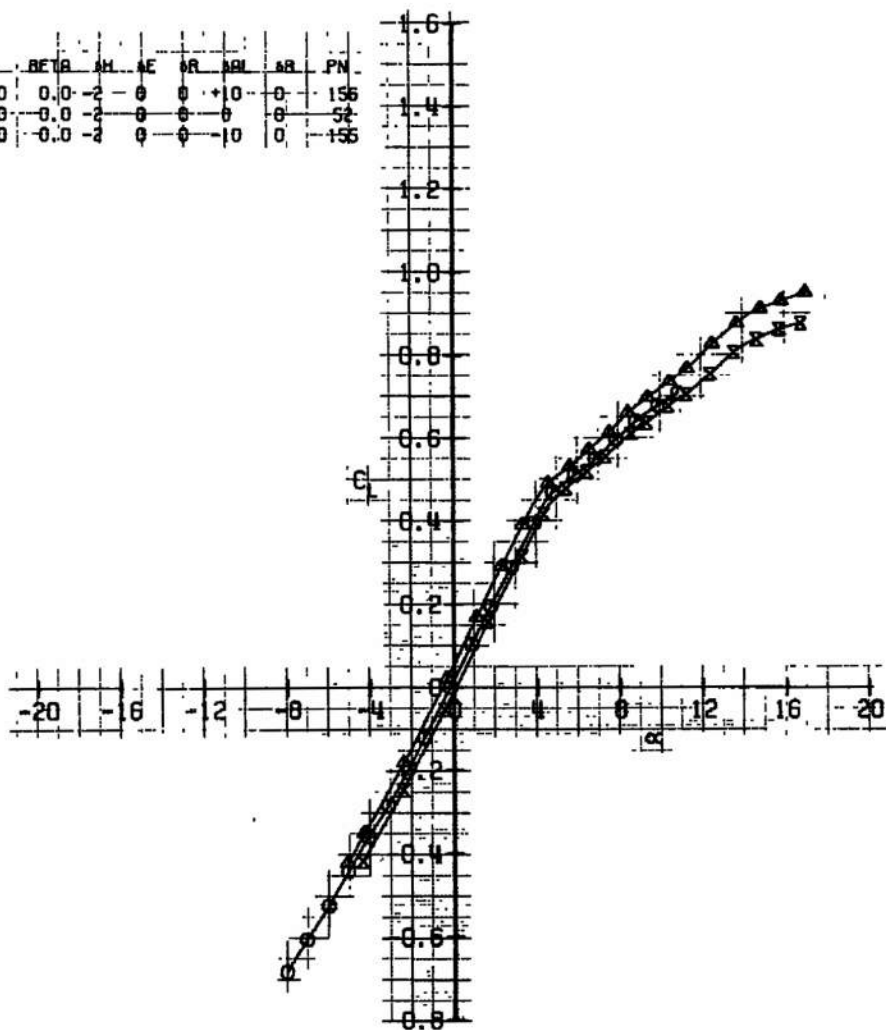


CONFIGURATION: $H_3S_2d_6N_2B_2C_2N_2$		M _w	No.	BETB	SH	EF	ER	ERI	EB	PN
□	D ₆ S ₁₋₆ V ₂ d ₆ r ₃ N ₂ C ₂	0.60	4-5	0	2	0	0	20	0	146
△	D ₆ S ₁₋₆ V ₂ d ₆ r ₃ N ₂ C ₂	0.60	4-5	0	2	0	0	10	0	146
◊	D ₆ S ₁₋₆ V ₂ d ₆ r ₃ N ₂ C ₂	0.60	4-5	0	2	0	0	5	0	150
○	D ₆ S ₁₋₆ V ₂ d ₆ r ₃ N ₂ C ₂	0.60	4-5	0	2	0	0	0	0	56
▽	D ₆ S ₁₋₆ V ₂ d ₆ r ₃ N ₂ C ₂	0.60	4-5	0	2	0	0	5	0	151
×	D ₆ S ₁₋₆ V ₂ d ₆ r ₃ N ₂ C ₂	0.60	4-5	0	2	0	0	10	0	152
†	D ₆ S ₁₋₆ V ₂ d ₆ r ₃ N ₂ C ₂	0.60	4-5	0	2	0	0	20	0	153

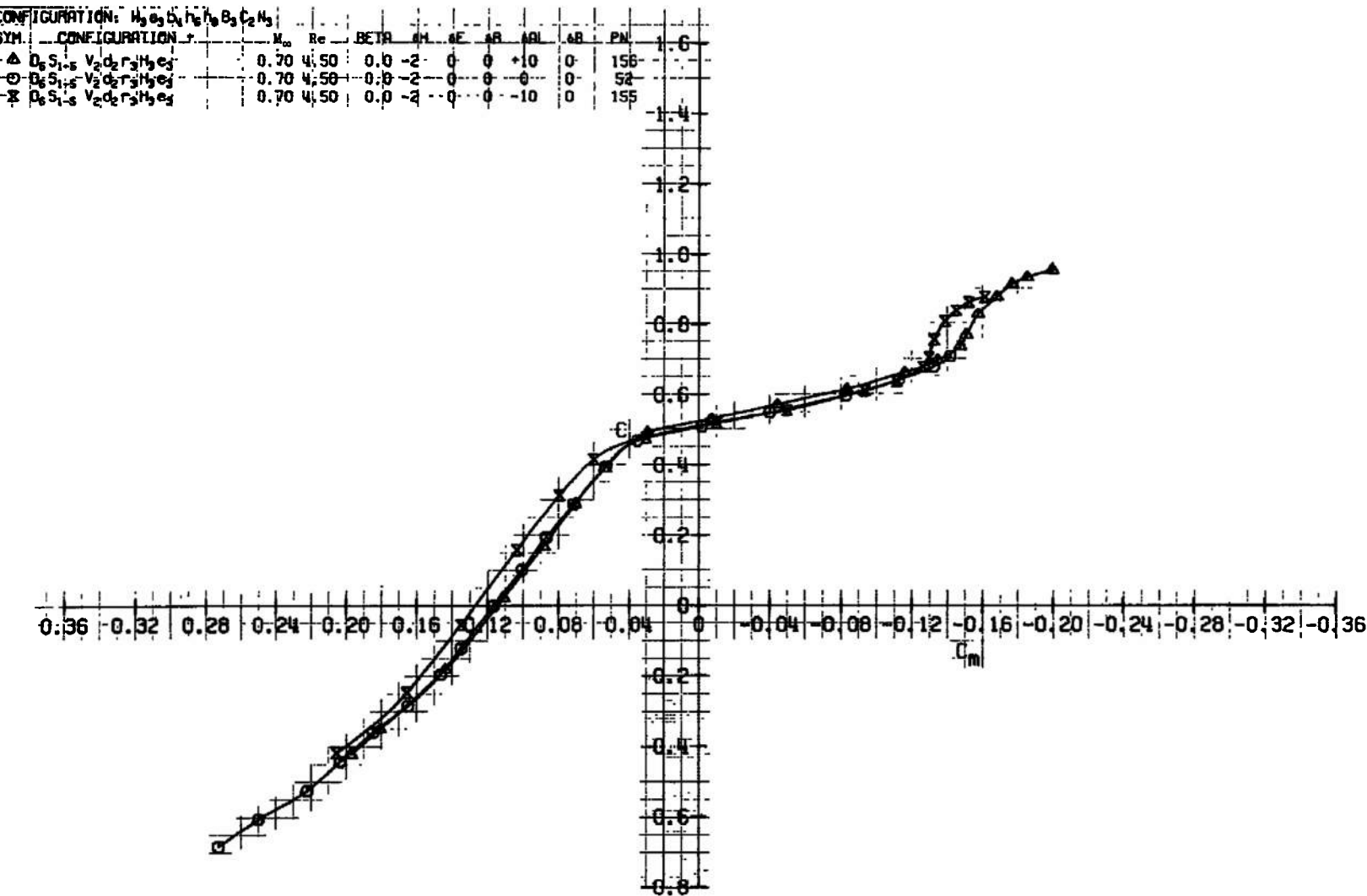


b. Concluded
Fig. 8 Continued

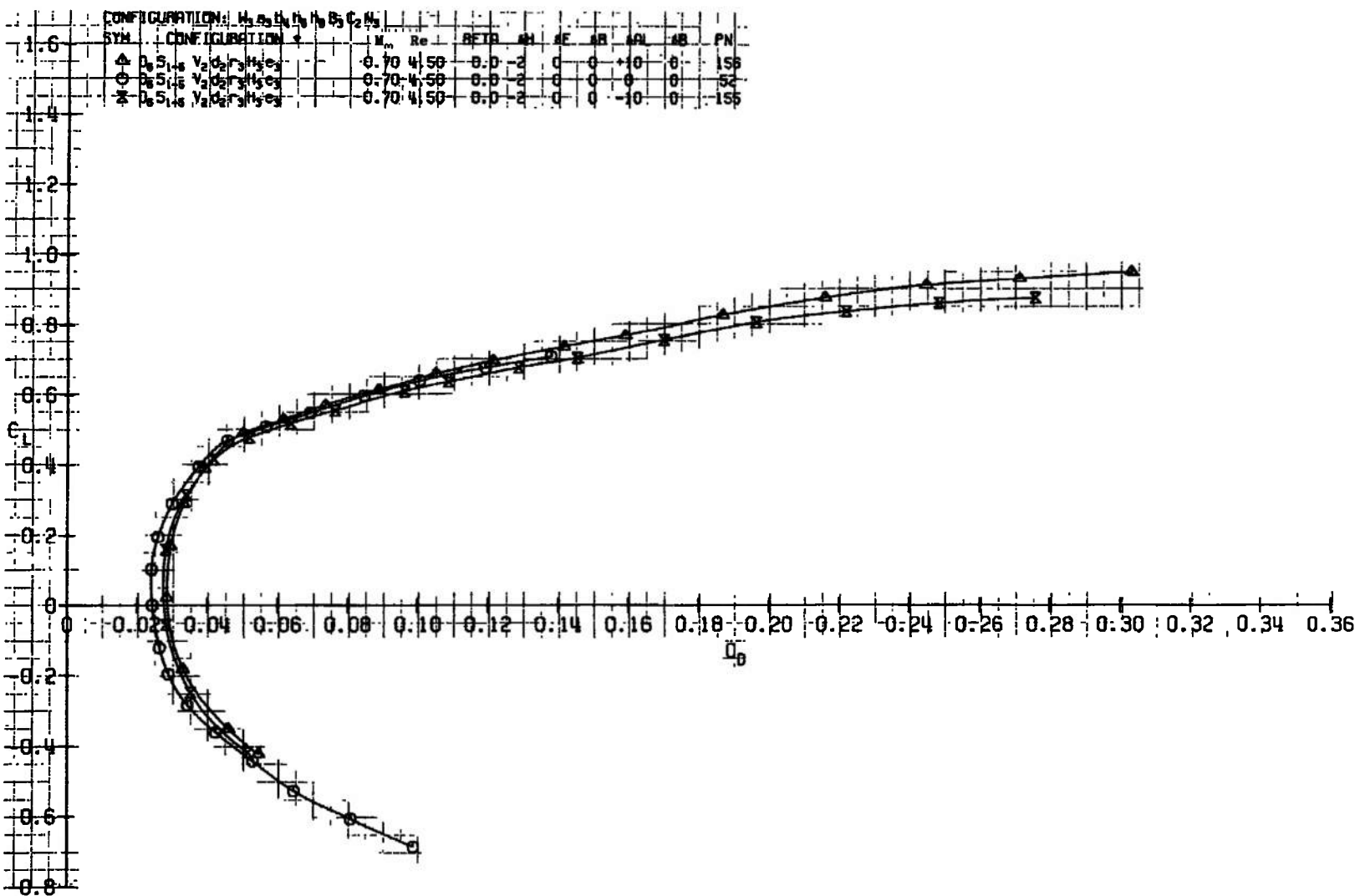
CONFIGURATION: $w_3 e_3 b_4 h_5 h_6 B_3 C_2 N_3$, ...
 SYM : CONFIGURATION + $\dots - M_{\infty} Re \beta \alpha_{\infty} \alpha_{\infty}^2 \alpha_{\infty}^3 \alpha_{\infty}^4 \alpha_{\infty}^5 \alpha_{\infty}^6 \alpha_{\infty}^7 \alpha_{\infty}^8 \alpha_{\infty}^9 \alpha_{\infty}^{10} \alpha_{\infty}^{11} \alpha_{\infty}^{12} \alpha_{\infty}^{13} \alpha_{\infty}^{14} \alpha_{\infty}^{15} \alpha_{\infty}^{16} \alpha_{\infty}^{17} \alpha_{\infty}^{18} \alpha_{\infty}^{19} \alpha_{\infty}^{20} \alpha_{\infty}^{21} \alpha_{\infty}^{22} \alpha_{\infty}^{23} \alpha_{\infty}^{24} \alpha_{\infty}^{25} \alpha_{\infty}^{26} \alpha_{\infty}^{27} \alpha_{\infty}^{28} \alpha_{\infty}^{29} \alpha_{\infty}^{30} \alpha_{\infty}^{31} \alpha_{\infty}^{32} \alpha_{\infty}^{33} \alpha_{\infty}^{34} \alpha_{\infty}^{35} \alpha_{\infty}^{36} \alpha_{\infty}^{37} \alpha_{\infty}^{38} \alpha_{\infty}^{39} \alpha_{\infty}^{40} \alpha_{\infty}^{41} \alpha_{\infty}^{42} \alpha_{\infty}^{43} \alpha_{\infty}^{44} \alpha_{\infty}^{45} \alpha_{\infty}^{46} \alpha_{\infty}^{47} \alpha_{\infty}^{48} \alpha_{\infty}^{49} \alpha_{\infty}^{50} \alpha_{\infty}^{51} \alpha_{\infty}^{52} \alpha_{\infty}^{53} \alpha_{\infty}^{54} \alpha_{\infty}^{55} \alpha_{\infty}^{56} \alpha_{\infty}^{57} \alpha_{\infty}^{58} \alpha_{\infty}^{59} \alpha_{\infty}^{60} \alpha_{\infty}^{61} \alpha_{\infty}^{62} \alpha_{\infty}^{63} \alpha_{\infty}^{64} \alpha_{\infty}^{65} \alpha_{\infty}^{66} \alpha_{\infty}^{67} \alpha_{\infty}^{68} \alpha_{\infty}^{69} \alpha_{\infty}^{70} \alpha_{\infty}^{71} \alpha_{\infty}^{72} \alpha_{\infty}^{73} \alpha_{\infty}^{74} \alpha_{\infty}^{75} \alpha_{\infty}^{76} \alpha_{\infty}^{77} \alpha_{\infty}^{78} \alpha_{\infty}^{79} \alpha_{\infty}^{80} \alpha_{\infty}^{81} \alpha_{\infty}^{82} \alpha_{\infty}^{83} \alpha_{\infty}^{84} \alpha_{\infty}^{85} \alpha_{\infty}^{86} \alpha_{\infty}^{87} \alpha_{\infty}^{88} \alpha_{\infty}^{89} \alpha_{\infty}^{90} \alpha_{\infty}^{91} \alpha_{\infty}^{92} \alpha_{\infty}^{93} \alpha_{\infty}^{94} \alpha_{\infty}^{95} \alpha_{\infty}^{96} \alpha_{\infty}^{97} \alpha_{\infty}^{98} \alpha_{\infty}^{99} \alpha_{\infty}^{100}$
 ▲ $D_6 S_{1-5} V_2 d_2 r_3 h_3 e_3$ 0.70 4.50 0.0 -2 0 0 +10 0 0 156
 ○ $B_6 S_{1-5} V_2 d_2 r_3 h_3 e_3$ 0.70 4.50 0.0 -2 0 0 0 0 0 54
 X $D_6 S_{1-5} V_2 d_2 r_3 h_3 e_3$ 0.70 4.50 0.0 -2 0 0 -10 0 0 156



c. $M_{\infty} = 0.70$
 Fig. 8 Continued

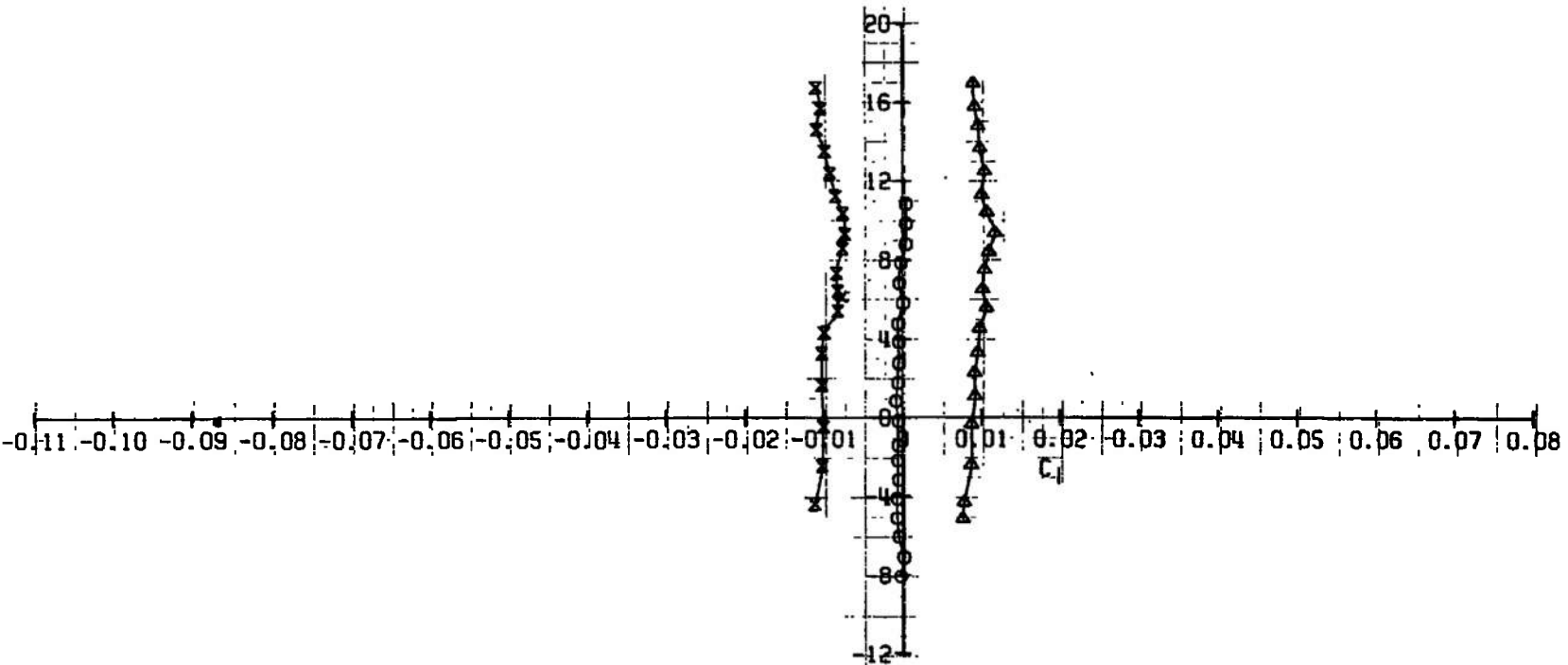


c. Continued
Fig. 8 Continued

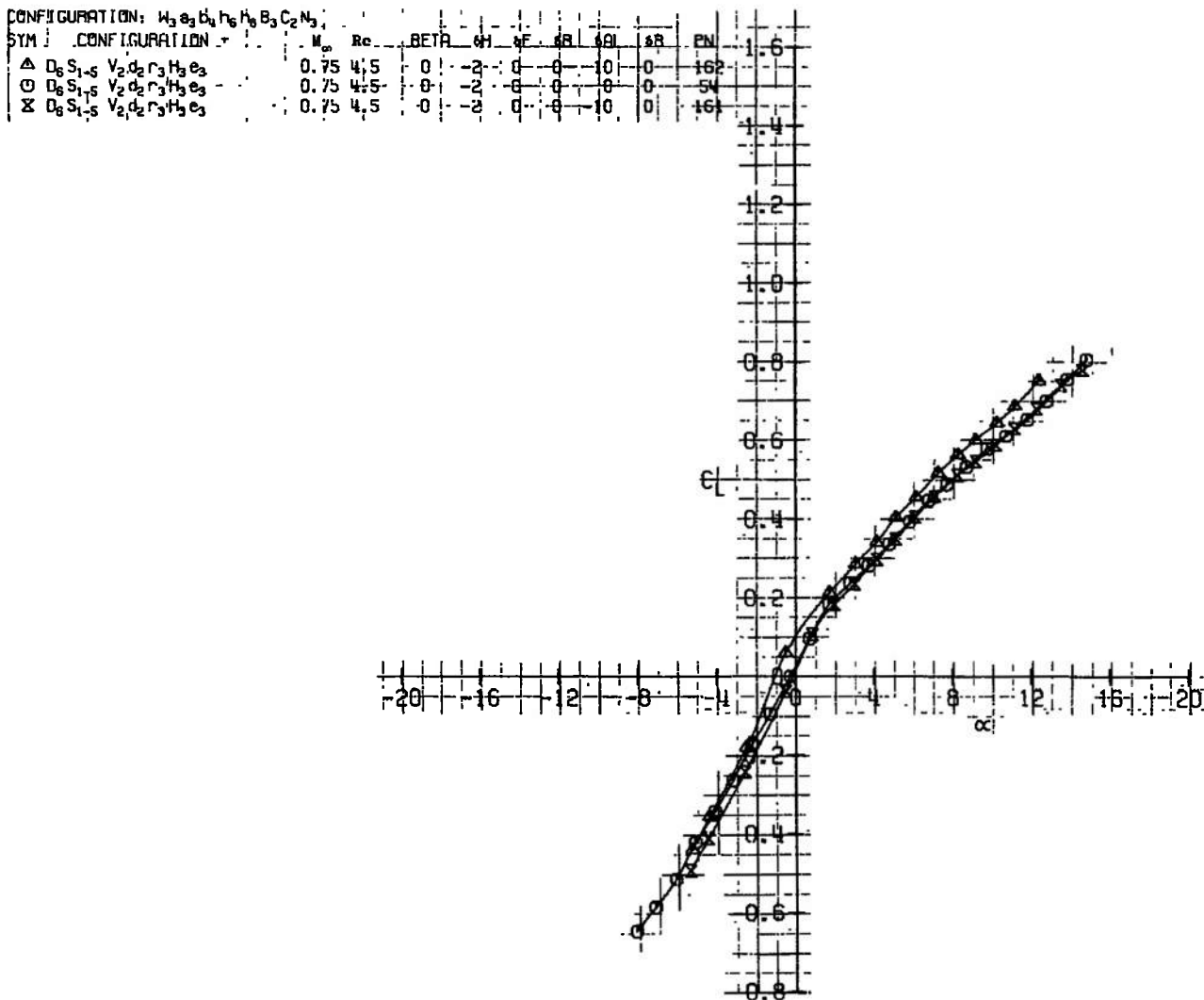


c. Continued
Fig. 8 Continued

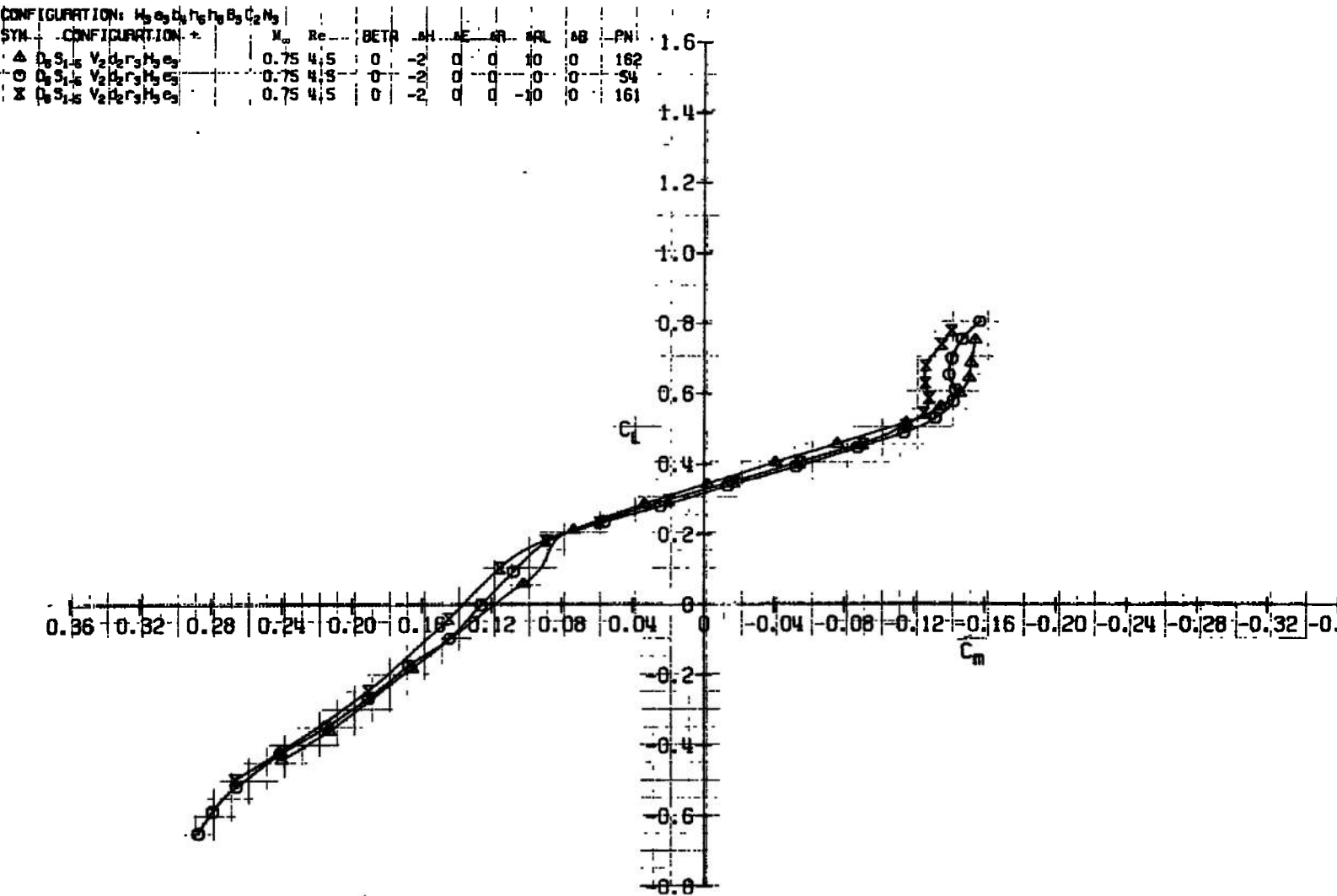
CONFIGURATION: H ₃ H ₅ H ₆ H ₇ H ₈ B ₃ C ₂ N ₃		M _a	Re	BETR	SH	CF	DR	ABL	AB	PN
△	D ₆ S _{1,6} V ₂ D ₂ R ₃ H ₃ C ₃	-	0.70	4.50	-0.0	-2	0	+10	0	156
○	D ₆ S _{1,6} V ₂ D ₂ R ₃ H ₃ C ₃	-	0.70	4.50	-0.0	-2	0	0	0	156
×	D ₆ S _{1,6} V ₂ D ₂ R ₃ H ₃ C ₃	-	0.70	4.50	-0.0	-2	-10	0	0	156



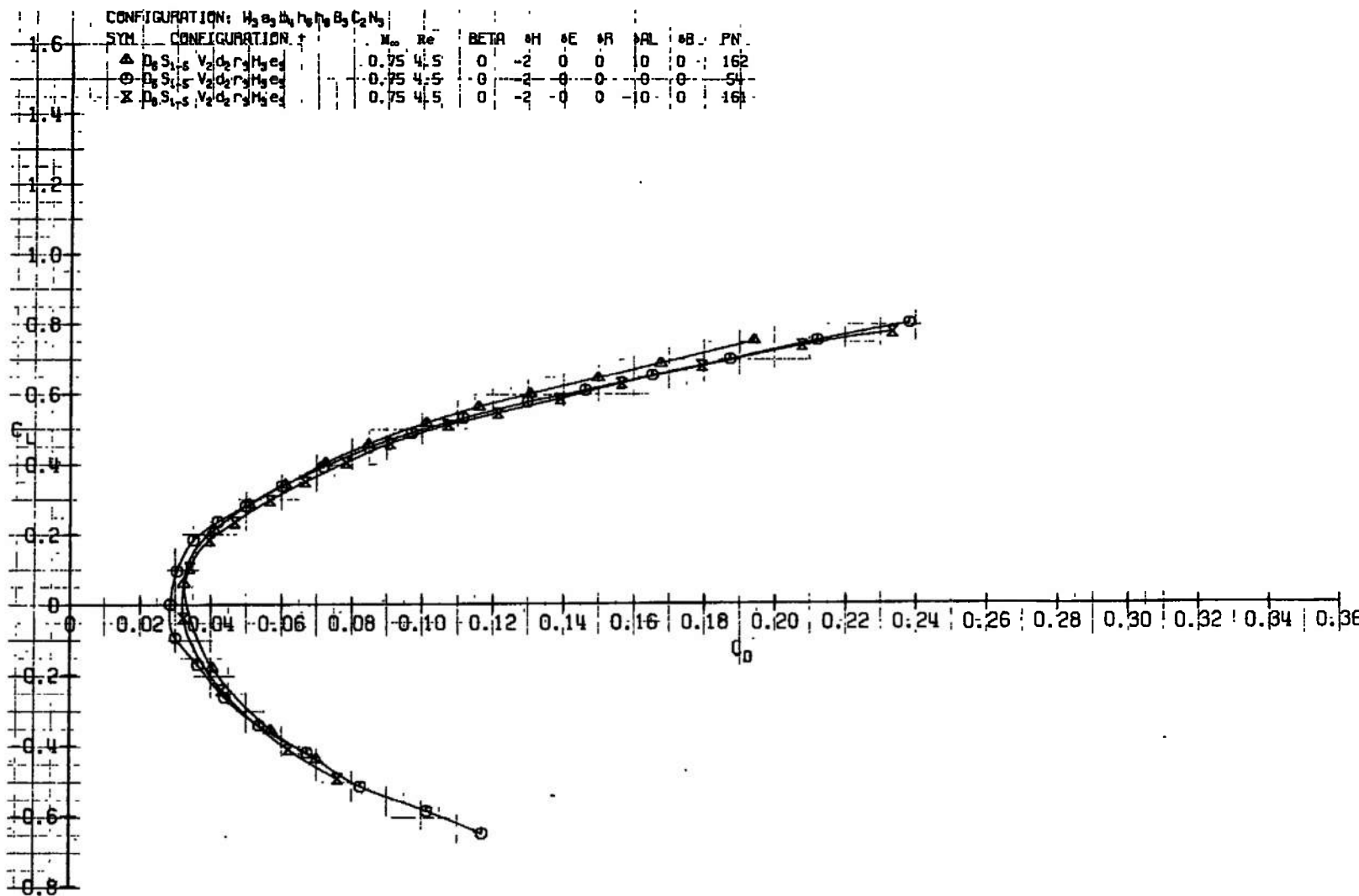
c. Concluded
Fig. 8 Continued



d. $M_\infty = 0.75$
Fig. 8 Continued

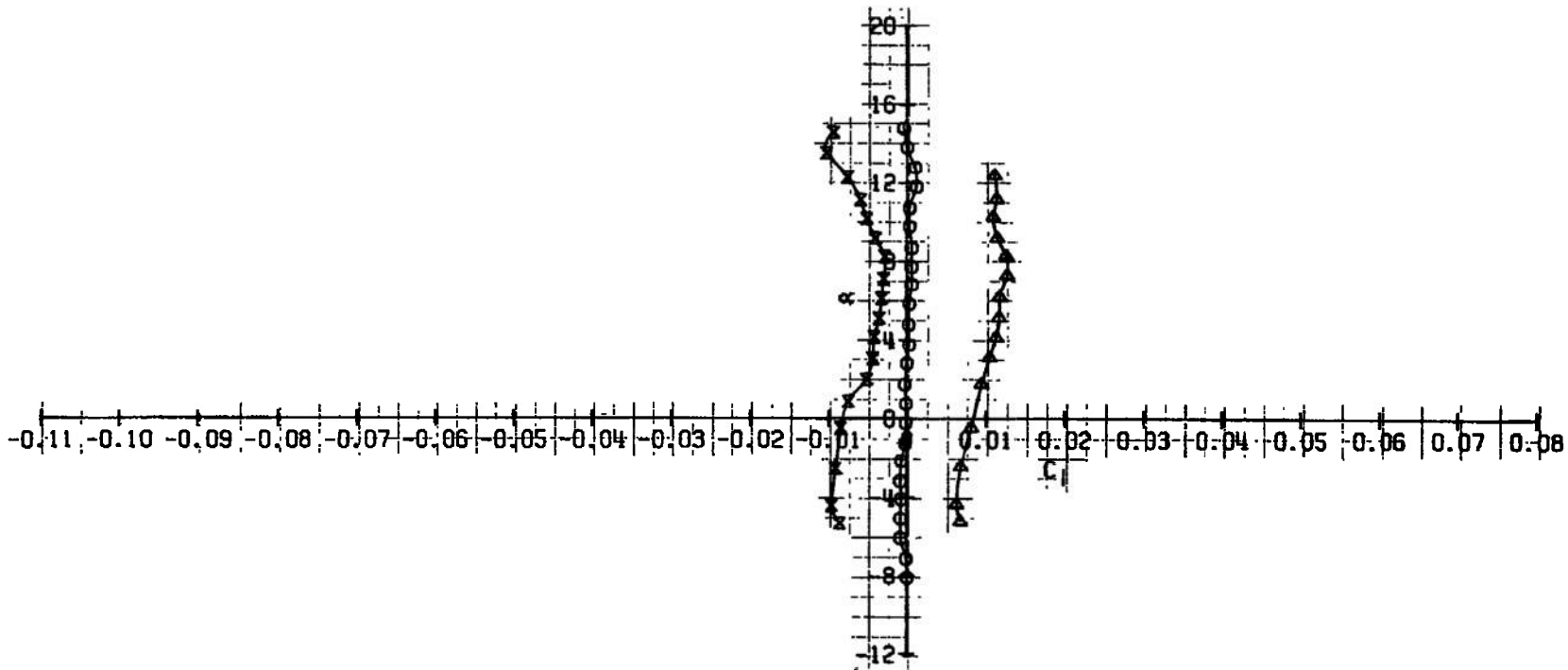


d. Continued
Fig. 8 Continued



d. Continued
Fig. 8 Continued

CONFIGURATION: $h_3 h_5 h_6 h_8 h_9 h_{10} C_2 N_3$		M _∞	Re	BETR	SH	EF	SR	SL	AB	PN
SYM - CONFIGURATION *										
Δ - $h_3 h_5 h_6 h_8 h_9 h_{10} C_2 N_3$		0.75	4.5	0	2	0	10	0	0	162
○ - $h_3 h_5 h_6 h_8 h_9 h_{10} C_2 N_3$		0.75	4.5	0	2	0	0	0	0	51
× - $h_3 h_5 h_6 h_8 h_9 h_{10} C_2 N_3$		0.75	4.5	0	2	0	10	0	0	161



d. Concluded
Fig. 8 Continued

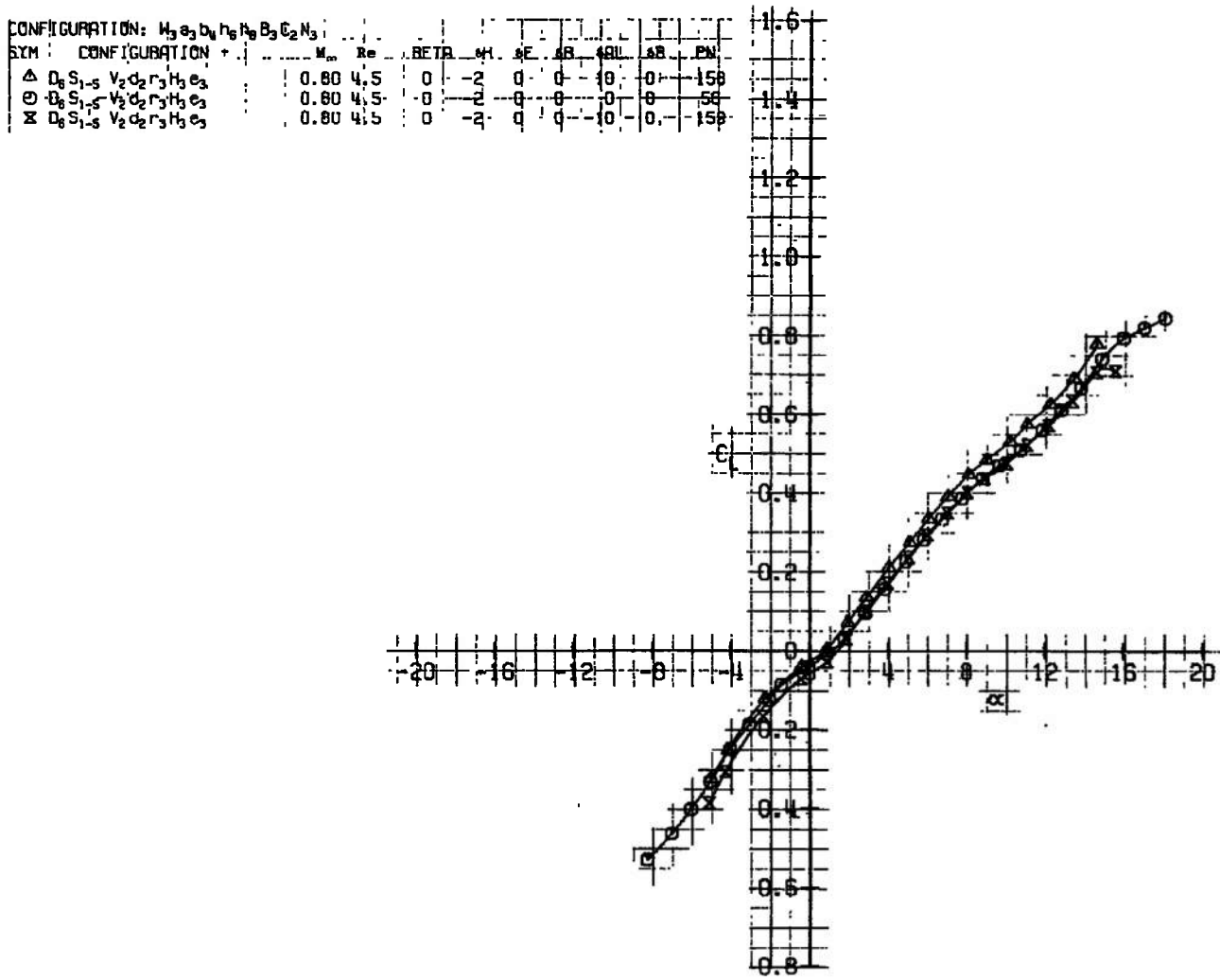
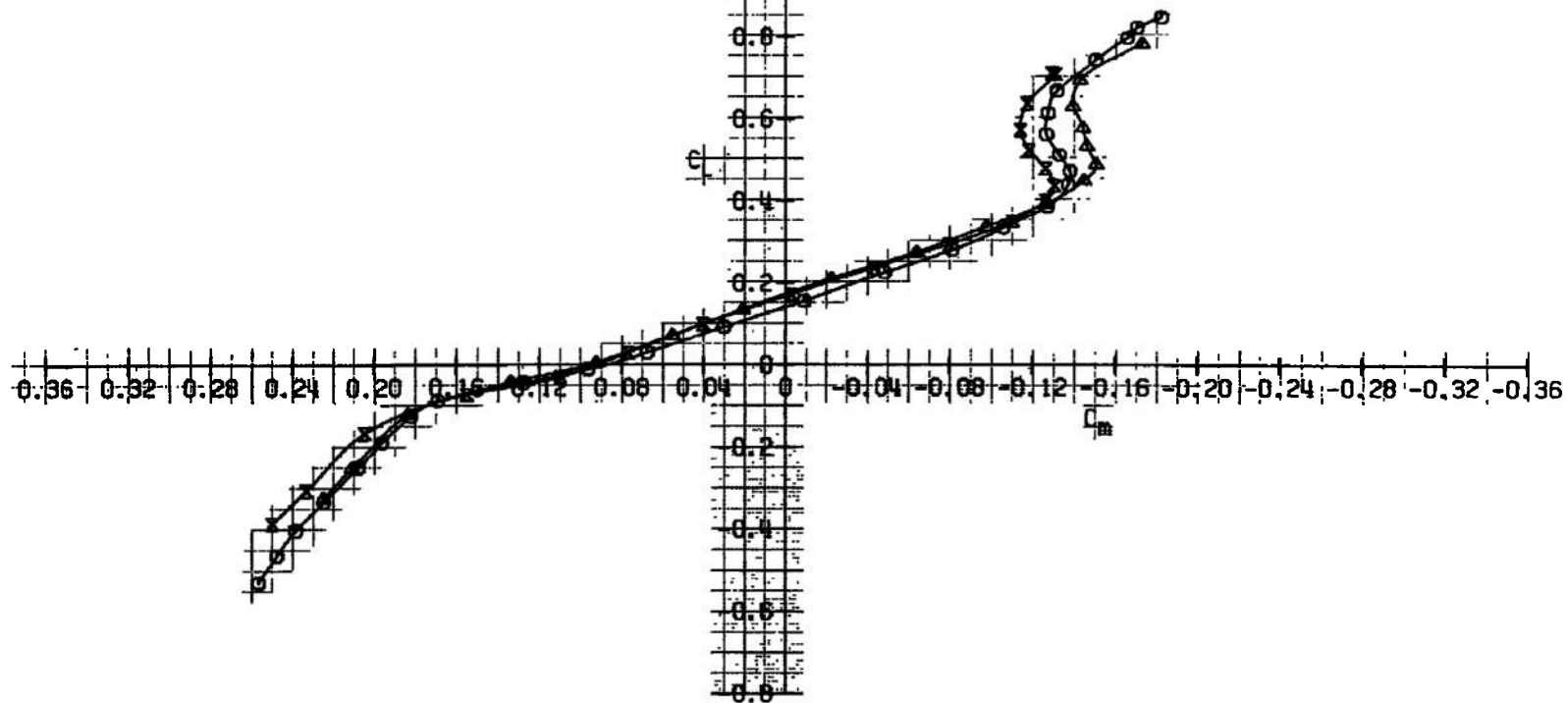
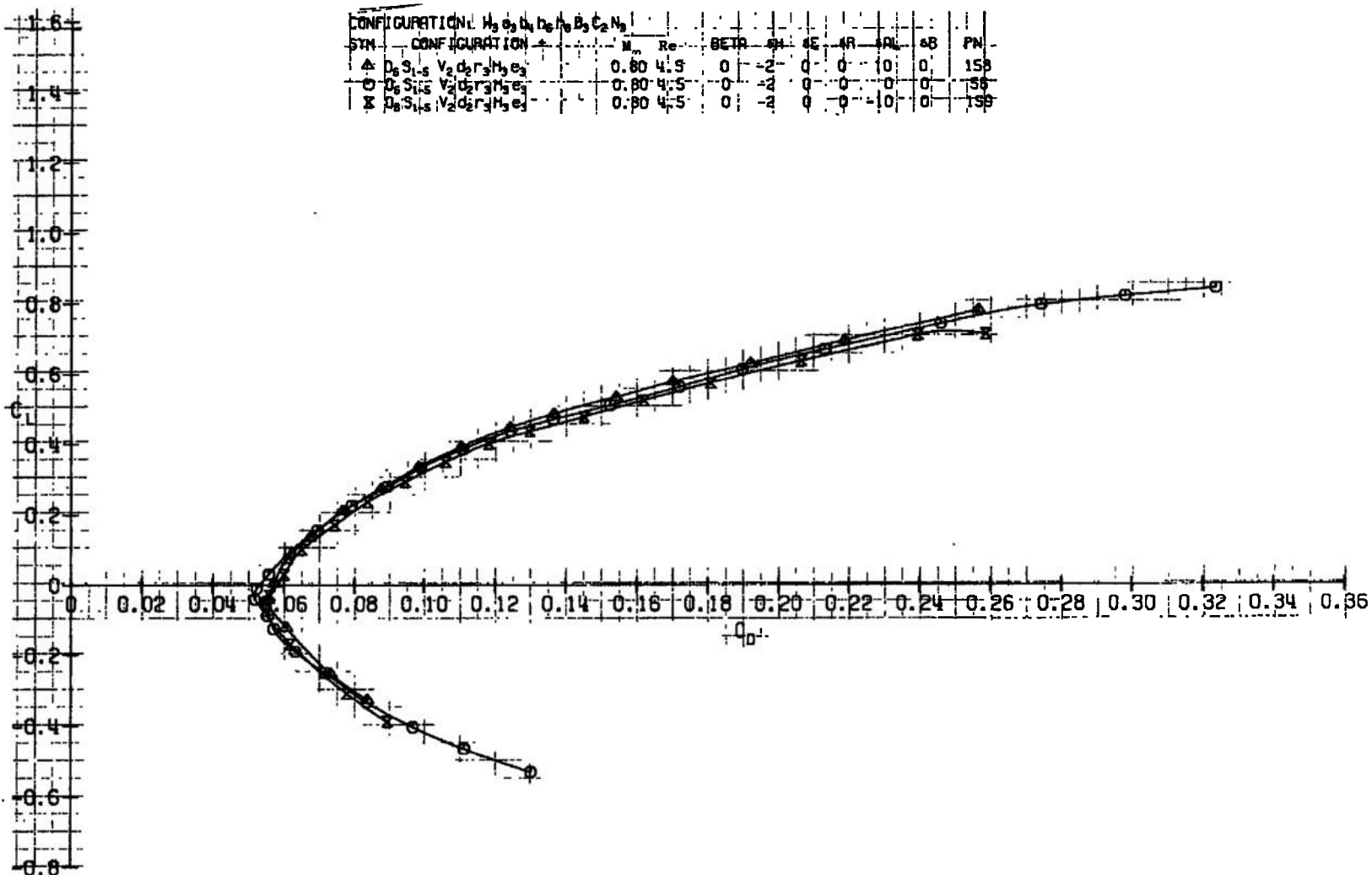
e. $M_{\infty} = 0.80$

Fig. 8 Continued

CONFIGURATION: $H_2S_1g^1 V_2d_2r_3H_3e_1$	M_∞	Re	BETA	SH	R _E	A _R	A _{RL}	A _B	PN
$D_2S_1g^1 V_2d_2r_3H_3e_1$	0.80	4.5	0	-7	0	0	0	0	150
$D_2S_1g^1 V_2d_2r_3H_3e_3$	0.80	4.5	0	-2	0	0	0	0	50
$\Delta D_2S_1g^1 V_2d_2r_3H_3e_3$	0.80	4.5	0	-2	0	0	-10	0	150

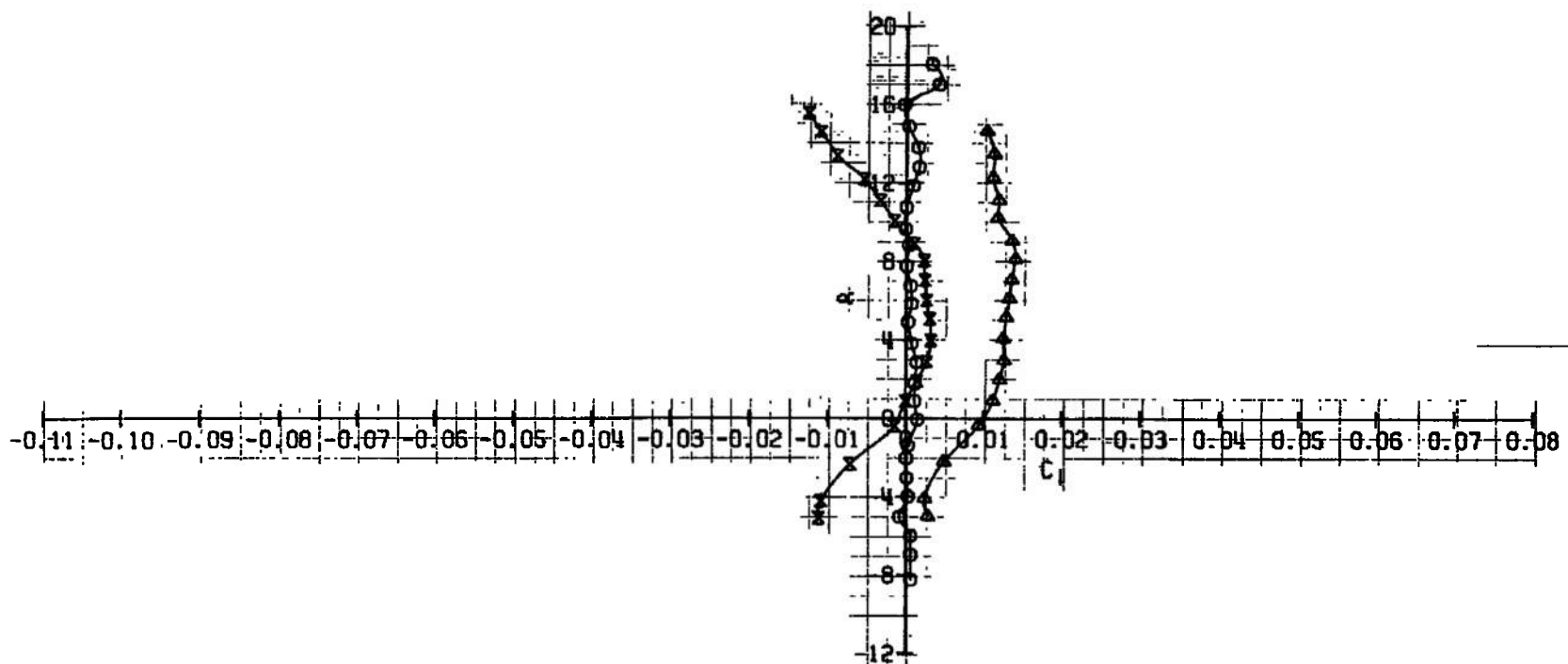


e. Continued
Fig. 8 Continued



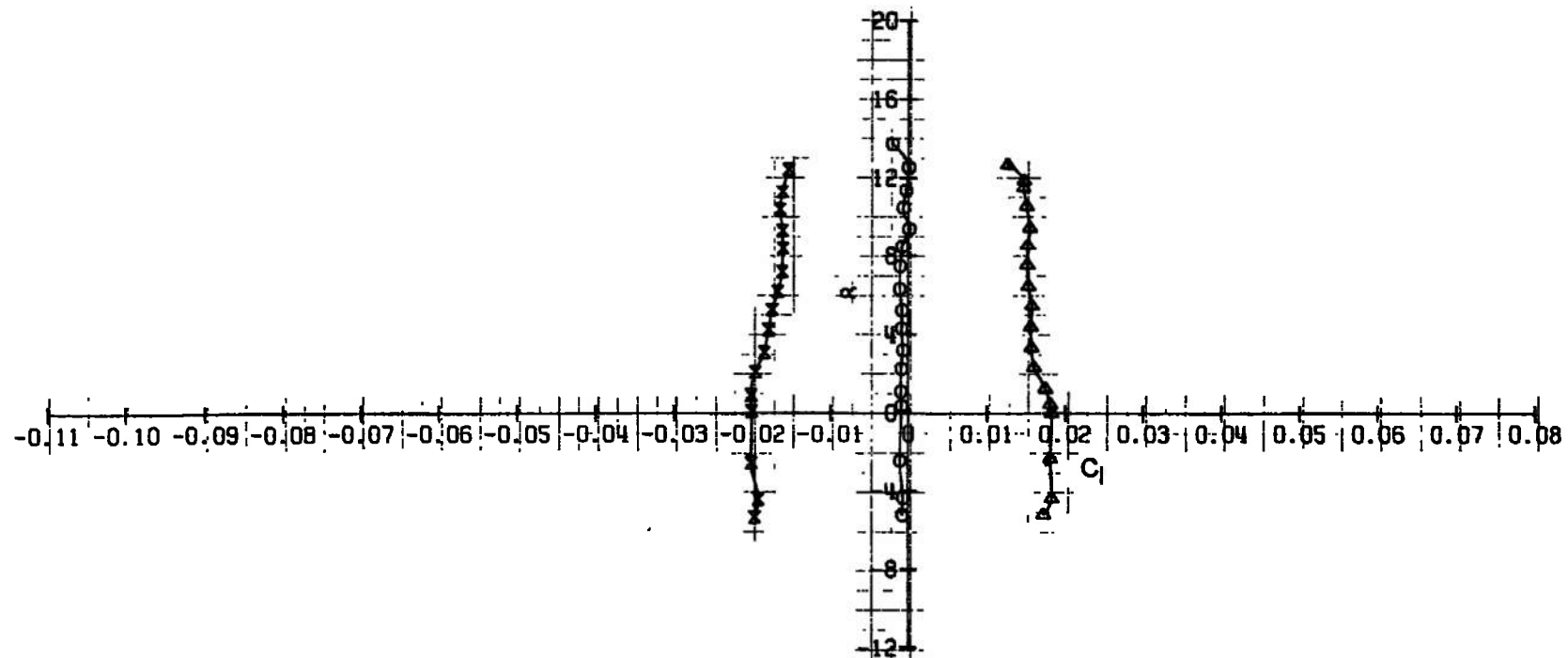
e. Continued
Fig. 8 Continued

CONFIGURATION: $H_3S_3D_3H_3B_1C_2N_3$		M ₀	R _c	BETH	SH	SF	AB	BC	AC	AB	PML
△	D ₆ S ₁₋₅ V ₂ D ₂ r ₃ H ₃ e ₃	-0.60	4.5	-	0	2	0	0	10	0	150
○	D ₆ S ₁₋₅ V ₂ D ₂ r ₃ H ₃ e ₃	0.60	4.5	-	0	2	0	0	0	0	150
X	D ₆ S ₁₋₅ V ₂ D ₂ r ₃ H ₃ e ₃	0.80	4.5	-	0	2	0	0	10	0	150



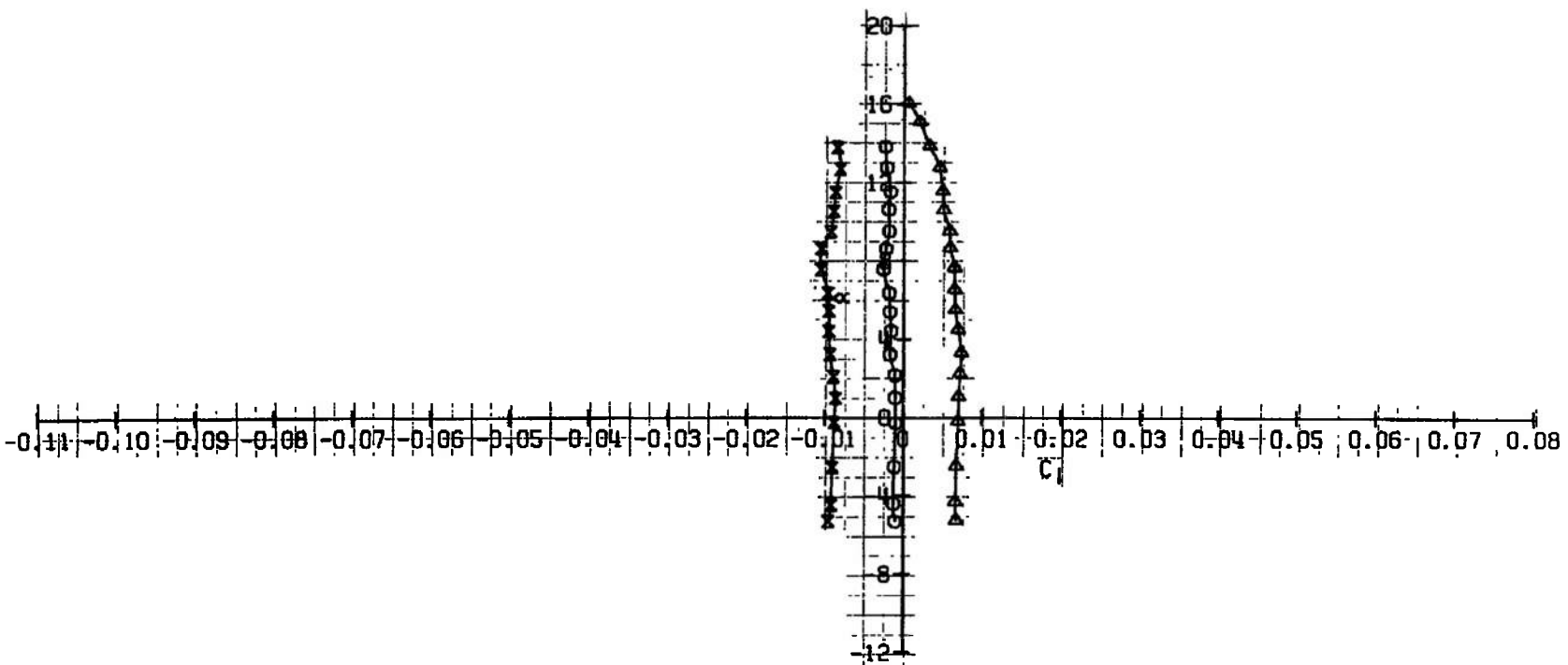
e. Concluded
Fig. 8 Continued

CONFIGURATION: $W_3 A_3 B_3 h_3 h_3 B_3 C_2 N_3$
 SYM. CONFIGURATION + N_∞ Re BETA M_L S_E S_P M_P S_B P_N
 Δ $D_3 S_{1/2} V_2 d_2 r_3 H_3 e_3$ 0.75 4.5 0 -2 0 0 10 20 180
 \circ $D_3 S_{1/2} V_2 d_2 r_3 H_3 e_3$ 0.75 4.5 0 -2 0 0 10 20 179
 \times $D_3 S_{1/2} V_2 d_2 r_3 H_3 e_3$ 0.75 4.5 0 -2 0 0 10 20 179



f. $M_\infty = 0.75$
Fig. 8 Continued

SYM.	CONFIGURATION	M_∞	Re	BETA	SH	AF	AB	AN	AB	PN
Δ	D ₈ S ₁ S ₁ V ₂ d ₃ r ₃ H ₃ e ₃	1	0.75	4.5	0	-2	0	10	60	196
○	D ₈ S ₁ S ₁ V ₂ d ₃ r ₃ H ₃ e ₃	1	0.75	4.5	0	-2	0	0	60	195
×	D ₈ S ₁ S ₁ V ₂ d ₃ r ₃ H ₃ e ₃	1	0.75	4.5	0	-2	0	-10	60	194



f. Concluded
Fig. 8 Continued

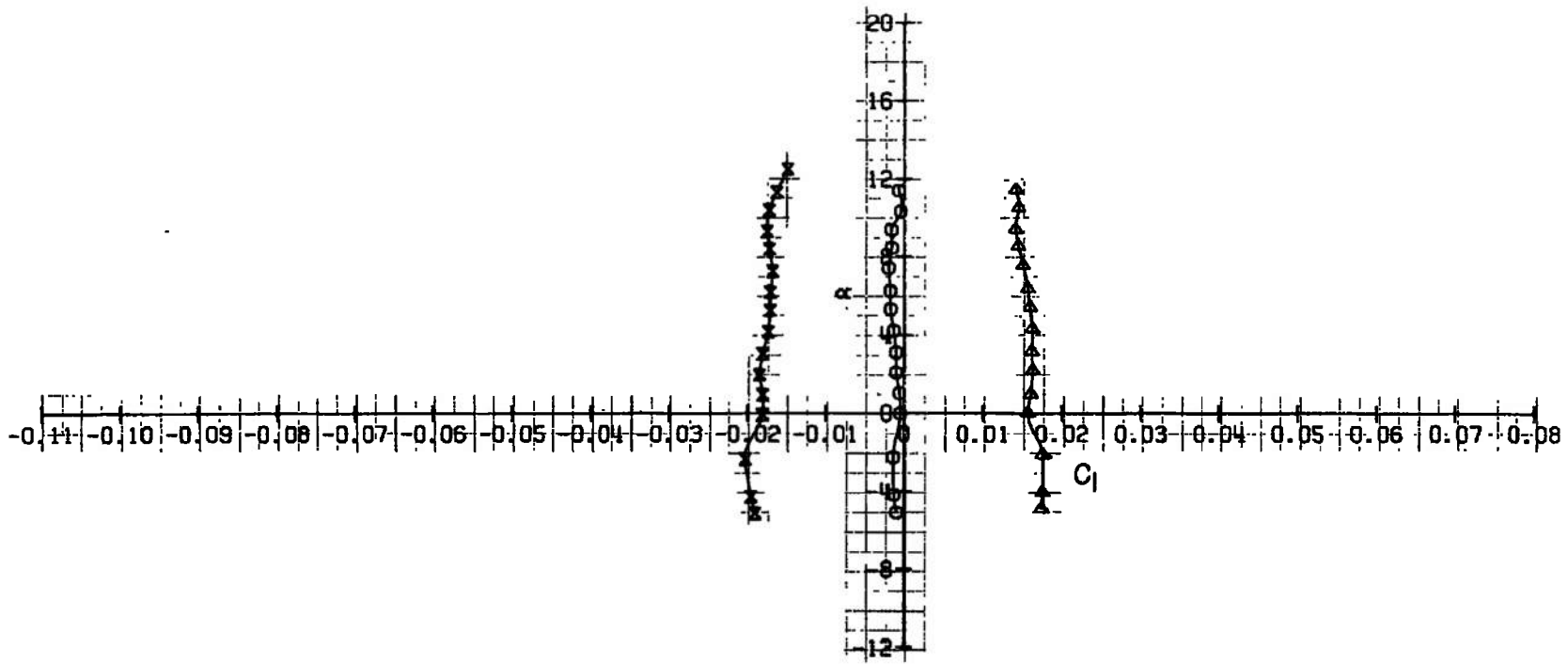
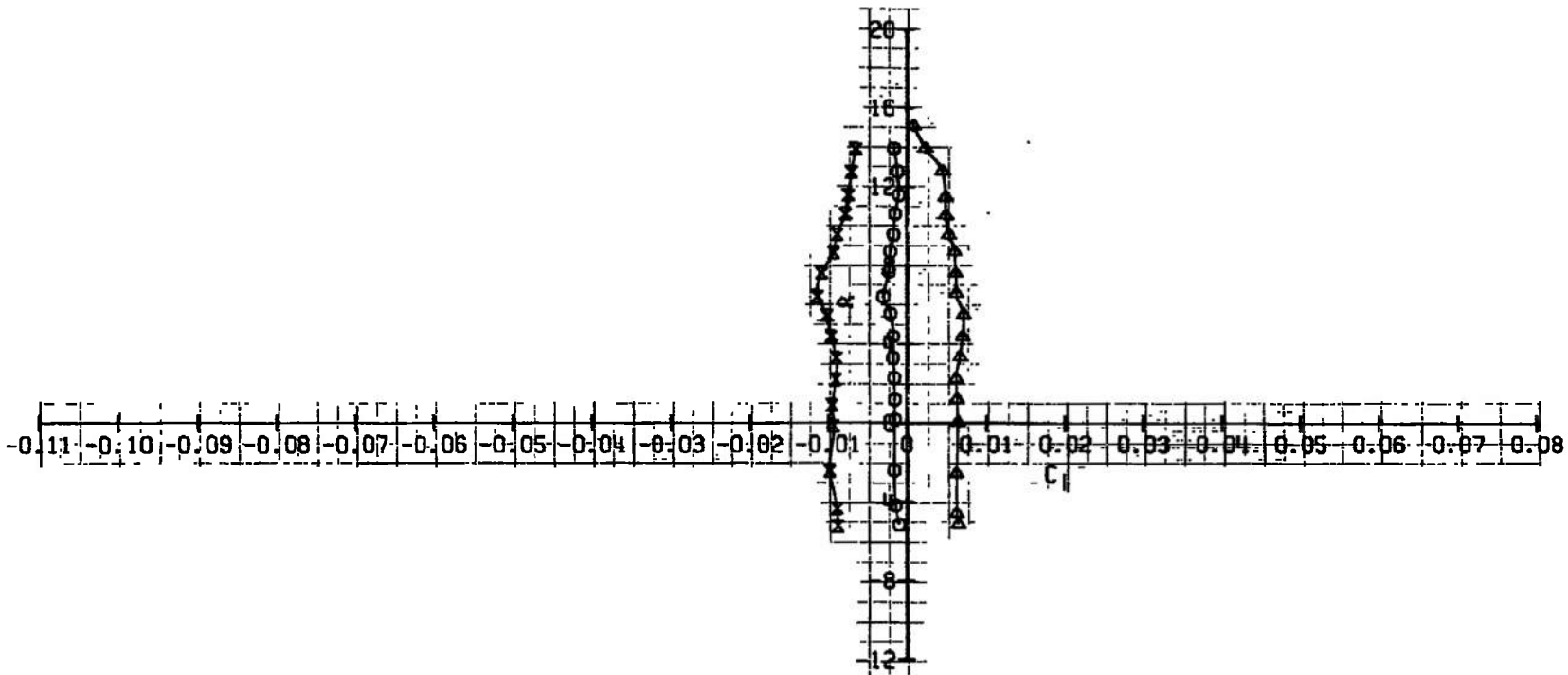


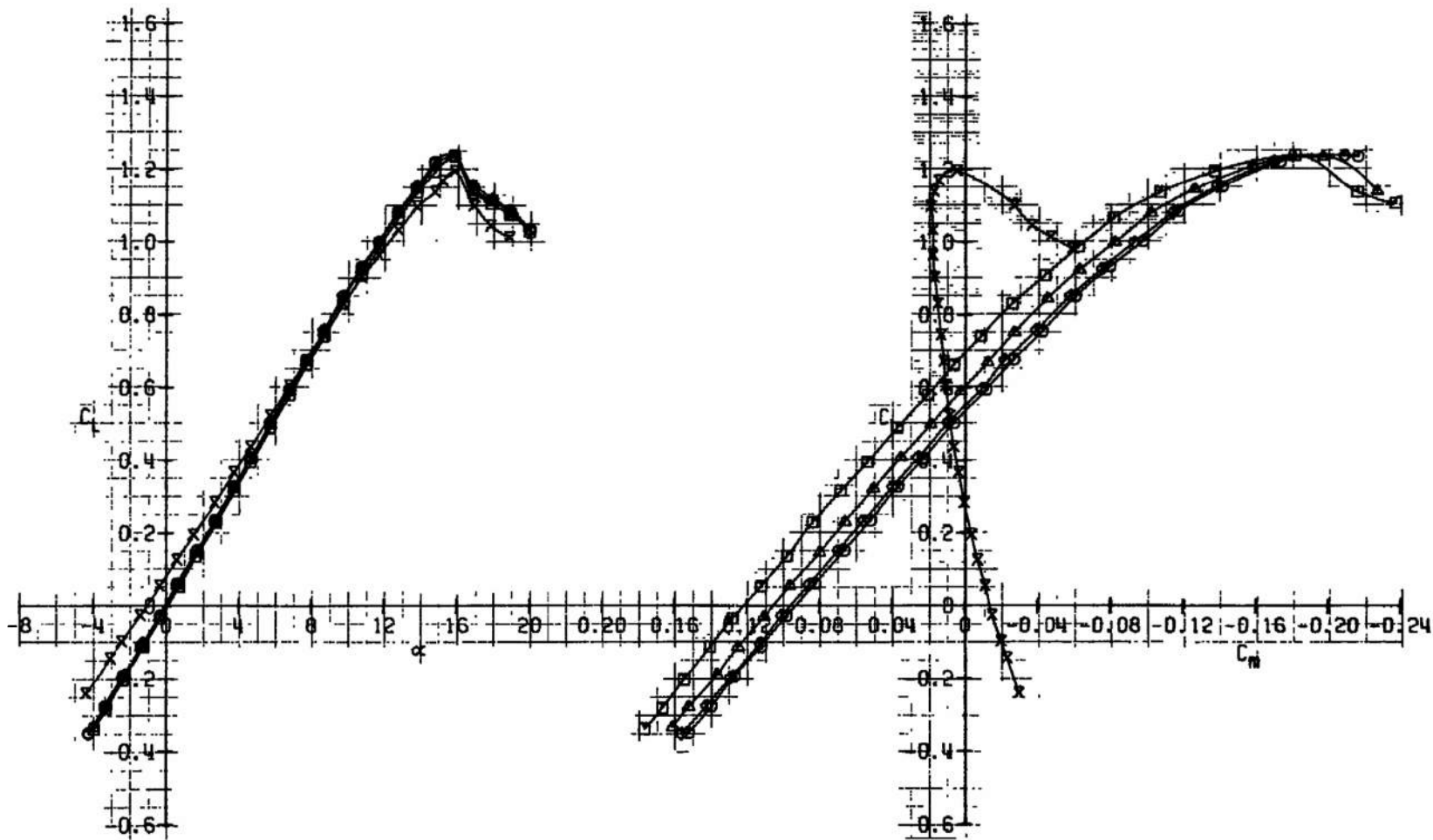
Fig. 8 Continued

CONFIGURATION: W ₃ S ₃ D ₃ H ₃ H ₃ B ₃ C ₂ N ₃		M _a	Re	BETR	AM	AF	AR	AC	AB	PW	
SYM	CONFIGURATION										
△	D ₃ S _{1,6} V ₂ D ₂ r ₃ H ₃ C ₃		0.80	4.5	0	2	0	0	10	60	191
○	D ₃ S _{1,6} V ₂ D ₂ r ₃ H ₃ C ₃		0.80	4.5	0	2	0	0	10	60	192
×	D ₃ S _{1,6} V ₂ D ₂ r ₃ H ₃ C ₃		0.80	4.5	0	2	0	0	-10	60	193



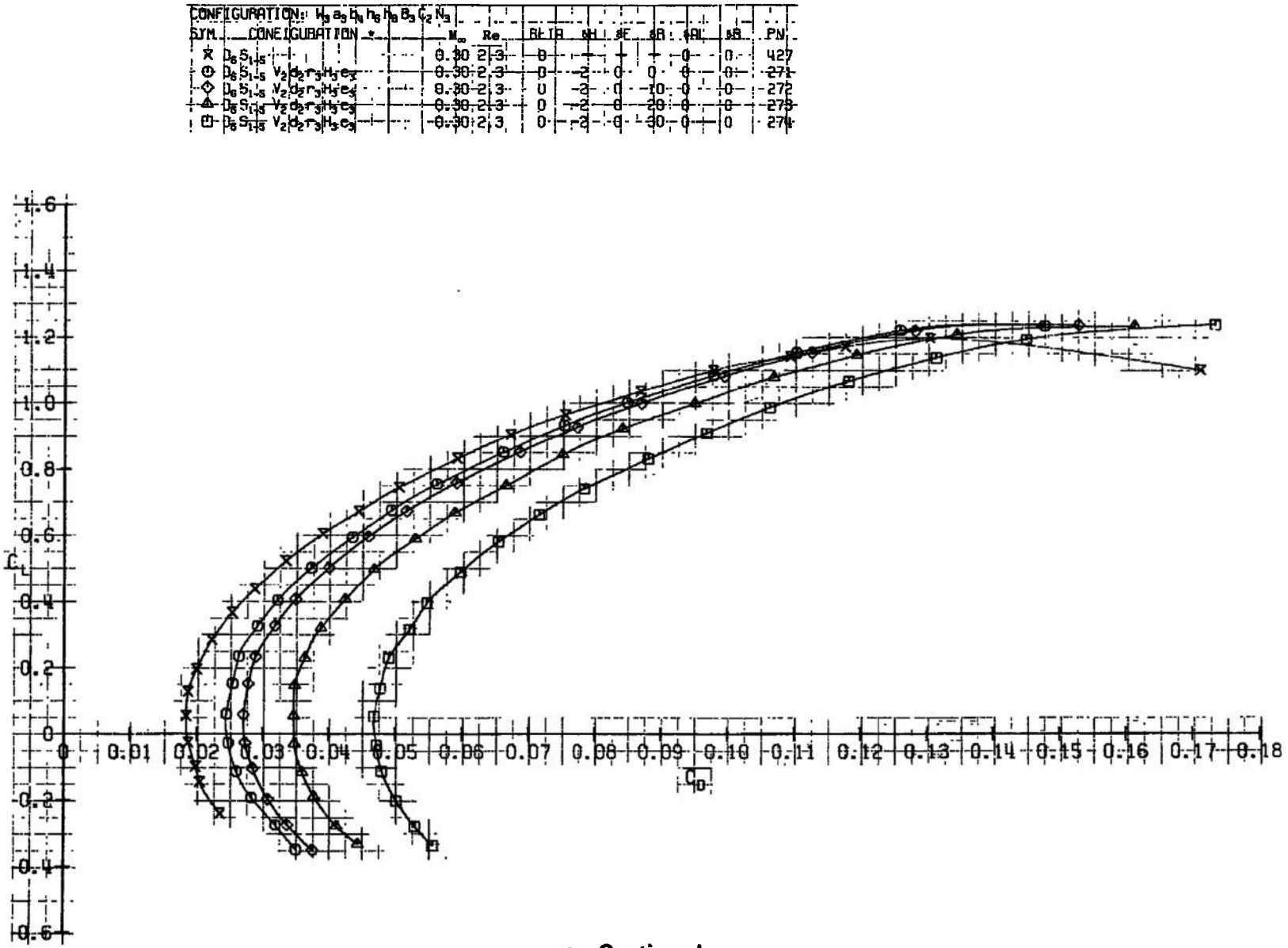
g. Concluded
Fig. 8 Concluded

CONFIGURATION: H_3 a_3 b_4 b_6 b_8 B_3 C_2 H_1							
SYM	CONFIGURATION	M_∞	Re	REF ID	W1	AF	AR
X	$D_6 S_1 S_5 T$	0.30	2.3	0	0	0	427
O	$B_6 S_1 S_3 V_2 d_2 r_3 h_2 e_3$	0.30	2.3	0	0	0	271
O	$D_6 S_1 S_3 V_2 d_2 r_3 h_2 e_3$	0.30	2.3	0	2	0	272
△	$D_6 S_1 S_5 V_2 d_2 r_3 h_2 e_3$	0.30	2.3	0	2	0	273
□	$B_6 S_1 S_5 V_2 d_2 r_3 h_2 e_3$	0.30	2.3	0	2	0	274



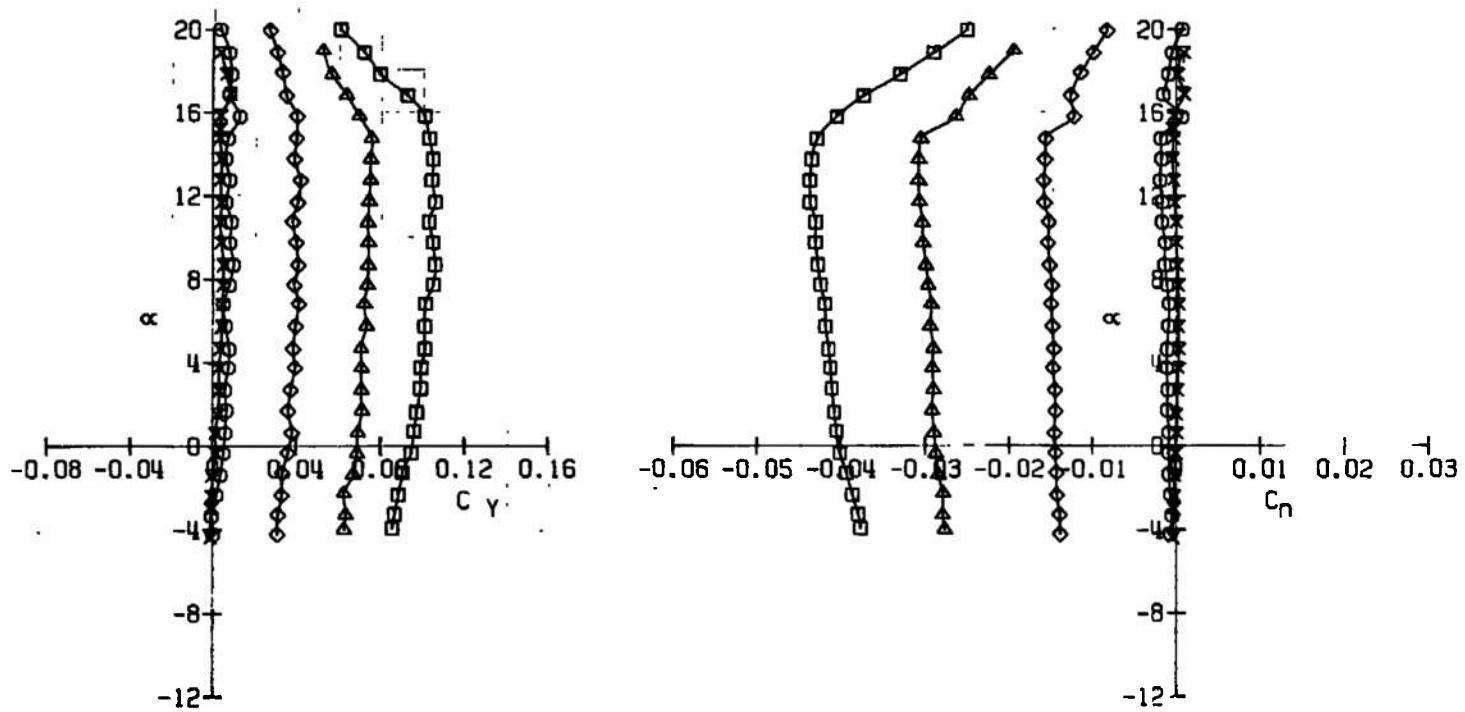
a. $M_\infty = 0.30$

Fig. 9 Rudder Effectiveness



a. Continued
Fig. 9 Continued

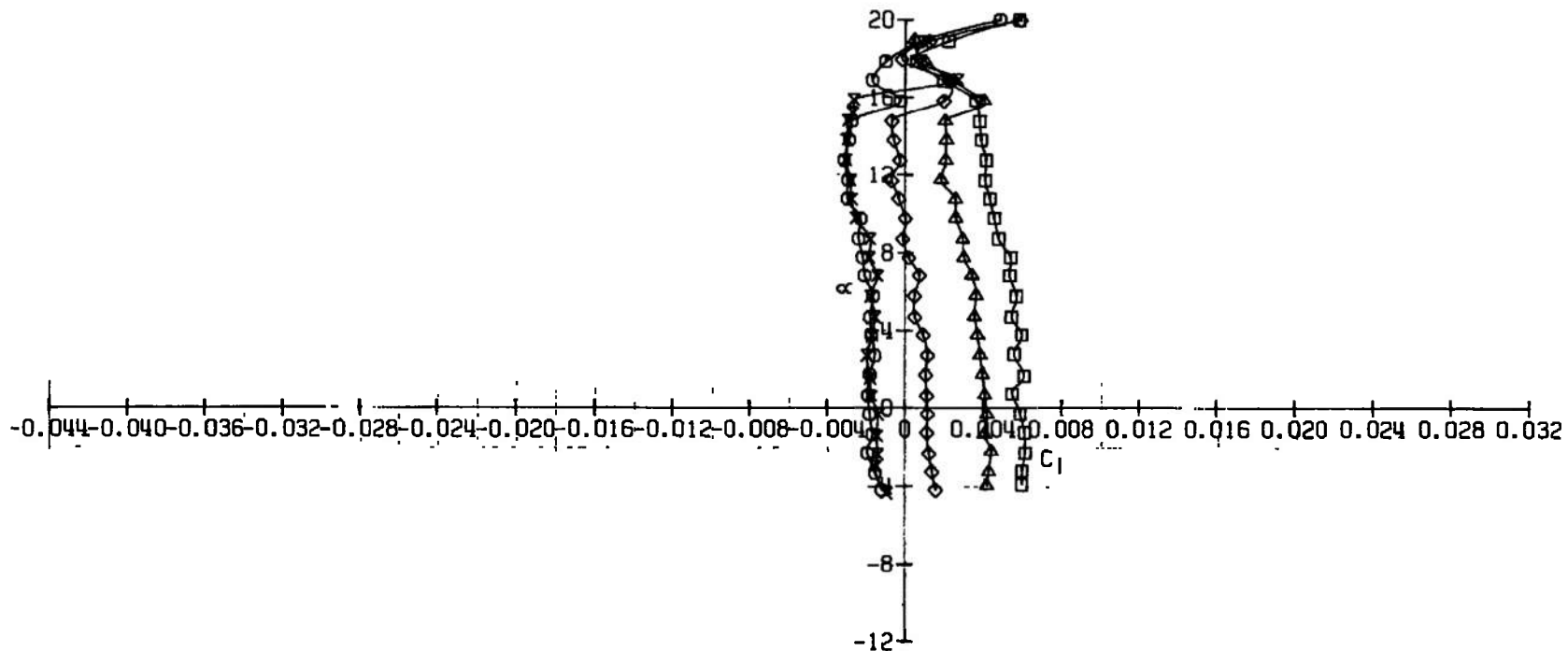
CONFIGURATION: $H_3e_3b_4h_6h_8B_3C_2N_3$		M _w	Re	BETA	SH	SE	SR	SL	BB	PN
X	D ₆ S ₁₋₅	0.30	2.3	0	-	-	-	0	0	427
O	D ₆ S ₁₋₅ V ₂ d ₂ r ₃ H ₃ e ₃	0.30	2.3	0	-	-	0	0	0	271
◊	D ₆ S ₁₋₅ V ₂ d ₂ r ₃ H ₃ e ₃	0.30	2.3	0	0	0	10	0	0	272
△	D ₆ S ₁₋₅ V ₂ d ₂ r ₃ H ₃ e ₃	0.30	2.3	0	0	0	20	0	0	273
□	D ₆ S ₁₋₅ V ₂ d ₂ r ₃ H ₃ e ₃	0.30	2.3	0	0	0	30	0	0	274



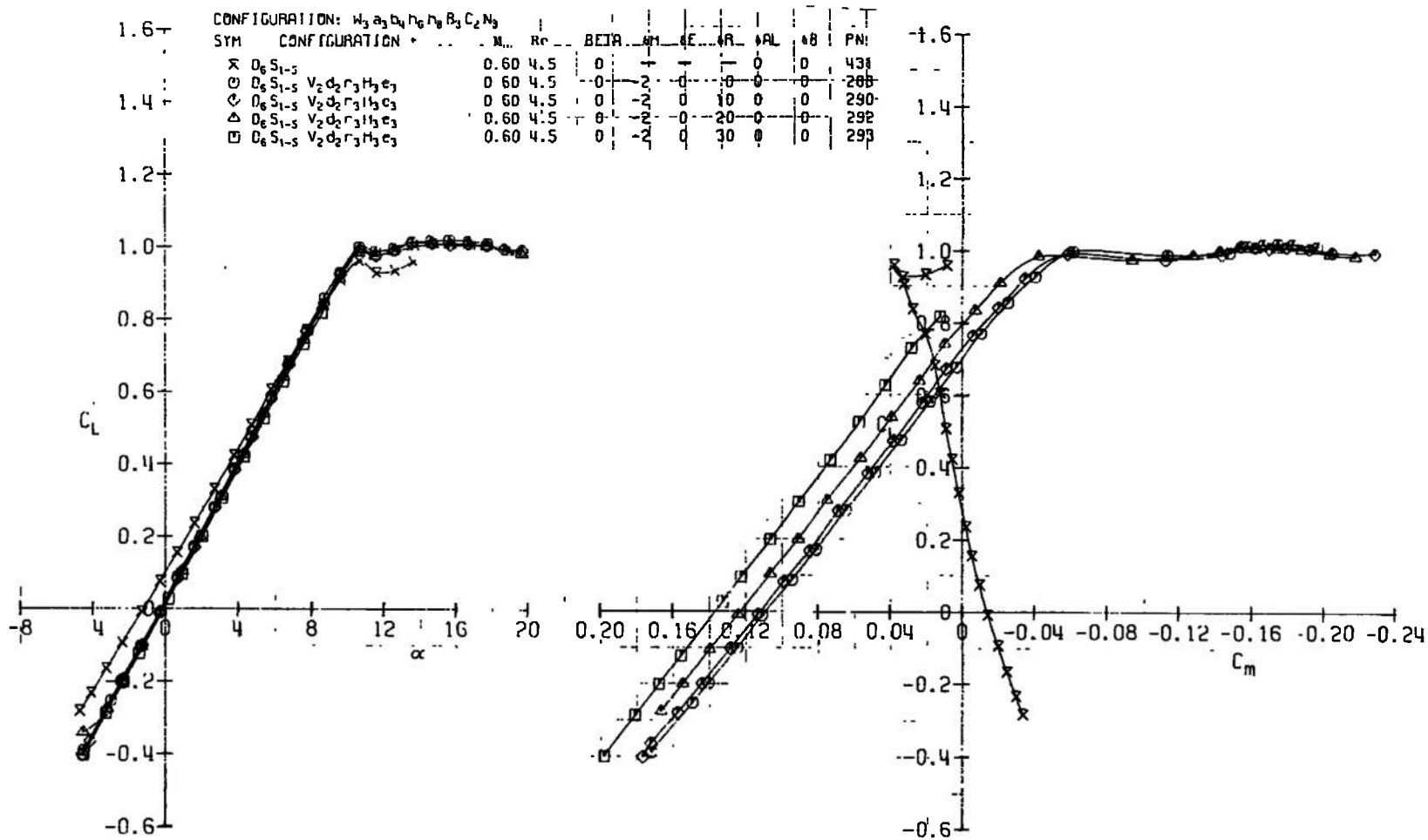
a. Continued
Fig. 9 Continued

CONFIGURATION: $H_3 a_3 b_3 h_6 h_9 B_3 C_2 N_3$

SYM	CONFIGURATION	+	M _w	R _c	BETA	SH	SE	SR	SRL	SB	PN
X	D ₆ S ₁₋₅		0.30	2.3	0	-1	-1	-1	0	0	427
O	D ₆ S ₁₋₅ V ₂ d ₂ r ₃ H ₃ e ₃		0.30	2.3	0	-2	0	0	0	0	271
◊	D ₆ S ₁₋₅ V ₂ d ₂ r ₃ H ₃ e ₃		0.30	2.3	0	-2	0	10	0	0	272
△	D ₆ S ₁₋₅ V ₂ d ₂ r ₃ H ₃ e ₃		0.30	2.3	0	-2	0	20	0	0	273
□	D ₆ S ₁₋₅ V ₂ d ₂ r ₃ H ₃ e ₃		0.30	2.3	0	-2	0	30	0	0	274

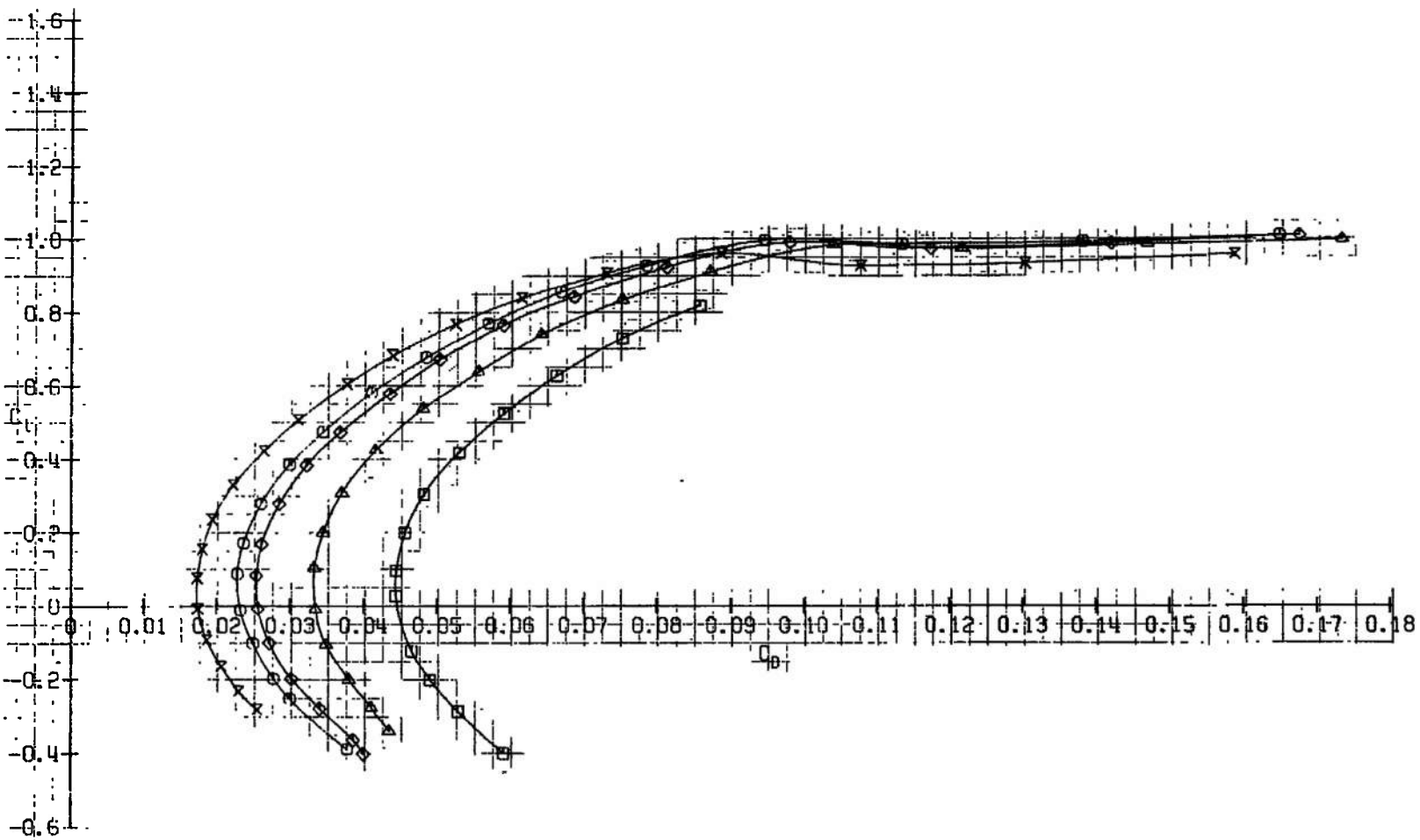


a. Concluded
Fig. 9 Continued



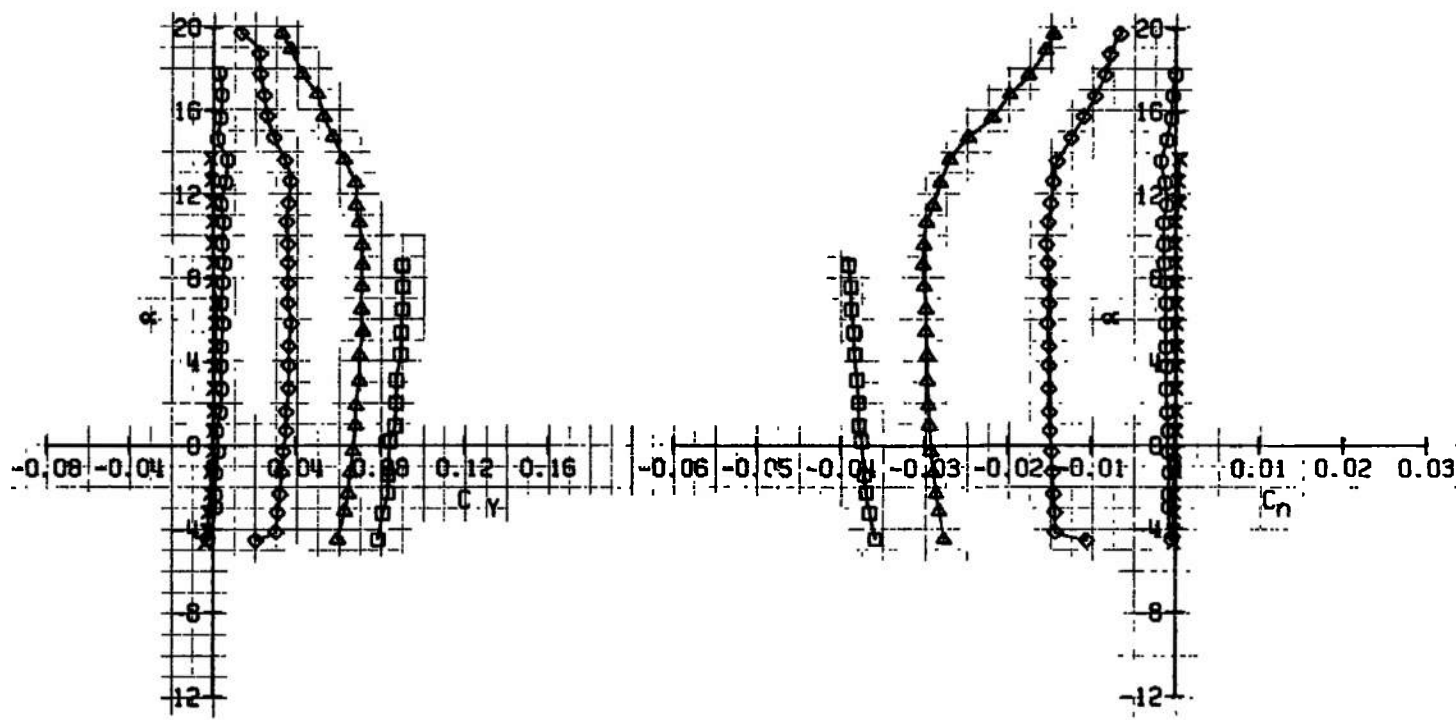
b. $M_\infty = 0.60$
Fig. 9 Continued

SYM.	CONFIGURATION	M_∞	Re	BETA	AH	AF	AG	AR	PN
X	D ₆ S ₁₋₅	0.60	475	0	2	0	0	0	431
O	D ₆ S ₁₋₅ V ₂ d ₃ r ₃ t ₃ e ₃	0.60	475	0	2	0	0	0	266
D	D ₆ S ₁₋₅ V ₂ d ₂ r ₃ t ₃ e ₃	0.60	475	0	2	0	10	0	290
A	D ₆ S ₁₋₅ V ₂ d ₂ r ₃ t ₃ b ₃ e ₃	0.60	475	0	2	0	20	0	256
D	D ₆ S ₁₋₅ V ₂ d ₂ r ₃ t ₃ b ₃ e ₃	0.60	475	0	2	0	30	0	295



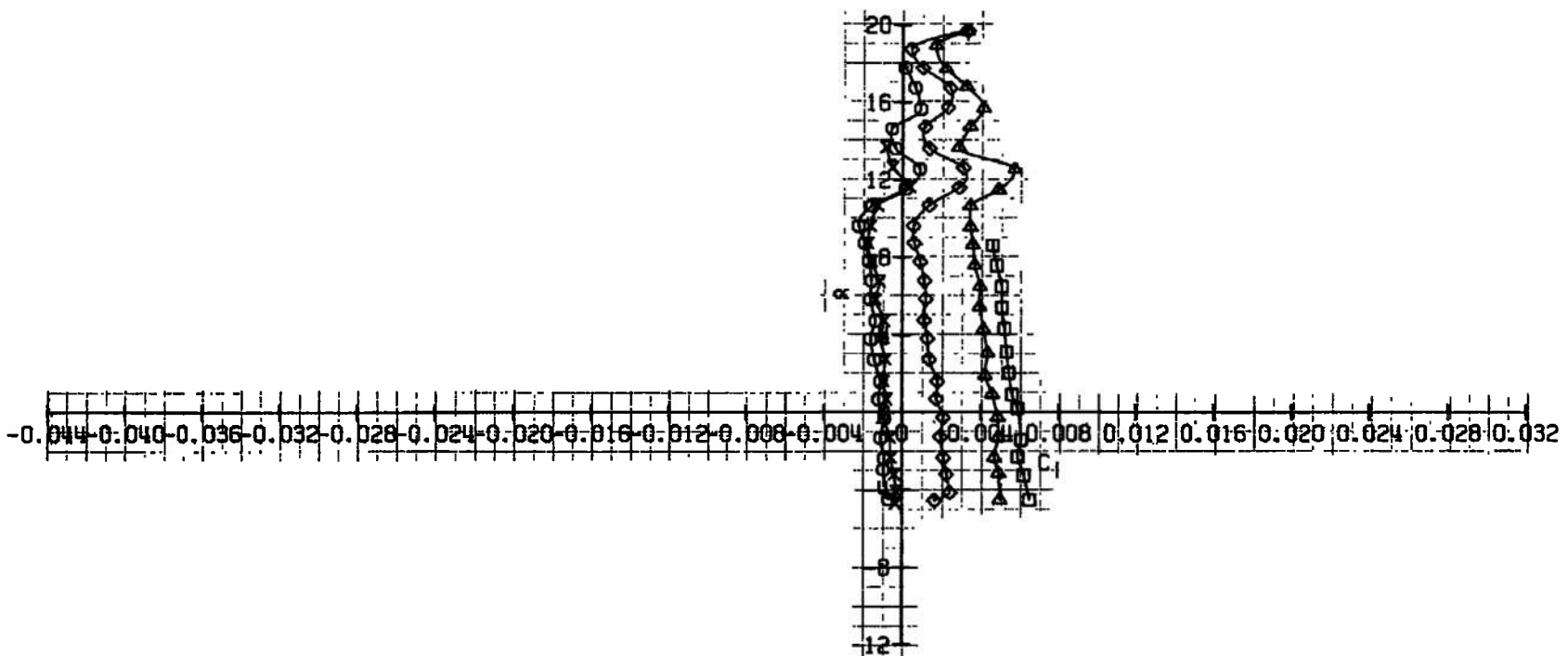
b. Continued
Fig. 9 Continued

SYM.	CONFIGURATION: N_2 σ_1^2 π_1^2 π_2^2 δ_1^2 δ_2^2 N_2	M _∞	Re	BETR	RH	RE	ANL	MB	PW
X	$S_{1,4}$	0.60	4.5	0	0	0	0	0	491
O	$S_{1,4}^2$ V_2 δ_1^2 π_1^2 π_2^2	0.60	4.5	0	0	0	0	0	289
D	$S_{1,4}^2$ V_2 δ_1^2 π_1^2 δ_2^2	0.60	4.5	0	0	10	0	0	289
▲	$S_{1,4}^2$ V_2 δ_1^2 π_1^2 δ_2^2	0.60	4.5	0	0	20	0	0	289
■	$S_{1,4}^2$ V_2 δ_1^2 π_1^2 δ_2^2	0.60	4.5	0	0	30	0	0	289

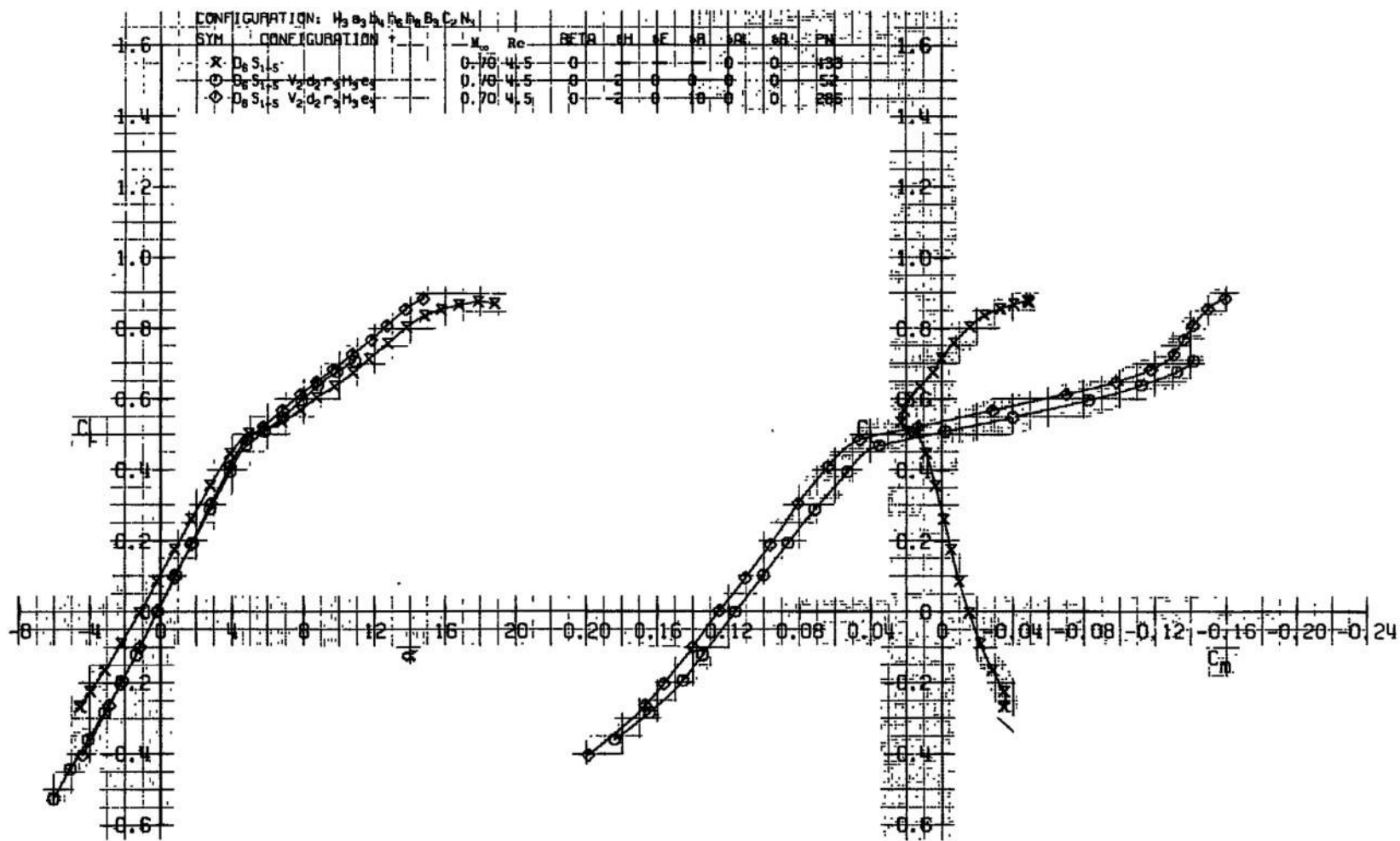


b. Continued
Fig. 9 Continued

CONFIGURATION: H ₃ S ₃ H ₃ H ₃ B ₃ C ₂ N ₃		M ₀	Re	BETA	AM	AE	AB	AL	AR	PN
SYM.	CONFIGURATION									
X	OsS ₃ H ₃		0.60	4.5	-	0	-	0	0	93
O	OsS ₃ H ₃ V ₂ deT ₃ H ₃ C ₃		0.60	4.5	-	2	0	0	0	288
D	OsS ₃ H ₃ V ₂ deT ₃ H ₃ C ₃		0.60	4.5	-	2	0	0	0	289
A	OsS ₃ H ₃ V ₂ deT ₃ H ₃ C ₃		0.60	4.5	-	2	0	0	0	292
-D	OsS ₃ H ₃ V ₂ deT ₃ H ₃ C ₃		0.60	4.5	-	2	0	0	0	293

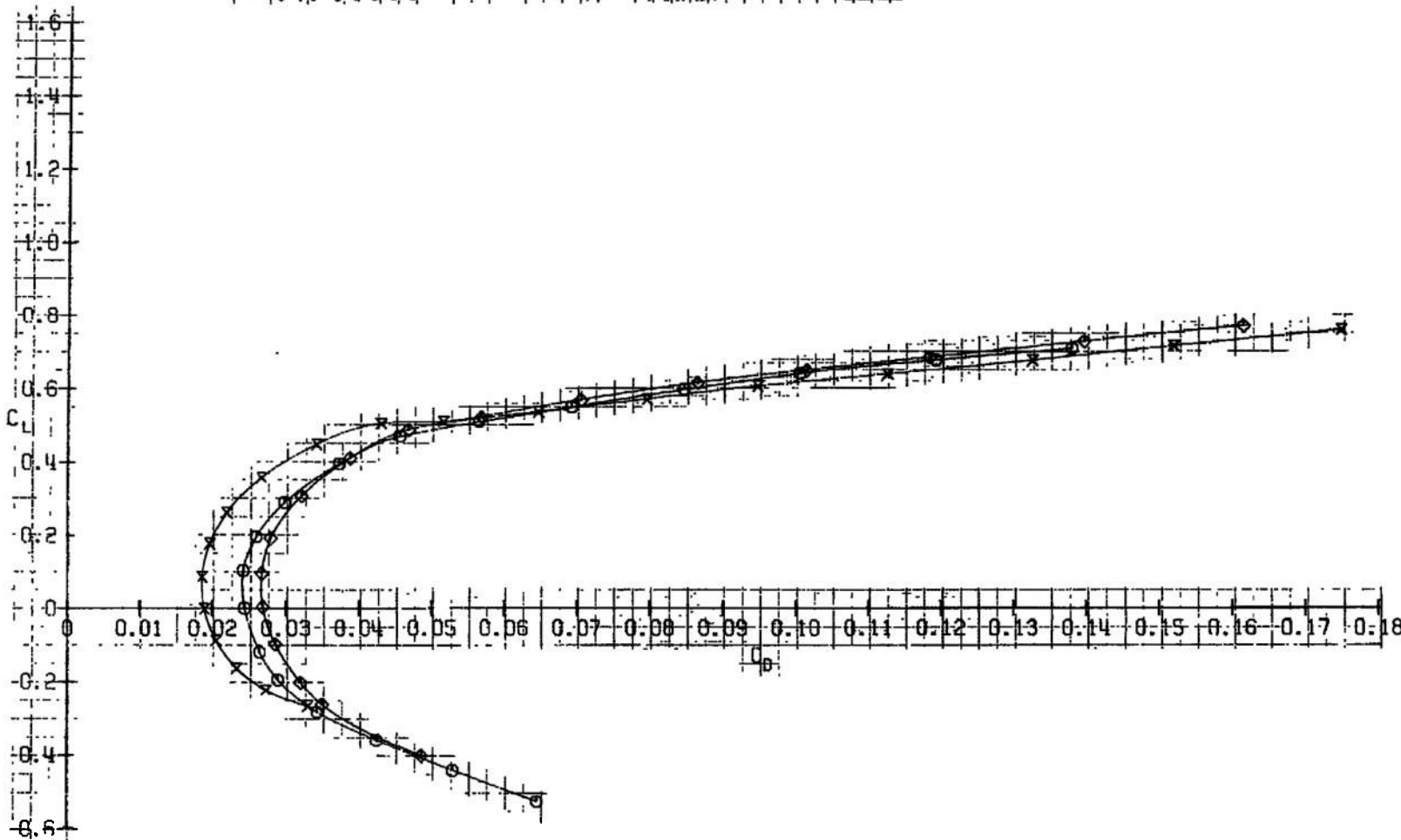


b. Concluded
Fig. 9 Continued



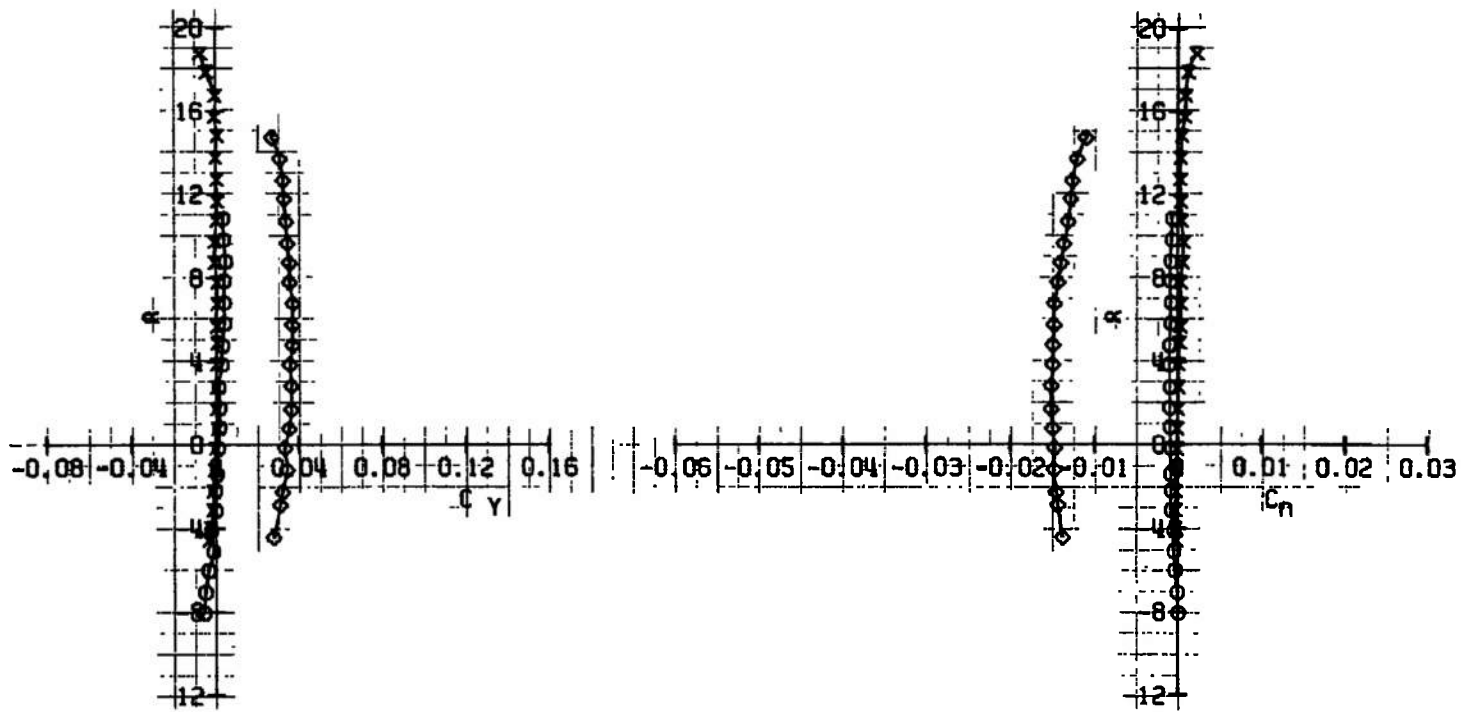
c. $M_\infty = 0.70$
Fig. 9 Continued

CONFIGURATION: $W_3 a_3 b_3 h_3 t_3 B_3 C_2 H_3$		Re	RFTD	SP	AB	BL	AB	BL	PN
SYM	CONFIGURATION								
X	$D_6 S_1 T_3$	0.70	4.5	P	0	0	0	0	130
O	$B_6 S_1 T_3 V_2 M_2 r_3 H_3 e_3$	0.70	4.5	P	2	0	0	0	132
◊	$D_6 S_1 T_3 V_2 M_2 r_3 H_3 e_3$	0.70	4.5	P	2	0	10	0	230



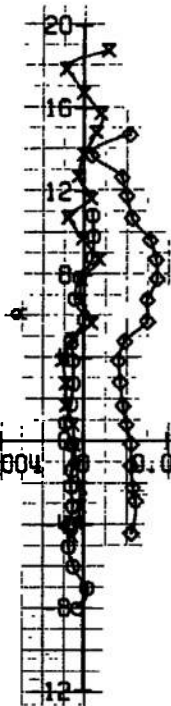
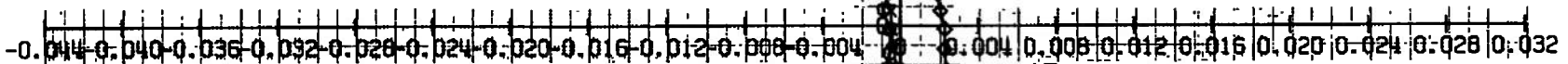
c. Continued
Fig. 9 Continued

CONFIGURATION: $H_2O_2 + H_2O + H_2 + O_2 + N_2$		x_w	Re	SETR	SH	SC	AB	PN
X	$D_{2,5,1,6}$	-0.70	4.5	0	0	0	0	435
O	$D_{2,5,1,6} \cap D_{2,5,1,7,8,9}$	-0.70	4.5	0	0	0	0	58
◊	$D_{2,5,1,6} \cap D_{2,5,1,7,8,9}$	-0.70	4.5	0	-1	0	10	285

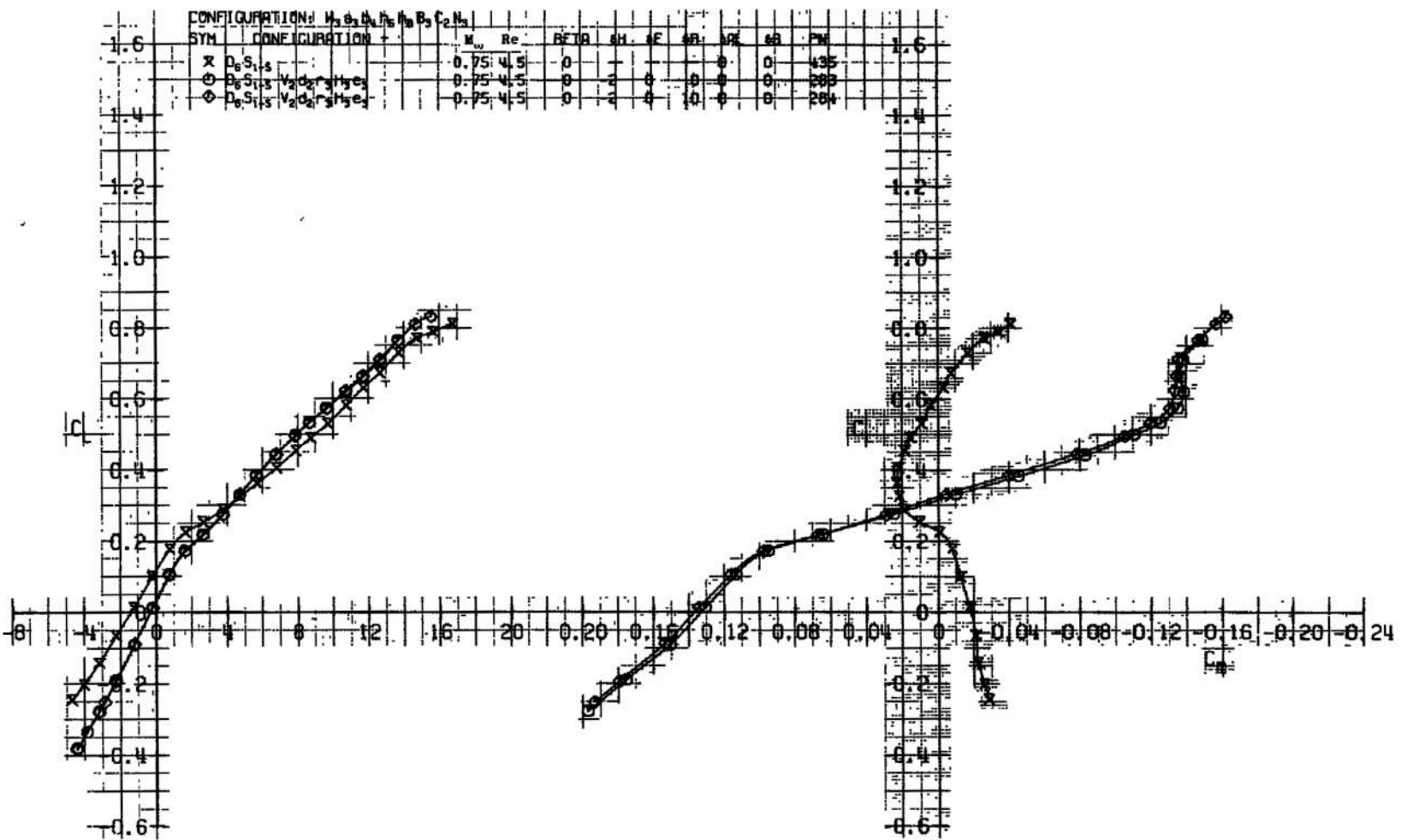


c. Continued
Fig. 9 Continued

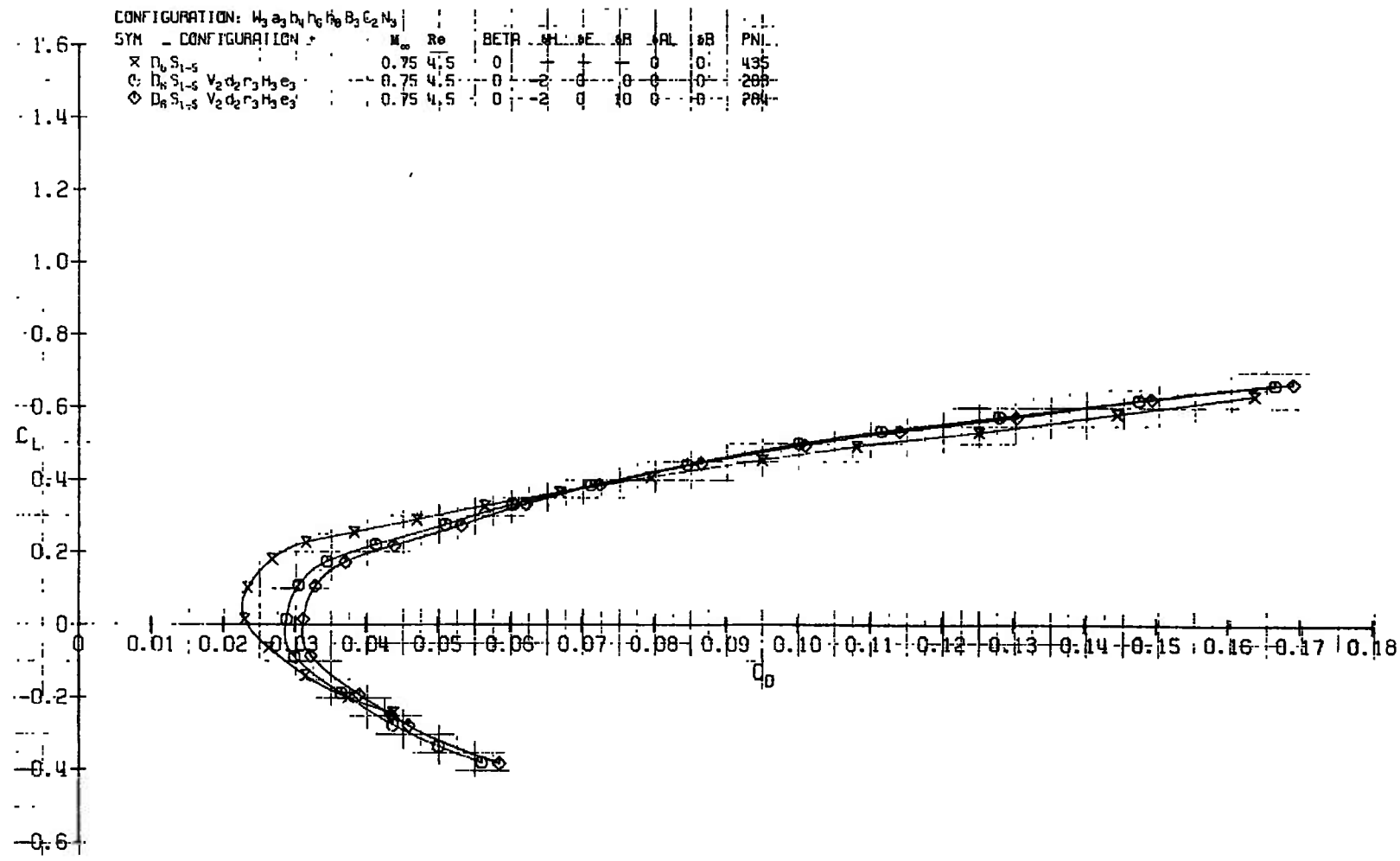
CONFIGURATION: H ₃ S ₃ B ₃ H ₃ B ₃ C ₂ N ₃		M _o	Re	BETD	SH	SE	AB	ACI	AB	PN
SYM.	CONFIGURATION									
X	D ₆ S ₁ H ₅	0.70	4.5	0	-	0	0	0	0	439
O	D ₆ S ₁ H ₅ V ₂ d ₂ r ₃ H ₃ e ₃	0.70	4.5	0	-2	0	0	0	0	52
◊	D ₆ S ₁ H ₅ V ₂ d ₂ r ₃ H ₃ e ₃	0.70	4.5	0	-2	0	10	0	0	286



c. Concluded
Fig. 9 Continued

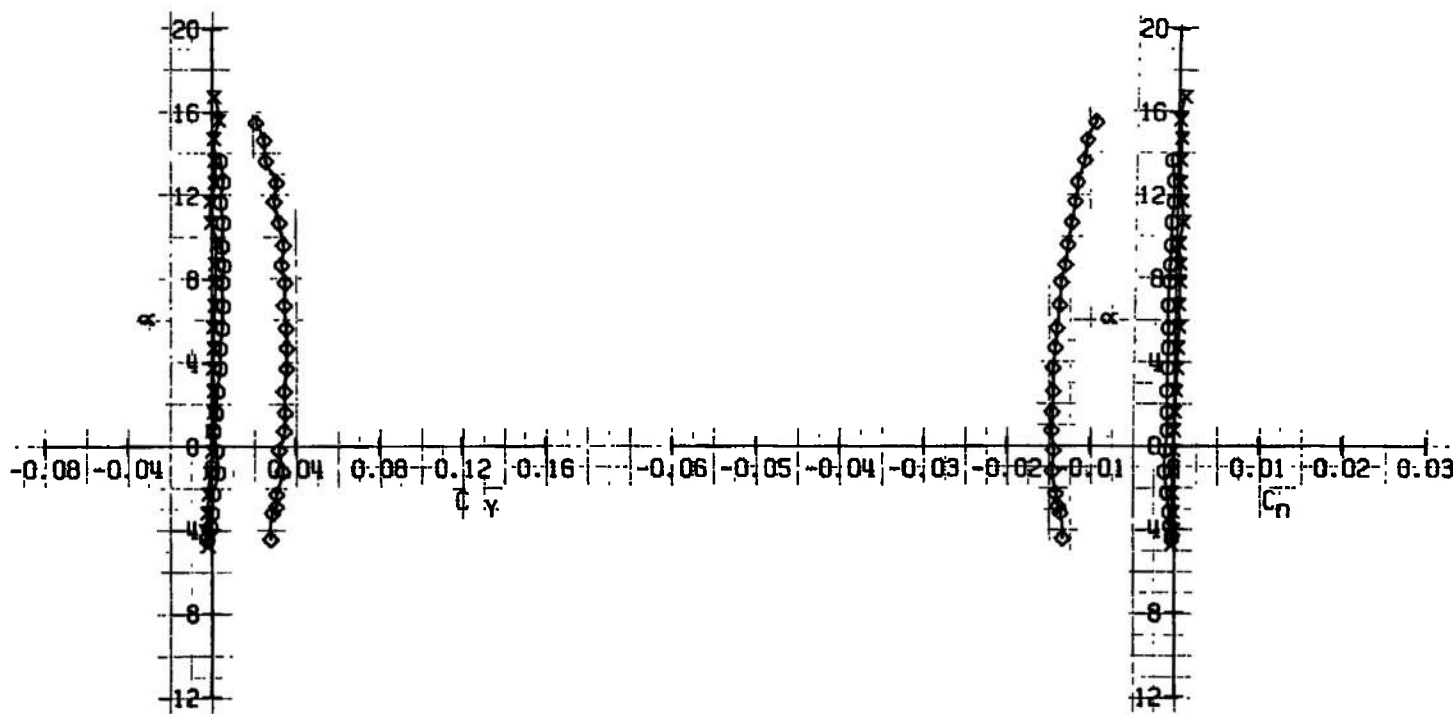


d. $M_\infty = 0.75$
Fig. 9 Continued



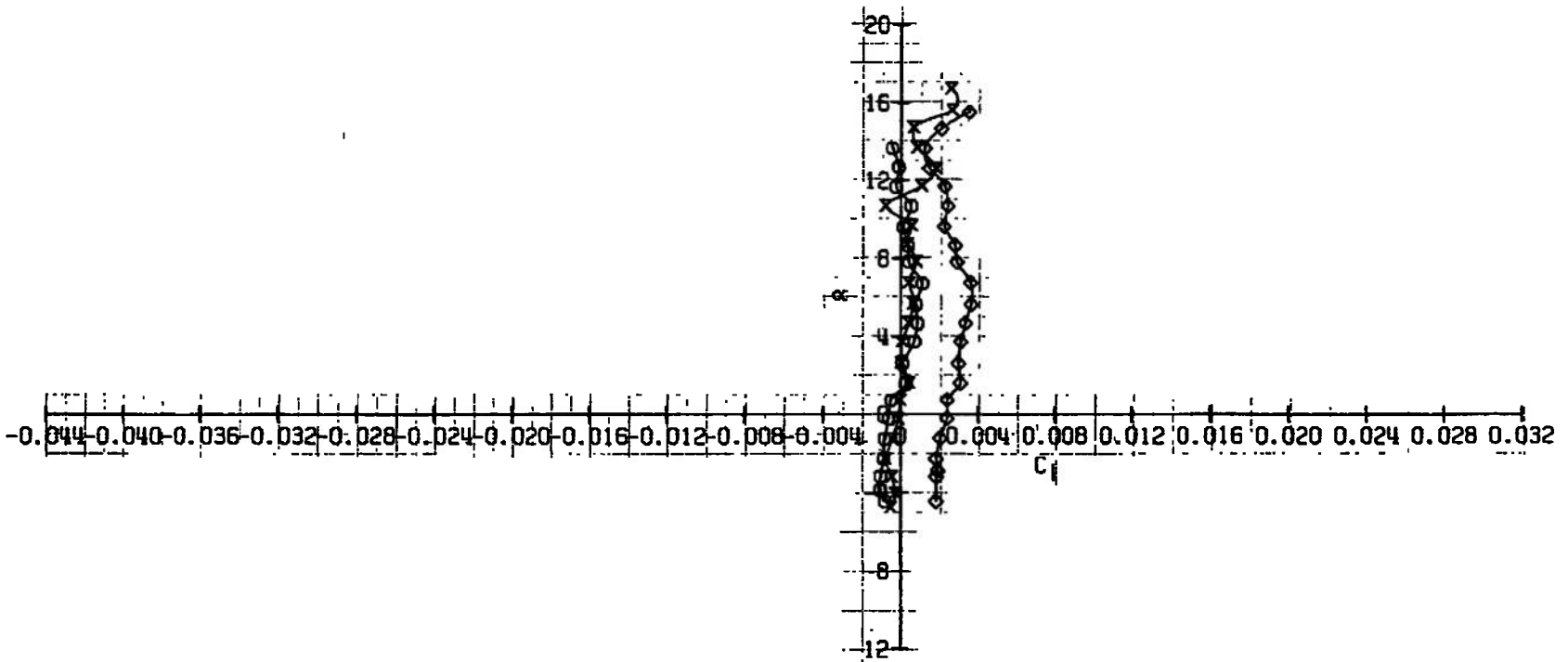
d. Continued
Fig. 9 Continued

CONFIGURATION: $H_3 a_3 b_3 h_3 h_3 B_3 C_2 N_3$
 SYM. CONFIGURATION: $D_6 S_{1-5}$
 X $D_6 S_{1-5}$ 0.75 4.5 0 + + 0 0 0 435
 O $D_6 S_{1-5} V_2 d_2 r_3 H_3 e_3$ 0.75 4.5 0 - + 0 0 0 263
 D $D_6 S_{1-5} V_2 d_2 r_3 H_3 e_3$ 0.75 4.5 0 - + 10 0 0 264



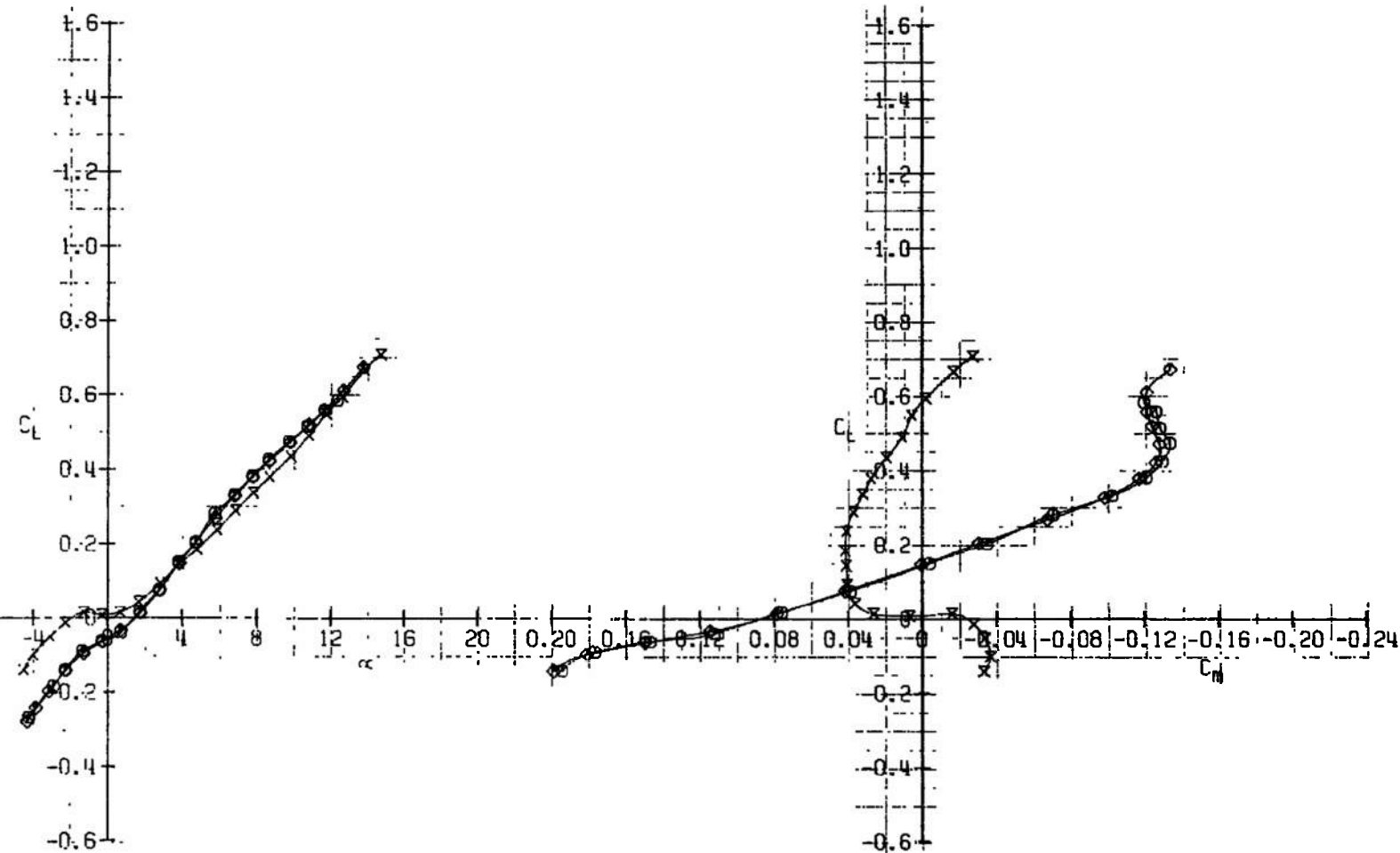
d. Continued
 Fig. 9 Continued

SYN.	CONFIGURATION	M_∞	Re	BETA	SH	ME	WB	SP	SB	PN
X	D ₀ S ₁₋₄	-	-	0.75	4.5	0	-	0	0	435
O	D ₀ S ₁₋₄ M ₂ D ₂ P ₃ R ₃ C ₃	-	-	0.75	4.5	0	2	0	0	263
Φ	D ₀ S ₁₋₄ M ₂ D ₂ P ₃ R ₃ C ₃	-	-	0.75	4.5	0	2	0	0	284



d. Concluded
Fig. 9 Continued

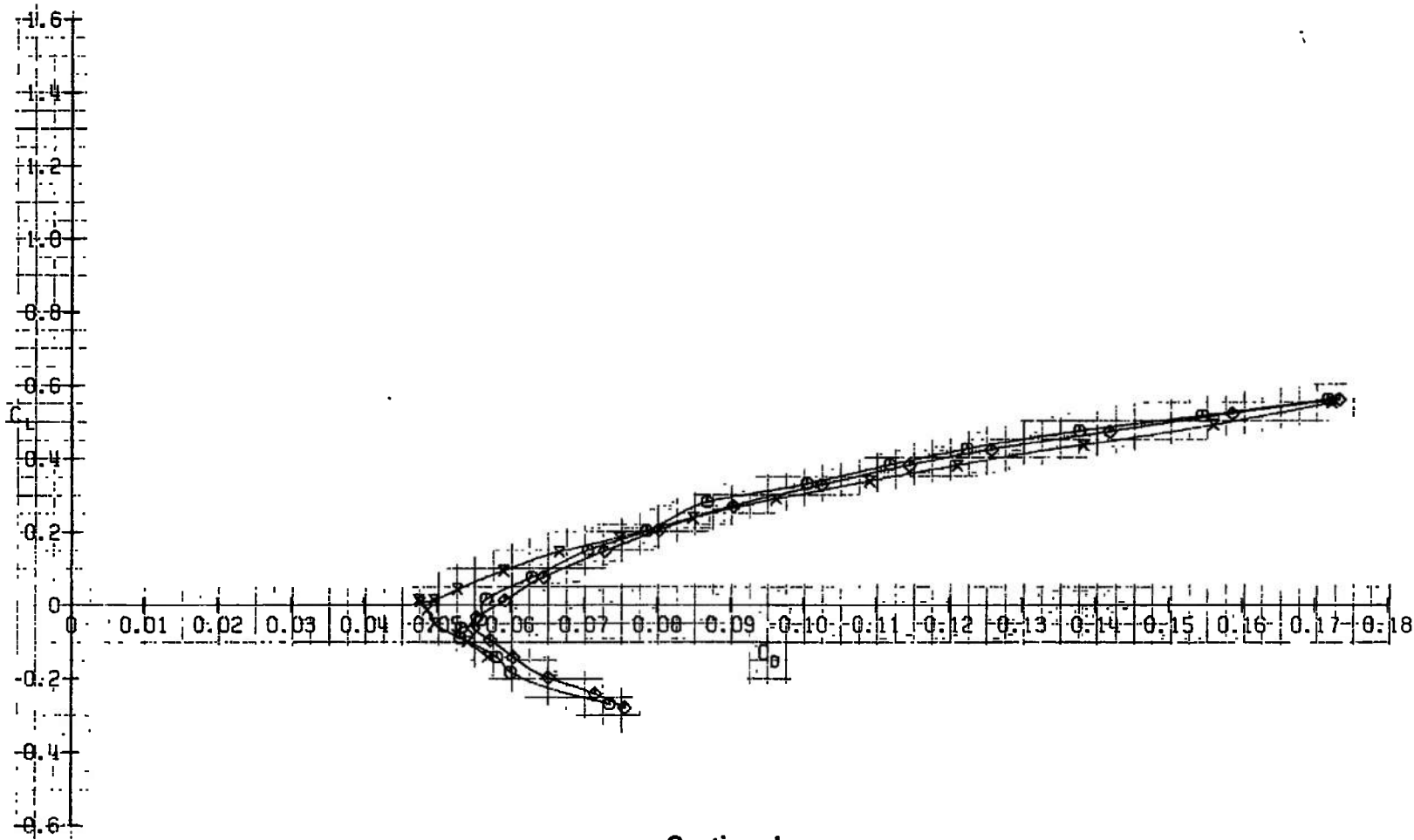
CONFIGURATION: W ₃ S ₃ H ₆ H ₆ B ₃ C ₂ N ₃	M _∞	Re	BE1B	SH	SE	SR	MR	LR	PN
X D ₆ S _{1,5}	-	-	0.80	4.5	-	0	-	0	437
O D ₆ S _{1,5} V ₂ D ₂ r ₃ H ₃ e ₃	-	-	0.80	4.5	-	2	0	0	299
◊ D ₆ S _{1,5} V ₂ D ₂ r ₃ H ₃ e ₃	-	-	0.80	4.5	+0	-2	0	-10	282



e. $M_\infty = 0.80$

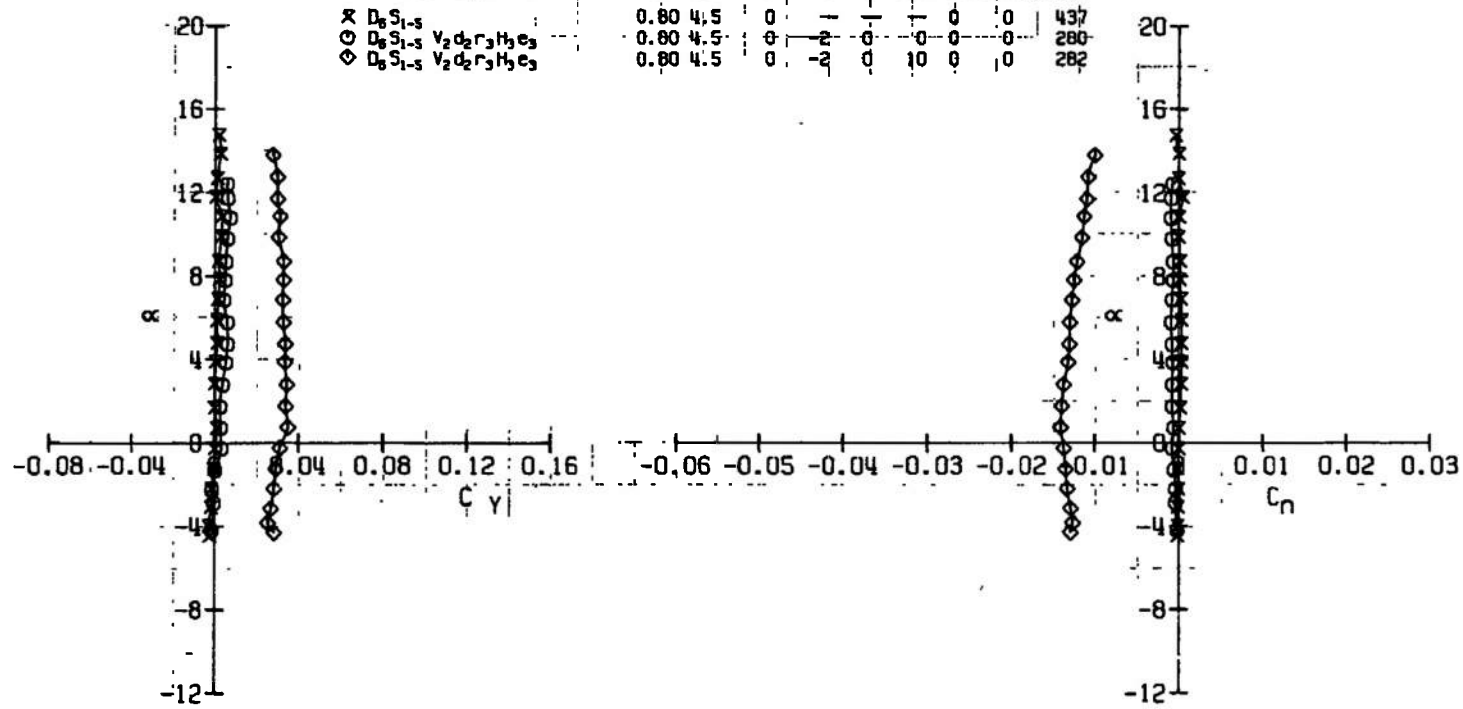
Fig. 9 Continued

CONFIGURATION	W_3	S_3	B_3	H_3	H_2	B_2	C_2	N_2					
SYM.	CONFIGURATION								M _∞	Re	REF.	SHR.	PN
*	D ₆	S ₁	S ₅						0.60	4.5	0	0	43
○	D ₆	S ₁	S ₅	V ₂	B ₂	T ₅	H ₃	C ₃	0.60	4.5	0	0	20
◊	D ₆	S ₁	S ₅	V ₂	B ₂	T ₅	H ₃	C ₃	0.60	4.5	0	0	20



e. Continued
Fig. 9 Continued

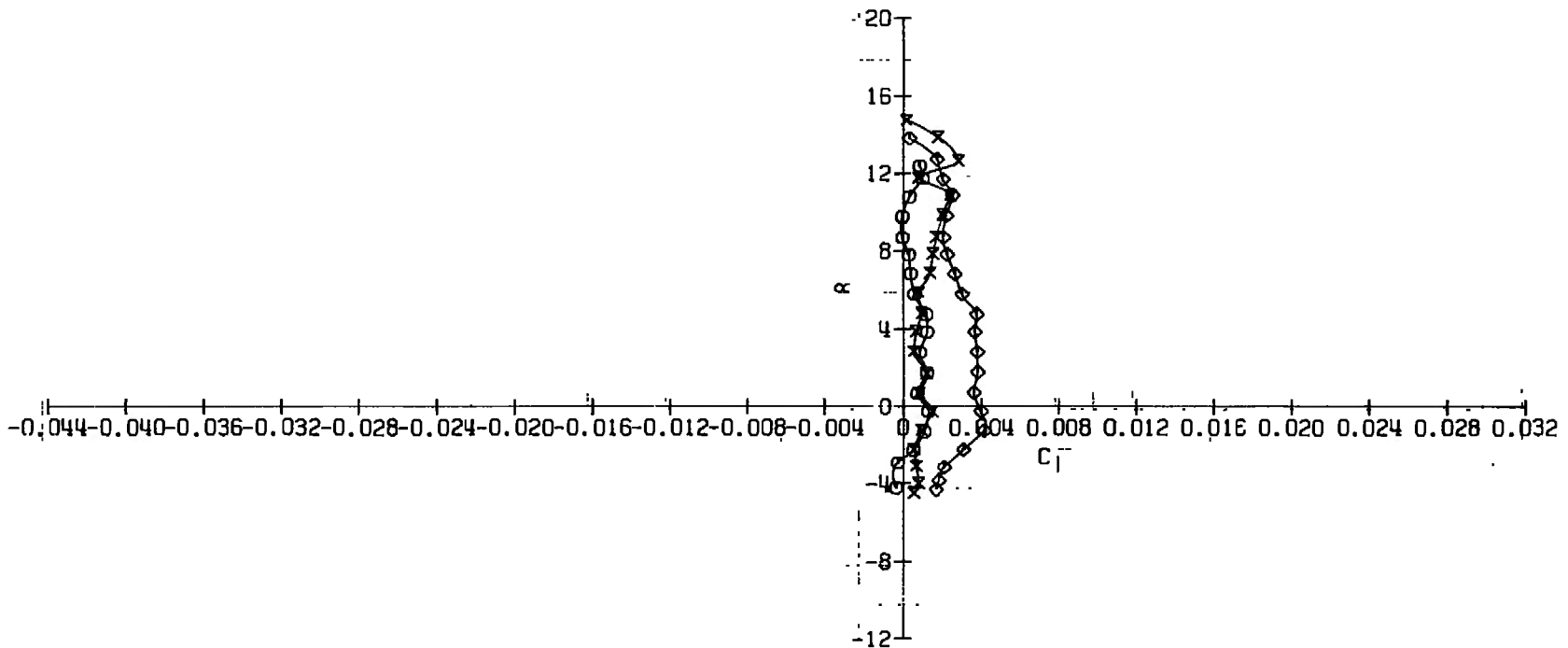
CONFIGURATION: $H_3a_2b_4h_6h_8B_3C_2N_3$
 M CONFIGURATION * M_∞ Re. BETR SH SE SB AL dB PNL
 X D_6S_{1-5} 0.80 4.5 0 -1 1 0 0 437
 O $D_6S_{1-5} V_2d_2r_3H_3e_3$ 0.80 4.5 0 -2 0 0 0 0 280
 $\diamond D_6S_{1-5} V_2d_2r_3H_3e_3$ 0.80 4.5 0 -2 0 10 0 0 282



e. Continued
 Fig. 9 · Continued

CONFIGURATION: $W_3 e_3 b_3 h_6 h_6 B_3 C_2 N_3$

SYM	CONFIGURATION	M ₀	Re.	BETA	SH	SE	SR	SL	SB	PN
X	D ₆ S ₁₋₅	0.80	4.5	0	-	-	0	0	0	437
O	D ₆ S ₁₋₅ V ₂ d ₂ r ₃ H ₃ B ₃	0.80	4.5	0	-2	0	0	0	0	280
◊	D ₆ S ₁₋₅ V ₂ d ₂ r ₃ h ₃ C ₃	0.80	4.5	0	-2	0	10	0	0	282



e. Concluded
Fig. 9 Concluded

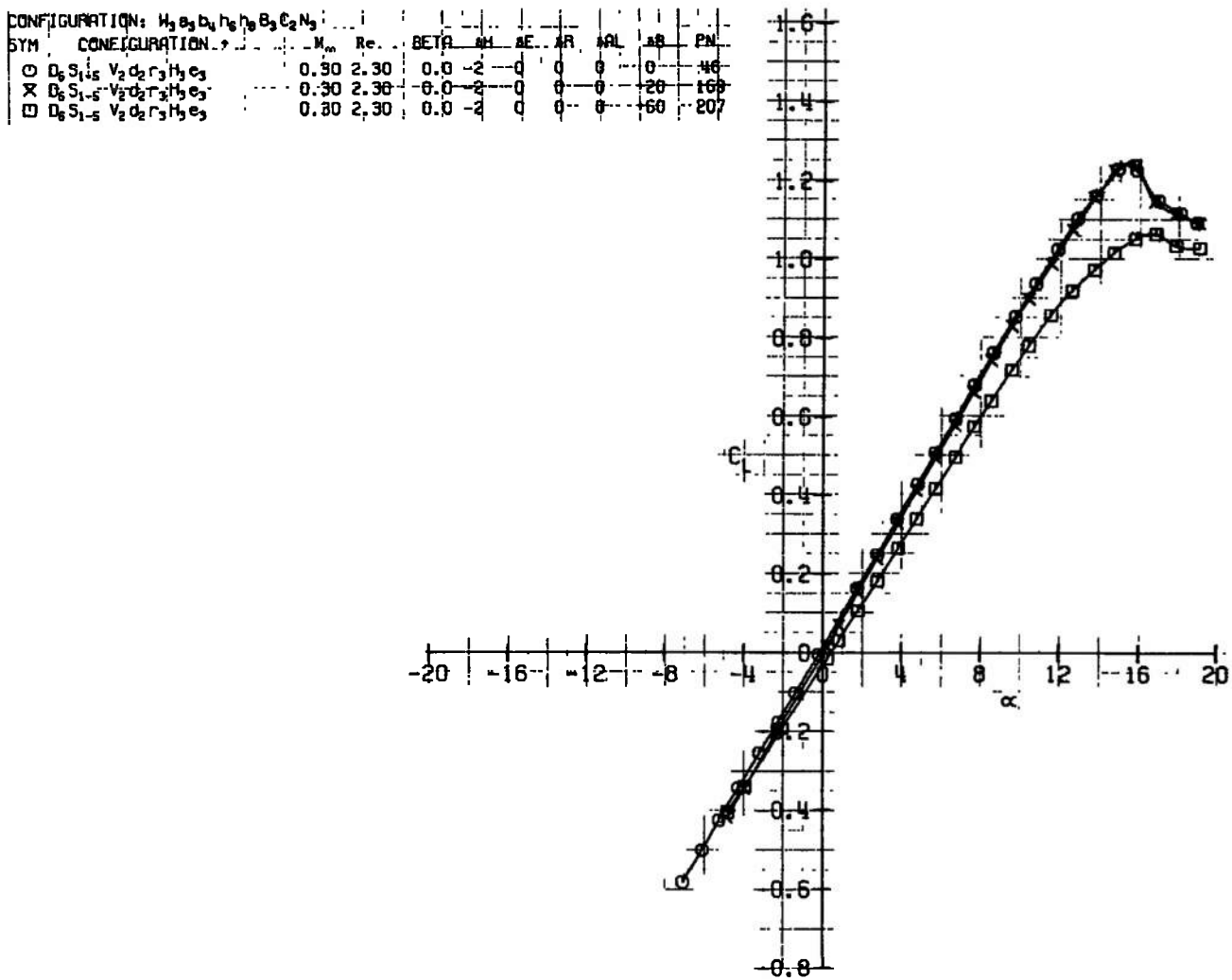
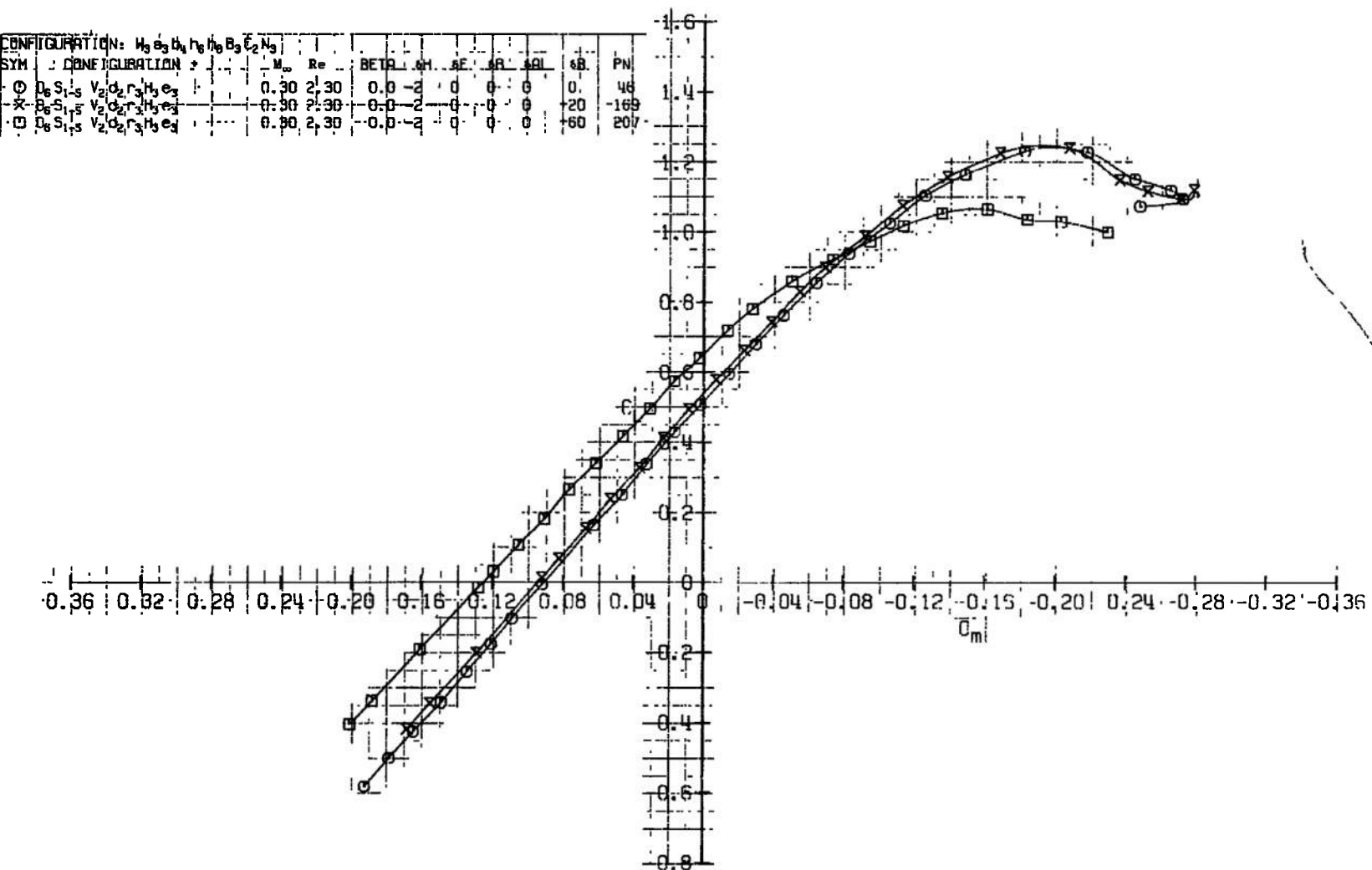
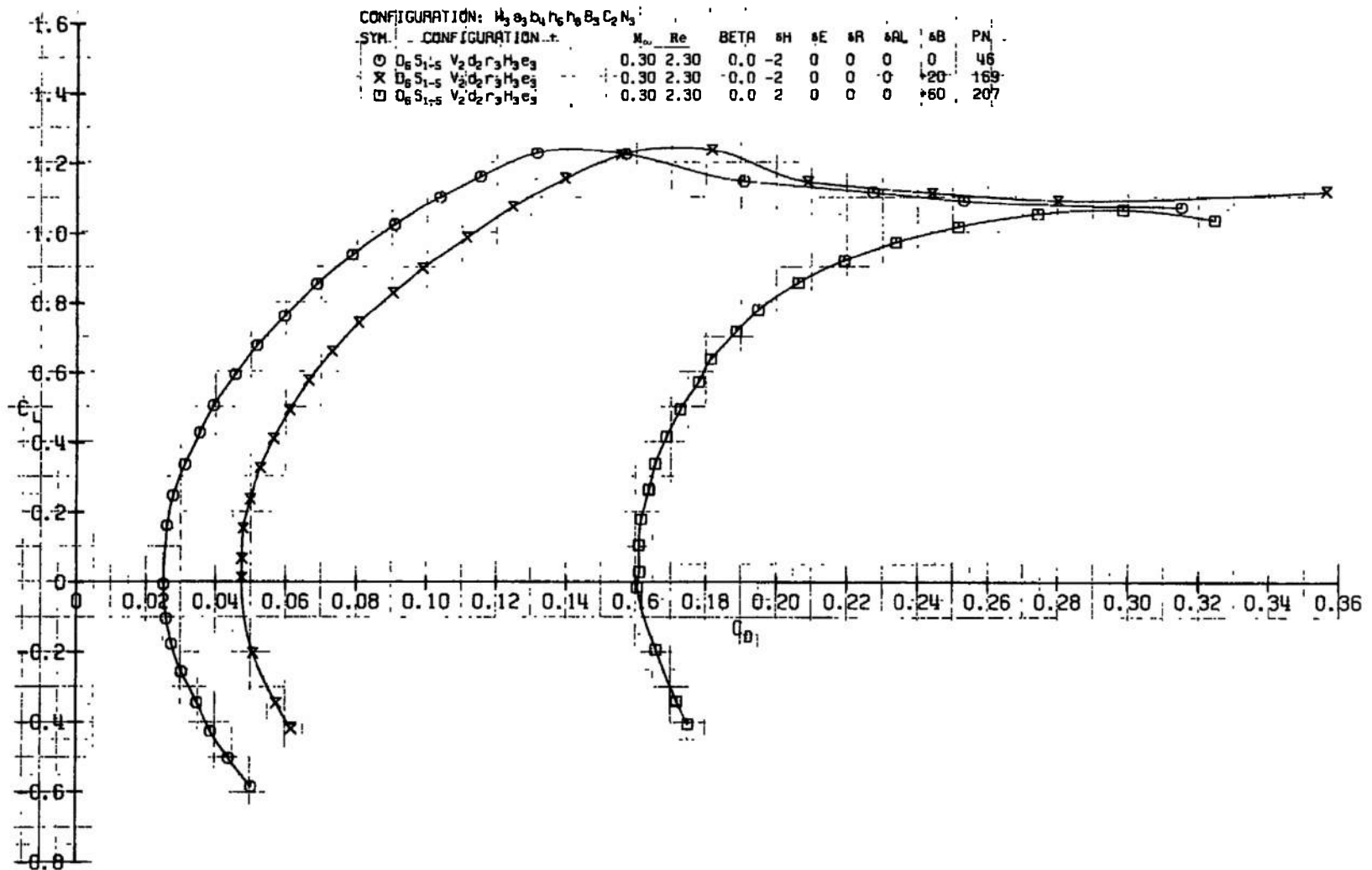
a. $M_\infty = 0.30$

Fig. 10 Speed Brake Effectiveness

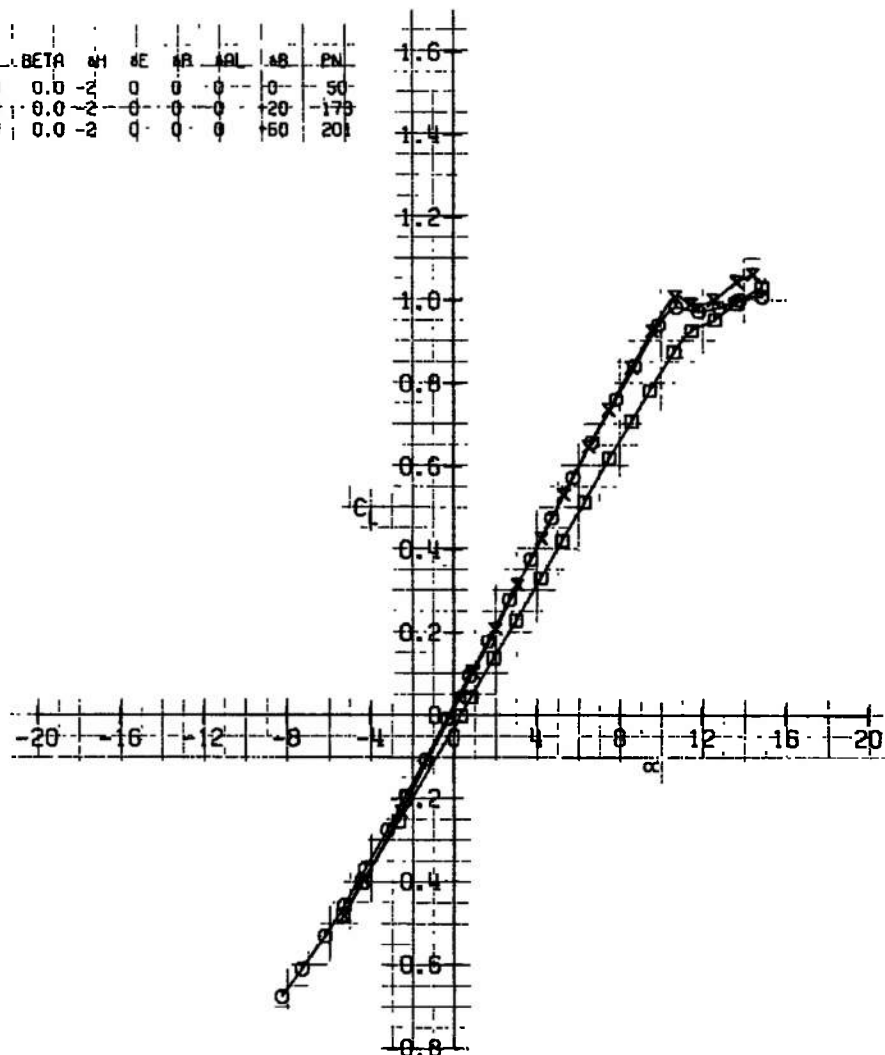


a. Continued
Fig. 10 Continued



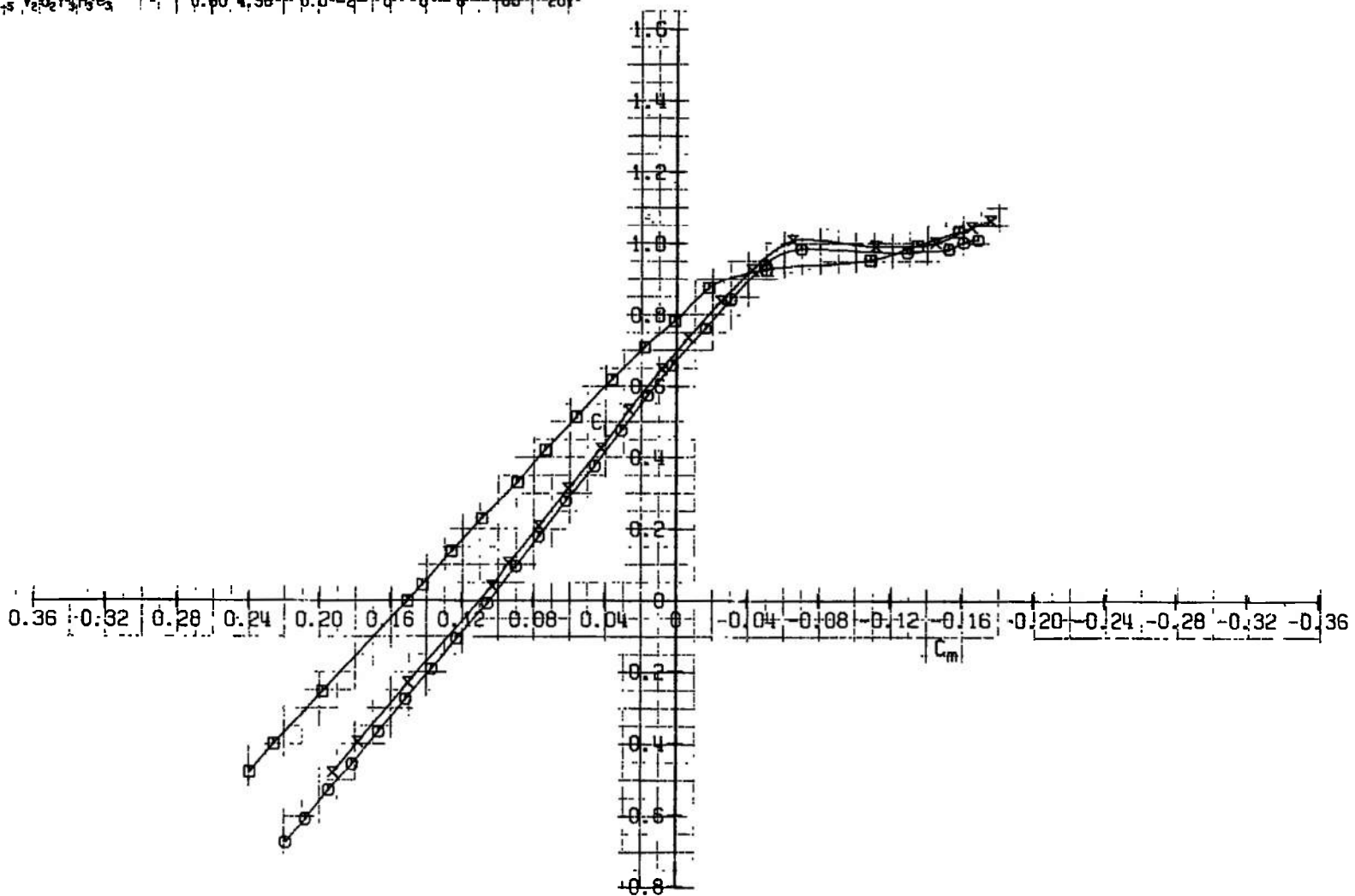
a. Concluded
Fig. 10 Continued

CONFIGURATION: $h_3 a_3 b_4 h_6 h_8 B_3 C_2 N_3$									
SYM	CONFIGURATION	M _∞	Re	BETA	SH	SE	SR	HL	LB
O	D ₆ S ₁₋₃ V ₂ d ₂ r ₃ H ₃ e ₃	0.60	4.50	0.0 -2	0	0	0	50	
X	D ₆ S ₁₋₃ V ₂ d ₂ r ₃ H ₃ e ₃	0.60	4.50	0.0 -2	0	0	0	120	170
□	D ₆ S ₁₋₃ V ₂ d ₂ r ₃ H ₃ e ₃	0.60	4.50	0.0 -2	0	0	0	150	200



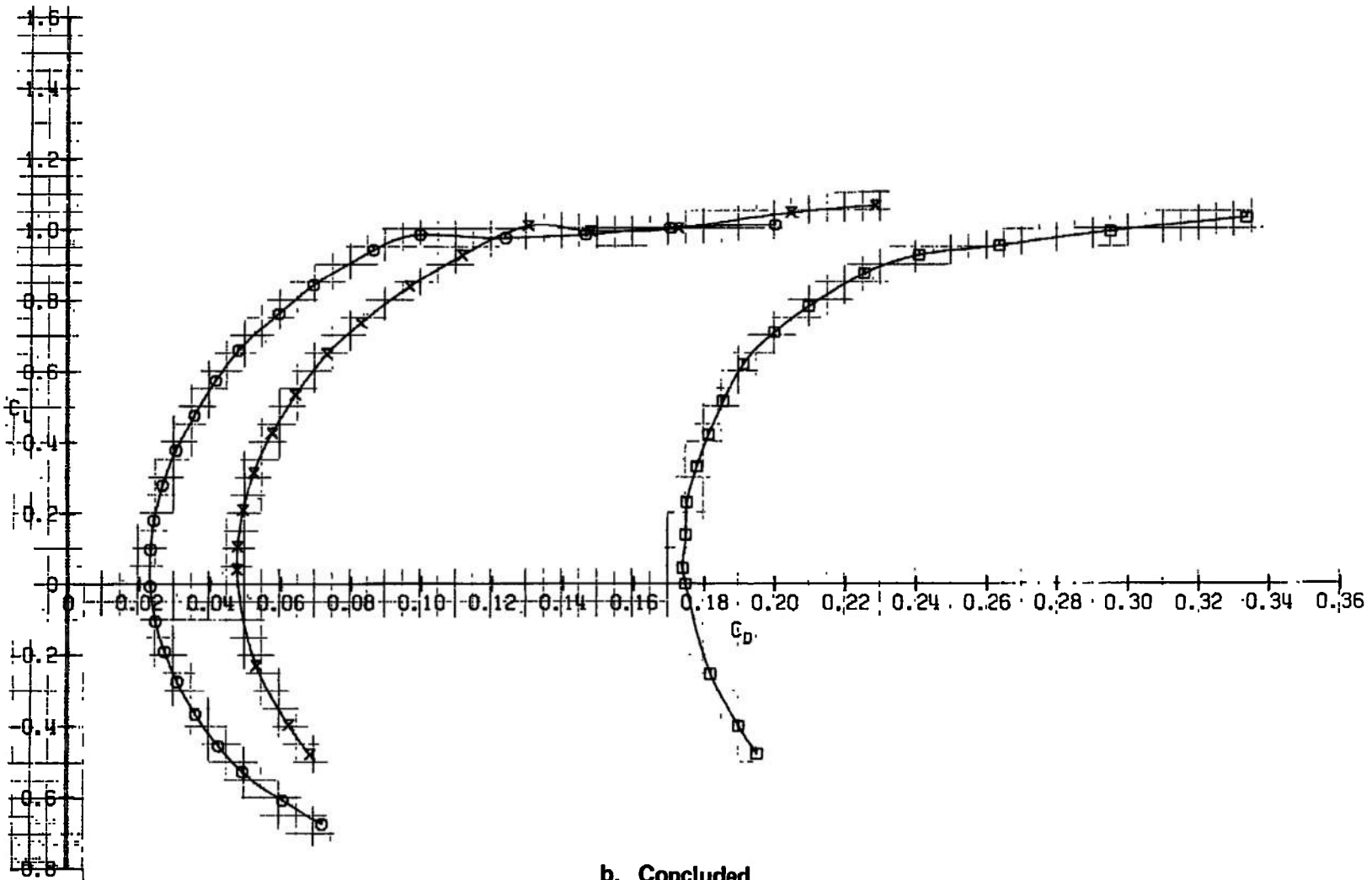
b. $M_\infty = 0.60$
Fig. 10 Continued

CONFIGURATION: $h_3 a_3 b_4 h_6 h_8 B_3 f_2 N_3$		M_∞	Re	BETR	ϕH	ϕE	ϕR	ϕL	ϕB	PN
○	$b_6 S_{1,5} V_2 D_2 r_3 H_3 e_3$	-	-	0.60	-4.50	0.0	-2	0	0	0
X	$b_6 S_{1,5} V_2 D_2 r_3 H_3 e_3$	-	-	0.60	-4.50	0.0	-2	0	0	175
□	$b_6 S_{1,5} V_2 D_2 r_3 H_3 e_3$	-	-	0.60	-4.50	0.0	-2	0	0	20



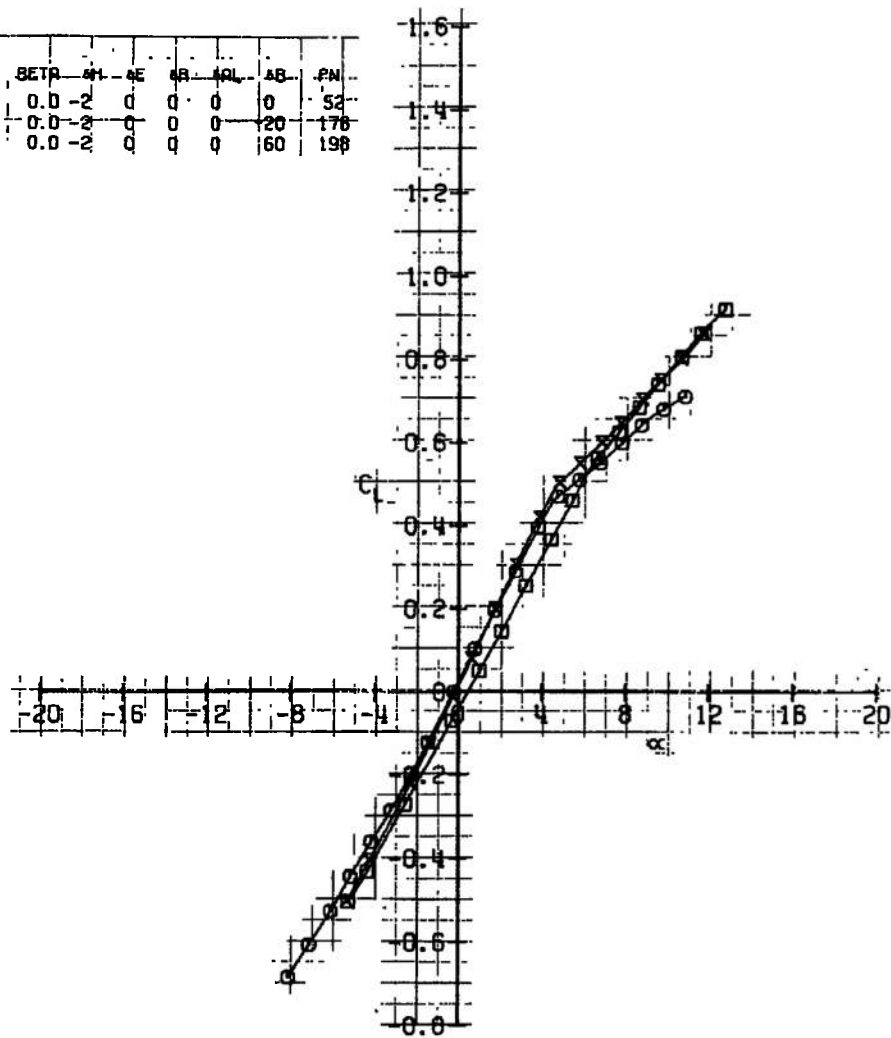
b. Continued
Fig. 10 Continued

CONFIGURATION	W_1	W_2	B_1	B_2	B_3	C_2	N_3						
SYM	CONF	R	M _∞	Re	REF	H	F	DR	AB	AB	PN		
○	$S_{1,5}$	V_2	d_2	r_2	H_2	e_2		0.60	4.50	0.0	-2	0	0
X	$S_{1,5}$	V_2	d_2	r_2	H_2	e_2		0.60	4.50	0.0	-2	0	0
□	$S_{1,5}$	V_2	d_2	r_2	H_2	e_2		0.60	4.50	0.0	-2	0	0



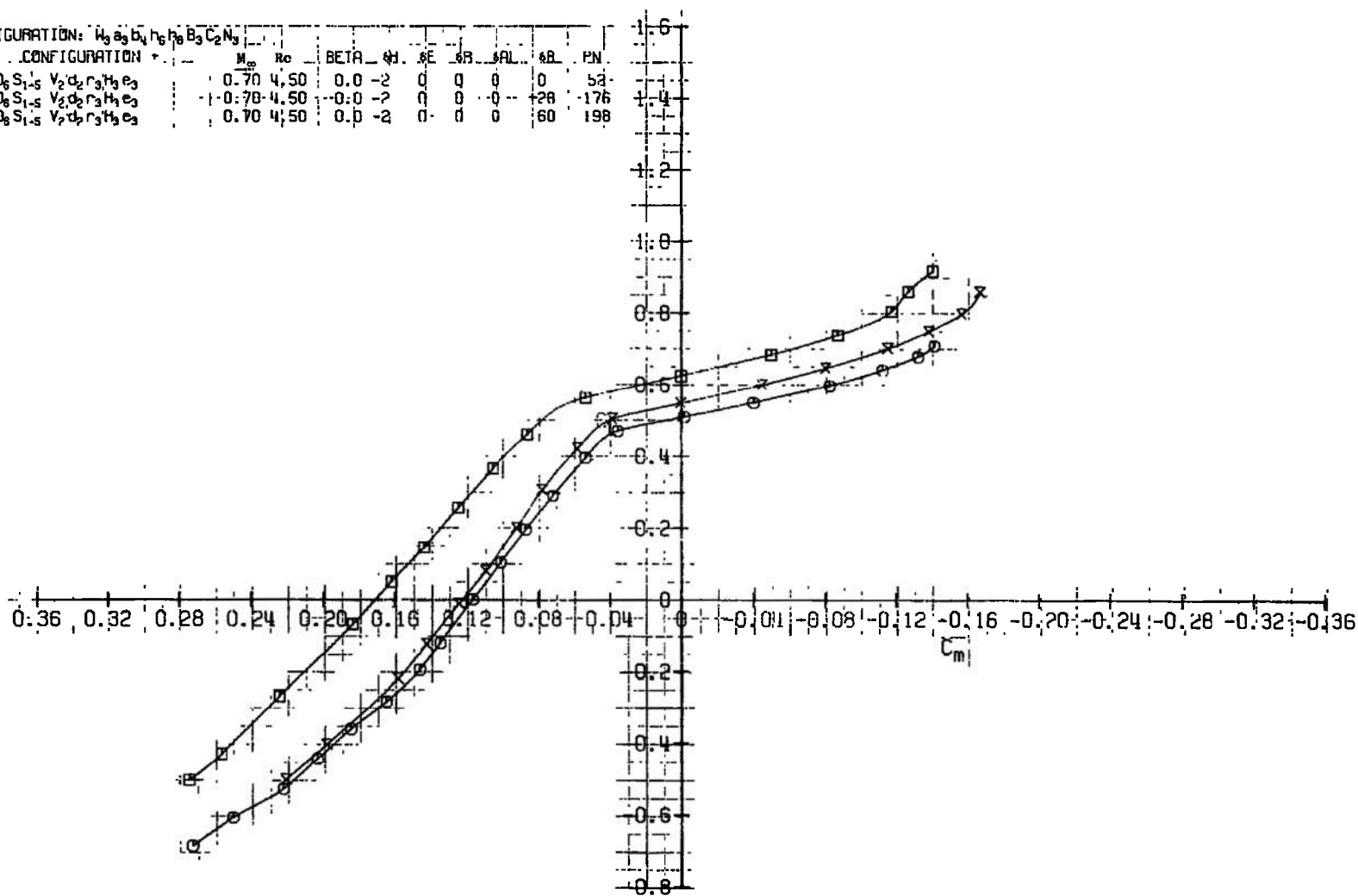
b. Concluded
Fig. 10 Continued

CONFIGURATION: H ₃ e ₃ b ₃ H ₆ H ₉ B ₃ C ₂ N ₃		M _∞	Ro	BETP	41°	4E	4B	4OL	AB	PN
DATA : CONFIGURATION.c										
O D ₆ S ₁₋₅ V ₂ d ₂ r ₃ H ₃ e ₃		0.70	4.50		0.0	-2	0	0	0	52
X D ₆ S ₁₋₅ V ₂ d ₂ r ₃ H ₃ e ₃		0.70	4.50		0.0	-2	0	0	20	176
□ D ₆ S ₁₋₅ V ₂ d ₂ r ₃ H ₃ e ₃		0.70	4.50		0.0	-2	0	0	160	196

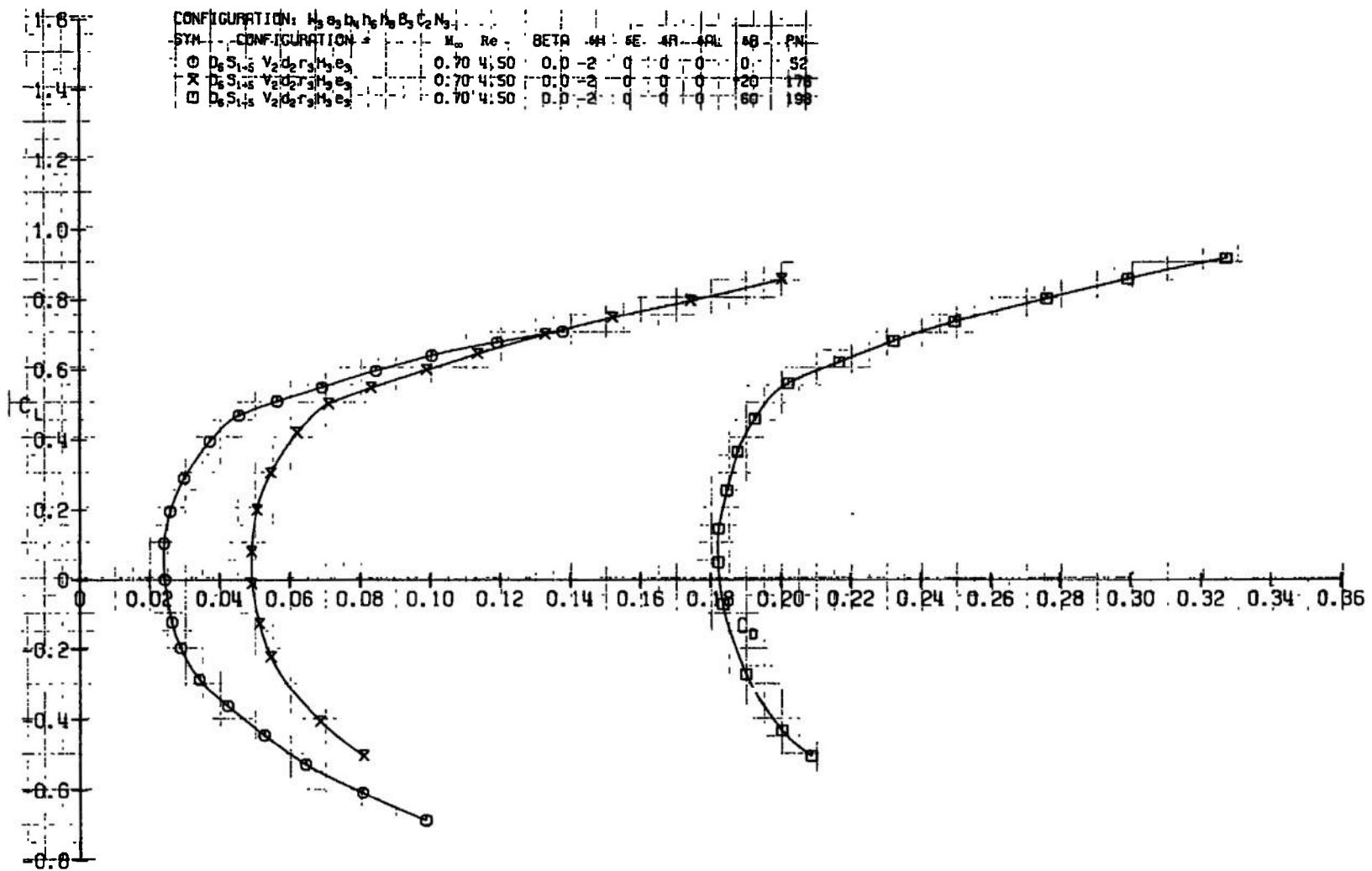


c. $M_{\infty} = 0.70$
Fig. 10 Continued

CONFIGURATION: $W_3 a_3 b_4 h_6 h_8 B_3 C_2 N_3$
 SYM
 CONFIGURATION + - - M_∞ Re BETA_4H SE SP SAL SB PN
 O D₆S₁₋₅ V₂d₂r₃h₃e₃ -0.70 4.50 0.0 -2 0 0 0 0 52
 X D₆S₁₋₅ V₂d₂r₃h₃e₃ -0.70 4.50 0.0 -2 0 0 0 20 176
 □ D₆S₁₋₅ V₂d₂r₃h₃e₃ 0.70 4.50 0.0 -2 0 0 0 60 198

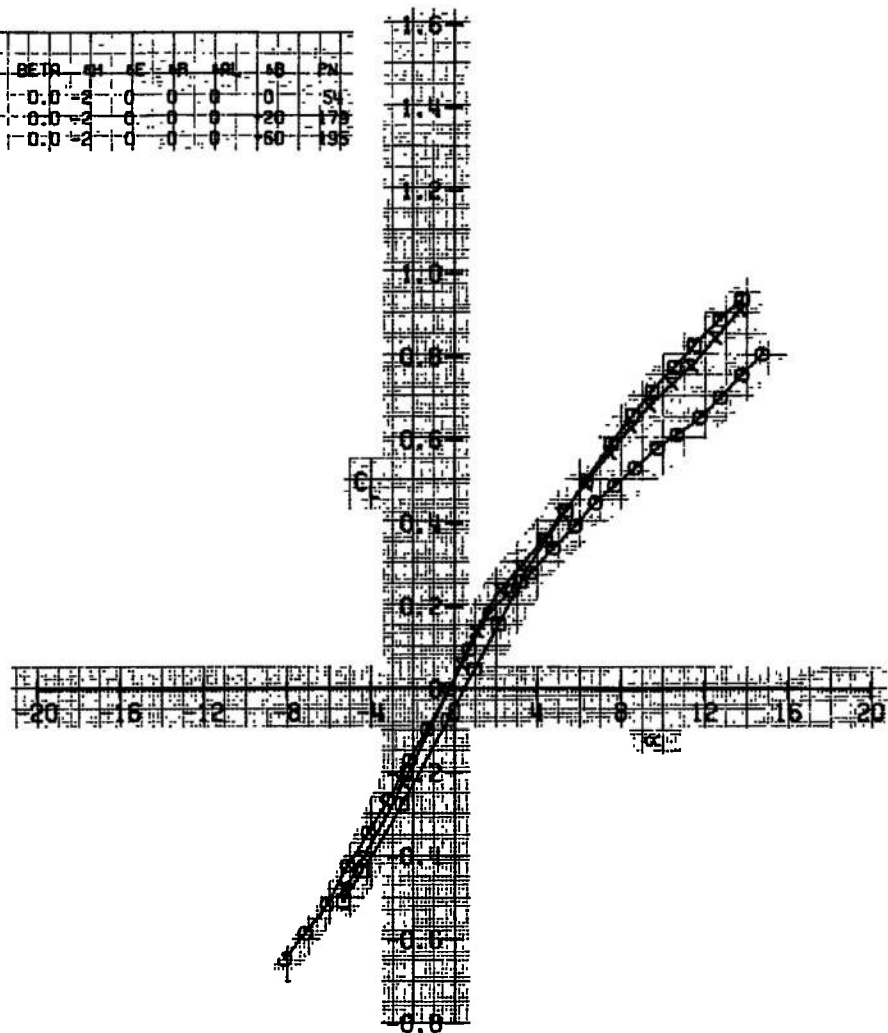


c. Continued
 Fig. 10 Continued



c. Concluded
Fig. 10 Continued

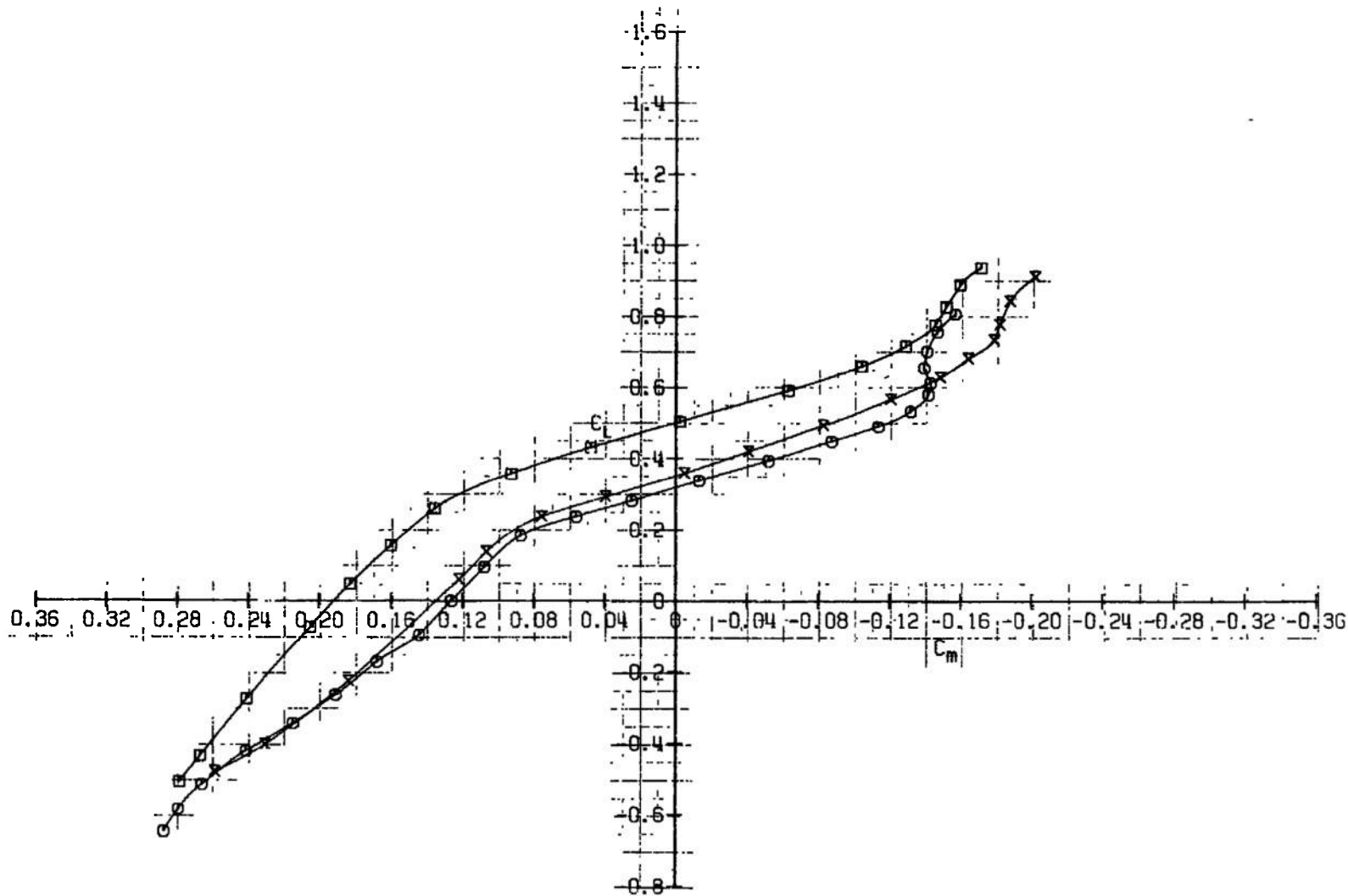
CONFIGURATION: H ₃ S ₃ B ₄ H ₆ H ₆ B ₂ C ₂ N ₃		M _a	Re	BETA	CH	SE	MR	AB	PN
SYM	CONFIGURATION								
O	D ₆ S ₁ S ₆ V ₂ d ₅ r ₃ H ₆ e ₃	0.75	4.50	0.0	-2	0	0	0	54
X	D ₆ S ₁ S ₆ V ₂ d ₅ r ₃ H ₆ e ₃	0.75	4.50	0.0	-2	0	0	0	178
□	D ₆ S ₁ S ₆ V ₂ d ₅ r ₃ H ₆ e ₃	0.75	4.50	0.0	-2	0	0	0	195



d. $M_a = 0.75$

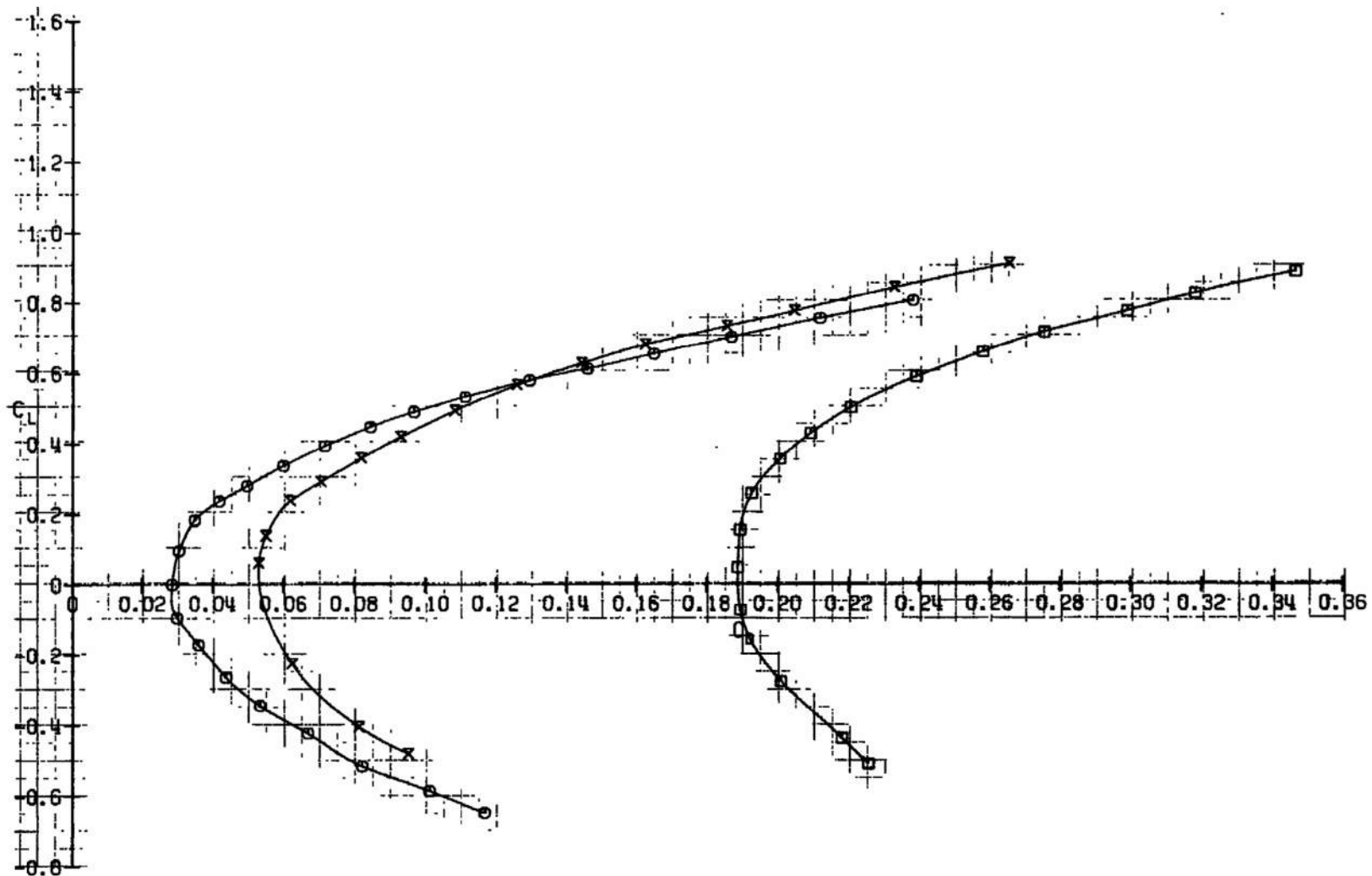
Fig. 10 Continued

CONFIGURATION: $W_3 a_3 b_4 h_6 H_8 B_3 C_2 N_3$
 SYM CONFIGURATION + : M_m Re BETA SH SF SR MFL SB PN
 O $D_8 S_{1-5} V_2 d_2 r_3 H_3 e_3$ 0.75 4.50 0.0 -2 0 0 0 0 0 54
 X $D_8 S_{1-5} V_2 d_2 r_3 H_3 e_3$ 0.75 4.50 0.0 -2 0 0 0 -20 179
 E $D_8 S_{1-5} V_2 d_2 r_3 H_3 e_3$ 0.75 4.50 0.0 -2 0 0 0 +60 195

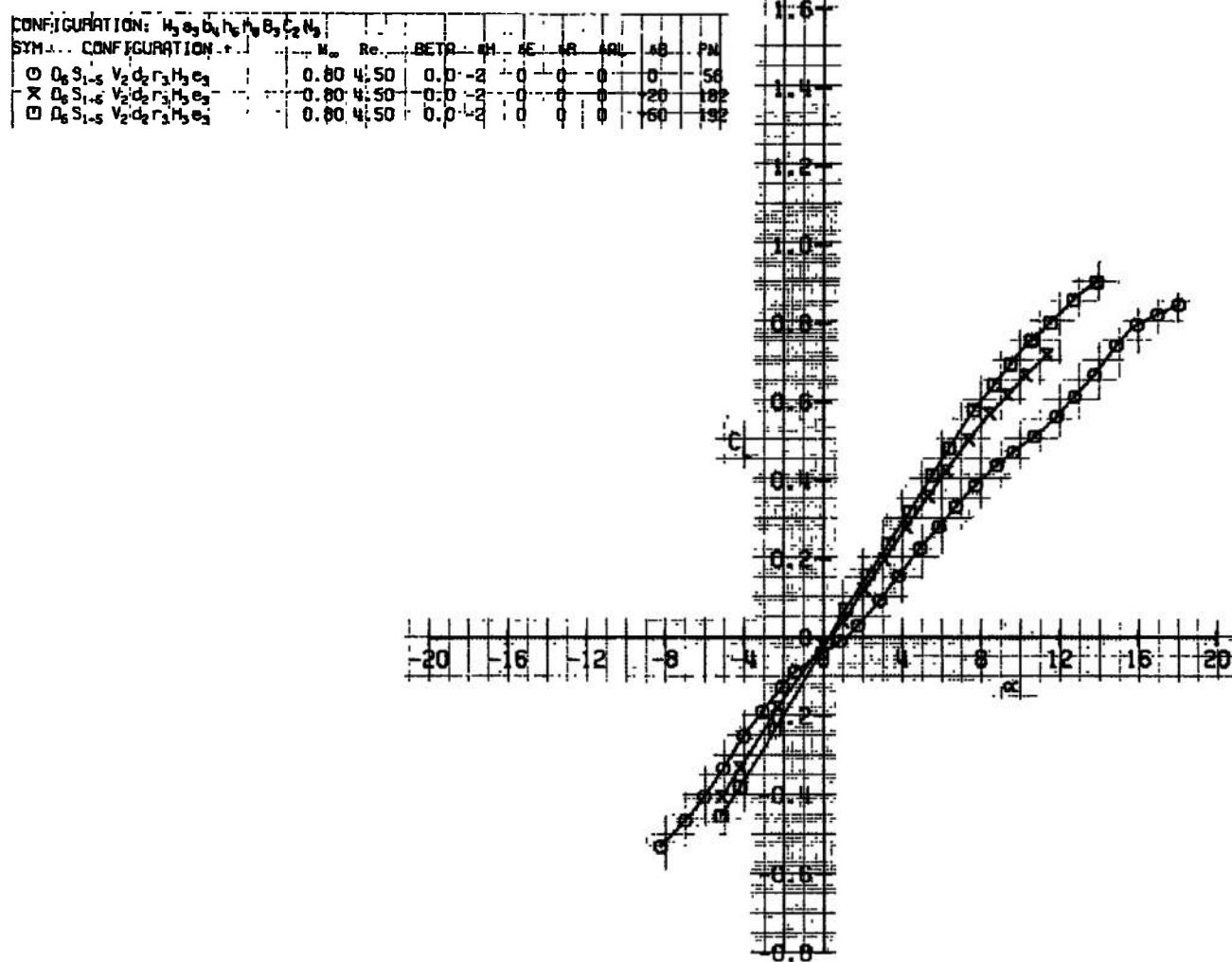


d. Continued
Fig. 10 Continued

CONFIGURATION: $H_3S_3B_4H_6B_3C_2N_3$
 SYM CONFIGURATION M_∞ Re BETAP 8H 8E 8R 8PL 8B PN
 O D₆S₁₋₅V₂d₂r₃H₃e₃ 0.75 4.50 0.0 -2 0 0 0 0 54
 X D₆S₁₋₅V₂d₂r₃H₃e₃ 0.75 4.50 0.0 -2 0 0 0 +20 178
 □ D₆S₁₋₅V₂d₂r₃H₃e₃ 0.75 4.50 0.0 -2 0 0 0 +60 196

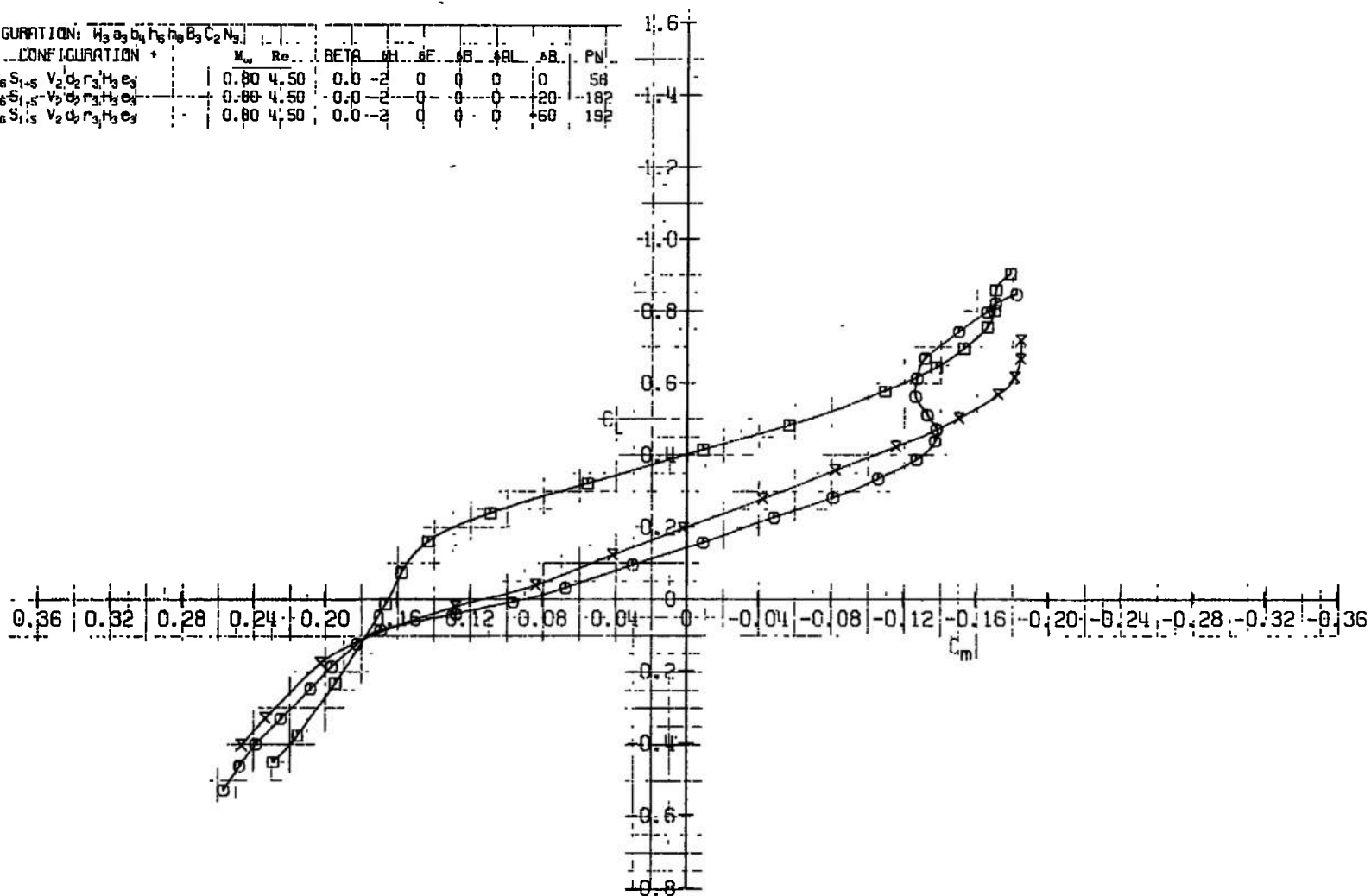


d. Concluded
 Fig. 10 Continued

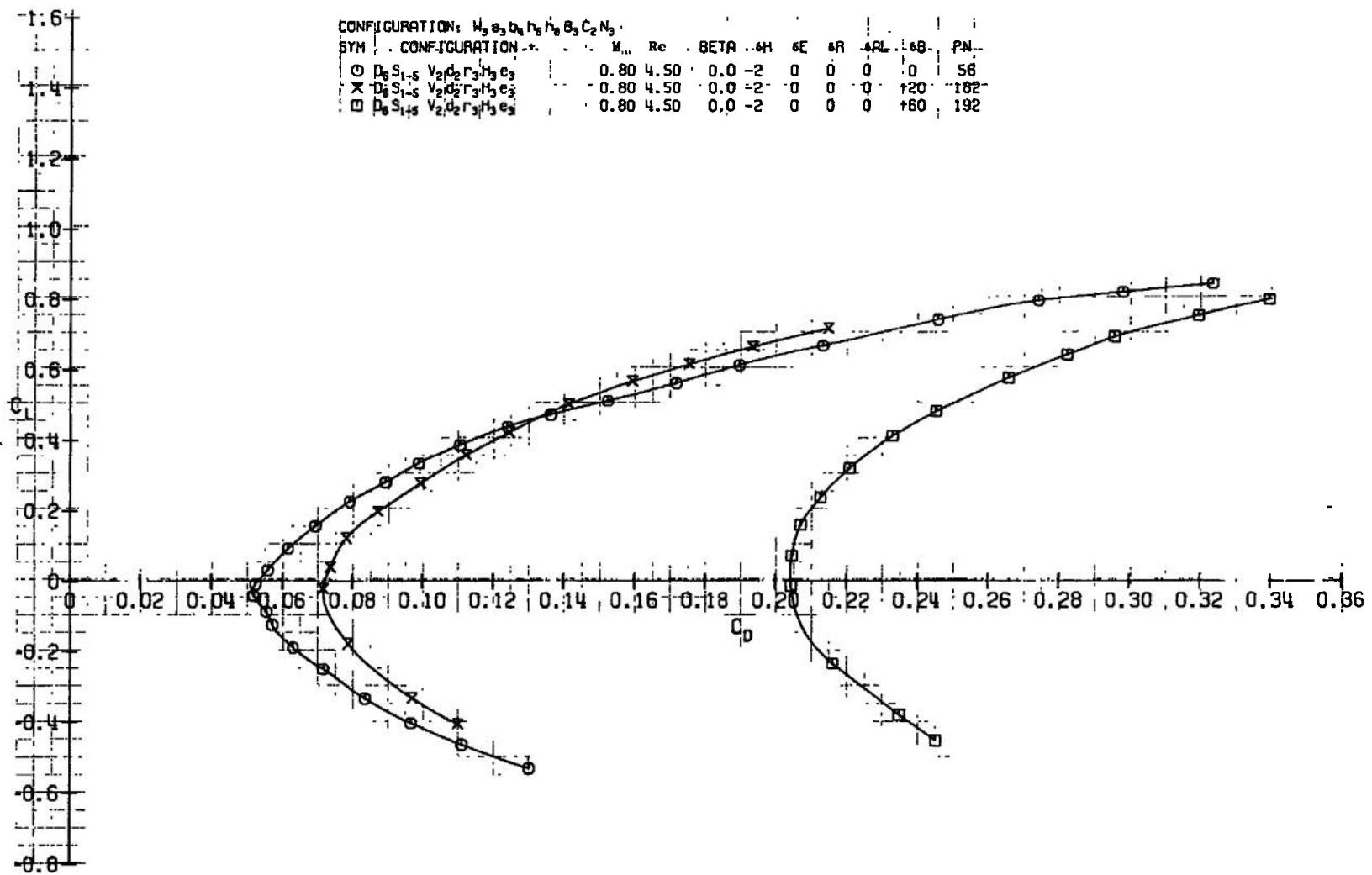


e. $M_\infty = 0.80$
Fig. 10 Continued

CONFIGURATION: $H_3^+ B_3^- b_4^- h_6^- h_8^- B_3^- C_2^- N_3^-$		SYM. CONFIGURATION +								
		M _w	Re _c	BETA	W _H	S _E	S _B	S _{BL}	S _{BR}	PN
-○-	D ₆ S _{1,-5} V ₂ d ₂ r ₃ H ₃ e ₃	0.80	4.50	0.0	-2	0	0	0	0	58
-×	D ₆ S _{1,-5} V ₂ d ₂ r ₃ H ₃ e ₃	0.80	4.50	0.0	-2	0	0	0	-20	182
□	D ₆ S _{1,-5} V ₂ d ₂ r ₃ H ₃ e ₃	0.80	4.50	0.0	-2	0	0	+60	192	



e. Continued
Fig. 10 Continued



e. Concluded
 Fig. 10 Concluded

TABLE I
INDEX TO MODEL COMPONENTS

Symbol	Components
a ₃	Aileron
B ₃	Body
b ₄	Speed Brake
C ₂	Canopy
d ₂	Dorsal
D ₆	Duct
D ₇	Duct with Core Cowl
h ₁	Dual Ejector Rack
H ₃ e ₃	Horizontal Tail with Elevator
h _{6, 8}	Flap Track
N ₃	Nacelle
S ₁₋₅	Pylons
V ₂ r ₃	Vertical Tail with Rudder
w ₁ ⁶	500-lb Bomb, six, MK82
w ₁ ¹⁸	500-lb Bomb, eighteen, MK82
w ₂ ¹⁰	Napalm Bomb, ten, BLU-1/B
W ₃	Wing

TABLE I (Concluded)

X	$W_3a_3h_6h_8B_3C_2N_3$ (Basic Configuration)
XD ₆	
XD ₆ S ₁₋₅	
XD ₆ S ₁₋₅ V ₂ d ₂ r ₃	
XD ₆ S ₁₋₅ V ₂ d ₂ r ₃ H ₃ e ₃	
XD ₇ S ₁₋₅ V ₂ d ₂ r ₃ H ₃ e ₃	
XD ₆ S ₁₋₅ V ₂ d ₂ r ₃ H ₄ e ₃	
XD ₆ S ₁₋₅ w ₁ ⁶ V ₂ d ₂ r ₃ H ₃ e ₃	
XD ₆ S ₁₋₅ w ₁ ¹⁸ V ₂ d ₂ r ₃ H ₃ e ₃	
XD ₆ S ₁₋₅ w ₂ ¹⁰ V ₂ d ₂ r ₃ H ₃ e ₃	

TABLE II
SUMMARY OF TEST DATA

Configuration X = W ₃ a ₃ b ₄ h ₆ h ₈ B ₃ C ₂ N ₃	α , deg	β , deg	RN x 10^{-6}	Controls	Mach Number								
					0.30	0.60	0.70	0.75	0.80				
						Part Number							
<u>Effect of M_∞ and RN</u>													
XD ₆	V	0	2.3		454	453	---	---	---				
XD ₆ S ₁₋₅					427	429	445	444	443				
XD ₆ S ₁₋₅ V ₂ r ₃					337	340	---	---	---				
XD ₆ S ₁₋₅ V ₂ r ₃ H ₃ e ₃					49/271	28/279	90	92	91				
XD ₆ S ₁₋₅ V ₂ r ₃ H ₄ e ₃					369	377	411	409	---				
XD ₆ S ₁₋₅ V ₂ r ₃ H ₃ e ₃			2.7		---	---	58	60	62				
XD ₆ S ₁₋₅			4.5		---	431	433	435	437				
XD ₆ S ₁₋₅ V ₂ r ₃					---	341	343	345	347				
XD ₆ S ₁₋₅ V ₂ r ₃ H ₃ e ₃					---	50/288	52/119	54/283	56/280				
XD ₆			7.0		---	449	450	451	452				
XD ₆ S ₁₋₅					---	430	440	441	442				
XD ₆ S ₁₋₅ V ₂ r ₃					---	350	351	352	353				
XD ₆ S ₁₋₅ V ₂ r ₃ H ₃ e ₃					---	56	68	70	72				
<u>Effect of Stores</u>													
XD ₆ S ₁₋₅ w ₁₋₃ ⁶ V ₂ d ₂ r ₃ H ₃ e ₃			2.3	10	260	261	263	266	267				
XD ₆ S ₁₋₅ h ₁₋₄ ¹⁸ w ₁₋₅ V ₂ d ₂ r ₃ H ₃ e ₃			2.3		241	243	245	247	249				
			4.5		---	---	253	251	---				
XD ₆ S ₁₋₅ w ₂₋₅ ¹⁰ V ₂ d ₂ r ₃ H ₃ e ₃			2.3		215	217	235	233	231				
			4.5		---	225	227	223	229				
			7.0		---	219	221	---	---				
<u>Elevator Effectiveness</u>													
XD ₆ S ₁₋₅ V ₂ d ₂ r ₃ H ₃ e ₃			2.3	10	97	109	---	---	---				
				5	99	104	---	---	---				
				0	46*	48*	---	---	---				
				-5	100	103	---	---	---				
				-10	101	102	---	---	---				

TABLE II (Continued)

Configuration $X = W_3 S_3 b_4 h_6 h_8 B_3 C_2 N_3$	α , deg	β , deg	RN x 10^{-6}	Controls	Mach Number						
					0.30	0.50	0.70	0.75	0.80		
					Part Number						
<u>Elevator Effectiveness (continued)</u>											
XD ₆ S ₁₋₅ V ₂ d ₂ r ₃ H ₃ e ₃	v	0	4.5	δ_E , deg	10	---	111	120	122	130	
					5	---	112	118	124	129	
					0	---	50*	52*	54*	56*	
					-5	---	113	117	123	128	
					-10	---	114	116	125	127	
					2.3	10	367	381	---	---	
					5	368	380	---	---	---	
					0	369	377	---	---	---	
					-5	371	376	---	---	---	
					-10	372	375	---	---	---	
					4.5	10	383	395	397	---	
					5	---	384	394	398	407	
					0	---	385	392	399	406	
					-5	---	387	391	401	405	
					-10	---	388	390	402	404	
<u>Horizontal Stabilizer Effectiveness</u>											
XD ₅ S ₁₋₅ V ₂ d ₂ r ₃ H ₃ e ₃			2.3	δ_H , deg	2	318	319	---	---	---	
					0	327	328	---	---	---	
					-2	46*	48*	---	---	---	
					4.5	2	---	320	321	322	323
					0	---	329	330	331	332	
					-2	---	50*	52*	54*	56*	
<u>Aileron Effectiveness</u>											
XD ₆ S ₁₋₅ V ₂ d ₂ r ₃ H ₃ e ₃			2.3	δ_A , deg	20	134	146	---	---	---	
					10	135	145	299	296	---	
					5	136	144	---	---	---	

TABLE II (Continued)

Configuration $X = W_3 a_3 b_4 n_6 h_8 B_3 C_2 N_3$	α , deg	β , deg	RN x 10^{-5}	Controls	Mac. Number					
					0.30	0.60	0.70	0.75	0.80	
					Part Number					
<u>Aileron Effectiveness (continued)</u>				δA , deg	δB , deg					
XD ₆ S ₁₋₅ V ₂ d ₂ r ₃ H ₃ e ₃	V	0	2, 3	0	0	46*	48*	80*	92*	91*
				-5		137	143	---	---	---
				-10		138	142	298	297	---
				-20		139	141	---	---	---
				4.5	20	---	148	---	---	---
					10	---	149	156	162	158
					5	---	150	---	---	---
					0	50*	52*	52*	54*	56*
					-5	---	151	---	---	---
					-10	---	152	155	161	159
					-20	---	153	---	---	---
				2, 3	30	20	167	---	---	---
						20	---	188	---	---
						10	168	187	---	---
						0	169	186	---	---
						-10	170	185	---	---
						-20	---	184	---	---
						-30	171	---	---	---
						4.5	10	174	175	180
							0	173	176	179
							-10	172	177	178
							2, 3	209	---	---
							10	208	203	---
							0	207	204	---
							-10	206	---	---
							-30	205	---	---
								202	197	196
										191

TABLE II (Continued)

Configuration X = W ₃ a ₃ b ₄ h ₆ h ₈ B ₃ C ₂ N ₃	α , deg	β , deg	RN 10^{-6}	Controls	Mach Number					
					0.30	0.60	0.70	0.75	0.80	
					Part Number					
<u>Aileron Effectiveness (continued)</u>										
XD ₆ S ₁₋₅ V ₂ d ₂ r ₃ H ₃ e ₃	V	0	4.5	0	60	---	201	198	195	192
			4.5	-10		---	200	199	194	193
<u>Horizontal Tail Dihedral Effects</u>										
XD ₆ S ₁₋₅ V ₂ d ₂ r ₃ H ₄ e ₃		2 3	0	0	369*	---	---	---	---	
		4.5	0	0	---	385*	392*	399	406*	
		2.3	0	-60	414	---	---	---	---	
		4.5	0	-60	---	418	420	421	422	
XD ₆ S ₁₋₅ V ₂ d ₂ r ₃ H ₃ e ₃		2.3	10	0	45*/271	---	---	---	---	
		4.5	10	0	---	50*/288	52*	54*	56*/280	
		2.3	10	-60	207*	---	---	---	---	
		4.5	10	-60	---	201*	198*	195*	192*	
<u>Rudder Effectiveness</u>										
XD ₆ S ₁₋₅ V ₂ d ₂ r ₃ H ₃ e ₃		2 3	0	46*/271	48*/279	---	92*	---	---	
			10	272	278	---	295	---	---	
			20	273	277	---	296	---	---	
			30	274	275	---	297	---	---	
		4.5	0	---	50/286	52*	54*/283	56*/280		
			10	---	290	286	284	282		
			20	---	292	---	290	---		
			30	---	293	---	291	---		
<u>Lateral-Directional Characteristics</u>										
XD ₆ S ₁₋₅		2.3			427*	429*	---	---	---	
XD ₆ S ₁₋₅ V ₂ d ₂ r ₃					337*	340*	---	---	---	
XD ₆ S ₁₋₅ V ₂ d ₂ r ₃ H ₃ e ₃					46*/271	48*/279	---	---	---	

TABLE II (Concluded)

Configuration $X = W_3a_3b_4c_6h_8B_3C_2N_3$	α , deg	β , deg	RN x 10 ⁻⁶	Controls	Mach Number								
					0.30	0.60	0.70	0.75	0.80				
Part Number													
<u>Lateral-Directional Characteristics (continued)</u>													
XD ₆ S ₁₋₅ V ₂ d ₂ r ₃ H ₄ e ₃	V	0	2.3		369*	377	---	---	---				
XD ₆ S ₁₋₅		5			428	430	---	---	---				
XD ₆ S ₁₋₅ V ₂ d ₂ r ₃					338	339	---	---	---				
XD ₆ S ₁₋₅ V ₂ d ₂ r ₃ H ₃ e ₃					270	294	---	---	---				
XD ₆ S ₁₋₅ V ₂ d ₂ r ₃ H ₄ e ₃					370	379	---	---	---				
XD ₆ S ₁₋₅		0	4.5		---	431*	433*	435*	437				
XD ₆ S ₁₋₅ V ₂ d ₂ r ₃					---	341*	343*	345*	247				
XD ₆ S ₁₋₅ V ₂ d ₂ r ₃ H ₃ e ₃					50*/288	52*	54*/283	54*/283	56*/280				
XD ₆ S ₁₋₅ V ₂ d ₂ r ₃ H ₄ e ₃					---	385	392*	399*	---				
XD ₆ S ₁₋₅		5			---	432	434	436	438				
XD ₆ S ₁₋₅ V ₂ d ₂ r ₃					---	342	344	346	348				
XD ₆ S ₁₋₅ V ₂ d ₂ r ₃ H ₃ e ₃					---	280	287	285	281				
XD ₆ S ₁₋₅ V ₂ d ₂ r ₃ H ₄ e ₃					---	380	393	400	---				
<u>Effect of Core Cow.</u>													
XD ₆ S ₁₋₅ V ₂ d ₂ r ₃ H ₃ e ₃		0	2.3		46*	48*	---	---	---				
XD ₇ S ₁₋₅ V ₂ d ₂ r ₃ H ₃ e ₃			2.3		304	305	---	---	---				
XD ₆ S ₁₋₅ V ₂ d ₂ r ₃ H ₃ e ₃			7.0		---	68*	68*	70*	72*				
XD ₇ S ₁₋₅ V ₂ d ₂ r ₃ H ₃ e ₃			7.0		---	309	307	312	313				
<u>Pressure Data</u>													
XD ₆ R _D _{7L} S ₁₋₅ V ₂ d ₂ r ₃ H ₃ e ₃			2.3		22	7	---	---	---				
			4.5		---	10	13	15	18				
			7.0		---	9	---	---	20				
<u>Internal Drag Data</u>													
XD ₆ S ₁₋₅ V ₂ d ₂ r ₃ H ₃ e ₃			2.3		27	39	---	---	---				
			4.5		---	38	36	---	---				
			7.0		---	34	32	30	29				

* Listed Elsewhere

UNCLASSIFIED

Security Classification

DOCUMENT CONTROL DATA - R & D

(Security classification of title, body of abstract and indexing annotation must be entered when the overall report is classified)

1. ORIGINATING ACTIVITY (Corporate author) Arnold Engineering Development Center Arnold Air Force Station, Tennessee 37389	2a. REPORT SECURITY CLASSIFICATION UNCLASSIFIED
	2b. GROUP N/A

3. REPORT TITLE

AERODYNAMIC CHARACTERISTICS OF A 0.12-SCALE MODEL OF THE A-9A AIRCRAFT AT MACH NUMBERS FROM 0.30 TO 0.80

4. DESCRIPTIVE NOTES (Type of report and inclusive dates)

Final Report - August 17 to 24, 1971

5. AUTHOR(S) (First name, middle initial, last name)

Warren E. White, ARO, Inc.

6. REPORT DATE December 1971	7a. TOTAL NO OF PAGES 132	7b. NO OF REFS 1
8a. CONTRACT OR GRANT NO	9a. ORIGINATOR'S REPORT NUMBER(S)	
b. PROJECT NO.	AEDC-TR-71-271	
c. Program Element 64211F	9b. OTHER REPORT NO(S) (Any other numbers that may be assigned this report)	
d. System 329A	ARO-PWT-TR-71-207	
10. DISTRIBUTION STATEMENT Distribution limited to U.S. Government agencies only; this report contains information on test and evaluation of military hardware; December 1971; other requests for this document must be referred to Aeronautical Systems Division (SDXT), Wright-Patterson AFB, OH 45433.		
11. SUPPLEMENTARY NOTES Available in DDC.	12. SPONSORING MILITARY ACTIVITY Aeronautical Systems Division (SDXT), Wright-Patterson AFB, OH 45433	

13. ABSTRACT

Wind tunnel tests were conducted at Mach numbers from 0.30 to 0.80 and Reynolds numbers from 2.3 to 7.0 million on a 0.12-scale model of the A-9A aircraft to determine the effects of control surface deflections on the aerodynamic characteristics of the airplane. The results showed that the horizontal stabilizer was 20 to 50 percent more effective in pitching moment per degree of deflection than the elevator, the rudder remained effective at all Mach numbers, and the aileron deflections produced significant effects on lift, drag, and pitching and rolling moment. Minimum drag was increased by approximately 100 and 600 percent for speed brake deflections of 20 and 60 deg, respectively, at Mach numbers from 0.70 to 0.80.

Distribution limited to U. S. Government agencies only; this report contains information on test and evaluation of military hardware; December 1971; other requests for this document must be referred to Aeronautical Systems Division (SDXT), Wright-Patterson AFB, OH 45433.

UNCLASSIFIED

Security Classification

14. KEY WORDS	LINK A		LINK B		LINK C	
	ROLE	WT	ROLE	WT	ROLE	WT
A-9A						
jet aircraft						
control surfaces						
aerodynamic characteristics						
subsonic flow						
transonic wind tunnels						